Design of Ionic Liquids for Homogeneous Liquid-Liquid Extraction and Aqueous Biphasic Extraction of Metal Ions

Daphne DEPUYDT

Supervisor:
Prof. Dr. Koen Binnemans

Co-supervisor:
Prof. Dr. Wim Dehaen

Members of the
Examination Committee:
Prof. Dr. Wim De Borggraeve
Prof. Dr. Christ Glorieux
Prof. Dr. Richard Hoogenboom
Prof. Dr. Erik Nies
Prof. Dr. Ir. Tom Van Gerven

Dissertation presented in partial fulfillment of the requirements for the degree of Doctor of Science (PhD): Chemistry

November 2017

Uitgegeven in eigen beheer, Daphne Depuydt, Celestijnenlaan 200F, B-3001 Heverlee

DANKWOORD

ABSTRACT

Ionic liquids (ILs) are solvents that consist entirely of ions. Major advantages of these solvents are their low flammability and low volatility, making them an environmentally friendly alternative for volatile organic solvents. The large variety in possible anion and cation combinations makes the design of an IL for any application feasible. Depending on its composition, the ionic liquid is miscible (hydrophilic) or immiscible (hydrophobic) with water. Currently, hydrophobic ionic liquids are of interest for the separation of molecules by solvent extraction. However, most hydrophobic ionic liquids have fluorinated anions such as the hexafluorophosphate ($[PF_6]^-$) or bis(trifluoromethylsulfonyl) imide ($[Tf_2N]^-$), which are under inquiry for being too expensive, not hydrolytically stable ($[PF_6]^-$ and $[BF_4]^-$) and persistent in nature. Therefore, in this PhD thesis, the synthesis of non-fluorinated ionic liquids was pursued. A versatile, halogen-free synthesis procedure for 1,3-dialkylimidazolium ionic liquids was developed to obtain a series of acetate ionic liquids which can be transformed into other ionic liquids by anion-exchange reactions. Via different synthetic approaches, the implementation of nitrate, tosylate, bis(2-ethylhexyl)phosphate, and docusate as anions in both phosphonium and imidazolium ionic liquids was achieved.

By variations in the alkyl chain length or the incorporation of a functional group, the water miscibility of the ionic liquids was tuned. If hydrophobicity and hydrophilicity were balanced correctly, an ionic liquid was obtained which shows temperature-dependent miscibility with water. Ionic liquids with both UCST (upper critical solution temperature) and LCST (lower critical solution temperature) phase behavior are known. In case the IL/solvent mixture has an UCST, one homogeneous phase is formed above the UCST and phase separation occurs below this temperature. In LCST, the IL/solvent mixture forms one homogeneous phase below the LCST and phase separates above this temperature.

The addition of (metal) salts largely affects the temperature-dependent miscibility of the ionic liquids. In general, with a salting-in salt, mutual solubility of the phases is improved and the homogeneous solution favored. In UCST systems, the cloud point curve will descend to lower temperatures. On the other hand, in LCST systems, the biphasic mixtures will only be reached at higher temperatures. Salting-out salts diminish the mutual solubility and favor the demixing of the phases. This increases cloud point temperatures in

UCST systems, but decreases them in LCST systems. The effect of the salts on the thermomorphic system can even suppress any temperature-dependent miscibility, as was observed for the [HHIM][NO_3]/water system. Yet, this led to a short-chain IL binary mixture for the separation of rare earths and 3d transition metals. Addition of salting-out agents to a homogeneous aqueous solution of an ionic liquid may induce the coexistence of two separate phases, and the formation of an *aqueous biphasic system* (ABS). An example on how an IL-based ABS can be used in solvent extraction of metals is studied in detail.

In conventional solvent extraction systems with ionic liquids, often intense mixing and high temperatures are needed because of slow mass transfer arising with the high viscosity of ionic liquids. This problem is already circumvented by IL-based ABS as the system is largely diluted by water. However, it is even more beneficial to apply the thermomorphic ionic liquid systems in an innovative technique called *homogeneous liquid-liquid extraction* (HLLE). Mixing on a molecular level in the homogeneous phase is achieved, drastically increasing the mass transfer and diffusion in the system. The HLLE is exploited in the extraction of critical metals. In fact, we presented the first example for HLLE of metal ions with an IL system showing LCST phase behavior.

SAMENVATTING

Ionische vloeistoffen zijn solventen die volledig uit ionen bestaan. De grootste voordelen van ionische vloeistoffen zijn hun verwaarloosbare dampspanning en laag ontvlambaar karakter. Ionische vloeistoffen worden vaak gezien als een milieuvriendelijk alternatief voor vluchtige organische solventen. De grote variëteit aan mogelijke combinaties van kationen en anionen maken het ontwerp van een ionische vloeistof voor elke toepassing toegankelijk. Afhankelijk van de moleculaire structuur van het ionenpaar kunnen zowel water-mengbare (hydrofiele) als water-onmengbare (hydrofobe) ionische vloeistoffen gesynthetiseerd worden. Hydrofobe ionische vloeistoffen zijn interessant voor de scheiding van moleculen via solventextractie vanuit waterige oplossingen. Echter, de meeste hydrofobe ionische vloeistoffen hebben gefluoreerde anionen zoals hexafluorofosfaat ($[PF_6]^-$) of bis(trifluoromethylsulfonyl)imide ($[Tf_2N]^-$). De gefluoreerde ionische vloeistoffen zijn echter duur en zijn dus minder interessant voor industriële toepassingen op grote schaal. Aangezien er bovendien ook problemen kunnen zijn met persistentie in de natuur en de hydrolytische stabiliteit van bepaalde fluorhoudende anionen ($[PF_6]^-$, $[BF_4]^-$), wordt er in deze dissertatie de voorkeur gegeven aan fluorvrije ionische vloeistoffen. Via een halogeenvrije synthese werden 1,3-dialkylimidazolium ionische vloeistoffen verkregen. Deze reeks van ionische vloeistoffen had acetaat als anion wat ons in staat stelde via een eenvoudige anionuitwisseling nitraat, tosylaat, bis(2-ethylhexyl)fosfaat imidazolium ionische vloeistoffen te verkrijgen. Daarenboven werden ook bij fosfonium ionische vloeistoffen bis(2-ethylhexyl)fosfaat en docusaat als anion geïmplementeerd via diverse synthetische procedures. Door variaties aan te brengen in de alkylketenlengte of door het toevoegen van een functionele groep in de ionische vloeistof, kan de watermengbaarheid van de ionische vloeistof worden aangepast. Indien de hydrofobiciteit en hydrofiliciteit op een correcte manier gebalanceerd worden, wordt een ionische vloeistof bekomen die temperatuursafhankelijke mengbaarheid met water vertoont. Sommige ionische vloeistof/solvent mengsels hebben een bovenste kritische oplossingstemperatuur (*upper critical solution temperature*, UCST). Deze vormen één homogene fase boven de UCST en ondergaan fasescheiding onder deze temperatuur. Andere ionische vloeistof/solvent mengsels hebben een laagste kritische oplossingstemperatuur (*lower critical solution temperature*, LCST). Deze vormen één homogene fase onder de LCST en de fasescheiding treedt op boven deze temperatuur. De

toevoeging van (metaal)zouten aan een ionische vloeistof/solvent mengsel heeft een grote impact op de temperatuursafhankelijke mengbaarheid van de ionische vloeistof. Over het algemeen zal met een inzoutend zout de gemeenschappelijke mengbaarheid van de fasen verbeterd worden en dus de homogene fase worden bevorderd. In UCST-systemen zal dit de mengbaarheidscurve doen dalen naar lagere temperaturen. Daarentegen, in LCST-systemen zullen de twee fasen pas bij hogere temperaturen bereikt worden. Uitzoutende zouten verminderen dan weer de oplosbaarheid, waardoor het bifasisch systeem geprefereerd wordt. Dit zal de overgangstemperaturen doen stijgen in UCST-systemen, maar een daling zal worden geobserveerd in LCST-systemen. Het effect van het toevoegen van zouten op de thermomorfe ionische vloeistoffen kan zeer drastisch zijn en leiden tot het volledig verdwijnen van de temperatuursafhankelijke mengbaarheid, wat werd waargenomen voor het [HHIM][NO_3]/water systeem. Dit leidde echter wel tot het verkrijgen van een binair mengsel met een korte keten ionische vloeistof, en kon worden gebruikt in de scheiding van zeldzame aarden van 3d-transitiemetalen. Het toevoegen van uitzoutende zouten aan een homogeen mengsel van twee componenten, zoals ionische vloeistof en water, kan het gelijktijdig bestaan van twee aparte fasen induceren, met de vorming van een waterig bifase systeem (*aqueous biphasic system*, ABS). Een voorbeeld van hoe een ionische vloeistof gebaseerde ABS gebruikt kan worden voor de solvent extractie van metalen werd in detail bestudeerd.

In traditionele solventextractiesystemen met ionische vloeistoffen zijn vaak intens roeren en hoge temperaturen noodzakelijk door de trage massatransfer omwille van de hoge viscositeit van ionische vloeistoffen. Dit probleem wordt al omzeild door gebruik te maken van een IL-gebaseerde ABS, aangezien hier het systeem grotendeels door water verdund wordt. Toch is het gunstiger van de thermomorfe ionische vloeistoffen toe te passen in een innovatieve techniek genaamd *homogene vloeistof-vloeistof extractie* (HLLE). Omdat hierbij het mengen op moleculair niveau gebeurd, worden de massatransfer en diffusie aanzienlijk verhoogd. HLLE wordt toegepast voor de extractie van metaalionen. Het eerste toepassingsvoorbeeld van deze techniek op een LCST systeem voor de extractie van metaalionen wordt in deze dissertatie beschreven.

ABBREVIATIONS

ABS	aqueous biphasic system
AOT	sodium bis(2-ethylhexyl)sulfosuccinate (= Aerosol OT)
ASC	adiabatic scanning calorimetry
ATPS	aqueous two-phase system
ATR-FTIR	attenuated total reflectance Fourier transform infrared
c_{aq}	metal concentration aqueous phase
CE	coalescence extraction
CHN	carbon, hydrogen, nitrogen elemental analysis
CIPS	composition induced phase separation
conc	concentration
c_{org}	metal concentration organic phase
$c_{org,0}$	metal concentration organic phase before stripping
$c_{org,s}$	metal concentration organic phase after stripping
CPE	cloud point extraction
D	distribution ratio
DEHPA	bis(2-ethylhexyl)phosphoric acid
DFT	density functional theory
DLLME	dispersive liquid-liquid microextraction
DLS	dynamic light scattering
DOSS	dioctyl sulfosuccinate (= docusate)
DSC	differential scanning calorimetry
EDTA	ethylenediaminetetraacetic acid
eq.	equivalents
ESI-MS	electrospray ionization mass spectrometry
EXAFS	extended X-ray absorption fine structure

FT-IR	Fourier-transform infrared
GC	gass chromatography
HLLE	homogeneous liquid-liquid extraction
HPLC	high performance liquid chromatography
ICP	inductively coupled plasma
IL	ionic liquid
IUPAC	international union of pure and applied chemistry
K_{extr}	extraction constant
KF	Karl Fischer
K_{ow}	octanol-water partition coefficient
K_{sp}	solubility product equilibrium constant
LCST	lower critical solution temperature
LLD	lower limit of detection
LLE	liquid-liquid equilibrium
m_{aq}	mass aqueous phase
MD	molecular dynamics
MEE	microemulsion extraction
MME	micelle-mediated extraction
mol%	molar percentage
m_{org}	mass organic phase
MS	mass spectrometry
n.d.	not determined
NIPS	non-solvent induced phase separation
NIST	national institute of standards and technology
NMR	nuclear magnetic resonance
pH_{eq}	equilibrium pH

pH_{in}	initial pH
ppm	parts per million
PTE	phase transition extraction
PUREX	plutonium uranium redox extraction
REE(s)	rare-earth element(s)
RTIL	room temperature ionic liquid
s	standard deviation
SAILs	surfactant ionic liquids
SIPS	solvent induced phase separation
T_b	boiling point
TBP	tri-*n*-butylphosphate
T_d	decomposition temperature
T_g	glass transition temperature
TGA	thermogravimetric analysis
TIPS	temperature induced phase separation
T_m	melting point
TM	transition metals
TMS	tetramethylsilane
TOPO	trioctylphosphine oxide
TXRF	total reflection X-ray fluorescence
UCST	upper critical solution temperature
VOC(s)	volatile organic compound(s)
wt%	weight percentage
%E	percentage extraction
%S	percentage stripping/scrubbing
η	viscosity

ρ	Density
$\alpha_{A,B}$	separation factor for metal ions A and B
$[Chol]^+$	Cholinium
$[C_nmim]^+$	1-alkyl-3-methylimidazolium
$[DEHP]^-$	bis(2-ethylhexyl)phosphate
$[Hbet]^+$	Betainium
$[P_{4444}]^+$	tetra-*n*-butylphosphonium
$[Tf_2N]^-$	bis(trifluoromethylsulfonyl)imide (= bistriflimide)
$[TsO]^-$	*p*-toluenesulfonate (= tosylate)

TABLE OF CONTENTS

THESIS OUTLINE

During the course of this PhD, several research results were published in peer-reviewed journals, these articles are the core of the PhD thesis.

In the introductory **Chapter 1**, three different subjects are discussed. To start with, *ionic liquids* (ILs) are introduced, their synthesis and functionalization towards their application as designer solvents is shortly reviewed. Since the ionic liquids discussed in this PhD thesis are specifically designed to show temperature-dependent miscibility, *phase behavior* is the main topic of the introduction. After the explanation of basic concepts, both phase behavior of common solvents and ionic liquids are explored. The last section addresses the area of *solvent extraction* as an application for ionic liquids.

Chapter 2 lists objectives and discusses the goal of the PhD thesis.

Chapters 3 to 7 describe the published results, starting with a full paper on the synthesis of symmetrical 1,3-dialkylimidazolium ionic liquids (**Chapter 3**). Next, a communication discusses the phase behavior of the 1,3-dihexylimidazolium nitrate ionic liquid in water, the salting-out with sodium nitrate and its application for metal extraction (**Chapter 4**). **Chapter 5** describes the first example of a homogeneous liquid-liquid extraction system for metal ions based on an ionic liquid with LCST phase behavior. Then, in **Chapter 6**, the effect of cation exchange on water solubility in docusate ionic liquids as well as their solvent extraction behavior is investigated. The solvent extraction of metal ions with an ionic liquid based aqueous biphasic system is explored in **Chapter 7**.

Chapter 8 contains the general conclusions and an outlook on future research.

The PhD thesis ends with health, safety and environmental aspects, a list of publications, attended conferences and seminars.

CHAPTER 1

INTRODUCTION

1.1 Ionic Liquids

Ionic liquids (ILs) are solvents that consist entirely of ions, and generally, they have melting points below 100 °C.[1–3] Some salts we would now consider as ionic liquids were discovered as early as the mid-19th century, but the research on ionic liquids has only recently attracted the attention it deserves. Their potential green application made them triumph as the greatest innovation of the 21st century in a Great British innovation vote.[4] It is not the purpose of this introductory part to review all the literature on ionic liquids, but just to inform the reader about these fascinating solvents.

Ethylammonium nitrate was the first IL reported in 1914 by Paul Walden.[5] Up to the present time, three generations of ILs exist: 1) chloroaluminate ILs, with 1,3-dialkylimidazolium or *N*-alkylpyridinium cations, which were popular room temperature ionic liquids (RTILs) due to their easy synthesis, but these types of ILs suffer from large air and water sensitivity; 2) moisture stable ammonium and phosphonium ILs based on weakly coordinating anions like tetrafluoroborate and hexafluorophosphate; 3) biodegradable, non-fluorinated or functionalized ILs with task specific groups on cation and/or anion. A selection of common ILs can be found in **Figure 1.1**. To a large extent, the properties of ionic liquids are determined by intermolecular interactions between anions and cations. In particular, Coulomb forces, hydrogen bonds, π-stacking and repulsion–dispersion forces are important in understanding the properties of ionic liquids. These interactions give an ionic liquid its characteristic viscosity, conductivity or melting point.

Ionic liquids have been widely studied in a wide variety of fields including organic synthesis and catalysis,[6–10] purification of organic and biomolecules,[11] biomass conversion,[12–14] electrochemistry,[15,16] metal processing[17], chemical industry[18] and solvent extraction.[19,20]

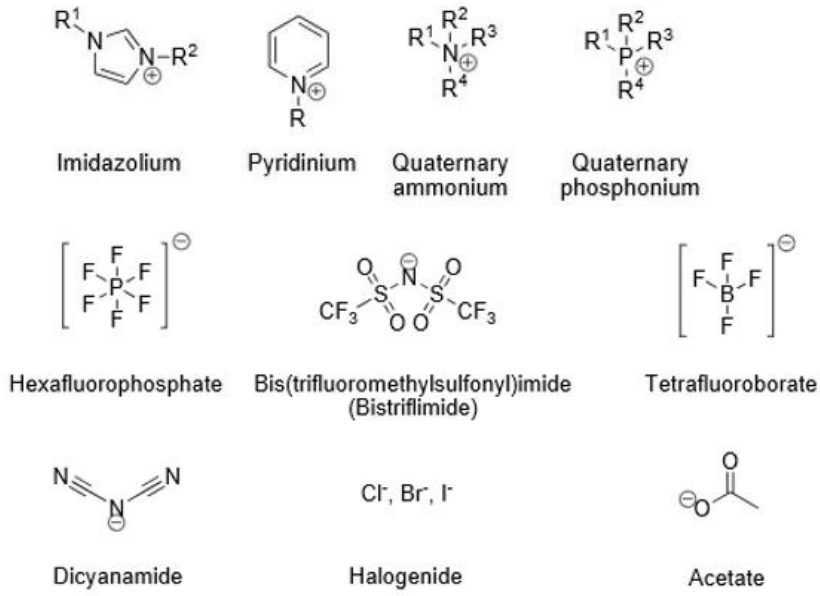

Figure 1.1 Selection of commonly used cations and anions in ionic liquids.

1.1.1 Synthesis

The cation defines the categorization of the ionic liquids, common ILs are imidazolium, pyridinium, quaternary phosphonium or ammonium. Generally, the synthesis of ionic liquids consists of two steps: the formation of the desired cation and the necessary anion exchange to receive the wanted product.[21]

Cations can be synthesized from their respective building blocks, but most often synthesis is carried out by protonation or by quaternization. The procedure to obtain protic ionic liquids is limited because of the reversible nature of the protonation of the base and the unfavorable equilibrium at high temperatures. The quaternization reaction is a nucleophilic substitution reaction (S_N2) of haloalkanes with readily available products like imidazole, pyridine, trialkyl amines or trialkylphosphines. Major advantages are the wide range of cheap and available haloalkanes, the smooth substitution reaction at reasonable temperatures and the fact that halides are easily converted with other anions afterwards. However, the affinity of the new anion for the ionic liquid must be high in order to achieve an easy anion exchange.[22] Water-immiscible ionic liquids can be treated with an aqueous solution of the salt of

the desired anion. Wilkes and Zaworotko performed the first anion metathesis reactions in the synthesis of ionic liquids based on 1-alkyl-3-methylimidazolium cations.[23] Since silver salts like $AgNO_3$, $AgBF_4$ and $Ag(CH_3COO)$ were used, this was an expensive procedure. Nowadays, the more common sodium, lithium and potassium salts are utilized in metathesis reactions.[24] Another option for water-immiscible ionic liquids is to introduce the anion via its corresponding acid, yet setting the limitation to strong acids (full dissociation). For water-miscible ionic liquids, an anion exchange resin loaded with the desired anion must be used for the anion exchange.[25] Most often anions like tetrafluoroborate, hexafluorophosphate and bistriflimide are introduced.

The versatility of ionic liquids, in which the chemical structure can be designed to fit any wanted application, is a great advantage of these solvents. An estimated number of 10^{18} combinations of ionic liquids are possible by combination of cations and anions.[26] Reliable structure–property relationships can help in the synthesis of ionic liquids with the desired set of properties.[27] Any ionic liquid with appropriate properties for a given application can be obtained, granting them their status as designer solvents.[3] Mostly the specific property is reached by introducing a functional group in the structure of the ionic liquid: functionalized ionic liquids.[28]

1.1.2 Functionalized ionic liquids

As mentioned in the previous section, functionalized ionic liquids are ionic liquids with a functional group incorporated in the ionic liquid cation and/or anion. In the literature, these ionic liquids are also often called '*task-specific ionic liquids*'.[26,28] The synthesis of this type of ionic liquids involves a multistep process, as a functionalized alkylating agent has to be designed first, followed by the alkylation of the desired cation precursor, further modification of the obtained salt might be necessary to obtain the desired functional group and finally, an anion exchange reaction. Obviously, as the number of steps increases and the specific features of the reaction become more complex, this implies an increasing cost of the ionic liquid.

Different synthesis routes are researched for the functionalized ionic liquids, as summarized for ammonium type of ionic liquids in **Scheme 1.1**: 1) a substitution reaction with functionalized alkyl halides seems the most plausible, as it is just a quaternization reaction with a functional group, yet incompatibility of the functional group in the reaction might request the need for protective groups, making the reaction more complex; 2) a Michael-type addition reaction of a tertiary amine or phosphine to an α,β-unsaturated compound, limiting to strongly electron-withdrawing groups like –COOR,-CN or -SO_3H;[29,30] 3) a ring-opening reaction, an effective way to yield functionalities as carboxylate, phosphate, alcohol or sulfonate, depending on the reactive ring used.

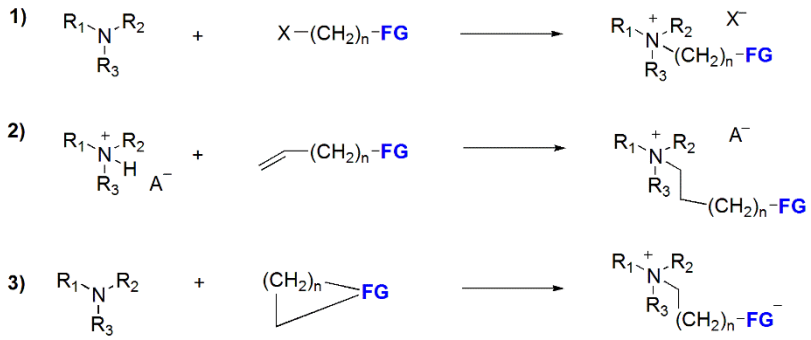

Scheme 1.1 Synthetic routes to functionalized ionic liquids (FG = functional group).

Due to their negligible vapor pressure and thus low volatility, ionic liquids can be environmentally friendlier than conventional molecular solvents.[31,32] Ionic liquids have recently gained a lot of interest because they have several other interesting properties such as a low flammability, a high thermal stability, and a broad electrochemical window and liquidus range.[3,21,33,34] Ionic liquids can be used as diluents in combination with traditional organic extracting agents,[35-37] yet they are also utilized in their undiluted form in extraction of metals.[38,39] Key for such conventional extraction methods is the mutual immiscibility of the ionic liquid and water. This lead to a classification of ionic liquids into hydrophobic and hydrophilic ionic liquids, depending on their miscibility with water. This classification is actually ambiguous, as ionic liquids with temperature-dependent miscibility exist. In the following, phase behavior of binary mixtures is introduced.

1.2 Phase Behavior

A phase is defined as a form of matter that is homogeneous in chemical composition and physical state. Liquid mixtures with different compositions that are not fully miscible in each other are counted as two different phases. This phase behavior of liquid-liquid binary mixtures is the point of discussion in this paragraph. The topic is first introduced with common solvents, yet the focus is on mixtures containing one ionic liquid phase. The restrictive choice to leave out the phase behavior of thermoresponsive polymers was made, as it is comprehensively reviewed elsewhere.[40]

1.2.1 Basic concepts

The ability of substances to form a solution depends on the chemical nature of the forming compounds, on temperature and on pressure. The expression "Like dissolves like" describes clearly how solvent chemistry works. Polar substances will only dissolve well in polar solvents and non-polar compounds only dissolve in likewise non-polar solvents. For liquids, the term *miscibility* is used, the property of substances to mix in all proportions, that is, to fully dissolve in each other at any concentration. Two solvents can either be immiscible (*e.g.* water and nitrobenzene) or be miscible (*e.g.* water and methanol or toluene and benzene). In these examples, the miscibility is complete, but *partial miscibility* in a certain temperature range is also possible (water/phenol or hexane/nitrobenzene). In partial miscibility, two distinct phases are formed, each containing certain amounts of the other liquid. The effect of temperature on the miscibility of binary mixtures is described by phase diagrams. The phase diagram shows a plot of the temperature as function of the composition of the mixture. To understand the construction of such a phase diagram, we must have a look at the thermodynamics of mixing liquids.[41]

Mixing of two components will occur when the excess Gibbs free energy of mixing $\Delta_{mix}G$, defined as the difference between the free energy of the system before and after mixing, is minimized (equation 1.1). The excess enthalpy term, $\Delta_{mix}H$, is known as the heat of mixing, the heat absorbed or evolved during the mixing process. $\Delta_{mix}S$ is the excess entropy difference between the mixed and unmixed state. These two parameters, together with temperature are the determining factors in the phase behavior. Enthalpy and volume changes occur when liquids mix, and additional contributions of entropy arise

from molecules which cluster together instead of mingling freely with others. A miscibility gap indicates a maximum in the excess Gibbs free energy in a specific range of compositions. The term partial miscibility is used for these types of mixtures.

$$\Delta_{mix}G = \Delta_{mix}H - T\Delta_{mix}S \quad (1.1)$$

The actual calculation of the $\Delta_{mix}G$ depends on the specific theory or model used and is out of the scope of this PhD thesis. In **Figure 1.2**, a representation is given of the excess Gibbs free energy of mixing as a function of the composition, including the corresponding phase diagram. During the liquid-liquid phase separation process, two scenarios are possible: *nucleation* and *spinodal decomposition*.[42] The *binodal* or *coexistence curve* is defined by the points of the common tangent to $\Delta_{mix}G$ (outer curve). At these compositions, the chemical potentials of the two components are equal and two phases can coexist. A *tie-line* or isotherm connects two nodes on the binodal, representing the final concentration of the phase components in top and bottom phases.[43] The inner curve on the phase diagram is the *spinodal*, which is defined by the points of inflection on the graph of $\Delta_{mix}G$. In this region, the system is unstable for even the smallest concentration fluctuations, and the phase separation process is called *spinodal decomposition*. The area between the binodal and the spinodal is a *metastable region*, and phase separation follows *nucleation and growth*. A free energy activation barrier has to be overcome and only concentration fluctuations exceeding the critical droplet size will result in phase separation. The point where the binodal and the spinodal curves meet is the *critical point*. The critical point is the lowest or highest temperature at which the phase transition occurs, all other points on the binodal are termed cloud points with their respective cloud point temperatures. The term *cloud point* is derived from the visual observation of a cloudy, turbid mixture when phase separation sets in. The phase demixing occurs with a turbid solution when two solutions with different refractive indices are mixed. On the other hand, also the term *clear point* can be used, indicating the formation of a clear homogeneous solution with complete miscibility.

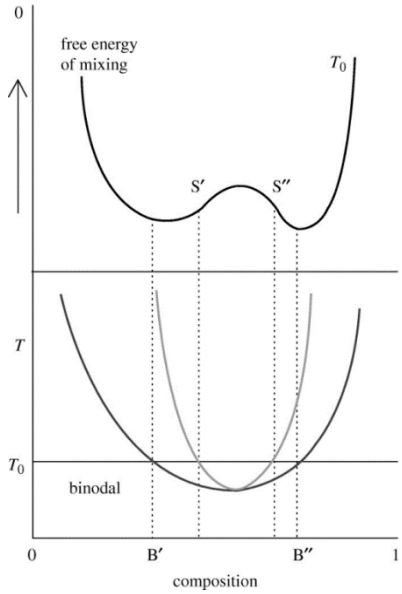

Figure 1.2 Plot of the excess Gibbs free energy of mixing as a function of composition at a chosen temperature T_0 (top) and its corresponding phase diagram showing the binodal (outer) and spinodal (inner) curves. Reprinted with permission from Higgins *et al.*, copyright 2010 The Royal Society Publishing.[44]

The fundamental physical chemistry behind phase separation of binary liquid mixtures has been intensively researched for several decades, both theoretically and experimentally.[45,46] Phase behavior is the result of several competing interactions in solution, mainly long-range Coulombic forces and short-range hydrogen bonding. Phase transitions can be expected to be driven by Coulombic interactions.[47] In spite of the long range nature of Coulombic interactions, the *3D Ising universality class* has been observed for liquid-liquid phase transitions of ionic solutions. This is a consequence of the shielding of the Coulombic interactions by the charge distribution surrounding the ion, so that the correlations become short range and the *Ising criticality* results.[48] It was indeed confirmed experimentally, by extensive measurements by high-resolution calorimetric techniques,[49] turbidity and light scattering,[47,50] dielectric and refractive index measurements[51] that critical points in ionic liquid binary mixtures belong to this 3D Ising universality class. Further reading on this subject can be found in literature.[48,52–58] Solution theory can be used to predict critical properties of mixtures,[59] or excess Gibbs energy models (NRTL, UNIQUAC) to correlate phase equilibria or excess molar enthalpies of mixing in binary mixtures.[60–62] Also, COSMO-RS, a predictive model based on unimolecular quantum chemistry calculations, was evaluated

for liquid–liquid equilibria of binary mixtures.[63,64] However, the discussion of the thermodynamic models for phase behavior are outside the scope of this PhD thesis. Merely, the different types of phase behavior for partially miscible liquids will be discussed here, first by introducing the concepts to common solvent systems and next to review the phase behavior of ionic liquids.

1.2.2 Phase behavior of common solvents

Two types of phase behavior for partially miscible liquids exist: *upper critical solution temperature* (UCST) behavior and *lower critical solution temperature* (LCST) behavior. Phase separation of the partially miscible liquids may occur when the temperature is below the UCST (highest temperature at which phase separation occurs) or above the LCST (temperature below which components mix in all proportions and above which they form two phases). Both types can be combined as well, giving rise to four types of phase diagrams (**Figure 1.3**).

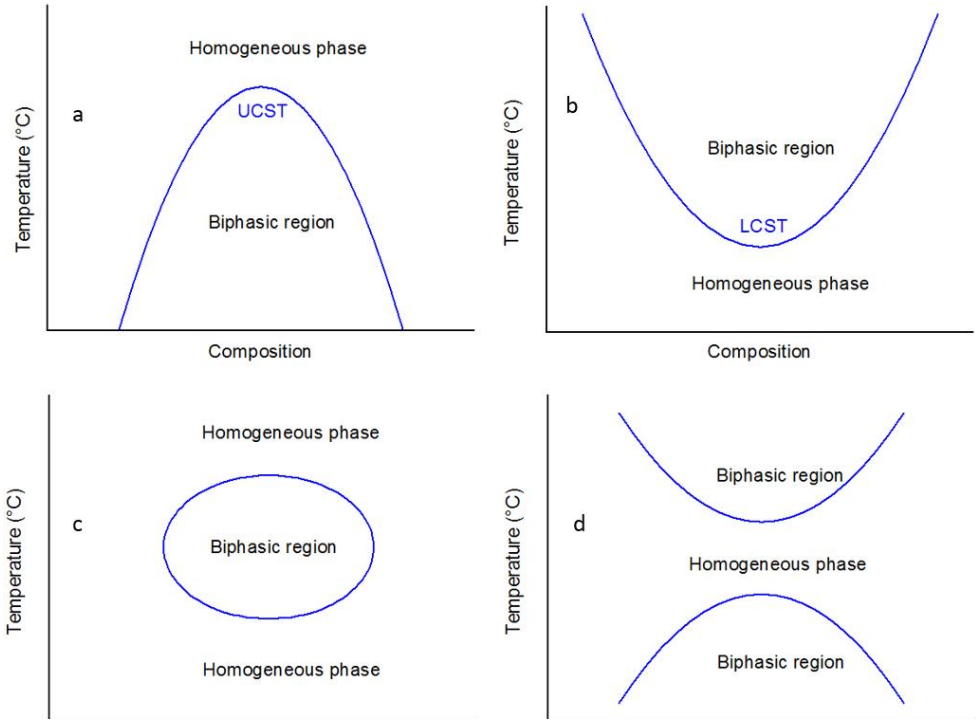

Figure 1.3 Four types of phase diagrams of partially miscible liquids. (a) Upper critical solution temperature, (b) Lower critical solution temperature, (c+d) both upper and lower critical solution temperature.

In the 1960s, Francis listed the critical solution temperature for more than 6,000 chemical systems.[65,66] Several liquid-liquid equilibrium data for solvent systems with critical solution temperatures are available in data collections.[67,68] The IUPAC Solubility Data Series is a database on solubility measurements, containing 1,800 chemical substances in the database and 5,200 systems, of which 473 have been critically evaluated.[69] This project is a product of the collaboration between the National Institute of Standards and Technology (NIST) and the IUPAC Analytical Chemistry Division, Commission on Solubility Data. This series compiles data on liquid-liquid systems, but a limited number of related solid-liquid, fluid-fluid and multicomponent (organic-water-salt) systems are included. For some of the systems listed, the two components are miscible in all proportions at certain temperatures and pressures. A selection of this data on miscibility gaps and upper and lower critical solution temperatures is discussed here, as examples on the phase behavior of partially miscible liquids.

In UCST phase behavior, the higher the temperature, the larger the mutual solubility of the two liquids, until complete miscibility is reached. Generally, the entropy in homogeneous mixtures is larger than in biphasic mixtures, so miscibility is favored in this regard from an entropic point of view. However, the contribution of the entropic effect is small at low temperatures, and miscibility will be governed solely by the minimization of enthalpy. At a molecular level, interactions between unlike molecules are significantly weaker than between like molecules, promoting the formation of a separate phase with the same kind of molecules. At the basis of this type of transition is thus an unfavorable enthalpy of mixing, it is said that the UCST is an enthalpy driven demixing. A typical example found in the literature is the hexane/nitrobenzene system (**Figure 1.4**). These two solvents are mixed in all proportions at 20 °C, but phase-separate at lower temperatures. Other UCST examples of binary solvent mixtures are: phenol/water (UCST 66 °C),[70] hexane/nitroethane (31 °C),[71] hexane/nitromethane (102 °C).[72] Liquid-liquid coexistence curves with methanol and hydrocarbons have been studied extensively.[73] The UCST of the binary systems depends on the molecular shape of the hydrocarbon used. It was observed that the solubility of the alkanes increased with increasing branching of structural isomers of hexane. Hence, the more branched isomers have a lower UCST.

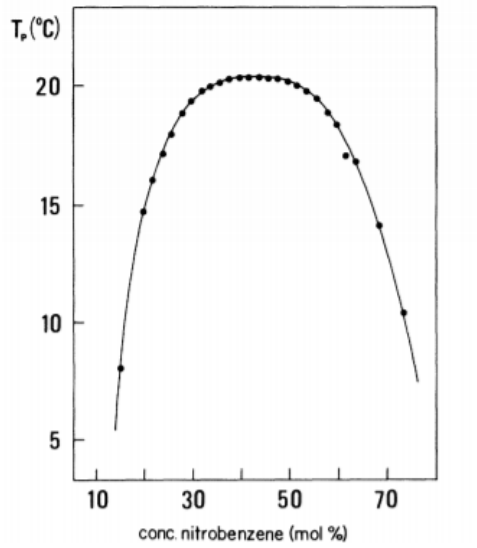

Figure 1.4 UCST phase diagram (temperature in function of fraction of nitrobenzene) of the hexane-nitrobenzene system. Reprinted with permission from Chen *et al.*, copyright 1983 American Physical Society.[74]

LCST phase behavior is contra-intuitive, since two phases are in their mixed state at lower temperature and become immiscible with higher temperature (**Figure 1.5**). LCST-type phase transitions are seen in mixtures involving strong interactions between the component species, like hydrogen bonding. Due to the strength of hydrogen bonding between the unlike molecules, the enthalpy of the miscible phase is lower than that of the immiscible one. Again, at low temperatures, no entropic effects can compete with this enthalpy decrease. As temperature increases, the disruption in hydrogen bonding results in the formation of the separate phases. The physical basis of this LCST phase behavior is found in the unfavorable entropy of mixing, LCST phase behavior is an entropy induced demixing. In the triethylamine/water system, the amine forms hydrogen bonds with water at temperatures below 19 °C, so the amine molecules remain associated to the water with loss of entropy.[42,75–77] The mixing of the phases is due to the enthalpy of formation of hydrogen bonds. At higher temperatures, the hydrogen bonds are broken up and the separate phases form. Another example of a common solvent mixture showing this LCST phase behavior is water and lutidine, which shows an LCST at 34 °C.[78,79]

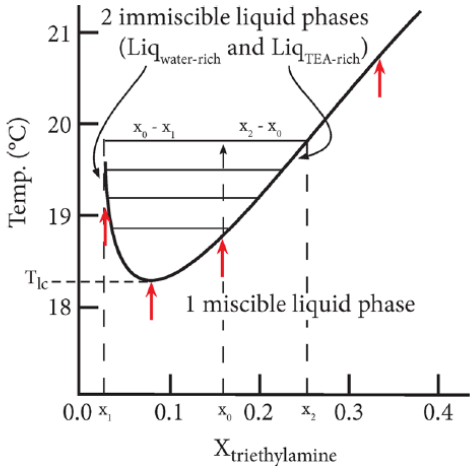

Figure 1.5 LCST phase diagram of the triethylamine/water mixture. Reprinted with permission from Erikson, copyright 2017 American Chemical Society.[75]

In 1898, Rothmund observed an upper critical solution temperature for the methyl ethyl ketone/water system. Additionally, he noticed the tendency to a lower critical solution temperature but he could not realize it because of the freezing of the water.[80] In 1904, Hudson discovered the miscibility gap in the phase diagram of nicotine/water, the first closed-loop coexistence curve ever reported (**Figure 1.6**).[81] The original goal of Hudson's experiments was to crystallize nicotine from its aqueous solution, and study the melting point of nicotine/water mixtures to prove the existence of the hypothetical nicotine hydrate. Hudson believed the reason for the mixing was the presence of the hydrate at low temperatures. At elevated temperatures this hydrate decomposes and the two liquids, water and nicotine, separate because the quantity of the mutual solvent, namely the hydrate, was greatly reduced. The early results of Hudson were further investigated by other researchers.[82,83] The nicotine/water system became the textbook example for a two-liquid system with both maximum and minimum critical solution temperatures, with an LCST of 61 °C and a UCST of 210 °C. Examples of binary systems which possess both UCST and LCST are methyl ethyl ketone/water, *sec*-butyl alcohol/water, β-picoline/water.[84] The 2-methylpiperidine/ water system forms a single closed loop of two immiscible phases surrounded by a single-phase region with the UCST approximately 140 °C higher than the LCST.[85,86] Tetrahydrofuran/water is another example of a binary solvent system that shows a closed-loop phase diagram.[87,88] For an exhaustive review of the theory and experimental results on closed miscibility gaps, the reader is referred to the review by Narayanan and Kumar.[89]

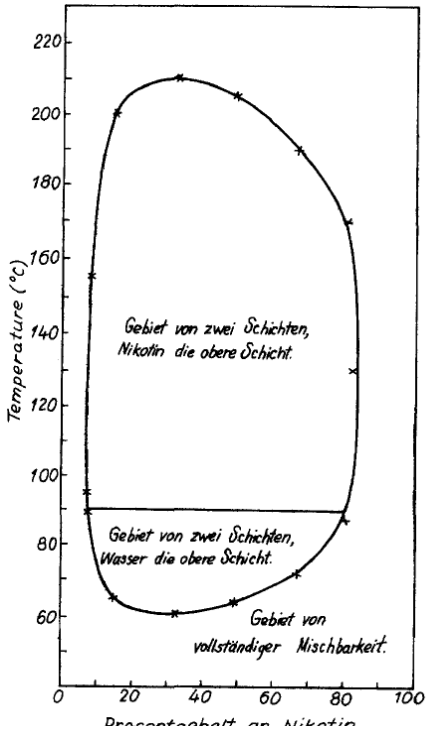

Figure 1.6 Closed-loop phase diagram of nicotine/water system.[81] Reprinted with permission from Narayanan and Kumar, copyright 1994 Elsevier.[89]

Another possibility for combined UCST and LCST phase behavior is found in sulfur/solvent systems (**Figure 1.7**). Liquid-liquid phase diagrams were determined for solutions of molten sulfur in different solvents: benzene, toluene, *o*-xylene, biphenyl, triphenylmethane and *cis*-decalin. In these systems, both an UCST and LCST is found, and between the two critical temperatures there is a region of complete miscibility.[90] This type of phase transitions occurs because of the polymerization ability of sulfur, the conversion of the eight sulfur atoms rings to very long diradical chains.[91] At temperatures well below this polymerization temperature of sulfur, there is immiscibility between unpolymerized sulfur and the solvent. The polymerization temperature increases as the concentration of solvent increases reaching a second region of immiscibility between the solvent and the partially polymerized sulfur at high temperatures.[92]

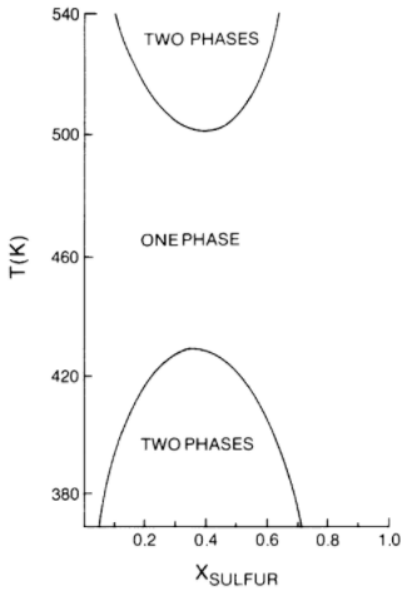

Figure 1.7 Partial miscibility exhibited by the sulfur/benzene system. Reprinted with permission from Acree, copyright 1984, Academic Press, Elsevier.[85]

1.2.3 Experimental methods to determine phase diagrams

The observation of cloud point temperatures and consecutive construction of the phase diagram can be performed in various ways. Thermal analysis is the study of properties of materials as they change with temperature. For liquid samples, enthalpy, thermal capacity, mass changes and the coefficient of heat expansion are the studied properties. Several different methods are included in thermal analysis like TGA (thermogravimetric analysis) and DSC (differential scanning calorimetry). DSC employs the measurement of phase transition energies. However, even with sophisticated instruments, high precision determination of UCST liquid-liquid transitions is not possible due to the small thermal signatures of these transitions. Additionally, samples cannot be stirred in the DSC method, which is essential for the investigation of phase transitions.[93] The sharp transitions in LCST behavior, however, can be detected via DSC. In addition, the thermophysical properties of binary mixtures can be studied by a photopyroelectric technique and by adiabatic scanning calorimetry (ASC). By photothermal analysis, besides highly accurate values for the thermal conductivity and effusivity, the detailed temperature dependence of both quantities for the upper and lower part of a

critical ionic liquid/water mixture in the neighborhood of the mixing-demixing phase transition can be determined with high resolution and accuracy. Experimental high resolution ASC data gives information on the critical behavior of the specific heat capacity of an ionic liquid/water mixture.[94–97]

A phase diagram of a thermomorphic ionic liquid/solvent system can be constructed gravimetrically. Therefore, the binary mixture is equilibrated at a given temperature, followed by analysis of the components in the IL-rich phase and solvent-rich phase. Since the ionic liquid is non-volatile, the composition of the phases can be determined by distilling out the solvent and comparing the original mass with the remaining ionic liquid mass. For volatile compounds, Ullmann's method of determination of the phase diagram can be used. The solvents composition in each of the coexisting phases was analyzed using gas chromatography. With varying the overall composition and the system temperature, the entire phase diagram can be constructed.[98] Other analysis methods to determine phase compositions can be carried out by using a combination of either optical rotation (for phase components containing an asymmetric center that can rotate a plane of polarized light), refractive index, dry weight or conductivity measurements.[43,99] The most straightforward method for cloud point determination is the visual observation of the appearance or disappearance of turbidity with changing temperature of the mixture in an observational cell. The method is also described as a dynamic cloud point method. An example of an apparatus for the cloud point method determination can be found in **Figure 1.8**.[100] Strey *et al.* constructed their experimental phase diagrams in a similar thermostatted water bath with the samples contained in sealed test tubes. Phase-transition temperatures were determined by visual inspection in transmitted light, scattered light and between crossed polarizers.[101] In the turbidometric titration technique, the solution is held at a constant temperature and is titrated by adding one of its components until turbidity is observed visually.[102]

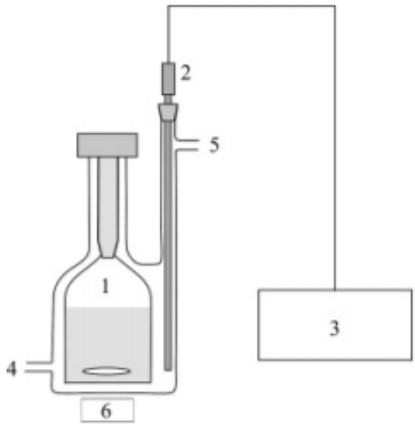

Figure 1.8 Cloud point method apparatus. 1 thermostatted equilibrium cell, 2 thermometer probe, 3 precision thermometer, 4 thermostat outlet, 5 thermostat inlet, 6, magnetic stirrer. Reprinted with permission from Bendová *et al.,* copyright 2006 American Chemical Society.[100]

Several researchers measure accurate phase diagrams using light scattering techniques. The phase separation is detected by monitoring low-angle forward scattered light, together with simultaneous loss in transmitted light. The light source can be a tungsten lamp,[103] yet mostly laser light sources (*e.g.* He–Ne laser) are used to illuminate the sample.[104,105] Schrödle reported an automated apparatus which operates unattended and measures six samples simultaneously. In this way, high quality phase-diagram data are produced in a reasonable time. The device takes advantage of the intensity changes in transmitted light which occur when the sample undergoes a phase change. The construction is based on light emitting diodes (LED) as light sources and light dependent resistors (LDR) or photodiodes as detectors, which are less expensive than optic equipment like lasers, glass fiber optics or photomultipliers.[93]

Nowadays, commercial automated turbidity analyzers are sold by multiple suppliers, *e.g.* Turbitronic (NovoMatics), Turbidity system (ABB). In principle, the method is based on automatic turbidity detection by light transmission. Infrared light is transmitted through the sample and is detected by a highly sensitive photoelectric sensor on the opposite side. Turbidity measurements can also be carried out in a temperature-controlled UV-vis spectrophotometer, by determination of the optical transmittance over a specific temperature range.

Vibrational spectroscopy can also be a helpful technique to investigate the hydrophilic/hydrophobic interactions in solutions, especially for the thermomorphic behavior. For instance, Fourier transform infrared spectroscopy (FT-IR) in combination with two-dimensional analysis methods, including perturbation correlation moving window (PCMW) and two-dimensional correlation spectroscopy (2Dcos), have been applied to illustrate the dynamic hydration behavior of polymers and the interactions between ILs and water.[106,107] These techniques, together with DSC, optical microscopy (microscopic observation of the phase transition process to follow the morphology of the separating phases[98]) and nuclear magnetic resonance (NMR) elucidate the detailed phase transition dynamic mechanisms, which is conducive in understanding the phase transition process.[108]

1.2.4 Phase behavior of ionic liquid/water systems

Most ILs are highly hygroscopic and water interacts with the ILs through hydrogen bonding. Early studies on ionic liquids report water as an impurity, as its presence largely affects the IL properties. Yet, the mixing of ionic liquids with water yields benefits, since the properties of both the IL and water can be exploited in various applications.[109]

Biphasic IL/water mixtures

The solubility of ionic liquids in water varies with the structure and polarity of the ionic liquid.[110] Freire *et al.* observed a decrease of the mutual solubility of water and 1-alkyl-3-methylimidazolium ionic liquids with increasing alkyl chain length.[111] This trend is also observed by increasing *n*-octanol/water partition coefficients (K_{ow}), a value which is calculated by dividing the concentration of IL in the *n*-octanol phase by that in the water phase of a biphasic solution.[112,113] K_{ow} is also used to estimate the hydrophobicity of anions, in order to list them according to higher hydrophobicity, *i.e.* lower water solubility:

$[BF_4]^- < [CH_3(C_2H_4O)_2SO_4]^- < [C(CN)_3]^- < [PF_6]^- < [Tf_2N]^-$

The mutual solubility of the ionic liquids and water in a biphasic IL/water mixture is of importance in the application of solvent extraction. The water phase can become polluted with IL, and valuable IL may get lost.

It is widely accepted that the phase behavior of IL/water mixtures is governed by the total hydrophobicity/hydrophilicity of the constituent cation and anion of the IL. In what follows, seminal examples of ionic liquids with temperature-dependent phase behavior are discussed. Thermomorphic ionic liquids were recently reviewed by Ohno and co-workers and by Qiao *et al.*[114,115]

IL/water systems with UCST phase behavior

The UCST phase behavior is mostly found in studies of fluid phase equilibria of binary mixtures of ionic liquids with 1-alkyl-3-methylimidazolium cations. A homogeneous mixture of $[C_4mim][BF_4]$/water, 1:1 w/w, is formed at temperatures above 5 °C and a two-phase mixture at lower temperatures.[116] Anthony *et al.* presented the liquid-liquid equilibrium (LLE) phase behavior of water with three ionic liquids: $[C_4mim][PF_6]$, $[C_8mim][PF_6]$ and $[C_8mim][BF_4]$.[117] The affinity for water is larger for ILs with $[BF_4]^-$, and the water affinity decreases with increasing alkyl chain length. In this study, only the $[C_4mim][PF_6]$ shows UCST phase behavior with water. The well-known tetrafluoroborate ($[BF_4]^-$) and hexafluorophosphate $[PF_6]^-$ anions have been commonly incorporated in ionic liquids for many years. The study of these types of ionic liquids with aqueous systems, however, is inadequate as these anions are not stable against hydrolysis.[118] Decomposition of the ionic liquid with formation of HF is the result, together with etching of the used glassware. Considering the study of the thermomorphic behavior of the ILs, substantial changes of the composition, phase volumes and transition temperatures are caused by this hydrolysis of the anion.[119]

The anion bis(trifluoromethylsulfonyl)imide (or bistriflimide, $[Tf_2N]^-$) is superior to $[BF_4]^-$ and $[PF_6]^-$, since it is hydrolytically stable and yields ionic liquids with lower viscosity. This anion is also more hydrophobic, so that smaller or more polar cations have to be introduced to give thermomorphic behavior with water. $[C_2C_2IM][Tf_2N]$ and $[C_4C_2IM][Tf_2N]$ water mixtures have increasing cloud point temperatures of 72 °C and 94 °C in 1:1 molar ratios. Introducing an ether group on the imidazolium core as in $[C_6H_{13}OCH_2MIM][Tf_2N]$ gives a UCST of 55 °C and two ether groups in $[(C_6H_{13}OCH_2)_2IM][Tf_2N]$, further lowers the transition temperature to 44 °C for 50/50 mol% mixtures with water.[120]

Our research group introduced the [Hbet][Tf_2N]/water mixture, with an UCST of 55.5 °C.[94] A longer linker between the nitrogen atom and the carboxylic acid functional group increased the critical temperature (C_3: 74 °C, C_4: 96 °C).[121] Pyridinium (55 °C), morpholinium (52 °C) and imidazolium (64 °C) betaine derivatives also tested positive for thermomorphic behavior.[122] Structures of the [Hbet][Tf_2N] and described derivatives are found in **Figure 1.9**.

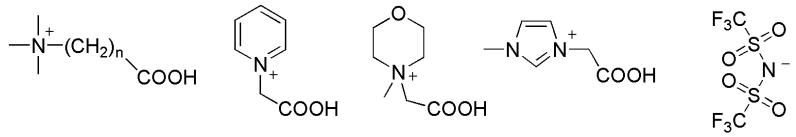

Figure 1.9 Structures of $[Hbet]^+$ and betaine derivatives with pyridinium, morpholinium and imidazolium cation, and structure of $[Tf_2N]^-$.

Köddermann *et al.* used DFT calculations and infrared spectroscopy on different ionic liquids mixed with water to show that hydrogen bonding can play an important role for the phase behavior of ionic liquids.[123] The water molecules are mainly forming hydrogen bonds with IL anions. Different types of structures were found in [C_2mim][Tf_2N]. A double donor conformer exists in which the water molecules form two hydrogen bonds to one $[Tf_2N]^-$ group. In a single donor conformer, the water molecules form a strong hydrogen bond to the anion. Therefore, the most probable explanation of the 'phase-switching' behavior of the [Hbet][Tf_2N]/water system is the loss of the cation-anion hydrogen bonding upon heating (**Figure 1.10**).

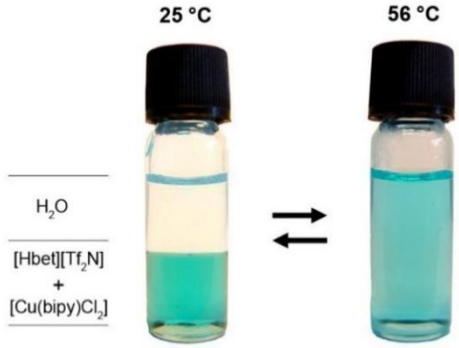

Figure 1.10 Temperature-dependent phase behavior of a binary [Hbet][Tf_2N]/water mixture. [Cu(bipy)Cl_2] was added to accentuate the phase boundaries. Reprinted with permission from Nockemann *et al.*, copyright 2006 American Chemical Society.[94]

An ionic liquid similar to betaine bistriflimide is choline bistriflimide, [Chol][Tf_2N], in which the carboxylic acid group is changed to an alcohol group (**Figure 1.11**).[95] Upon heating a mixture of [Chol][Tf_2N] and water, a homogeneous phase is observed for a 1:1 w/w mixture at 72 °C. The IL/water mixture was studied by ^1H NMR. It could be concluded that upon heating, with an increase of miscibility with water, the hydrogen bonding between hydroxyl proton of the choline cation and oxygen of bistriflimide was diminished. The hydrogen bond between anion and cation is fully broken upon formation of the single phase system.

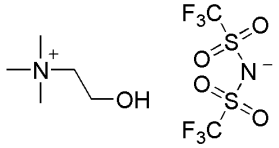

Figure 1.11 Structure of choline bistriflimide [Chol][Tf_2N].

Costa *et al.* continued the work on cholinium-derived bistriflimide ionic liquids, expanding to longer alkyl chains on the nitrogen atom ([N_{11n2}OH][Tf_2N]; n = 1, 2, 3, 4, and 5).[124] The ionic liquid/water systems have UCST behavior, the higher the alkyl chain length, the higher the UCST. The phase diagrams are almost symmetrical if the composition of the system is given in mass fraction (**Figure 1.12, right**). This means that at a given temperature the mutual solubilities of the IL in water and water in IL are similar if expressed in mass percentage. This symmetry is not preserved if the phase diagram is represented as a function of the mole fraction (**Figure 1.12, left**), since there is a large difference in molar mass between the ionic liquid and water.

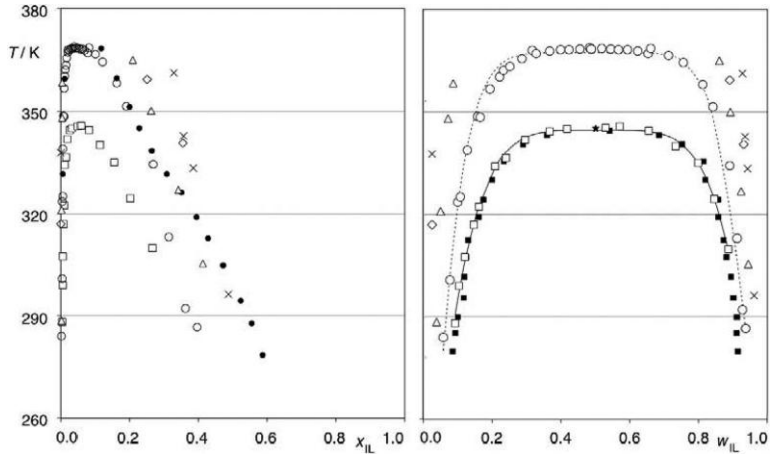

Figure 1.12 Phase diagrams showing the liquid-liquid equilibrium behavior of binary mixtures of $[N_{11n2}OH][Tf_2N]$. Left: mole fraction (x_{IL}), right: mass fraction (w_{IL}). Reprinted with permission from Costa *et al.*, copyright 2012 American Chemical Society.[124]

Another example are ionic liquid analogues of Girard's reagents (**Figure 1.13**), with bistriflimide anions that show UCST.[125] Not all ionic liquids showing thermomorphic behavior have fluorinated anions, examples are aqueous solutions of tetra-*n*-pentylammonium bromide (UCST at 136 °C at 0.3 MPa),[126] or tetra-*iso*-pentylammonium bromide (UCST at 96 °C at 0.1 MPa).[127]

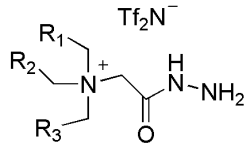

Figure 1.13. Structures of ionic liquid analogues of Girard's reagents.[125]

IL/water systems with LCST phase behavior

Ohno and co-workers discovered the first LCST type of phase changes in amino acid based ionic liquids (**Figure 1.14**).[128] Valine, leucine, *iso*-leucine and phenylalanine were chosen as starting materials, and all derived ionic liquids show the LCST-type phase behavior. The respective cloud point temperatures for the IL/water mixtures (50/50 by wt%) of 1.14a until 1.14d were 40, 25, 25, and 15 °C. In **Figure 1.15**, a photographical view on a typical cloud point determination is shown. Furthermore, in ionic liquids where the carboxylic acid residue on the anion was protected by a methyl ester group, no LCST-type phase separation was found. These results imply that free carboxyl

groups on the hydrophobic amino acid anions play a key role in the LCST-type phase separation.

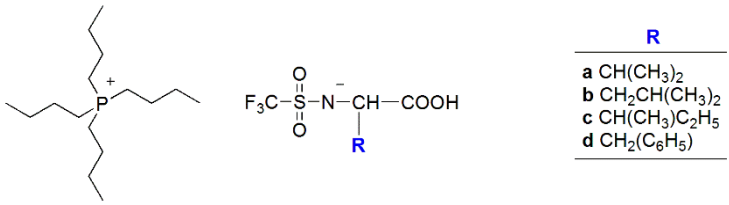

Figure 1.14 ILs which show LCST phase behavior, anions based on the amino acids a) valine, b) leucine, c) *iso*-leucine and d) phenylalanine.

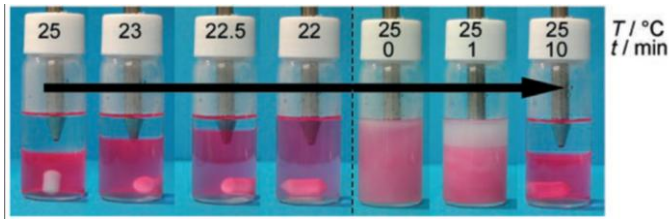

Figure 1.15 Temperature-dependence of the phase behavior of a $[P_{4444}][Tf\text{-}Leu]$/water mixture. The IL-phase was colored by Nile Red. Left: increase of water miscibility in the IL-phase with decreasing temperature. Right: turbidity of mixed IL/water mixture with settling until full phase separation after 10 min. Reprinted with permission from Fukumoto *et al.*, copyright 2007 Wiley.[129]

The tetra-*n*-butylphosphonium *N*-trifluoromethane sulfonyl leucine ($[P_{4444}][Tf\text{-}Leu]$)/water system is discussed further (1.3) as it was used for the extraction of proteins.[129,130] Both lysine- and aspartic acid-based amino acid ionic liquids $[P_{6668}][Lys]$ and $[P_{6668}][Asp]$ are fully water miscible, yet a mixture of both gives LCST phase separation in water.[131] The mechanism of this phase separation was studied by molecular dynamics (MD) simulations on the amino acid ILs. Hydrogen bonding between the $–NH_2$ or –COOH group of one anion with the –COO group of another anion was found. An increase of temperature strengthens this kind of hydrogen bonding interaction between anions whilst weakens the anion–water electrostatic interaction, leading to the LCST-type phase separation of the mixed ILs in water.[132]

Ohno and co-workers made ample contributions to this field and found that mostly phosphonium ionic liquids show LCST phase behavior with water. The LCST transition occurs in ILs that are on the border between hydrophilic and hydrophobic. The ionic liquid tetra-*n*-butylphosphonium trifluoroacetate, $[P_{4444}][CF_3COO]$, exhibits an LCST at 29 °C.[133] A total of 7 to 14 water molecules are present per $[P_{4444}][CF_3COO]$ ion pair, in the separated IL-rich

phase above the LCST, the number of water molecules in the IL-rich phase decreases with increasing temperature.[134] Investigation of density fluctuations indicated that the water molecules were largely localized near the critical point.[135] The $[P_{4444}][CF_3COO]$ molecules can form long-living aggregates in an aqueous solution of certain concentrations at temperatures below the LCST as identified by dynamic light scattering (DLS) measurements. Certain compositions of the $[P_{4444}][CF_3COO]$/water binary system display the physical characteristics of microemulsions, such as swelling behavior, solubilization capacity and tunable micropolarity, yet it is a surfactant-free microemulsion-like system.[136]

The larger and more hydrophobic tetraoctylphosphonium cation, $[P_{8888}]^+$ combined with polar phosphonate-derived anions ($(EtO)RPO_2$, R= CH_2OCH_3, CH_2OH, or NH_2) shows LCST phase behavior with water. Furthermore, these mixtures displayed thermo-reversible viscosity changes despite a large water content due to the occurrence of *rheopectic gelation* of the ionic liquid/water mixtures by external stimuli such as shear stress.[137]

IL/water systems with both UCST and LCST

Glasbrenner and Weingärtner reported an aqueous solution of tetra-*n*-butylammonium thiocyanate ($[N_{4444}]SCN$, T_m = 127 °C) that shows both UCST- and LCST-type phase transitions (**Figure 1.16**).[138]

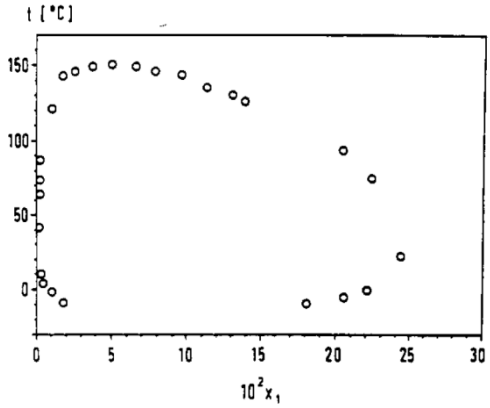

Figure 1.16 Liquid-liquid coexistence curve for tetra-*n*-butylammonium thiocyanate and water. x_1 being the mole fraction of the salt. Reprinted with permission from Glasbrenner *et al.*, copyright 1989 American Chemical Society.[138]

Aqueous solutions of tri-*n*-butyl-*n*-propylammonium iodide ($[N_{3444}]I$) represent a model system for investigating liquid-liquid phase transitions

driven by the hydrophobic effect of alkyl chains of organic cations in water (**Figure 1.17**).[139]

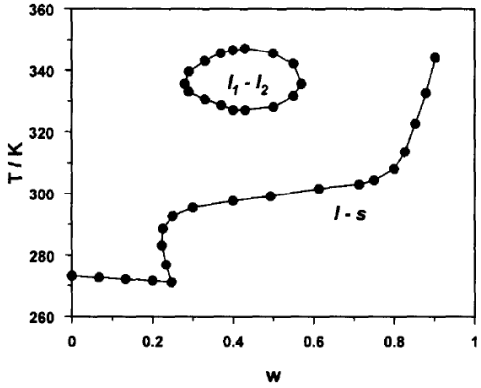

Figure 1.17 Phase diagram of the tri-*n*-butyl-*n*-propyl-ammonium iodide/water system. l_1-l_2 indicates the liquid-liquid miscibility gap, l-s the crystallization curve and w the weight fraction of the IL. Reprinted with permission from Kleemeier *et al.*, copyright 1997 Elsevier.[139]

Zwitterionic-type of ionic liquids contain the structure of both the cation and anion in one molecule. The advantage of these zwitterions is related to the fact that with mixing of different ionic liquids, undesired ion pairs can be formed due to anion exchange, sometimes with undesirable properties. Ammonium based zwitterions studied by Ohno and co-workers show both LCST and UCST type phase transitions after mixing with water in a very narrow temperature range (**Figure 1.18**).[140]

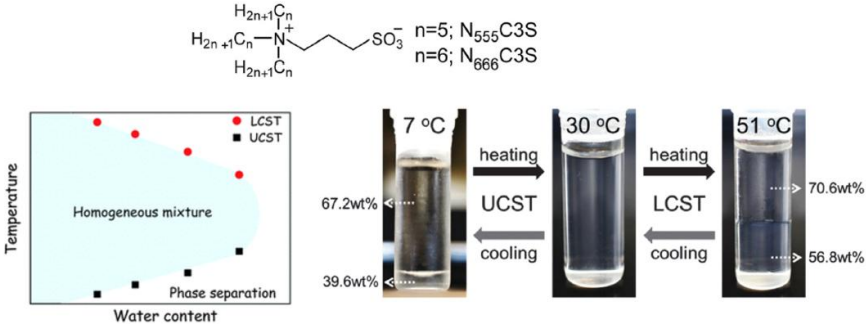

Figure 1.18 Top: structures of the ammonium based zwitterions, bottom left: representation of the phase diagram showing both LCST and UCST type phase transitions, bottom right: visual appearance of the water content of the mixture of $N_{555}C_3S$ and $N_{666}C_3S$ (0.67:0.33) and water (35 water molecules per zwitterion). Adapted with permission from Saita *et al.*, copyright 2014 The Royal Society of Chemistry.[140]

Fumarate and maleate tetra-*n*-butylphosphonium ionic liquids also show an exceptional case. They basically have the same anion, yet in a different *cis-trans* conformation. This conformation change has a significant impact on their solubility in water (**Figure 1.19**). Ohno and co-workers suggest that the low proton donor properties of the fumarate (*trans* conformation) are responsible for the low solubility of the IL in water. Fumarate anions also take part in intermolecular hydrogen bonding with other fumarate anions. With higher temperatures, these will be broken and the fumarate becomes hydrated. Investigation of the maleate (*cis* conformation) ionic liquid showed no intermolecular hydrogen bonding, yet an intramolecular hydrogen bond which led to delocalization of the negative charge and a resulting weakening of the electrostatic interaction with the cation. Raman studies on the interaction between water molecules and the ionic liquid showed water hydrated to $[P_{4444}]$[maleate] mainly on the CH and C=O moiety of the maleate anion.[141]

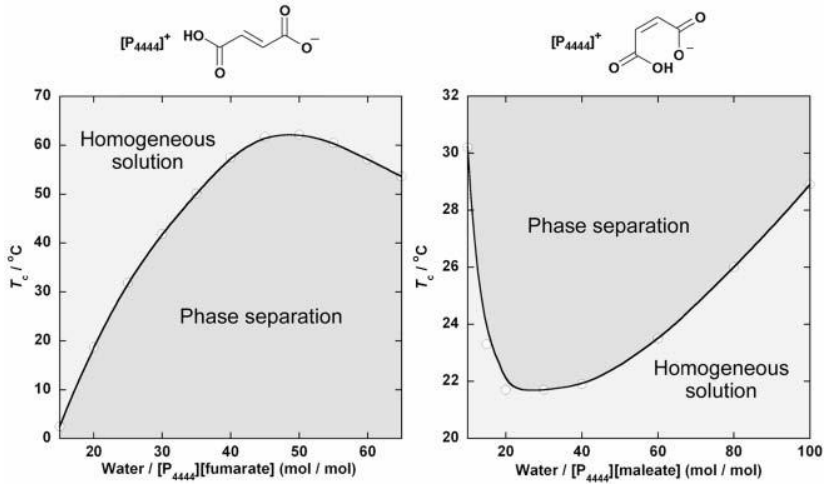

Figure 1.19 Water content dependence of cloud point temperature for tetra-*n*-butylphosphonium fumarate (left-showing UCST phase behavior) and tetra-*n*-butylphosphonium maleate (right-showing LCST phase behavior). Reproduced with permission from Fukaya *et al.*, copyright 2007 The Royal Society of Chemistry.[141]

1.2.5 Phase behavior of ionic liquid/organic solvent systems

ILs can have strong effects on chemical reactions and processes and are often used as catalysts in synthetic reactions.[21] Thus, the ability of the IL to interact with potential solvents is an important feature of its behavior.

IL/organic systems with UCST phase behavior

UCST phase behavior is the most common partial miscibility found in ionic liquid-organic solvent systems. Qiao *et al.* listed a high number of systems, which can be divided into two major classes: IL/alcohol and IL/hydrocarbon systems.[114] A limited number of systems is discussed here.

Like water, alcohols have a great ability to form hydrogen bonds, thus it comes as no surprise that these solvents also generate thermomorphic systems. In many binary systems of ILs with alcohols, the observations of the UCST were limited by the boiling temperature of the alcohol.[142] In imidazolium/alcohol systems, the effect on the UCST phase behavior of the alkyl chain length on the ionic liquid as well as type of alcohol was studied.[143–145] The UCST increases as the chain of the alcohol increases due to less interaction with the IL through hydrogen bonding, dipolar and Coulombic forces (**Figure 1.20, left**).[146] Increasing the alkyl chain length on the imidazolium from hexyl to octyl, the UCST of the system is significantly lowered (**Figure 1.20, right**). This decrease of the UCST with longer alkyl chains on the imidazolium is due to higher mutual solubilities because of higher dispersion interactions between the alkyl chain of the cation and the alcohol chain. An increase in UCST is noticed by replacing the acidic C2 hydrogen of the imidazolium to a methyl group, since this lowers the hydrogen bonding of the alcohol with the cation.[119] On the other hand, the introduction of alkoxy groups in the imidazolium increases hydrogen bonding opportunities with the solvent, resulting in an increase in solubility and lower UCST.[120] The hydrogen bonding acceptor capability of the alcohol is the most important parameter, alcohol solubility in ILs follows the order of alcohol branching: tertiary > secondary > primary, correlated with the relative basicity of the alcohols.[114] Not only cation and alcohol affect the phase behavior, also the anions' affinity towards the alcohol was largely studied. The trend observed was: $[N(CN)_2]^-$ > $[CF_3SO_3]^-$ > $[Tf_2N]^-$ > $[BF_4]^-$ > $[PF_6]^-$, an increase in the hydrogen bond strength between the anion and the alcohol results in higher mutual solubilities and a lower UCST.[143]

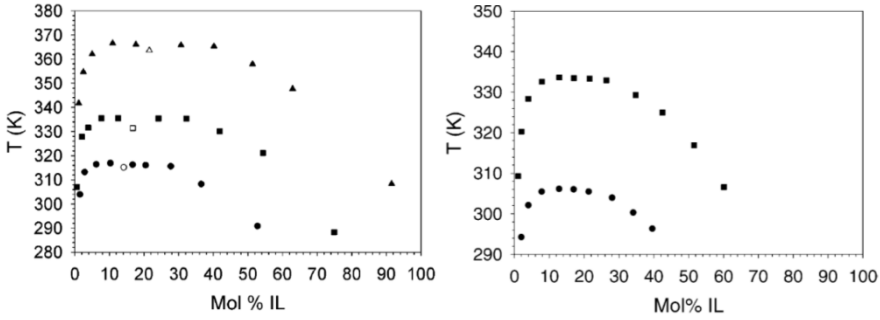

Figure 1.20 Left: Phase diagram for $[C_4mim][BF_4]$ with 1-propanol (●), 1-butanol (■) and 1-hexanol (▲). Right: Phase diagram for $[C_8mim][Tf_2N]$ (●) and $[C_6mim][Tf_2N]$ (■) with 1-octanol. Reprinted with permission from Crosthwaite *et al.*, copyright 2004 American Chemical Society, copyright 2005 Elsevier.[143,144]

Domańska *et al.* reported numerous ionic liquid phase equilibria studies, including IL/hydrocarbon binary systems.[147–153] For example, $[C_2mim][PF_6]$ and $[C_4mim][PF_6]$, were investigated in different aromatic hydrocarbons (benzene, toluene, ethylbenzene, *o*-xylene, *m*-xylene, *p*-xylene), in different *n*-alkanes (pentane, hexane, heptane, octane), and in two cyclohydrocarbons (cyclopentane, cyclohexane). The ionic liquids can act both as hydrogen-bond acceptor ($[PF_6]^-$) and donor (cations), thus can interact with solvents which have both accepting and donating sites, the aromatic hydrocarbons are known to form n-π interactions. The liquid-liquid phase diagrams for the mixtures under study exhibited UCST phase behavior of which the observation was limited by the boiling temperature of the solvents. The increase in the chain length of the alkyl substituent at the imidazole ring from $[C_2mim]^+$ to $[C_4mim]^+$ lowers the UCST, the temperature of the miscibility gap increases with an increase of the alkyl chain length of the *n*-alkanes for $[C_4mim][PF_6]$.[148]

IL/organic systems with LCST phase behavior

Critical behavior of ionic solutions in common solvents mainly show upper critical solution temperatures, examples with LCST are scarce. LCST behavior of $[N_{4444}]Br$ in toluene with a nearly closed miscibility loop was reported by Dittmar and Schröer.[154] Cholinium-based ILs were further researched by Costa *et al.* in their mutual solubility with different ethers.[155] Higher LCST values were obtained with longer alkyl chains on the cholinium cation.

In the $[C_4mim][SCN]$/thiophene system, the specific spatial orientation of the sulfur atom of the anion with the thiophene protons was suggested to be

responsible for the LCST behavior.[156] Also the binary equilibria of $[C_2mim][Tf_2N]$ and $[C_4mim][Tf_2N]$ with fluorinated benzenes[157] and amines (diethylamine and triethylamine)[158] have been discussed in literature as examples of lower critical solution phase behavior.

IL/organic systems with both UCST and LCST

Lachwa *et al*. have discovered IL/organic solvent systems that present a high temperature LCST plus a closed-loop $[LCST_1 < UCST < LCST_2]$ in $[C_mmim][Tf_2N]$/chloroform binary systems (**Figure 1.21 I**). By mixing $[C_4mim][Tf_2N]$ and $[C_5mim][Tf_2N]$ in different compositions with chloroform, this extraordinary kind of phase diagram was discovered. The addition of CCl_4 in a quasi-binary system $[C_5mim][Tf_2N]/(CHCl_3 + CCl_4)$ illustrates a case of an LCST at a temperature higher than that of the UCST (**Figure 1.21 II**).[159] Examples showing both UCST and LCST with organics are scarce, the only other case is found in $[C_{10}mim][Tf_2N]$/benzene.[160]

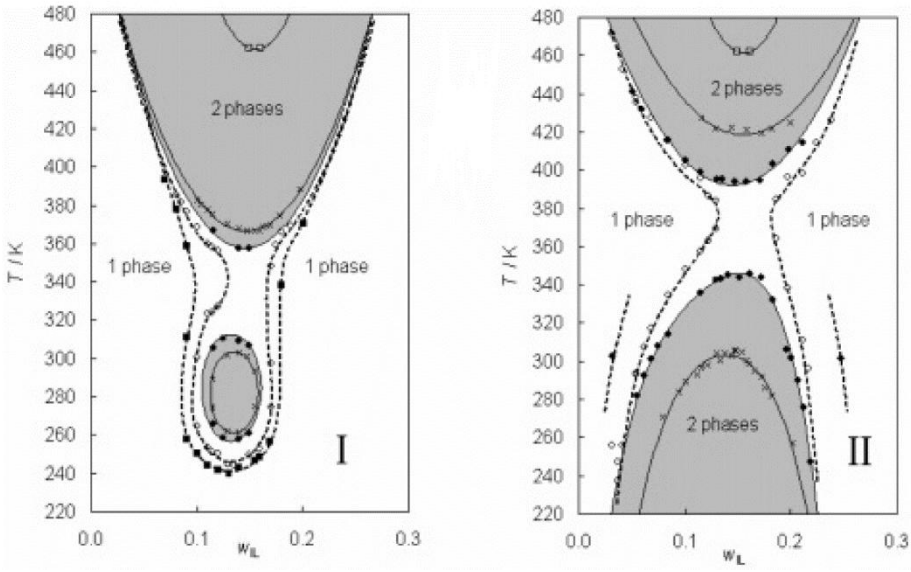

Figure 1.21 I Phase diagram of $[C_mmim][Tf_2N]$ + $CHCl_3$ (□) m = 5.000; (×) m = 4.337;(●) m = 4.330; (○) m = 4.320; (■) m = 4.300. The shaded areas depict the demixing regions for m = 4.330; **II** phase diagram for $[C_5mim][Tf_2N]/(CHCl_3 + CCl_4)$ for different concentrations of CCl_4, c is the weight percentage ratio of CCl_4 in $CHCl_3$ (□) c = 0%; (×) c = 6.5%; (●) c = 7.6%; (○) c = 8.0%; (◆) c = 10.5%. The hatched areas depict the demixing regions for c = 7.6%. w_{IL} is the weight fraction of IL (nominal pressure of 1 bar). Reprinted with permission from Lachwa *et al.*, copyright 2005 American Chemical Society.[159]

1.2.6 Factors that affect phase behavior

Solvents

Most definitely, the solvent and the type of IL play the key role in phase behavior. It could be observed from the IL/water and IL/organic systems that the effect of the cation alkyl chain length on the phase behavior is opposite. In IL/water system, longer alkyl chain lengths decrease the mutual solubility (*e.g.* higher UCST) whilst in IL/organic systems the mutual solubility of IL and solvent increase with longer alkyl chain lengths (*e.g.* lower UCST). In solvent systems with a high dielectric constant ε (*solvophobic systems*), hydrogen bonds and hydrophobic interactions are the driving forces for phase transitions. In media with a low dielectric constant (*Coulombic systems*), the Coulombic forces are much stronger and the responsible actors for the phase separation.[161] Binnemans and co-workers reported a predictive model for the phase behavior of ILs based on the charge density (hydration) of the IL anion (**Figure 1.22**).[22] In IL/water biphasic systems, ILs with poorly hydrated (low charge density) anions (such as bis(trifluoromethylsulfonyl)imide or iodide), UCST phase behavior is found, whilst the incorporation of more strongly hydrated (high charge density) anions (chloride or trifluoroacetate), the systems show LCST phase behavior. A reversal of these observations is found in IL/apolar solvent systems, because the hydrophobic anions have a higher affinity for the solvent.

	weakly-hydrated IL anion (e.g. Tf_2N^-, PF_6^-, BF_4^-)	**highly-hydrated IL anion** (e.g. Cl^-, Br^-, CF_3COO^-)
polar solvent	**UCST**	**LCST**
apolar solvent	**LCST**	**UCST**

Figure 1.22 Prediction model for rational design of ILs with UCST or LCST phase behavior. Reprinted with permission from Dupont *et al.*, copyright 2015 American Chemical Society.[22]

Of course, the cloud point temperature can be tuned by changing the composition of the phases, as evident from the phase diagrams. Yet, different additives affect the thermomorphic systems. Although technically speaking, from the moment additives are added, the binary system is lost, the effects of metal salts and organics on IL/water systems are an important issue in view of the application to separations.

Salts in aqueous solutions

As early as 1888, Hofmeister investigated the effect of metal salts on the solubility of the protein ovalbumin in aqueous solutions, leading to the so-called *Hofmeister series* which ranks the ions from salting-in to salting-out, whether the dissolution of the compound is promoted or has the effect of excluding the solute from solution.[162] Adding metal salts to a homogeneous aqueous solution of two components may induce the coexistence of two separate phases, in this particular case, and the formation of an *aqueous biphasic system* (ABS) (discussed in 1.2.7). The effect of metal salts on the phase behavior of thermomorphic ionic liquids differs whether the system has LCST or UCST phase behavior. In **Figure 1.23**, a series of salting-in and salting-out anions and cations for ionic liquids is illustrated.[22] It should be mentioned that this series corresponds to the Hofmeister series, yet has a reversed cation series since Hofmeister established his series with a negatively charged protein. The salting-in salts improve mutual solubility of the phases and thus favor the homogeneous solution. In UCST systems, the cloud point curve descends to lower temperatures. On the other hand, in LCST systems, the biphasic mixtures are reached only at higher temperatures. Salting-out salts diminish the mutual solubility and favor the demixing of the phases. This increases the cloud point temperatures in UCST systems,[163] but a decrease is noticed in LCST systems. Both the cation and anion of the salt affect the phase behavior, yet the salt anion has the largest effect due to the poorer solvation of anions in water compared to cations.[164] For example, the addition of cesium nitrate to the triethylamine/water system slightly reduces the LCST with 2 °C, even though the Cs^+ is a strong salting-in cation.[165]

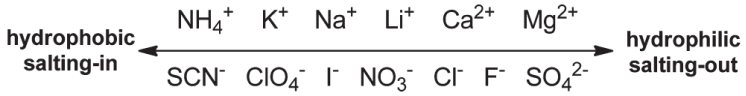

Figure 1.23 Salting-in/salting-out series for uncharged molecular solvents and ionic liquids. Reprinted with permission from Dupont *et al.,* copyright 2015 American Chemical Society.[22]

Ohno and co-workers also evaluated the effect of the addition of ionic liquid 'salts' on the LCST of $[P_{4444}][CF_3COO]$. The addition of water-soluble ILs, $[P_{4444}]CH_3SO_3$, $[P_{4444}]Cl$, $[P_{4444}]Br$, $[P_{4444}]NO_3$, and $[P_{4444}][TsO]$ increased the cloud point temperatures in respect to these of the $[P_{4444}]CF_3COO$/water mixture. Water-immiscible ionic liquids $[P_{4444}]BF_4$, $[P_{4444}]CF_3SO_3$ and

$[P_{4444}][Tf_2N]$ caused lowering of the LCST. The added ionic liquids will be present in the IL-rich phase rather than the aqueous phase, so the IL cannot be evaluated based on salting-in or salting-out effect since the water structuring is not influenced. The ILs only affect the hydrophilicity or hydrophobicity of the $[P_{4444}][CF_3COO]$-layer. This temperature-sensitive LCST-type phase transition of the IL/water mixtures was used as a simple system for listing decreasing hydrophilicity of target anions: $[CH_3SO_3]^-$ > Cl^- > Br^- > $[TsO]^-$ > NO_3^- > $[CF_3COO]^-$ > $[BF_4]^-$ > $[CF_3SO_3]^-$ > $[Tf_2N]^-$.[166]

Organics in aqueous solutions

The addition of an apolar organic to an aqueous solution of two mutually miscible solvents can induce partial miscibility, in the *ternary system*. To introduce the concept, the ternary phase diagram of a system of ethanol, benzene, and water at 30 °C and 1 bar is given in **Figure 1.24**.[167] In the area labeled P = 1, a homogeneous mixture is formed of which the composition is described by the position of the point. The one-phase area extends to the sides of the triangle representing binary mixtures of ethanol/benzene and ethanol/water, as ethanol and benzene mix in all proportions, and so do ethanol and water. In the area labeled P = 2, two separate liquid phases are present. The determination of the compositions of the phases is done via the tie lines which must be determined experimentally. Numerous examples of ternary systems for common solvents are found in literature.[168–173] Also the research on ionic liquid- ternary systems is plentiful.[174–178] Ternary systems of hydrophilic ionic liquids with water and salts form aqueous biphasic systems, as discussed in the next subchapter.

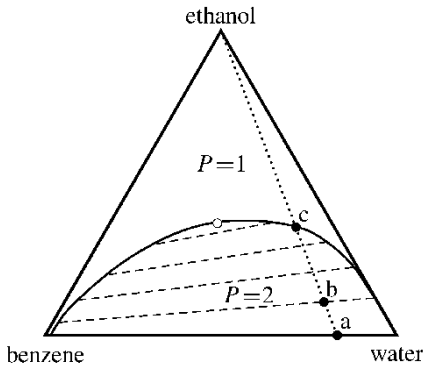

Figure 1.24 Ternary phase diagram of ethanol, benzene and water (30 °C, 1 bar).

Reprinted with permission from Brandani *et al.,* copyright 1985 American Chemical Society.[167]

1.2.7 Aqueous Biphasic Systems

Since reviews on the topic of aqueous biphasic systems and IL-based aqueous biphasic systems exist,[179,180] this subject will only be shortly introduced here. Conventional *aqueous biphasic systems* (ABS) or *aqueous two-phase systems* (ATPS) are polymer-polymer, polymer-salt, and salt-salt systems.[181] The two components are water-soluble, yet two separate phases are formed above a certain concentration. One of the aqueous phases will be enriched in one of the components, while in the other phase, prevalence for the second component is obtained. ABS has been extensively used for separation and analytical studies of biomaterials,[182] in the recovery and purification of proteins and nucleic acids,[181,183] and for the preconcentration of solutes from small samples of metal chelates and porphyrins.[184,185] The number of examples for extraction of metal ions with the aqueous two-phase systems is limited[186–189] and can be described by three different categories of ABS: 1) extraction using a water-soluble extractant; 2) extraction of metal ions as metal complexes with inorganic anions and 3) extraction by the polymer-rich phase.[190]

In an IL-based ABS, the aqueous solution of an ionic liquid undergoes liquid-liquid demixing upon addition of a salting-out agent.[191] The salting-out agent chemically induces phase separation with the formation of a binary system consisting of an IL-rich phase and a salt-rich phase. This phase separation is a *composition induced phase separation* (CIPS). **Figure 1.25** depicts both a ternary phase diagram for an IL-based ABS and its orthogonal representation. The graphs can be read in the following way: for the ternary phase diagram, all mixtures with compositions below the binodal curve (A–B–C–D) will phase separate, while those above the line form a single homogeneous phase. At point C, the critical point, the biphasic system ceases to exist. For a mixture with composition M under the binodal curve, the compositions of each separate phase formed is read by following the specific tie-line to its end-points (nodes) B and D. The orthogonal representation, where the water concentration is omitted, is the tool mostly used to depict ABS in the literature. Here, mixtures with compositions above the binodal fall into the biphasic regime, whereas mixture compositions below the binodal form homogeneous solutions.[180]

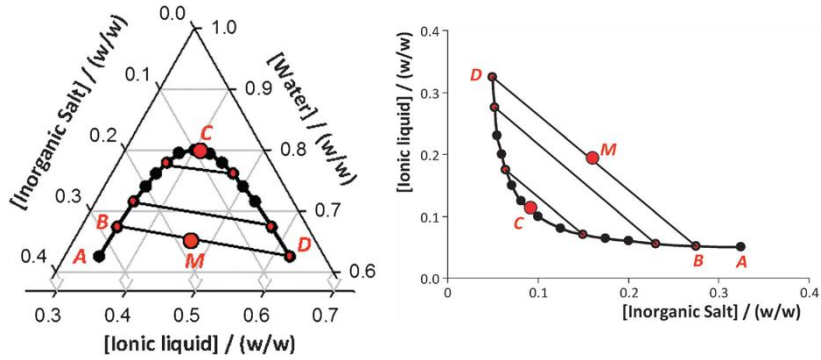

Figure 1.25 Left: ternary phase diagram of IL-based ABS, right: orthogonal representation. Reproduced with permission from Freire *et al.*, copyright 2012 The Royal Society of Chemistry.[180]

The miscibility of the ionic liquid is controlled by the salting-out agent, which is essential for separation technologies. Both the anions' and cations' ability to induce the salting-out of the ionic liquid closely follows the Hofmeister series.[162,192,193] As mentioned above, in the Hofmeister series, two types of salts can be defined: salting-out salts (kosmotropic salts or kosmotropes) and salting-in salts (chaotropic salts or chaotropes). The ionic *kosmotropes* tend to be small with high charge density and well hydrated ions, they have a water-structuring ability. *Chaotropes*, on the other hand, are the large and low charged salts which have poorly hydrated ions that have a water-disrupting ability. In this fashion, the phase behavior of IL-based ABS and conventional electrolytes was explained, based on the Gibbs free energy of hydration of the salt ions.[194] However, recent studies demonstrate that bulk water structure is not central to the Hofmeister effect.[180,193,195,196] Instead, it was shown that the magnitude of the salting-out effect correlates with the molar entropy of hydration of the ions, which means that the salting-out by inorganic salts from aqueous media is driven by an entropic process resulting from the formation of water-ion complexes. It is the interaction of water with the salt ions and the consecutive formation of hydration complexes, which further cause the dehydration of the ionic liquid ions, which rules the formation of IL-based aqueous biphasic systems.

Not only CIPS, also *temperature induced phase separation* (TIPS) is found in IL-based ABS, these systems can thus be considered thermomorphic.[180,197–200] The IL-based ABS open the door to a new, greener solvent extraction system. IL-based ABS have been mainly used in the extraction of biomolecules and

other added-value compounds.[180,201] ABS also offers an alternative approach for the removal and recovery of ionic liquids from aqueous media.[180,202] Few examples are reported on the use of IL-based ABS for metal extraction. Akama *et al.* described an aqueous two phase systems with tetrabutylammonium bromide, for the extraction of cadmium and chromium(VI).[202,203] Binnemans and co-workers separated Co(II) and Ni(II) using a $[P_{44414}][Cl]/NaCl/H_2O$ ionic liquid-based aqueous biphasic system.[196]

It must be noted that in this PhD thesis, an IL-based ABS is a three component system: a hydrophilic IL, a salting-out salt and water. In the literature, other definitions are possible, this topic is discussed further (1.3.1). An IL-based ABS for metal extraction is introduced in Chapter 7.

1.2.8 Other triggers

To conclude the discussion on phase behavior, other triggers than temperature to induce the phase-switching feature are investigated. In CIPS (*composition induced phase separation*), a homogeneous solution is formed by mixing a primary solvent with a solute, the addition of a secondary solvent induces the phase separation.[205] CIPS can be performed with pH variation, ion-pair formation and by salting-out with inorganic salts or organic solvents. In polymer systems, besides the TIPS (*temperature induced phase separation*) and CIPS (composition induced phase separation) which are evident, also SIPS (*solvent induced phase separation*) and NIPS (*non-solvent induced phase separation*) are possible phase separation processes.[206]

The $[P_{4444}]$[Tf-Leu]/water system shows a reversible phase transition of the LCST type by bubbling CO_2 and N_2 through the mixture. This phase change is driven by a slight pH change in the mixture.[207] pH-Dependent phase behavior was also found with a biphasic mixture of [Hbet]$[Tf_2N]$ and water. In alkaline environment (by the addition of a solution of the alkali-metal hydroxide LiOH, NaOH, or KOH), a homogeneous phase is obtained, because the alkali metal salts of betaine bis(trifluoromethylsulfonyl)imide are water soluble. Acidification of the solution regenerated the hydrophobic [Hbet]$[Tf_2N]$ ionic liquid and phase separation occurred.[94]

1.3 Application of ILs in Solvent Extraction

The potential of ionic liquids is unlimited and in recent years, there has been an explosion of interest in applications of ionic liquids. The innovative uses of ionic liquids span a large variety of fields, of which the most important applications are listed in **Table 1.1**. Most commonly, ionic liquids are used as solvents, in particular for organic synthesis,[1] but also in separation processes.[17] Ionic liquids are also of high importance for catalytic applications.[7] IL-based chemical processes are expected to revolutionize the chemical industry in the future.[18] In this PhD thesis, only the application of separations via solvent extraction is introduced.

Table 1.1 Applications of ionic liquids.

Field	Applications	Reference
Analytics	Matrices for MS, GC columns, stationary phases HPLC	208
Solvent chemistry	Synthesis, multiphase reactions and extractions, microwave chemistry, dissolution of polymers	21,209,210
Catalysis	Hydrogenation and rearrangement reactions, cleavage reactions, coupling reactions	2,6–10,211
Engineering	Coatings, surfactants, lubricants, plasticizers	212,213
Physical chemistry	Thermodynamics, high refractive index fluid, binary and ternary systems, heat storage	114,214,215
Electrochemistry	Electrolyte, metal plating, solar panels, batteries, fuel cells, electro-optics, ion propulsion	15,16,216
Biological issues	Biomass processing, biocides, bioseparations	12–14
Pharmaceutical	Drug delivery, personal care, embalming	18,19
Food industry	Natural compounds, food analysis, extraction, additive as antimicrobial and enzymatic activity enhancer	217
Separations	Metal extraction, gas absorption and separation, protein separation	17,130,218,219

The concept of a solvent extraction procedure is simple, a solute containing feed solution is contacted with a solvent to which the solute will be extracted. The solvent/feed mixture is normally immiscible, but it may be partially miscible. The basis of this technique is the preferential distribution of a solute between two phases. Generally, the feed is an aqueous solution containing the dissolved solute brought into contact with an immiscible organic phase. The solute distributes between the two phases until equilibrium is reached. This equilibration is accelerated by strong agitation (stirring or shaking) in case of mutually immiscible phases, to increase the phase boundary area between the organic and aqueous phase at which diffusion of the solute occurs.[220]

Specific extractants can be designed to achieve certain selectivity to a certain metal ion, showing the great versatility of solvent extraction as a separation technique. Three main groups of extractants are distinguished, representing different extraction mechanisms (**Figure 1.26**).[220,221] The acidic extractants work via a cation exchange mechanism, examples are carboxylic acids (*e.g.* Versatic acid 10), acidic organophosphorus extractants (*e.g.* DEHPA) or chelating extractants (*e.g.* β-diketonates). Neutral extractants extract via a solvating mechanism, typical examples are TBP, TOPO and Cyanex® 923. An anion exchange mechanism is found for basic extractants like protonated mono-, di- or tri-alkyl amines and phosphines or quaternary ammonium or phosphonium salts (*e.g.* Aliquat® 336 or Cyphos® IL 101).

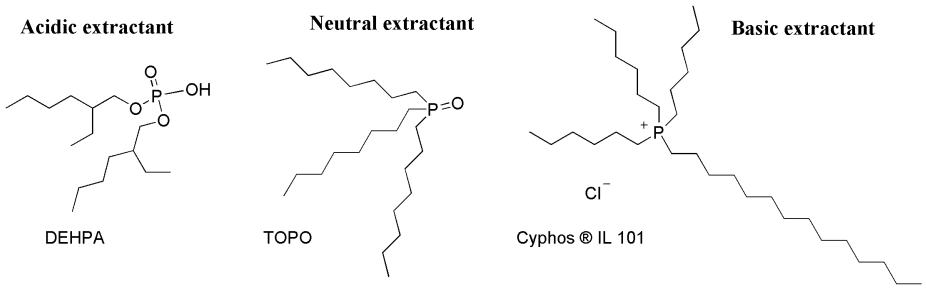

Figure 1.26 Examples of common extractants. Left: bis(2-ethylhexyl)phosphoric acid (DEHPA), middle: trioctylphosphine oxide (TOPO), right: trihexyltetradecylphosphonium chloride (Cyphos® IL 101).

Solvent extraction is then usually carried out by dissolving these extractants in an organic solvent and contacting it with the metal-containing aqueous phase.[220] The volatility of organic solvents such as kerosene and toluene (VOCs) poses safety and environmental threats. The negligible vapor pressure and low flammability of ionic liquids make them excellent alternatives.[222] Moreover, ILs are electrically conductive, so they are electrostatically safer since sparks caused by static electricity cannot be created.[223] The water-immiscible ILs have been used as solvents in conventional ionic liquid solvent extractions, both undiluted or due to the high viscosity of ILs, diluted in another solvent.[35,36,38,39,224–228]

1.3.1 Solvent extraction with partially miscible ionic liquids

The solvent is the heart of the solvent extraction process, and as said before solvent and feed solution can be immiscible or partially miscible. In the literature, different terms can be found that describe separation processes based on liquid-liquid extraction using mixtures with a critical point of miscibility. The most straightforward term is *homogeneous liquid-liquid extraction* (HLLE),[229,230] clearly indicating the homogeneous phase formed at the operational temperature. Other terms used are: *phase transition extraction* (PTE),[98,231] *coalescence extraction* (CE)[205,232–235] or TIPS, extraction via *temperature induced phased separation*.[236] The principles are the same, in a liquid mixture, a homogeneous phase is formed by heating above the critical temperature (in case of UCST). Next, the mixture is cooled again to the region below the miscibility curve to induce the phase separation.

Replacing conventional isothermal liquid-liquid extraction by the HLLE grants faster kinetics to the extraction and inhibits the formation of stable emulsions.[98,205,232] As explained before, a phase diagram can be divided into two regions (**Figure 1.2**): a metastable region and an unstable region. In the metastable region, classical nucleation theory is followed. Phase separation starts when the activation energy or critical droplet size is exceeded.[237–239] On the other hand, in the unstable region, there is no energy activation barrier to overcome. Even the smallest concentration fluctuations can cause the phase separation, the spinodal decomposition process. The time scale for spinodal decomposition is very small for fluids.[205] In HLLE, this spinodal decomposition is also the actor that induces phase separation as large temperature or composition differences are applied, hence the fast kinetics of

the process. Stable emulsions are caused by the adsorption of emulsion stabilizing particles to the phase boundary, yet no well-defined boundaries are formed during spinodal decomposition, so emulsions cannot be established.[98] In HLLE, extraction occurs in the homogeneous phase so strong agitation is not necessary, since mixing occurs at a molecular level.

Other, yet similar extraction techniques also exist, for example, by the use of microemulsions as solvent media for metal extraction. The microemulsion is formed spontaneously by two immiscible liquids, a surfactant and occasionally a short-chained alcohol as co-surfactant. The surfactant dissolves in the liquids after sonication yielding a clear and transparent phase. To this microemulsion phase, an aqueous metal feed solution is then added for the so-called *microemulsion extraction* (MEE).[240–244] Similarly, a sample pre-treatment liquid-liquid microextraction technique called *dispersive liquid-liquid microextraction* (DLLME), induces a cloudy solution by the addition of a dispenser which induces phase separation to a mixture of aqueous feed solution and an organic solvent. An organic or biological solute will be extracted to the organic phase, with or without the help of an extractant and the sedimented organic phase is separated by centrifugation.[245,246] In addition, *temperature-controlled ionic liquid dispersive liquid-liquid microextraction* was designed, based on the temperature change making the IL completely disperse in the aqueous phase. By cooling, the IL containing the target molecule was concentrated into one drop.[247,248] *Micelle-mediated extraction* (MME) is another specific technique that uses temperature as the trigger to induce phase separation. Here, a surfactant and a chelating agent are added to an aqueous metal feed solution. Micelles are created by the surfactant and the chelating agent forms a hydrophobic complex with the metal ions which become entrapped in the hydrophobic environment of the micelles. Via a temperature increase, two separate phases are formed, and the surfactant-rich phase containing the metal ions can be isolated. This micelle-mediated extraction is often also labeled with the term *cloud point extraction* (CPE), and is frequently applied to preconcentrate metal ions previous to analytical determination.[249,250] Confusingly, in analytical chemistry, CPE technology also is the procedure based on the phase separation, which occurs in aqueous solutions of non-ionic surfactants when heated above the so-called cloud point temperature. Again, different terms can be identified to designate the same process, as this technique is mainly addressed as homogeneous liquid-liquid extraction for preconcentration as well.[251] The HLLE technique is a simple

and powerful preconcentration method that reduces reagent consumption, extraction time, cost of analysis and the exposure to the organic solvents.[252] All terms used for describing separation processes based on liquid-liquid extraction using mixtures with a critical point of miscibility are summarized in **Figure 1.27**.

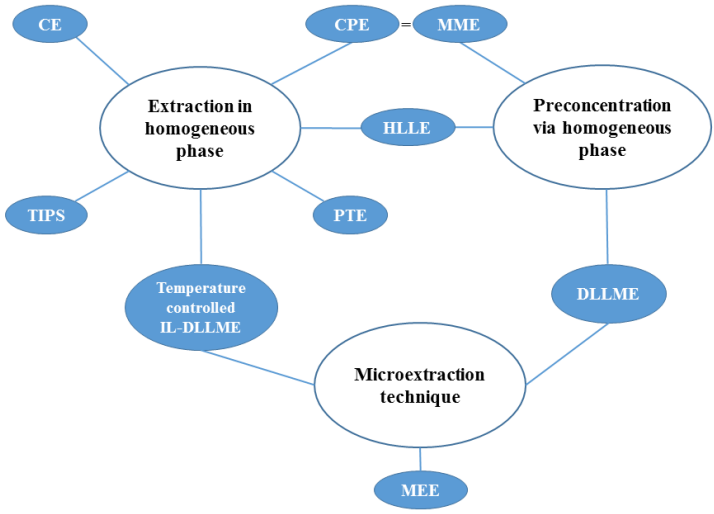

Figure 1.27 Summary of techniques describing separation processes based on liquid-liquid extraction using mixtures with a critical point of miscibility.

In the remainder of the subchapter, the term homogeneous liquid-liquid extraction (HLLE) will be used. HLLE using ionic liquids as a solvent extraction tool is discussed for biological and organic molecules and for the separations of metal ions. Examples of all three types of applications are investigated here, with the focus on the HLLE for metal ion extraction.

Biomolecules

Ohno and co-workers made seminal contributions to the extraction of biomolecules by ionic liquids with LCST phase behavior. A 1:1 w/w mixture of tetra-*n*-butylphosphonium *N*-trifluoromethanesulfonyl leucine ([P_{4444}][Tf-Leu])/water starts to phase separate at 22 °C. At 25 °C, two distinct clear phases were observed. A change of temperature of a few degrees induced LCST-type phase behavior, making this system suitable for the extraction of biopolymers such as proteins. The system [P_{4444}][Tf-Leu]/water could extract the protein cytochrome c (cyt. c) (**Figure 1.28**). The IL-phase contained 21 wt% of water after phase separation. The hydrated IL could also extract the proteins lysozyme, chymotrypsin, hemoglobin, albumin and myoglobin.[130,134]

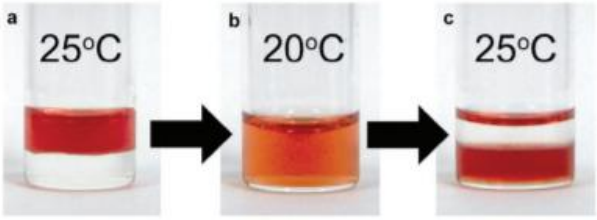

Figure 1.28 Extraction of cyt. c from aqueous to [P_{4444}][Tf-Leu] phase by changing the temperature. A) cyt. c in aqueous phase (red color) b) homogeneous phase after cooling to 20 °C c) temperature increase to 25 °C phase separation occurs, cyt. c in IL phase. Reproduced with permission from Kohno *et al.*, copyright 2011 The Royal Society of Chemistry.[130]

Organic molecules

Dyes are used in the textiles and leather industry, producing large amounts of wastewater containing disperse dyes. The treatment of this waste is a challenge because of the dyes' low water solubility and high capacity to form suspensions.[253,254] Ionic liquids are ideal solvents for these types of solutes that are ionizable but nonetheless hydrophobic in nature. Dyes color the ionic liquid phase and are therefore commonly added to thermomorphic mixtures to clearly show phase boundaries, like the Nile Red in **Figure 1.15**. Nockemann and co-workers used ionic liquid analogues of Girard's reagents, shown in **Figure 1.29**, to extract Rhodamine B. These types of ILs show UCST phase behavior and could be utilized in homogeneous liquid-liquid extraction. After heating an aqueous solution of Rhodamine B with [N_{222}hcm][Tf_2N] to 60 °C, the phases merged. Upon cooling, the dye had been completely transferred to

the ionic liquid phase. The extraction mechanism is presumed to be the interaction of the carboxylic acid functionality on the Rhodamine B with the hydrazide group of the ionic liquid. Also methyl red or fluorescein dyes could be extracted via this method from water to most of the described ionic liquids.[125] Also other groups have reported on the transfer of dyes from water into different classes of ionic liquids via a temperature-controlled mechanism.[254–256]

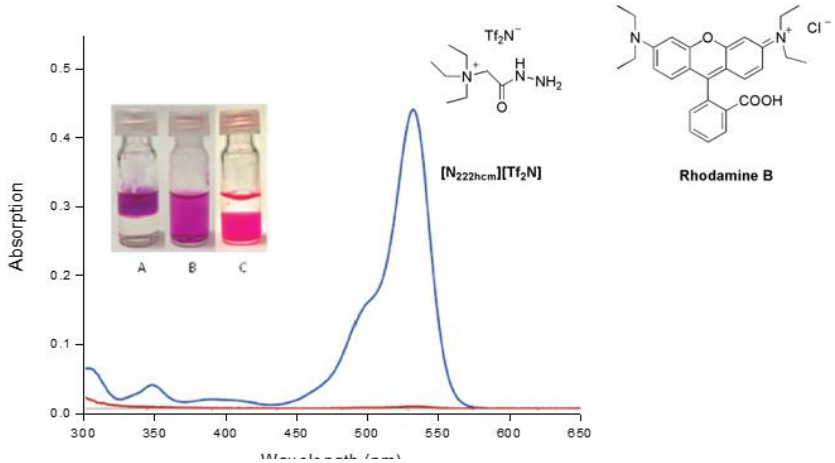

Figure 1.29 Electronic absorption spectra of an aqueous Rhodamine B solution before (blue) and after (red) contact with $[N_{222}hcm][Tf_2N]$. The photographs (inset) illustrate the extraction process: A) colored aqueous top phase with Rhodamine B before heating, B) homogeneous phase after heating to 60 °C, C) cooling phase separates the mixture, Rhodamine B is in the bottom IL phase. Adapted with permission from Blesic *et al.*, copyright 2014 The Royal Society of Chemistry.[125]

Metal ions

Critical metals are economically important metals with a high supply risk.[257] The shortage of these metals can be tackled by investments in primary mining, research for the substitution of the critical elements in their applications and the development of recycling schemes.[258] New technologies are being developed in order to maintain supplies of critical metals, in particular for rare-earth elements (REEs), as they are becoming essential for high-tech applications.[224,259] Ionic liquid design can provide new innovative solutions to the recycling of critical metals from end-of-life products. A key aspect in the design of these recycling processes is ensuring a low or even zero waste valorization scheme.[258] Not only are ionic liquids not emitted into the air, causing less pollution than VOCs, they can also be recycled after extraction. Many studies exist on the conventional solvent extraction of metal

ions with ionic liquids.[35,36,38,39,224–228] In what follows, the use of thermomorphic systems in homogeneous liquid-liquid extraction of metals is discussed.

In 1972, Murata *et al.* introduced the concept of homogeneous liquid-liquid extraction for the extraction of Fe(III) with thenoyl trifluoroacetone from a water/propylene carbonate mixture having an UCST of 73 °C.[229] By using HLLE, much faster reaction kinetics were obtained, also in the extraction and separation of uranium from other fission products.[260] HLLE towards dinitrile organic phases has been reported for the extraction of Pb(II) and Sr(II),[233,235] a broad range of alkali, alkaline earth and some transition metals.[234,261] Billard extensively reviewed the literature on ionic liquid based ABS for metal extraction.[262] As noted before, an IL-based ABS is a three component system: a hydrophilic IL, a salting-out salt and water. Yet, in this review, the author chose to add to this definition, systems displaying either an UCST or LCST. Indeed, for the application of metal extraction with thermomorphic systems, the addition of extra components as common salts, salts to be extracted (metallic salts), extracting agents, mineral acids are required, hence the term IL-ABS. Yet, for clarity, in this PhD thesis, the term 'IL-based ABS' will only be used when meaning the induction of a two phase system by the addition of a salting-out salt to an aqueous solution of an ionic liquid. The thermomorphic systems used for homogeneous liquid-liquid extraction of metal ions discussed in this subchapter are not labeled as IL-ABS.

Our group made several contributions to the field of ionic liquid homogeneous liquid-liquid extraction for metal ions.[229,230,260,263–266] Before the publication of the HLLE system with the ionic liquid [Hbet][Tf_2N], only one example of temperature induced phase separation with ionic liquids was described. Vaezzadeh *et al.* exploited the HLLE of Ag(I) by a mixture of [C_6mim][BF_4], water, the complexing agent 4,4-bis(dimethylamino) thiobenzophenone and $NaPF_6$. A temperature decrease below 50 °C induced phase separation with silver concentrated in the ionic liquid phase.[267] However, as repeatedly acknowledged, the use of tetrafluoroborate and hexafluorophosphate should be avoided due to hydrolysis in contact with water.[118]

Let us consider the [Hbet][Tf_2N]/water system in detail. The binary mixture [Hbet][Tf_2N]/water has an UCST of 55.5 °C.[94] Although this thermomorphic phenomenon is acknowledged by Ikeda and co-workers, in their extraction of U(VI), Pd(II), Rh(III) and Ru(III) with the system, they did not take advantage of it.[268,269] Performing extractions above the UCST accelerates the kinetics of the extraction, yet no thermodynamical enhancement in the percentage extraction (*%E*) and distribution ratio (*D*) values is seen. The [Hbet][Tf_2N]/water system can extract Sc(III) and Fe(III) as observed in a study by Onghena *et al.*[266] Brennecke and co-workers observed a significant drop in UCST by Nd_2O_3 loading in the [Hbet][Tf_2N]/water system, yet it is unclear if this decrease is due to HTf_2N and water formation during the dissolution or by the increased metal loading.[270] In order to extract lanthanides from aqueous solutions, betaine has to be added as a complexing agent.[263] **Figure 1.30** shows the homogeneous liquid-liquid extraction of Pr(III). The Pr(III) ions can be stripped from the IL by contact with a HCl solution.[263,264]

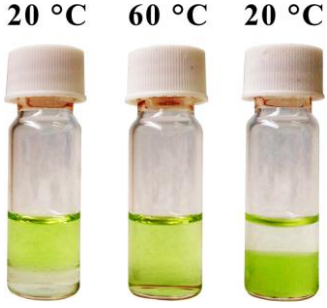

Figure 1.30 Homogeneous liquid-liquid extraction of Pr(III) ions from an aqueous bistriflimide medium with betaine as extractant in the [Hbet][Tf_2N]/water system. Left: initial stage, middle: homogeneous stage, right: after settling. The aqueous phase is on top and the IL is the bottom layer. Reprinted with permission from Vander Hoogerstraete *et al.*, copyright 2013 American Chemical Society.[263]

Via a slope analysis study, a plausible extraction mechanism (equation 1.2) was proposed for the extraction of Nd(III) in the presence of betaine:[262,264]

$$2\,Nd^{3+} + 3\,[Tf_2N]^- + 3\,bet + x\,H_2O \leftrightarrows \overline{Nd_2(bet)_3(H_2O)_x(Tf_2N)_3} \quad (1.2)$$

The upper bar represents species in the ionic liquid phase.

The interesting features of the thermomorphic behavior of the [Hbet][Tf_2N]/water system and its ability to dissolve oxides were also exploited in research on the recycling of NdFeB magnets. The [Hbet][Tf_2N]/water system was able to dissolve milled NdFeB magnet particles and after cooling, the IL contained iron while the rare earths (Nd, Dy) and Co stayed in the water phase. The thermomorphic system was thus a step in the integrated recycling process which started with the milling of NdFeB magnets until the production of pure rare earth oxides.[271] Also in the recycling of lamp phosphor waste, the thermomorphic [Hbet][Tf_2N]/water system is beneficial from an energy-saving point of view. Europium and yttrium could be recovered by stripping with an aqueous acid solution at 80 °C without shaking thanks to the formation of a homogeneous phase.[272]

[Chol][Tf_2N]/water is a similar system with a critical temperature of 72 °C, it was applied in homogeneous liquid-liquid extraction of neodymium with hexafluoroacetylacetone (Hhfac).[265] Also, the previously discussed ionic liquid analogues of Girard's reagents can perform in the HLLE of transition metals.[125] In **Table 1.2**, all known thermomorphic systems for metal extractions using ionic liquid technology are summarized.

Table 1.2 Summary of metal extraction application using thermomorphic IL systems.

System	Phase behavior	Metal ions	Additives	Ref
[Hbet][Tf_2N]/water	UCST	Rare earths, In, Ga	Betaine	263,264
[Hbet][Tf_2N]/water	UCST	Sc, Fe		266,271
[Chol][Tf_2N]/water	UCST	Nd	[chol][hfac]	265
[HMIM][BF_4]/water	UCST	Ag	$NaPF_6$	267
Girard IL/water	UCST	Co, Cu, Ni, Zn		125
[P_{44414}]Cl/water	LCST	Co, Ni	NaCl	197
[$P_{444}E_3$][DEHP]/water	LCST	Co, Cu, Ni, Zn		273
Docusate IL/water	LCST	Sc, La, Sm, Co, Ni		274

1.3.2 Industrial processes

Metal processing is probably one the largest sources of low-grade waste and one of the largest users of energy of any industrial sector. Most processes are based on either high temperature (pyrometallurgy) or hydrometallurgical methodologies.[17] The pyrometallurgical processes have been used for many centuries in metal processing, only in the beginning of the 20th century, hydrometallurgy was developed, operating at much lower temperatures (20-200 °C) and making use of water as a solvent. Recently, solvometallurgy was introduced as a similar technique to hydrometallurgy, yet the extraction of metals from ores, industrial process residues, production scrap, and urban waste uses non-aqueous solutions (discrete amounts of water).[275] The focus of this PhD thesis is on hydrometallurgy. Different steps are part of a hydrometallurgical process: leaching, *i.e.* the dissolution of the ore into an aqueous medium, concentration and separation of the metal using solvent extraction and the recovery of the metal from the aqueous solution by precipitation, ion exchange, electrodeposition or cementation.[17,221,276] The first use of a solvent extraction processes on large scale was the PUREX process for the recovery of uranium and plutonium from spent nuclear fuel.[277] Also the separation of cobalt and nickel and the separation of the rare earths are industrial processes.[277] For solvent extraction processes on industrial scale, different equipment was designed: centrifugal extractors, columns or stage-type extractors.[278] The only industrial choice for the technology of rare-earth separation batteries are mixer-settlers, the most common stage-type extractors (**Figure 1.31**). These are relatively easy to design and flexible to run in operation and have an excellent stage efficiency. In the mixing chamber, the two phases are first mixed together and then guided to a settling chamber where the two phases separate again by gravity.

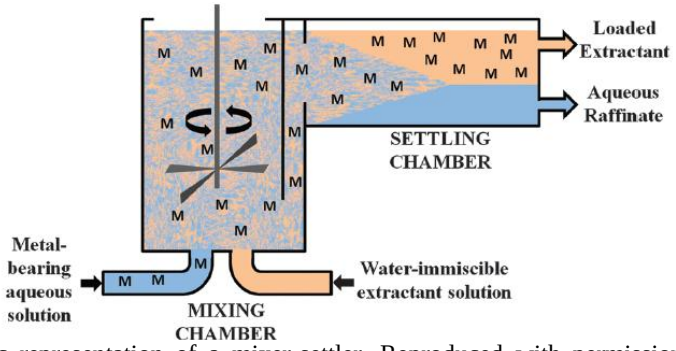

Figure 1.31 Schematic representation of a mixer-settler. Reproduced with permission from Wilson *et al.*, copyright 2014 The Royal Society of Chemistry.[221]

A disadvantage in the process is the fact that the water-immiscible organic phase often consists of a volatile and flammable solvent, such as kerosene, toluene, dichloromethane or diethyl ether. The implementation of ionic liquids into the process would ensure a greener, environmentally friendlier and safer alternative for the VOCs currently used. The use of mixer-settlers for metal extraction by ionic liquids was demonstrated by our group.[279] In practice, consecutive mixer-settlers are combined in an automated continuous counter-current extraction process, where the organic solvent flows in the opposite direction to the aqueous layer containing the solute. This provides higher selectivity, maximum equilibrium efficiency and quantitative separation for the recovery of the desired product at minimum time and expense. The two solvents are mixed in a mechanical mixer and the liquid dispersion is then separated in a settler. Intense agitation is necessary to break up the discontinuous phase into finely divided droplets to increase the surface area in contact between the two phases. Without this, the mass transfer of the solute or solutes between the phases would be extremely slow, making the extraction process inefficient.

To tackle the mass transfer issue, a patented invention describes a vertical column setup and mixer-settler setup for the application of solvent extraction with thermomorphic solvents.[280] The selection of the thermomorphic solvents makes sure that, at a first temperature, complete miscibility and, at a second temperature, full or partial immiscibility are achieved. The setups can be used for both UCST and LCST type of transitions. With this process, better mass transfer and, therefore, a faster approach to equilibrium in each stage and accordingly, a higher stage efficiency at a given throughput is achieved.

In **Figure 1.32**, five mixer zones (designated by the letter M) and five settler zones (letter S) are connected in counter-current.

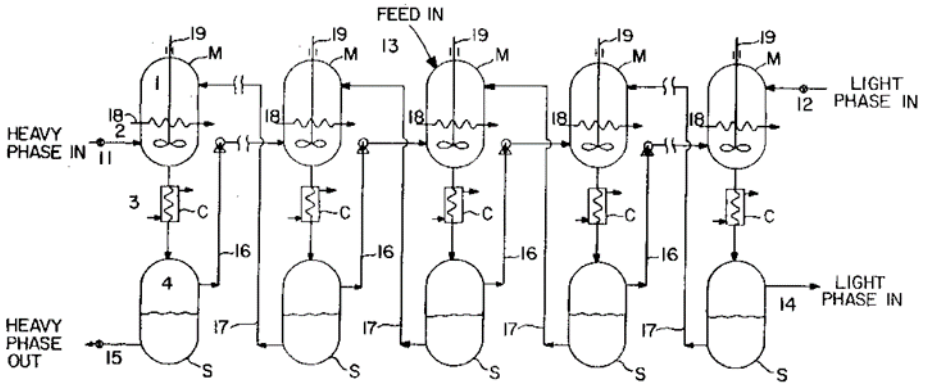

Figure 1.32 Application of heating and cooling devices to a mixer-settler extraction system, here separate discrete mixer (M) and settler (S) zones are employed. Cooling devices (C) are introduced between the mixer and settler zones. Reprinted from US Patent 4,954,260.[280]

To this limited amount of mixer settlers, additional stages can of course be added. The heavy phase and light phase are introduced via the lines 11 and 12, respectively, and the feed solution is fed via line 13 to the middle mixer zone. In case of an UCST process, in the mixing section, the temperature is above the critical point. By use of heating elements (18) at the bottom or on the side of the mixer, the formation of this single homogeneous phase is facilitated due to thermal convection. This way, mechanical mixing can be limited to soft agitation (19) to facilitate mixing and heat transfer. Next, the homogeneous phase is transferred from the bottom of the tank to the settler. Prior to introduction into the settler, the mixture is cooled below its critical temperature so that the two phases rapidly form in the settler. The throughput of the equipment is dominated by the phase separation in the settler. Fortunately, in the phase transfer from a single phase to two phases by cooling, the rate of coalescence is generally high. After settling, the light phase is pumped to the next right mixer zone (16) and similarly, the heavy phase is pumped from the settler zone to the next left mixer zone by means of a pump (17). Thus, these solvents are passed in counter-current flow through a multi-stage separation path of a series of alternating mixer and settler zones. In the meantime, the solute shows a preferential solubility in one of the solvents for selective extraction. Then, one solvent may be recovered rich in solute content and the second solvent as lean in solute amount. A pair of

solutes can be separated if their distribution ratios towards the solvents are different. The closer the distribution coefficients of the solutes, the more stages will be required to perform the separation to the same degree of purity. The exiting first solvent will be rich in the one solute and lean in the second, while the reverse will be true for the exiting second solvent.[280] Essential for this type of mixer-settler is only to operate them with a mixture of solvents which, by alternate heating and cooling, undergo a transition between a single homogeneous phase and two phases, *i.e.* a thermomorphic mixture.

1.4 References

1 T. Welton, *Chem. Rev.*, 1999, **99**, 2071.
2 P. Wasserscheid and W. Keim, *Angew. Chemie Int. Ed.*, 2000, **39**, 3772.
3 R. D. Rogers and K. R. Seddon, *Science*, 2003, **302**, 792.
4 Ionic liquids win Great British Innovation Vote | News | Chemistry World, https://www.chemistryworld.com/news/ionic-liquids-win-great-british-innovation-vote/6018.article.
5 P. Walden, *Bull. Russ. Acad. Sci.*, 1914, 405.
6 J. Dupont, R. F. de Souza and P. A. Z. Suarez, *Chem. Rev.*, 2002, **102**, 3667.
7 T. Welton, *Coord. Chem. Rev.*, 2004, **248**, 2459.
8 F. van Rantwijk and R. A. Sheldon, *Chem. Rev.*, 2007, **107**, 2757.
9 V. I. Pârvulescu and C. Hardacre, *Chem. Rev.*, 2007, **107**, 2615.
10 H. Olivier-Bourbigou, L. Magna and D. Morvan, *Appl. Catal. A*, 2010, **373**, 1.
11 M. M. Pereira, J. A. P. Coutinho and M. G. Freire, in *Ionic Liquids in the Biorefinery Concept: Challenges and Perspectives*, Royal Society of Chemistry, Cambridge, U.K., 2015, pp. 227–257.
12 H. Wang, G. Gurau and R. D. Rogers, *Chem. Soc. Rev.*, 2012, **41**, 1519.
13 J. Hulsbosch, D. E. De Vos, K. Binnemans and R. Ameloot, *ACS Sustain. Chem. Eng.*, 2016, **4**, 2917.
14 A. Farrán, C. Cai, M. Sandoval, Y. Xu, J. Liu, M. J. Hernáiz and R. J. Linhardt, *Chem. Rev.*, 2015, **115**, 6811.
15 M. Armand, F. Endres, D. R. MacFarlane, H. Ohno and B. Scrosati, *Nat. Mater.*, 2009, **8**, 621.
16 H. Liu, Y. Liu and J. Li, *Phys. Chem. Chem. Phys.*, 2010, **12**, 1685.
17 A. P. Abbott, G. Frisch, J. Hartley and K. S. Ryder, *Green Chem.*, 2011, **13**, 471.
18 N. V. Plechkova and K. R. Seddon, *Chem. Soc. Rev.*, 2008, **37**, 123.
19 H. Zhao, S. Xia and P. Ma, *J. Chem. Technol. Biotechnol.*, 2005, **80**, 1089.
20 X. Sun, H. Luo and S. Dai, *Chem. Rev.*, 2012, **112**, 2100.
21 P. Wasserscheid and T. Welton, *Ionic Liquids in Synthesis*, Wiley-VCH, Weinheim, 2008.
22 D. Dupont, D. Depuydt and K. Binnemans, *J. Phys. Chem. B*, 2015, **119**, 6747.
23 J. S. Wilkes and M. J. Zaworotko, *J. Chem. Soc. Chem. Commun.*, 1992, **213**, 965.
24 P. Bonhôte, A. P. Dias, N. Papageorgiou, K. Kalyanasundaram and M. Grätzel, *Inorg. Chem.*, 1996, **35**, 1168.
25 E. Alcalde, I. Dinares, A. Ibanez and N. Mesquida, *Molecules*, 2012, **17**, 4007.
26 A. E. Visser, R. P. Swatloski, W. M. Reichert, R. Mayton, S. Sheff, A. Wierzbicki, J. Davis and R. D. Rogers, *Chem. Commun.*, 2001, 135.
27 R. Ludwig, E. Maginn and S. Balasubramanian, *ChemPhysChem*, 2012, **13**, 1603.
28 H. Davis, *Chem. Lettt.*, 2004, **33**, 1072.
29 P. Wasserscheid, B. Drießen-Hölscher, R. van Hal, H. C. Steffens and J.

Zimmermann, *Chem. Commun.*, 2003, 2038.
30 T. A. Wielema and J. B. F. N. Engberts, *Eur. Polym. J.*, 1987, **23**, 947.
31 M. Freemantle, *Chem. Eng. News Arch.*, 1998, **76**, 12.
32 G. Huddleston and R. D. Rogers, *Chem. Commun.*, 1998, 1765.
33 M. Freemantle, *An introduction to ionic liquids*, RSC Publishing, Cambridge, U.K., 2009.
34 K. E. Gutowski, G. A. Broker, H. D. Willauer, J. G. Huddleston, R. P. Swatloski, J. D. Holbrey and R. D. Rogers, *J. Am. Chem. Soc.*, 2003, **125**, 6632.
35 R. K. K. Mishra, P. C. C. Rout, K. Sarangi and K. C. C. Nathsarma, *Hydrometallurgy*, 2011, **108**, 93.
36 M. Regel-Rosocka and M. Wisniewski, *Hydrometallurgy*, 2011, **110**, 85–90.
37 D. Kogelnig, A. Stojanovic, M. Galanski, M. Groessl, F. Jirsa, R. Krachler and B. K. Keppler, *Tetrahedron Lett.*, 2008, **49**, 2782.
38 T. Vander Hoogerstraete, S. Wellens, K. Verachtert and K. Binnemans, *Green Chem.*, 2013, **15**, 919.
39 S. Wellens, B. Thijs and K. Binnemans, *Green Chem.*, 2012, **14**, 1657–1665.
40 R. Hoogenboom, in *Smart Polymers and their Applications*, Woodhead Publishing, Cambridge, U.K., 2014, pp. 15–44.
41 P. Atkins and J. Paula, *Physical chemistry*, Oxford University Press, Oxford, UK, 8th edn., 2006.
42 W. Xing, A. K. Vutha, X. Yu, A. Ullmann, N. Brauner and Y. Peles, *Int. J. Heat Mass Transf.*, 2017, **107**, 53.
43 A. Kaul, in *Aqueous Two-Phase Systems: Methods and Protocols*, Humana Press Inc., Totowa, NJ, 2000, vol. 11, pp. 11–21.
44 J. S. Higgins, J. E. G. Lipson and R. P. White, *Philos. Trans. R. Soc. A Math. Phys. Eng. Sci.*, 2010, **368**, 1009.
45 M. A. Anisimov, *Critical phenomena in liquids and liquid crystals*, Gordon and Breach Science Publishers, Philadelphia, 1991.
46 P. M. Chaikin and T. C. Lubensky, *Principles of Condensed Matter*, Cambridge University Press, Cambridge, U.K., 1995.
47 H. Weingärtner, M. Kleemeier, S. Wiegand and W. Schröer, *J. Stat. Phys.*, 1995, **78**, 169.
48 W. Schröer and V. R. R. Vale, *J. Phys. Condens. Matter*, 2009, **21**, 424119.
49 J. Thoen, J. Hamelin and T. Bose, *Phys. Rev. E*, 1996, **53**, 6264.
50 O. Müller and J. Winkelmann, *Phys. Rev. E*, 1999, **59**, 2026.
51 H. S. Nalwa, Ed., *Handbook of Low and High Dielectric Constant Materials and Their Applications*, Academic Press, London, UK, 1999.
52 J. Rotrekl, J. Storch, P. Velíšek, W. Schröer, J. Jacquemin, Z. Wagner, P. Husson and M. Bendová, *J. Solution Chem.*, 2017, **46**, 1456.
53 H. Weingärtner and W. Schröer, *Adv. Chem. Physics*, 2001, **116**, 1.
54 M. L. Japas and J. M. H. L. Sengers, *J. Phys. Chem.*, 1990, **94**, 5361.
55 S. Wiegand, M. E. Briggs, J. M. H. Levelt Sengers, M. Kleemeier and W. Schröer, *J. Chem. Phys.*, 1998, **109**, 9038.
56 M. Wagner, O. Stanga and W. Schröer, *Phys. Chem. Chem. Phys.*, 2004, **6**, 4421.
57 W. Schröer, M. Wagner and O. Stanga, *J. Mol. Liq.*, 2006, **127**, 2.

58 W. Schröer, *Contrib. to Plasma Phys.*, 2012, **52**, 78.
59 C. G. Panayiotou, *Can. J. Chem. Eng.*, 1984, **62**, 578.
60 J. Mollerup, *Fluid Phase Equilib.*, 1981, **7**, 121.
61 L. D. Simoni, Y. Lin, J. F. Brennecke and M. A. Stadtherr, *Ind. Eng. Chem. Res.*, 2008, **47**, 256.
62 G. Nagatani, J. Ferrari, L. Cardozo Filho, C. C. R. S. Rossi, R. Guirardello, J. V. Oliveira and M. L. Corazza, *Brazilian J. Chem. Eng.*, 2008, **25**, 571.
63 M. G. Freire, L. M. N. B. F. Santos, I. M. Marrucho and J. A. P. Coutinho, in *Molten Salts and Ionic Liquids: Never the Twain*, John Wiley & Sons, Hoboken, New Jersey, 2010, pp. 101–121.
64 M. Wlazło, E. I. Alevizou, E. C. Voutsas and U. Domańska, *Fluid Phase Equilib.*, 2015, **424**, 16.
65 A. W. Francis, in *Advances in Chemistry Series No. 31*, ed. American Chemical Society, Washington, D.C., 1961.
66 A. W. Francis, *Liquid-liquid equilibriums*, Interscience, New York, 1963.
67 W. Arlt, M. E. A. Macedo, P. Rasmussen and J. M. Sørensen, *Liquid-liquid equilibrium data collection*, DECHEMA, Deutsche Gesellschaft für Chemisches Apparatewesen, Frankfurt/Main, 1979.
68 J. M. Sørensen, T. Magnussen, P. Rasmussen and A. Fredenslund, *Fluid Phase Equilib.*, 1979, **2**, 297.
69 IUPAC Solubility data series (online), https://srdata.nist.gov/solubility/IUPAC/iupac.aspx.
70 J. B. Ferguson, *J. Phys. Chem.*, 1927, **160**, 757.
71 D. K. Beridze and A. K. Karshibaev, *Fiz. i Fiz. zhidkostei*, 1976, **3**, 138.
72 M. Rolla, P. Franzosini, R. L. Riccardi and Z. Bottelli, *Naturforsch.*, 1967, **22A**, 48.
73 A. Trejo, P. Yañez and R. Eustaquio-Rincón, *J. Chem. Eng. Data*, 2006, **51**, 1070.
74 S. Chen, C. Lai, J. Rouch and P. Tartaglia, *Phys. Rev. A*, 1983, **27**, 1086.
75 J. P. Erikson, *J. Chem. Educ.*, 2017, **94**, 75.
76 A. Ullmann, I. Lipstein and N. Brauner, in *Proceedings of the 15th International Heat Transfer Conference*, Begellhouse, Connecticut, 2014.
77 J. Thoen, E. Bloemen and W. Van Dael, *J. Chem. Phys.*, 1978, **68**, 735.
78 A. W. Loven and O. K. Rice, *Trans. Faraday Soc.*, 1963, **59**, 2723.
79 M. A. Handschy, R. C. Mockler and W. J. O'Sullivan, *Chem. Phys. Lett.*, 1980, **76**, 172.
80 V. Rothmund, *Z. Phys. Chem.*, 1898, **26**, 433.
81 C. S. Hudson, *Z. Phys. Chem.*, 1904, **47**, 113.
82 D. E. Tsakalotos, *Bull. Soc. Chim. Fr.*, 1909, **5**, 397.
83 P. Leone, *Atti congr. nazl. chim. pura ed appl. 2nd Congr*, 1926, 1209.
84 H. L. Cox and L. H. Cretcher, *J. Am. Chem. Soc.*, 1926, **48**, 451.
85 W. E. Acree, in *Thermodynamic Properties of Nonelectrolyte Solutions*, Academic Press, Orlando, 1984, pp. 240–256.
86 O. Flaschner and B. Macewen, *J. Chem. Soc.*, 1908, **93**, 1000.
87 J. Matous, J. P. Novak, J. Sobr and J. Pick, *Collect. Czechoslov. Chem. Commun.*, 1972, **37**, 2653.
88 W. Hayduk, H. Laudie and O. H. Smith, *J. Chem. Eng. Data*, 1973, **18**, 373.

89 T. Narayanan and A. Kumar, *Phys. Rep.*, 1994, **249**, 135.
90 J. A. Larkin, J. Katz and R. L. Scott, *J. Phys. Chem.*, 1967, **71**, 352.
91 E. M. Anderson and S. C. Greer, *J. Chem. Phys.*, 1988, **88**, 2666.
92 R. L. Scott, *J. Phys. Chem.*, 1965, **69**, 261.
93 S. Schrödle, R. Buchner and W. Kunz, *Fluid Phase Equilib.*, 2004, **216**, 175.
94 P. Nockemann, B. Thijs, S. Pittois, J. Thoen, C. Glorieux, K. Van Hecke, L. Van Meervelt, B. Kirchner and K. Binnemans, *J. Phys. Chem. B*, 2006, **110**, 20978.
95 P. Nockemann, K. Binnemans, B. Thijs, T. N. Parac-Vogt, K. Merz, A. V. Mudring, P. C. Menon, R. N. Rajesh, G. Cordoyiannis, J. Thoen, J. Leys and C. Glorieux, *J. Phys. Chem. B*, 2009, **113**, 1429.
96 S. Pittois, B. Van Roie, C. Glorieux and J. Thoen, *J. Chem. Phys.*, 2004, **121**, 1866.
97 S. Pittois, B. Van Roie, C. Glorieux and J. Thoen, *J. Chem. Phys.*, 2005, **122**, 24504.
98 A. Ullmann, Z. Ludmer and R. Shinnar, *AIChE J.*, 1995, **41**, 488.
99 P. A. Albertsson and F. Tjerneld, in *Methods in Enzymology: Aqueous Two-Phase Systems*, Academic Press, San Diego, CA, Vol. 228., 1994, pp. 3–13.
100 M. Bendová and Z. Wagner, *J. Chem. Eng. Data*, 2006, **51**, 2126.
101 R. Strey, R. Schomäcker, D. Roux, F. Nallet and U. Olsson, *J. Chem. Soc., Faraday Trans.*, 1990, **86**, 2253.
102 M. S. Calado, Z. Petrovski, M. S. Manic, V. Najdanovic-Visak, E. A. Macedo and Z. P. Visak, *Fluid Phase Equilib.*, 2013, **337**, 67.
103 K. Ochi, M. Tada and K. Kojima, *Fluid Phase Equilib.*, 1990, **56**, 341.
104 J. Szydlowski, L. P. Rebelo and W. A. Van Hook, *Rev. Sci. Instrum.*, 1992, **63**, 1717.
105 A. Heintz, J. K. Lehmann and C. Wertz, *J. Chem. Eng. Data*, 2003, **48**, 472.
106 B. Sun and P. Wu, *J. Phys. Chem. B*, 2010, **114**, 9209.
107 J. Shi, P. Wu and F. Yan, *Langmuir*, 2010, **26**, 11427.
108 G. Wang and P. Wu, *Soft Matter*, 2015, **11**, 5253.
109 Y. Kohno and H. Ohno, *Chem. Commun.*, 2012, **48**, 7119.
110 C. Chiappe, C. S. Pomelli and S. Rajamani, *J. Phys. Chem. B*, 2011, **115**, 9653.
111 M. G. Freire, L. M. N. B. Santos, A. M. Fernandes, J. A. P. Coutinho and I. M. Marrucho, *Fluid Phase Equilibr.*, 2007, **261**, 449.
112 U. Domańska, E. Bogel-Łukasik and R. Bogel-Łukasik, *Chem. Eur. J.*, 2003, **9**, 3033.
113 L. Ropel, L. S. Belvèze, S. N. V. K. Aki, M. A. Stadtherr and J. F. Brennecke, *Green Chem.*, 2005, **7**, 83.
114 Y. Qiao, W. Ma, N. Theyssen, C. Chen and Z. Hou, *Chem. Rev.*, 2017, **117**, 6881.
115 Y. Kohno, S. Saita, Y. Men, J. Yuan and H. Ohno, *Polym. Chem.*, 2015, **6**, 2163.
116 J. E. L. Dullius, P. A. Z. Suarez, S. Einloft, R. F. de Souza and J. Dupont, *Organometallics*, 1998, **17**, 815.
117 J. L. Anthony, E. J. Maginn and J. F. Brennecke, *J. Phys. Chem. B*, 2001, **105**, 10942.

118 R. P. Swatloski, J. D. Holbrey and R. D. Rogers, *Green Chem.*, 2003, **5**, 361.
119 M. Wagner, O. Stanga and W. Schröer, *Phys. Chem. Chem. Phys.*, 2003, **5**, 3943.
120 U. Domańska and A. Marciniak, *Fluid Phase Equilib.*, 2007, **260**, 9.
121 D. Depuydt, Master thesis KU Leuven, 2013.
122 P. Nockemann, B. Thijs, T. N. Parac-Vogt, K. Van Hecke, L. Van Meervelt, B. Tinant, I. Hartenbach, T. Schleid, V. T. Ngan, M. T. Nguyen and K. Binnemans, *Inorg. Chem.*, 2008, **47**, 9987.
123 T. Köddermann, C. Wertz, A. Heintz and R. Ludwig, *ChemPhysChem*, 2006, **7**, 1944.
124 A. J. L. Costa, M. R. C. Soromenho, K. Shimizu, I. M. Marrucho, J. M. S. S. Esperança, J. N. C. Lopes and L. P. N. Rebelo, *J. Phys. Chem. B*, 2012, **116**, 9186.
125 M. Blesic, H. Q. N. Gunaratne, J. Jacquemin, P. Nockemann, S. Olejarz, K. R. Seddon and C. R. Strauss, *Green Chem.*, 2014, **16**, 4115.
126 M. L. Japas and J. M. H. Levelt-Sengers, *J. Phys. Chem.*, 1990, **94**, 5361.
127 H. Weingärtner and E. Steinle, *J. Phys. Chem.*, 1992, **96**, 2407.
128 H. Ohno and K. Fukumoto, *Acc. Chem. Res.*, 2007, **40**, 1122.
129 K. Fukumoto and H. Ohno, *Angew. Chemie Int. Ed.*, 2007, **46**, 1852.
130 Y. Kohno, S. Saita, K. Murata, N. Nakamura and H. Ohno, *Polym. Chem.*, 2011, **2**, 862.
131 S. Saita, Y. Kohno, N. Nakamura and H. Ohno, *Chem. Commun.*, 2013, **49**, 8988.
132 Y. Zhao, H. Wang, Y. Pei, Z. Liu and J. Wang, *Phys. Chem. Chem. Phys.*, 2016, **18**, 23238.
133 Y. Kohno, H. Arai, S. Saita and H. Ohno, *Aust. J. Chem.*, 2011, **64**, 1560.
134 Y. Kohno and H. Ohno, *Phys. Chem. Chem. Phys.*, 2012, **14**, 5063.
135 A. Nitta, T. Morita, S. Saita, Y. Kohno and H. Ohno, *Chem. Phys. Lett.*, 2015, **628**, 108.
136 R. Wang, W. Leng, Y. Gao and L. Yu, *RSC Adv.*, 2014, **4**, 14055.
137 Y. Fukaya, T. Nakano and H. Ohno, *Aust. J. Chem.*, 2016, **70**, 74.
138 H. Glasbrenner and H. Weingärtner, *J. Phys. Chem.*, 1989, **93**, 3378.
139 M. Kleemeier, W. Schröer and H. Weingärtner, *J. Mol. Liq.*, 1997, **73**–**74**, 501.
140 S. Saita, Y. Mieno, Y. Kohno and H. Ohno, *Chem. Commun.*, 2014, **50**, 15450.
141 Y. Fukaya, K. Sekikawa, K. Murata, N. Nakamura and H. Ohno, *Chem. Commun.*, 2007, 3089.
142 U. Domańska, *Thermochim. Acta*, 2006, **448**, 19.
143 J. M. Crosthwaite, S. N. V. K. Aki, E. J. Maginn and J. F. Brennecke, *J. Phys. Chem. B*, 2004, **108**, 5113.
144 J. M. Crosthwaite, S. N. V. K. Aki, E. J. Maginn and J. F. Brennecke, *Fluid Phase Equilib.*, 2005, **228**–**229**, 303.
145 J. M. Crosthwaite, M. J. Muldoon, S. N. V. K. Aki, E. J. Maginn and J. F. Brennecke, *J. Phys. Chem. B*, 2006, **110**, 9354.
146 U. Domańska and R. Bogel-Łukasik, *Fluid Phase Equilib.*, 2005, **233**, 220.
147 U. Domańska, M. Królikowski and K. Ślesińska, *J. Chem. Thermodyn.*,

2009, **41**, 1303.
148 U. Domańska and A. Marciniak, *J. Chem. Eng. Data*, 2003, **48**, 451.
149 U. Domańska and K. Paduszynski, *J. Phys. Chem. B*, 2008, **112**, 11054.
150 U. Domańska, M. Zawadzki, M. Królikowski and A. Lewandrowska, *Chem. Eng. J.*, 2012, **181**–**182**, 63.
151 U. Domańska and M. Królikowski, *J. Chem. Thermodyn.*, 2011, **43**, 1488.
152 U. Domańska, M. Zawadzki, M. Marc Tshibangu, D. Ramjugernath and T. M. Letcher, *J. Chem. Thermodyn.*, 2010, **42**, 1180.
153 T. M. Letcher, D. Ramjugernath, K. Tumba, M. Królikowski and U. Domańska, *Fluid Phase Equilib.*, 2010, **294**, 89.
154 H. R. Dittmar and W. H. Schröer, *J. Phys. Chem. B*, 2009, **113**, 1249.
155 A. J. L. Costa, M. R. C. Soromenho, K. Shimizu, J. M. S. S. Esperança, J. N. C. Lopes and L. P. N. Rebelo, *RSC Adv.*, 2013, **3**, 10262.
156 M. L. S. Batista, L. I. N. Tomé, C. M. S. S. Neves, E. M. Rocha, J. R. B. Gomes and J. A. P. Coutinho, *J. Phys. Chem. B*, 2012, **116**, 5985.
157 M. B. Shiflett and A. Yokozeki, *J. Chem. Eng. Data*, 2008, **53**, 2683.
158 J. Jacquemin, M. Bendová, Z. Sedláková, M. Blesic, J. D. Holbrey, C. L. Mullan, T. G. A. Youngs, L. Pison, Z. Wagner, K. Aim, M. F. C. Gomes and C. Hardacre, *ChemPhysChem*, 2012, **13**, 1825.
159 J. Lachwa, J. Szydlowski, V. Najdanovic-Visak, L. P. N. Rebelo, K. R. Seddon, M. Nunes da Ponte, J. M. S. S. Esperança and H. J. R. Guedes, *J. Am. Chem. Soc.*, 2005, **127**, 6542.
160 J. Lachwa, J. Szydlowski, A. Makowska, K. R. Seddon, J. M. S. S. Esperanca, H. J. R. Guedes and L. P. Rebelo, *Green Chem.*, 2006, **8**, 262.
161 R. D. Rogers and K. R. Seddon, Eds., *Ionic Liquids III A: Fundamentals, Progress, Challenges, and Opportunities*, American Chemical Society, Washington, DC, 2005, vol. 901.
162 F. Hofmeister, *Pathol. Pharmacol.*, 1888, **24**, 247.
163 J. R. Trindade, Z. P. Visak, M. Blesic, I. M. Marrucho, J. A. P. Coutinho, J. N. C. Lopes and L. P. N. Rebelo, *J. Phys. Chem. B*, 2007, **111**, 4737.
164 Z. Yang, *J. Biotechnol.*, 2009, **144**, 12.
165 K. K. Il'in and D. G. Cherkasov, *Russ. J. Phys. Chem. A*, 2013, **87**, 598.
166 S. Saita, Y. Kohno and H. Ohno, *Chem. Commun.*, 2013, **49**, 93.
167 V. Brandani, A. Chianese and M. Rossi, *J. Chem. Eng. Data*, 1985, **30**, 27.
168 T. Wongsawa, M. Hronec, A. W. Lothongkum, U. Pancharoen and S. Phatanasri, *J. Mol. Liq.*, 2014, **196**, 98.
169 J. R. Alvarez Gonzalez, E. A. Macedo, M. E. Soares and A. G. Medina, *Fluid Phase Equilib.*, 1986, **26**, 289.
170 E. A. Macedo, M. E. Soares and A. G. Medina, *Fluid Phase Equilib.*, 1986, **31**, 117.
171 A. Frolkova, D. Zakharova, A. Frolkova and S. Balbenov, *Fluid Phase Equilib.*, 2016, **408**, 10.
172 Z. Shen, Q. Wang, L. Chen, Z. Xiong and C. Chen, *Fluid Phase Equilib.*, 2016, **414**, 48.
173 F. Lei, Q. Wang, X. Gong, L. Li, Q. Wu and W. Zhang, *Fluid Phase Equilib.*, 2014, **382**, 65.
174 M. S. Selvan, M. D. McKinley, R. H. Dubois and J. L. Atwood, *J. Chem.*

Eng. Data, 2000, **45**, 841.
175 Y. Cao, H. Xing, Q. Yang, Z. Li, T. Chen, Z. Bao and Q. Ren, *Ind. Eng. Chem. Res.*, 2014, **53**, 10784.
176 A. Arce, O. Rodríguez and A. Soto, *J. Chem. Eng. Data*, 2004, **49**, 514.
177 T. M. Letcher and N. Deenadayalu, *J. Chem. Thermodyn.*, 2003, **35**, 67.
178 T. M. Letcher, N. Deenadayalu, B. Soko, D. Ramjugernath and P. K. Naicker, *J. Chem. Eng. Data*, 2003, **48**, 904.
179 S. Raja, V. R. Murty, V. Thivaharan, V. Rajasekar and V. Ramesh, *Sci. Technol.*, 2012, **1**, 7.
180 M. G. Freire, A. F. Claudio, J. M. M. Araujo, J. A. P. Coutinho, I. M. Marrucho, J. N. C. Lopes and L. P. Rebelo, *Chem. Soc. Rev.*, 2012, **41**, 4966.
181 P. A. Albertsson, *Partitioning of Cell Particles and Macromolecules*, Wiley, New York, 3rd edn., 1986.
182 R. Hatti-Kaul, in *Aqueous Two-Phase Systems: Methods and Protocols*, Humana Press Inc., Totowa, New Jersey, 2000, pp. 1–10.
183 B. Y. Zaslavsky, *Aqueous Two-Phase Partitioning*, Marcel Dekkers Inc., New York, 1994.
184 H. Watanabe and H. Tanaka, *Talanta*, 1978, **25**, 585.
185 S. Igarashi and T. Yotsuyanagi, *Mikrochim. Acta*, 1992, **106**, 37.
186 R. D. Rogers and M. A. Eiteman, Eds., *Aqueous Biphasic Separations: Biomolecules to Metal Ions*, Plenum Press, New York, 1995.
187 R. D. Rogers, A. H. Bond, C. B. Bauer, J. Zhang and S. T. Griffin, *J. Chromatogr. B Biomed. Sci. Appl.*, 1996, **680**, 221.
188 S. Lahiri and K. Roy, *J. Radioanal. Nucl. Chem.*, 2009, **281**, 531.
189 M. C. H. Silva, L. H. M. Silva, F. J. Paggioli, J. S. R. Coimbra and L. A. Minim, *Quim. Nova*, 2006, **29**, 1332.
190 R. D. Rogers, A. H. Bond and C. B. Bauer, *Separ. Sci. Technol.*, 1993, **28**, 1091.
191 M. H. Abraham, A. M. Zissimos, J. G. Huddleston, H. D. Willauer, R. D. Rogers and W. E. Acree, *Ind. Eng. Chem. Res.*, 2003, **42**, 413.
192 Y. Zhang and P. Cremer, *Curr. Opin. Chem. Biol.*, 2006, **10**, 658.
193 S. Shahriari, C. M. S. S. Neves, M. G. Freire and J. A. P. Coutinho, *J. Phys. Chem. B*, 2012, **116**, 7252.
194 N. J. Bridges, K. E. Gutowski and R. D. Rogers, *Green Chem.*, 2007, **9**, 177.
195 M. G. Freire, Ed., *Ionic-Liquid- Based Aqueous Biphasic Systems*, Springer-Verlag, Berlin-Heidelberg, 2016.
196 M. G. Freire, C. M. S. S. Neves, A. M. S. Silva, L. M. N. B. F. Santos, I. M. Marrucho, L. P. N. Rebelo, J. K. Shah, E. J. Maginn and J. A. P. Coutinho, *J. Phys. Chem. B*, 2010, **114**, 2004.
197 B. Onghena, T. Opsomer and K. Binnemans, *Chem. Commun.*, 2015, **51**, 15932.
198 H. Passos, A. Luis, J. A. P. Coutinho and M. G. Freire, *Sci. Rep.*, 2016, **6**, 20276.
199 M. Dilip, N. J. Bridges, H. Rodríguez, J. F. B. Pereira and R. D. Rogers, *J. Solution Chem.*, 2015, **44**, 454.
200 A. M. Ferreira, H. Passos, A. Okafuji, M. G. Freire, J. A. P. Coutinho and H. Ohno, *Green Chem.*, 2017, **19**, 4012.

201 M. G. Freire, C. M. S. S. Neves, I. M. Marrucho, J. N. Canongia Lopes, L. P. Rebelo and J. A. P. Coutinho, *Green Chem.*, 2010, **12**, 1715.
202 C. M. S. S. Neves, M. G. Freire and J. A. P. Coutinho, *RSC Adv.*, 2012, **2**, 10882.
203 Y. Akama, M. Ito and S. Tanaka, *Talanta*, 2000, **53**, 645.
204 Y. Akama and A. Sali, *Talanta*, 2002, **57**, 681.
205 A. Schaadt and H. J. Bart, *Chem. Eng. Technol.*, 2003, **26**, 469.
206 F. Tasselli, in *Encyclopedia of Membranes*, Springer-Verlag, Berlin-Heidelberg, 2014, pp. 1–3.
207 Y. Kohno, H. Arai and H. Ohno, *Chem. Commun.*, 2011, **47**, 4772.
208 J. L. Anderson and D. W. Armstrong, *Anal. Chem.*, 2003, **75**, 4851.
209 P. J. Dyson and T. J. Geldbach, *Electrochem. Soc. Interface*, 2007, 50.
210 Richard P. Swatloski, Scott K. Spear, A. John D. Holbrey and R. D. Rogers, *J. Am. Chem. Soc.*, 2002, **124**, 4974.
211 C. M. Gordon, *Appl. Catal. A Gen.*, 2001, **222**, 101.
212 S. T. Handy, Ed., *Applications of ionic liquids in science and technology*, InTechOpen, Rijeka, Croatia, 2011.
213 M. D. Bermúdez, A. E. Jiménez, J. Sanes and F. J. Carrión, *Molecules*, 2009, **14**, 2888.
214 M. Deetlefs, M. Shara and K. R. Seddon, in *Ionic Liquids III: Fundamentals, Progress, Challenges, and Opportunities*, eds. R. D. Rogers and K. R. Seddon, ACS Symposium Series, 2005, pp. 219–233.
215 M. E. V. Valkenburg, R. L. Vaughn, M. Williams and J. S. Wilkes, *Thermochim. Acta*, 2005, **425**, 181.
216 H. Ohno, *Electrochemical aspects of ionic liquids*, John Wiley & Sons, Inc., Hoboken, New Jersey, 2011.
217 A. A. C. Toledo Hijo, G. J. Maximo, M. C. Costa, E. A. C. Batista and A. J. A. Meirelles, *ACS Sustain. Chem. Eng.*, 2016, **4**, 5347.
218 J. Huang, A. Riisager, P. Wasserscheid and R. Fehrmann, *Chem. Commun.*, 2006, **36**, 4027.
219 L. A. Neves, J. G. Crespo and I. M. Coelhoso, *J. Membr. Sci.*, 2010, **357**, 160.
220 J. Rydberg, M. Cox, C. Musikas and G. R. Choppin, Eds., *Solvent Extraction: Principles and Practice*, Marcel Dekker Inc., New York, 2nd edn., 2004.
221 A. M. Wilson, P. J. Bailey, P. A. Tasker, J. R. Turkington, R. A. Grant and J. B. Love, *Chem. Soc. Rev.*, 2014, **43**, 123.
222 M. L. Dietz, *Separ. Sci. Technol.*, 2006, **41**, 2047.
223 J. N. N. Chubb, P. Lagos and J. Lienlaf, *J. Electrostat.*, 2005, **63**, 119.
224 K. Binnemans, P. T. Jones, K. Vanacker, B. Blanplain, B. Mishra and D. Apelian, *JOM*, 2013, **65**, 846.
225 S. Raiguel, D. Depuydt, T. Vander Hoogerstraete, J. Thomas, W. Dehaen and K. Binnemans, *Dalt. Trans.*, 2017, **46**, 5269.
226 D. Dupont, S. Raiguel and K. Binnemans, *Chem. Commun.*, 2015, **51**, 9006.
227 A. E. Visser, R. P. Swatloski, W. M. Reichert, H. D. Willauer, J. G. Huddleston and R. D. Rogers, in *Green Industrial Applications of Ionic Liquids*, Springer Netherlands, Dordrecht, 2002, vol. 92, pp. 137–156.

228 D. Kogelnig, A. Stojanovic, F. Jirsa, W. Körner, R. Krachler and B. K. Keppler, *Sep. Purif. Technol.*, 2010, **72**, 56.
229 K. Murata, Y. Yokoyama and S. Ikeda, *Anal. Chem.*, 1972, **44**, 805.
230 H. Itoh, K. Murata and S. Ikeda, *J. Inorg. Nucl. Chem.*, 1973, **35**, 3632.
231 F. Califano, G. Nozadze, A. Ly van Manh and A. Farhat, *Int. J. Phys. Sci.*, 2014, **9**, 350.
232 A. Schaadt and H. J. Bart, *Chemie Ing. Tech.*, 2002, **74**, 66.
233 J. D. Lamb and R. T. Peterson, *Separ. Sci. Technol.*, 1995, **30**, 3237.
234 N. Alizadeh and K. Ashtari, *Sep. Purif. Technol.*, 2005, **44**, 79.
235 J. D. Lamb, A. Y. Nazarenko and R. J. Hansen, *Sep. Sci. Technol.*, 1999, **34**, 2583.
236 R. Gupta, R. Mauri and R. Shinnar, *Ind. Eng. Chem. Res.*, 1996, **35**, 2360.
237 K. Binder, *Phys. A Stat. Mech. Appl.*, 1986, **140**, 35.
238 J. W. Cahn and J. E. Hilliard, *J. Chem. Phys.*, 1958, **28**, 258.
239 J. W. Cahn and J. E. Hilliard, *J. Chem. Phys.*, 1959, **31**, 688.
240 Y. Tong, L. Han and Y. Yang, *Ind. Eng. Chem. Res.*, 2012, **51**, 16438.
241 T. N. Castro Dantas, *Talanta*, 2002, **56**, 1089.
242 T. N. Castro Dantas, A. A. Dantas Neto, M. C. P. A. Moura, E. L. B. Neto, K. R. Forte and R. H. L. Leite, *Water Res.*, 2003, **37**, 2709.
243 T. N. Castro Dantas, K. R. Oliveira, A. A. Dantas Neto and M. C. P. A. Moura, *Water Res.*, 2009, **43**, 1464.
244 H. Naganawa, H. Suzuki, S. Tachimori, J. Williams, R. K. Heenan and F. J. Leng, *Phys. Chem. Chem. Phys.*, 2000, **2**, 3247.
245 Q. Zhou, X. Zhang and J. Xiao, *J. Chromatogr. A*, 2009, **1216**, 4361.
246 C. Yao and J. L. Anderson, *Anal. Bioanal. Chem.*, 2009, **395**, 1491.
247 Q. Zhou, H. Bai, G. Xie and J. Xiao, *J. Chromatogr. A*, 2008, **1177**, 43.
248 M. Zeeb, P. Tayebi Jamil, A. Berenjian, M. Ganjali and M. R. Talei Bavil Olyai, *DARU J. Pharm. Sci.*, 2013, **21**, 63.
249 C. D. Stalikas, *TrAC Trends Anal. Chem.*, 2002, **21**, 343.
250 E. K. Paleologos, D. L. Giokas and M. I. Karayannis, *TrAC Trends Anal. Chem.*, 2005, **24**, 426.
251 A. N. Anthemidis and K.-I. G. Ioannou, *Talanta*, 2009, 413.
252 H. Ebrahimzadeh, Y. Yamini, F. Kamarei and S. Shahab, *Anal. Chim. Acta*, 2007, **594**, 93.
253 R. Vijayaraghavan, N. Vedaraman, M. Surianarayanan and D. R. MacFarlane, *Talanta*, 2006, **69**, 1059.
254 D. R. Bhatt, K. C. Maheria and J. Parikh, *J. Environ. Chem. Eng.*, 2015, **3**, 1365.
255 J. Liu, L. Wang, W. Zhu, C. Jia, Q. Deng and S. Yao, *Sep. Sci. Technol.*, 2014, **49**, 146.
256 Z. Talbi, B. Haddou, H. Ghouas, M. Kameche, Z. Derriche and C. Gourdon, *Chem. Eng. Commun.*, 2014, **201**, 41.
257 European Commission, *Report on Critical Raw Materials for the EU*, DG Enterprise & Industry, Brussels, 2014.
258 K. Binnemans, P. T. Jones, B. Blanpain, T. Van Gerven and Y. Pontikes, *J. Clean. Prod.*, 2015, **99**, 17.
259 K. Binnemans, P. T. Jones, B. Blanpain, T. Van Gerven, Y. Yang, A. Walton

and M. Buchert, *J. Clean. Prod.*, 2013, **51**, 1.
260 J. Xu, N. Rajapakse and H. L. Finston, *Radiochim. Acta*, 1990, **49**, 135.
261 M. H. Hosseini and N. Alizadeh, *Ind. Eng. Chem. Res.*, 2010, **49**, 7068.
262 I. Billard, in *Ionic-Liquid- Based Aqueous Biphasic Systems*, Springer-Verlag, Berlin-Heidelberg, 2016, pp. 183–220.
263 T. Vander Hoogerstraete, B. Onghena and K. Binnemans, *J. Phys. Chem. Lett.*, 2013, **4**, 1659.
264 T. Vander Hoogerstraete, B. Onghena and K. Binnemans, *Int. J. Mol. Sci.*, 2013, **14**, 21353.
265 B. Onghena, J. Jacobs, L. Van Meervelt and K. Binnemans, *Dalt. Trans.*, 2014, **43**, 11566.
266 B. Onghena and K. Binnemans, *Ind. Eng. Chem. Res.*, 2015, **54**, 1887.
267 M. Vaezzadeh, F. Shemirani and B. Majidi, *J. Anal. Chem.*, 2012, **67**, 28.
268 K. Sasaki, K. Takao, T. Suzuki, T. Mori, T. Arai and Y. Ikeda, *Dalt. Trans.*, 2014, **43**, 5648.
269 K. Sasaki, T. Suzuki, T. Mori, T. Arai, K. Takao and Y. Ikeda, *Chem. Lettt.*, 2014, **43**, 775.
270 D. P. Fagnant, G. S. Goff, B. L. Scott, W. Runde and J. F. Brennecke, *Inorg. Chem.*, 2013, **52**, 549.
271 D. Dupont and K. Binnemans, *Green Chem.*, 2015, **17**, 2150.
272 D. Dupont and K. Binnemans, *Green Chem.*, 2015, **17**, 856.
273 D. Depuydt, L. Liu, C. Glorieux, W. Dehaen and K. Binnemans, *Chem. Commun.*, 2015, **51**, 14183.
274 D. Depuydt, W. Dehaen and K. Binnemans, *Chempluschem*, 2017, **82**, 458.
275 K. Binnemans and P. T. Jones, *J. Sustain. Metall.*, 2017, **3**, 570.
276 F. Habashi, *Hydrometallurgy*, 2005, **79**, 15.
277 Y. Marcus and A. S. Kertes, *Ion Exchange and Solvent Extraction of Metal Complexes*, Wiley-Interscience, New York, USA, 1969.
278 C. Hanson, in *Hydrometallurgical Process Fundamentals*, Springer, Boston, 1984, pp. 499–514.
279 S. Wellens, R. Goovaerts, C. Moller, J. Luyten, B. Thijs and K. Binnemans, *Green Chem.*, 2013, **15**, 3160.
280 Z. Ludmer, R. Shinnar and V. Yakhot, Countercurrent separation process and apparatus, US Patent 4,954,260, 1989.

CHAPTER 2

OBJECTIVES

The main research hypothesis of this PhD thesis is that structural variations in ionic liquids allow for the design of thermomorphic ILs. The synthesis of non-fluorinated ionic liquids which can show temperature-dependent miscibility with water and the use of these IL/water systems for the separation of metal ions by solvent extraction are the core of the PhD thesis. To start, an easy synthesis from readily available starting materials in few steps to achieve high purity ionic liquids is key in ionic liquid technology for separation of metals. A challenge in the use of undiluted ionic liquids for solvent extraction is their high viscosity and slow mass transfer. By designing ionic liquids with temperature-dependent miscibility with water, homogeneous liquid-liquid extraction (HHLE) can be used as a solvent extraction technique. Here, mixing on a molecular level in the homogeneous phase is achieved, drastically increasing the mass transfer and diffusion in the system. For a better understanding of the solvent extraction process, different parameters are investigated to gain insights for future IL-based systems.

The specific objectives of this PhD research are:

1) To synthesize and characterize new functionalized ionic liquids with non-fluorinated anions;
2) To investigate the temperature-dependent miscibility of the ionic liquids with water;
3) To determine the upper/lower critical solution temperatures and phase diagrams of the systems;
4) To use the ionic liquids for homogeneous liquid-liquid extraction of metal ions;
5) To investigate different extraction parameters, the underlying extraction mechanism, stripping of the metal ion from the ionic liquid and the possibility to recycle the ionic liquid.

CHAPTER 3

HALOGEN-FREE SYNTHESIS OF IMIDAZOLIUM IONIC LIQUIDS

This chapter has been published and is reproduced here with permission from The Royal Society of Chemistry.

Depuydt, D., Van den Bossche, A., Dehaen, W., Binnemans, K. (2016). Halogen-free synthesis of symmetrical 1,3-dialkylimidazolium ionic liquids using non-enolisable starting materials. *RSC Advances, 6* (11), 8848-8859.

The experimental work was executed by Arne Van den Bossche under supervision of this thesis' author. The publication was written by the latter.

The supplementary information of this publication, containing all ^{1}H NMR and ^{13}C NMR spectra of the synthesized compounds can be found online:

http://www.rsc.org/suppdata/c5/ra/c5ra22798d/c5ra22798d1.pdf

Graphical Abstract

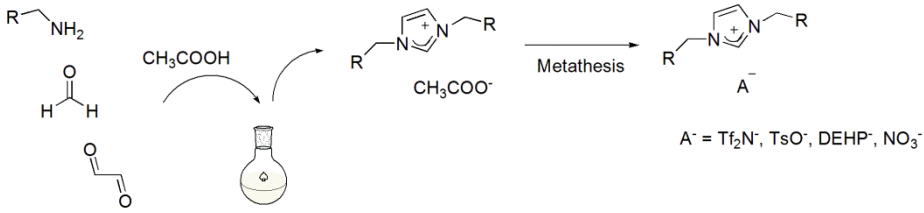

Halogen-free synthesis of symmetrical 1,3-dialkylimidazolium ionic liquids starting from their building blocks followed by metathesis reaction towards desired anions.

Abstract

Imidazolium ionic liquids were synthesized from readily available molecules: aldehydes, 1,2-carbonyl components, alkyl amines and acids in a halogen-free procedure. Since the use of enolizable carbonyl functions is not compatible with the modified Debus-Radziszewski reaction, symmetrical 1,3-dialkyl imidazolium ionic liquids were made. The use of strong acids, like sulfuric acid, leads to protonation of the amine, low yields and side products that are difficult to remove. Changing the acid in the synthesis to acetic acid greatly improved the isolated yield and produced pure imidazolium acetate ionic liquids. From these imidazolium acetate compounds, many other ionic liquids could be prepared using different metathesis strategies. These strategies were dependent on the acidity of the conjugate acid of the anion, the acid volatility and the hydrophilicity of the used reagents and resulting ionic liquid. The following anions were introduced: bis(trifluoromethylsulfonyl)imide ($[Tf_2N]^-$), *p*-toluenesulfonate (tosylate, $[TsO]^-$), bis(2-ethylhexyl)phosphate ($[DEHP]^-$) and nitrate ($[NO_3]^-$). The impact of the different anions on the properties of the ionic liquids was investigated.

3.1 Introduction

Ionic liquids (ILs) consist entirely of ion pairs and preferably melt below 100 °C.[1-3] The low volatility, high thermal stability and non-flammable character of ILs make these compounds of interest as replacements for volatile organic solvents or catalysts in industrial processes.[3,4] Imidazolium heterocycles are popular cations in ILs since their aromaticity makes them highly stable. The most investigated imidazolium compounds are 1-alkyl-3-methylimidazolium salts, due to the easy alkylation of commercially available *N*-methylimidazoles.[5-11] The most intensively studied imidazolium compounds contain the cations 1-ethyl-3-methylimidazolium $[C_2mim]^+$ or 1-butyl-3-methylimidazolium $[C_4mim]^+$, because these ionic liquids are the cheapest to prepare and possess relatively low melting points and viscosities. Imidazolium compounds with more than two alkyl chains are rarely used as ILs, as they require more complex synthetic procedures. The synthesis of highly substituted imidazoles is therefore under-explored. Maton *et al*. have described the synthesis of highly substituted imidazolium ionic liquids from readily available molecules, at 120 °C in pressure vials, yet the products were obtained in low yields.[12,13] In the literature on imidazole synthesis, phenyl is the most often used substituent. For instance, the oldest synthetic route to obtain imidazole is the Debus-Radziszewski method where a benzil (1,2-diphenylethane-1,2-dione) molecule reacts with formaldehyde and two ammonia equivalents to form an imidazole ring.[14] This approach was used in the synthesis of lophine (2,4,5-triphenylimidazole) by Radziszewski.[15] In the modified Debus-Radziszewski method, an improvement was made yielding a tetrasubstituted imidazole ring.[16] One of the ammonia equivalents is replaced by an alkylamine in this modification, which results in an extra substituent on the final imidazole product. An acid is added as a catalyst. To limit the amount of reagents and thus to simplify the reaction procedure, the ammonia and acid are mostly added as one compound: an ammonium salt. The reaction couples all five functionalities, primary amine, ammonium and three carbonyl groups, into an imidazole ring with four side chains. The possible side chains however, are limited. First of all, none of the side chains should contain a functional group which can react with amines or carbonyl functions or which may interfere in another way in the reaction. No selectivity is observed for the incorporation of asymmetric 1,2-diketones, resulting in a mixture of imidazole rings with mirrored substitution of the diketone substituents. This problem can

easily be avoided by using symmetric 1,2-diketones with identical substituents, as described in a patent by Arduengo *et al*.[16] A library of mono-, di-, tri- and tetra-substituted imidazoles was synthesized by Gelens *et al.* using microwave irradiation in a multicomponent reaction.[17] Interestingly, this procedure only works for benzils and very poor yields were observed for combinations using enolizable 1,2-dioxoalkanes. The direct synthesis of imidazolium compounds can also be performed by replacing the ammonium salt by another amine equivalent. This method was described by Zimmermann *et al.* for the synthesis of hydrophilic imidazolium ionic liquids, where glyoxal and formaldehyde were used as 1,2-carbonyl components and aldehyde, respectively, in the reaction with the two amine equivalents.[18] The acid used in the synthesis is needed in a stoichiometric amount since the conjugate base will become the anion required by the imidazolium cation, forming an ionic liquid. Using a mixture of amines would result in a statistical mixture of three different imidazolium salts, so only one amine can be used, leading to symmetrically substituted 1,3-dialkylimidazolium salts. A major advantage, however, is that this synthetic method directly yields the imidazolium ionic liquids in one step, which can even be performed in a halogen-free fashion if the correct acid is chosen.[18] In this paper, it is shown that the direct synthesis of highly substituted imidazolium ionic liquids (*i.e.* with more than two substituents) is not feasible when enolizable starting materials are used. A versatile, halogen-free synthesis procedure for 1,3-dialkylimidazolium ionic liquids was developed to obtain a series of acetate ionic liquids which can be transformed into other ionic liquids by anion-exchange reactions.

A library of symmetrical 1,3-dialkylimidazolium ionic liquids was synthesized (**Figure 3.1**).

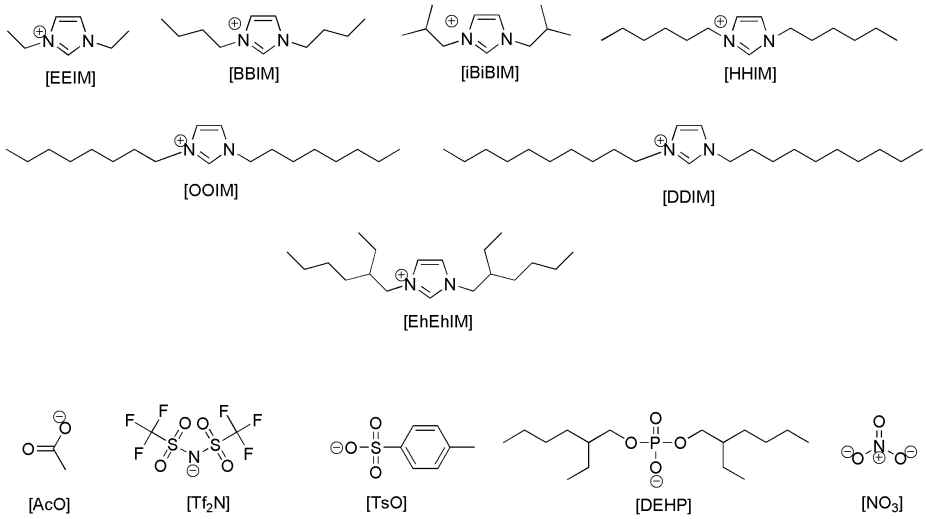

Figure 3.1 Overview of all the synthesized ILs, combination of cations 1,3-diethylimidazolium $[EEIM]^+$, 1,3-diisobutylimidazolium $[iBiBIM]^+$, 1,3-dibutylimidazolium $[BBIM]^+$, 1,3-dihexylimidazolium $[HHIM]^+$, 1,3-bis(2-ethylhexyl)imidazolium $[EhEhIM]^+$, 1,3-dioctylimidazolium $[OOIM]^+$ and 1,3-didecylimidazolium $[DDIM]^+$ and anions acetate $[AcO]^-$, bis(trifluoromethylsulfonyl)imide $[Tf_2N]^-$, *p*-toluenesulfonate $[TsO]^-$, bis(2-ethylhexyl)phosphate $[DEHP]^-$ and nitrate $[NO_3]^-$.

3.2 Experimental

3.2.1 Chemicals

Glyoxal (40 wt% in water), *n*-butylamine (99.5%), ethylamine (70 wt% in water), 2-ethylhexylamine (99%) and *n*-octylamine (99+%) were purchased from Acros Organics (Geel, Belgium). Diethyl ether (technical grade) and sodium hydroxide (Normapur) were obtained from VWR (Heverlee, Belgium). *n*-Decylamine (98%) was purchased from TCI Europe (Zwijndrecht, Belgium). Hydrogen bis(trifluoromethylsulfonyl)imide (80 wt% in water) was bought from Iolitec (Heilbronn, Germany). Bis(2-ethylhexyl)phosphate (97%), isobutylamine (99%), *n*-hexylamine (99%), *p*-toluenesulfonic acid monohydrate (≥98.5%) and nitric acid (65% in water) were bought from Sigma-Aldrich (Diegem, Belgium). Dichloromethane (analytical reagent grade), acetic acid (analytical reagent grade) and formaldehyde (37 wt% in water) were obtained from Fisher Scientific Limited (Loughborough, UK). All chemicals were used without purification.

3.2.2 General

The ^{1}H NMR and ^{13}C NMR spectra were recorded on a Bruker Avance 300 spectrometer (operating at 300 MHz for ^{1}H, 75 MHz for ^{13}C). The chemical shifts are noted in parts per million (ppm), referenced to TMS for ^{1}H and ^{13}C. All solutions were made in $CDCl_3$ or DMSO-d_6. The spectra were analyzed with SpinWorks software. All spectra can be found in the Electronic Supporting Information. The Fourier Transform Infrared (FTIR) spectra of the ILs were recorded by a Bruker Vertex 70 spectrometer via the attenuated total reflectance (ATR) technique with a Bruker Platinum ATR accessory. The OPUS software package was used for analysis of the FTIR spectra. The water content was determined by coulometric KF titration using a Mettler-Toledo DL39 titrator. The viscosity of the ionic liquids was measured using an automatic Brookfield plate-cone viscometer, Model LVDV-II CP (Brookfield Engineering Laboratories, USA) equipped with a CPE-40 cone spindle. The elemental analysis of carbon, hydrogen and nitrogen (CHN analysis) was performed on a CE-instruments EA-1110 elemental analyzer for acetate and bistriflimide ionic liquids, the tosylate, bis(2-ethylhexyl)phosphate and nitrate ionic liquids were measured on an Interscience Flash 2000 CHNS/O analyzer. TGA measurements were performed on a TGA-Q500 (TA Instruments).

3.2.3 Synthesis

General reaction procedure for synthesis of acetate ILs

Two equivalents of amine were cooled down to 0 °C in an ice bath. A mixture of formaldehyde (37 wt% in water, 1 eq.) and acetic acid (1.5 eq.) was added dropwise while keeping the temperature below 10 °C. The mixture was stirred for 30 min at 0 °C, after which the glyoxal (40 wt% in water, 1 eq.) was added and the reaction mixture was stirred overnight at RT. The solution was washed with diethyl ether until the organic phase was colorless and the water was removed with a rotary evaporator. The product was dried on a Schlenk line at 50 °C overnight.

1,3-Diethylimidazolium acetate [EEIM][AcO]

Dark orange oil (21.60 g, 0.117 mol, 94%). ^{1}H NMR: (300 MHz, DMSO-d_6, δ/ppm): 9.77 (s, 1H, CH), 7.85 (s, 2H, 2 CH), 4.22 (m, 4H, 2 CH_2-N), 1.64 (s, 3H, CH_3), 1.42 (m, 6H, 2 CH_3). ^{13}C NMR: (75 MHz, DMSO-d_6, δ/ppm): 173.04 (C=O), 136.21 (N-CH-N), 122.02 (2 CH-N), 44.02 (2 CH_2-N), 24.85 (2 CH_3), 15.08 (CH_3). FTIR: (v/cm^{-1}): 2960, 2934, 2874 (C-H stretch), 1577 (C=O stretch), 1381 (C-O stretch). CHN analysis: (calculated for $C_9H_{16}N_2O_2 \cdot 2H_2O$) (220.27 g mol^{-1}): C 48.20% (49.08%), H 8.87% (9.15%), N 12.65% (12.72%).

1,3-Dibutylimidazolium acetate [BBIM][AcO]

Dark orange oil (24.49 g, 0.102 mol, 82%). ^{1}H NMR: (300 MHz, DMSO-d_6, δ/ppm): 9.96 (s, 1H, CH), 7.88 (s, 2H, 2 CH), 4.21 (m, 4H, 2 CH_2-N), 1.78 (m, 4H, 2 CH_2), 1.63 (s, 3H, CH_3), 1.23 (m, 4H, 2 CH_2), 0.90 (m, 6H, 2 CH_3). ^{13}C NMR: (75 MHz, DMSO-d_6, δ/ppm): 173.52 (C=O), 137.50 (N-CH-N), 122.86 (2 CH-N), 49.00 (CH_2-N), 48.82 (CH_2-N), 31.84 (2 CH_2), 25.61 (2 CH_2), 19.24 (2 CH_3), 13.70 (CH_3). FTIR: (v/cm^{-1}): 2960, 2934, 2874 (C-H stretch), 1577 (C=O stretch), 1381 (C-O stretch). CHN analysis: (calculated for $C_{13}H_{24}N_2O_2 \cdot H_2O$) (258.36 g mol^{-1}): C 59.57% (60.44%), H 10.42% (10.14%), N 10.63% (10.84%).

1,3-Diisobutylimidazolium acetate [iBiBIM][AcO]

Dark orange solid (26.93 g, 0.112 mol, 90%). ^{1}H NMR: (300 MHz, DMSO-d_6, δ/ppm): 9.97 (s, 1H, CH), 7.88 (s, 2H, 2 CH), 4.08 (m, 4H, 2 CH_2-N), 2.11 (m, 2H, 2 CH), 1.67 (s, 3H, CH_3), 0.87 (m, 6H, 2 CH_3). ^{13}C NMR: (75 MHz, DMSO-d_6, δ/ppm): 173.47 (C=O), 137.15 (N-CH-N), 122.74 (2 CH-N), 55.33

(2 CH_2-N), 28.67 (2 CH), 24.71 (4 CH_3), 18.98 (CH_3). FTIR: (v/cm^{-1}): 2954, 2929, 2869 (C-H stretch), 1574 (C=O stretch), 1381 (C-O stretch). CHN analysis: (calculated for $C_{13}H_{24}N_2O_2 \cdot H_2O$) (258.36 g mol^{-1}): C 60.65% (60.44%), H 10.14% (10.14%), N 10.55% (10.84%).

1,3-Dihexylimidazolium acetate [HHIM][AcO]

Dark orange oil (26.42 g, 0.089 mol, 71%). ^{1}H NMR: (300 MHz, DMSO-d_6, δ/ppm): 9.91 (s, 1H, CH), 7.87 (s, 2H, 2 CH), 4.19 (m, 4H, 2 CH_2-N), 1.79 (m, 4H, 2 CH_2), 1.62 (s, 3H, CH_3), 1.25 (m, 12H, 6 CH_2), 0.85 (m, 6H, 2 CH_3). ^{13}C NMR: (75 MHz, DMSO-d_6, δ/ppm): 173.35 (C=O), 137.46 (N-CH-N), 123.00 (CH-N), 122.86 (CH-N), 49.15 (2 CH_2-N), 30.96 (2 CH_2), 29.75 (2 CH_2), 25.67 (CH_3), 25.57 (CH_2), 22.33 (2 CH_2), 14.22 (2 CH_3). FTIR: (v/cm^{-1}): 2956, 2928, 2859 (C-H stretch), 1579 (C=O stretch), 1381 (C-O stretch). CHN analysis: (calculated for $C_{17}H_{32}N_2O_2 \cdot 1.5H_2O$) (323.47 g mol^{-1}): C 63.23% (63.12%), H 12.91% (10.91%), N 8.65% (8.66%).

1,3-Dioctylimidazolium acetate [OOIM][AcO]

Dark orange oil (24.38 g, 0.069 mol, 55%). ^{1}H NMR: (300 MHz, DMSO-d_6, δ/ppm): 9.97 (s, 1H, CH), 7.89 (s, 2H, 2 CH), 4.29 (m, 4H, 2 CH_2-N), 1.79 (m, 4H, 2 CH_2), 1.63 (s, 3H, CH_3), 1.24 (m, 20H, 10 CH_2), 0.85 (m, 6H, 2 CH_3). ^{13}C NMR: (75 MHz, DMSO-d_6, δ/ppm): 173.53 (C=O), 137.55 (N-CH-N), 123.02 (CH-N), 122.86 (CH-N), 49.13 (2 CH_2-N), 31.60 (2 CH_2), 29.82 (2 CH_2), 28.98 (2 CH_2), 28.77 (2 CH_2), 25.94 (2 CH_2), 25.62 (CH_3), 22.50 (2 CH_2), 14.32 (2 CH_3). FTIR: (v/cm^{-1}): 2956, 2924, 2856 (C-H stretch), 1576 (C=O stretch), 1385 (C-O stretch). CHN analysis: (calculated for $C_{21}H_{40}N_2O_2 \cdot H_2O$) (370.57 g mol^{-1}): C 68.60% (68.06%), H 13.88% (11.42%), N 7.57% (7.56%).

1,3-Didecylimidazolium acetate [DDIM][AcO]

Brown oil (27.07 g, 0.066 mol, 53%). ^{1}H NMR: (300 MHz, DMSO-d_6, δ/ppm): 9.76 (s, 1H, CH), 7.86 (s, 2H, 2 CH), 4.19 (m, 4H, 2 CH_2-N), 1.79 (m, 4H, 2 CH_2), 1.76 (s, 3H, CH_3), 1.23 (m, 28H, 14 CH_2), 0.85 (m, 6H, 2 CH_3). ^{13}C NMR: (75 MHz, DMSO-d_6, δ/ppm): 172.98 (C=O), 137.52 (N-CH-N), 122.87 (2 CH-N), 52.02 (2 CH_2-N), 30.64 (2 CH_2), 29.30 (2 CH_2), 27.66 (2 CH_2), 24.67 (CH_3), 22.74 (2 CH_2), 22.34 (4 CH_2), 22.33 (4 CH_2), 13.76 (2 CH_2), 10.10 (2 CH_3). FTIR: (v/cm^{-1}): 2958, 2926, 2853 (C-H stretch), 1578 (C=O stretch), 1385 (C-O stretch). CHN analysis: (calculated for $C_{25}H_{48}N_2O_2$) (408.66 g mol^{-1}): C 74.54% (73.48%), H 14.92% (11.84%), N 6.58% (6.85%).

1,3-Bis(2-ethylhexyl)imidazolium acetate [EhEhIM][AcO]

Highly viscous, dark orange oil (20.83 g, 0.059 mol, 47%). ^{1}H NMR: (300 MHz, DMSO-d_6, δ/ppm): 9.83 (s, 1H, CH), 7.87 (s, 2H, 2 CH), 4.13 (d, 7.0 Hz, 4H, 2 CH_2-N), 1.84 (m, 2H, 2 CH), 1.65 (s, 3H, CH_3), 1.25 (m, 16H, 8 CH_2), 0.85 (m, 12H, 4 CH_3). ^{13}C NMR: (75 MHz, DMSO-d_6, δ/ppm): 173.10 (C=O), 136.90 (N-CH-N), 122.40 (2 CH-N), 48.7 (2 CH_2-N), 31.28 (2 CH), 30.61 (2 CH_2), 29.32 (2 CH_2), 28.87 (2 CH_2), 28.70 (2 CH_2), 28.68 (2 CH_2), 28.34 (2 CH_2), 25.45 (CH_3), 24.38 (2 CH_2), 22.08 (2 CH_2), 13.87 (4 CH_3). FTIR: (v/cm^{-1}): 2959, 2928, 2861 (C-H stretch), 1578 (C=O stretch). CHN analysis: (calculated for $C_{21}H_{40}N_2O_2 \cdot H_2O$) (370.57 g mol^{-1}): C 68.35% (68.06%), H 13.70% (11.42%), N 7.54% (7.56%).

General reaction procedure for synthesis of bis(trifluoromethylsulfonyl) imide ILs

Hydrogen bis(trifluoromethylsulfonyl)imide is a superacid,[19] therefore the acid was used in the metathesis reaction. 1,3-Dialkylimidazolium acetate (5 mmol) and hydrogen bis(trifluoromethylsulfonyl)imide (80 wt% in water, 5 mmol, 1.76 g) were dissolved in water and stirred at room temperature for 2 h. A hydrophobic layer appeared. Dichloromethane was added to the reaction mixture until the entire hydrophobic liquid was dissolved. The dichloromethane layer was separated from the water phase and washed with water. After removing the dichloromethane by evaporation, the product was dried on a Schlenk line at 50 °C.

1,3-Diethylimidazolium bis(trifluoromethylsulfonyl)imide [EEIM][Tf_2N]

Brown oil (1.428 g, 3.52 mmol, 71%). ^{1}H NMR: (300 MHz, DMSO-d_6, δ/ppm): 9.18 (s, 1H, CH), 7.80 (s, 2H, 2 CH), 4.19 (m, 4H, 2 CH_2), 1.43 (m, 6H, 2 CH_3). ^{13}C NMR: (75 MHz, DMSO-d_6, δ/ppm): 134.40 (N-CH-N), 122.18 (2 CH-N), 119.48 (q, 320 Hz, 2 CF_3), 45.29 (2 CH_2-N), 14.88 (2 CH_3). FTIR: (v/cm^{-1}): 3153, 3118, 2991 (C-H stretch), 1566 (aromatic C-N stretch), 1455 (aromatic C-C stretch), 1347, 1330, 1135 (S=O stretch), 1180 (C-F stretch), 1053 (N-S stretch), 613 (SO_2 bending), 570, 513 (C-F bending). CHN analysis: (calculated for $C_9H_{13}N_3O_4S_2F_6$) (405.34 g mol^{-1}): C 27.11% (26.67%), H 3.72% (3.23%), N 10.23% (10.37%).

1,3-Dibutylimidazolium bis(trifluoromethylsulfonyl)imide
[BBIM][Tf_2N]

Brown oil (2.023 g, 4.38 mmol, 88%). ^{1}H NMR: (300 MHz, $CDCl_3$, δ/ppm): 8.78 (s, 1H, CH), 7.36 (s, 2H, 2 CH), 4.18 (t, 7.5 Hz, 4H, 2 CH_2-N), 1.85 (m, 4H, 2 CH_2), 1.36 (m, 4H, 2 CH_2), 0.96 (t, 7.5 Hz, 6H, 2 CH_3). ^{13}C NMR: (75 MHz, $CDCl_3$, δ/ppm): 130.55 (N-CH-N), 117.65 (2 CH-N), 115.07 (q, 320 Hz, 2 CF_3), 45.16 (2 CH_2-N), 27.21 (2 CH_2), 14.54 (2 CH_2), 8.41 (2 CH_3). FTIR: (v/cm^{-1}): 2967, 2939, 2879 (C-H stretch), 1565 (aromatic C-N stretch), 1465 (aromatic C-C stretch), 1348, 1330, 1135 (S=O stretch), 1181 (C-F stretch), 1054 (N-S stretch), 614 (SO_2 bending), 570, 512 (C-F bending). CHN analysis: (calculated for $C_{13}H_{21}N_3O_4S_2F_6$) (461.44 g mol^{-1}): C 33.82% (33.84%), H 5.27% (4.59%), N 9.06% (9.11%).

1,3-Diisobutylimidazolium bis(trifluoromethylsulfonyl)imide
[iBiBIM][Tf_2N]

Brown oil (1.382 g, 2.99 mmol, 60%). ^{1}H NMR: (300 MHz, $CDCl_3$, δ/ppm): 8.81 (s, 1H, CH), 7.33 (s, 2H, 2 CH), 4.02 (d, 7.5 Hz, 4H, 2 CH_2-N), 2.15 (m, 2H, 2 CH), 0.95 (d, 6.5 Hz, 12H, 4 CH_3). ^{13}C NMR: (75 MHz, $CDCl_3$, δ/ppm): 135.90 (N-CH-N), 122.77 (2 CH-N), 119.83 (q, 320 Hz, 2 CF_3), 56.92 (2 CH_2-N), 29.44 (2 CH), 19.09 (4 CH_3). FTIR: (v/cm^{-1}): 2967, 2926, 2856 (C-H stretch), 1564 (aromatic C-N stretch), 1465 (aromatic C-C stretch), 1349, 1135 (S=O stretch), 1185 (C-F stretch), 1056 (N-S stretch), 616 (SO_2 bending), 571, 513 (C-F bending). CHN analysis: (calculated for $C_{13}H_{21}N_3O_4S_2F_6$) (461.44 g mol^{-1}): C 33.92% (33.84%), H 5.12% (4.59%), N 8.95% (9.11%).

1,3-Dihexylimidazolium bis(trifluoromethylsulfonyl)imide
[HHIM][Tf_2N]

Orange oil (2.372 g, 4.58 mmol, 92%). ^{1}H NMR: (300 MHz, $CDCl_3$, δ/ppm): 8.80 (s, 1H, CH), 7.35 (s, 2H, 2 CH), 4.18 (t, 7.5 Hz, 4H, 2 CH_2-N), 1.86 (m, 4H, 2 CH_2), 1.31 (m, 12H, 6 CH_2), 0.88 (m, 6H, 2 CH_3). ^{13}C NMR: (75 MHz, $CDCl_3$, δ/ppm): 135.32 (N-CH-N), 122.41 (2 CH-N), 119.85 (q, 320 Hz, 2 CF_3), 50.16 (2 CH_2-N), 30.90 (2 CH_2), 30.04 (2 CH_2), 25.67 (2 CH_2), 22.26 (2 CH_2), 13.75 (2 CH_3). FTIR: (v/cm^{-1}): 2960, 2933, 2863 (C-H stretch), 1564 (aromatic C-N stretch), 1465 (aromatic C-C stretch), 1348, 1135 (S=O stretch), 1183 (C-F stretch), 1055 (N-S stretch), 615 (SO_2 bending), 570, 513

(C-F bending). CHN analysis: (calculated for $C_{17}H_{29}N_3O_4S_2F_6$) (517.55 g mol^{-1}): C 39.29% (39.45%), H 6.34% (5.65%), N 8.04% (8.12%).

1,3-Dioctylimidazolium bis(trifluoromethylsulfonyl)imide [OOIM][Tf_2N]

Orange oil (2.65 g, 4.62 mmol, 93%). ^{1}H NMR: (300 MHz, $CDCl_3$, δ/ppm): 8.81 (s, 1H, CH), 7.33 (s, 2H, 2 CH), 4.18 (t, 7.5 Hz, 4H, 2 CH_2-N), 1.86 (m, 4H, 2 CH_2), 1.29 (m, 20H, 10 CH_2), 0.87 (m, 6H, 2 CH_3). ^{13}C NMR: (75 MHz, $CDCl_3$, δ/ppm): 135.32 (N-CH-N), 122.38 (2 CH-N), 119.82 (q, 320 Hz, 2 CF_3), 50.18 (2 CH_2-N), 31.58 (2 CH_2), 30.10 (2 CH_2), 28.91 (2 CH_2), 28.77 (2 CH_2), 26.04 (2 CH_2), 22.51 (2 CH_2), 13.96 (2 CH_3). FTIR: (v/cm^{-1}): 2928, 2859 (C-H stretch), 1564 (aromatic C-N stretch), 1465 (aromatic C-C stretch), 1349, 1135 (S=O stretch), 1184 (C-F stretch), 1055 (N-S stretch), 616 (SO_2 bending), 570, 513 (C-F bending). CHN analysis: (calculated for $C_{21}H_{37}N_3O_4S_2F_6$) (573.66 g mol^{-1}): C 43.94% (43.97%), H 7.36% (6.50%), N 7.29% (7.32%).

1,3-Didecylimidazolium bis(trifluoromethylsulfonyl)imide [DDIM][Tf_2N]

Orange oil (1.523 g, 2.42 mmol, 48%). ^{1}H NMR: (300 MHz, $CDCl_3$, δ/ppm): 8.83 (s, 1H, CH), 7.30 (s, 2H, 2 CH), 4.19 (t, 7.5 Hz, 4H, 2 CH_2-N), 1.87 (m, 4H, 2 CH_2), 1.28 (m, 28H, 14 CH_2), 0.87 (m, 6H, 2 CH_3). ^{13}C NMR: (75 MHz, $CDCl_3$, δ/ppm): 135.38 (N-CH-N), 122.36 (2 CH-N), 119.81 (q, 320 Hz, 2 CF_3), 50.22 (2 CH_2-N), 31.82 (2 CH_2), 30.12 (2 CH_2), 29.39 (2 CH_2), 29.29 (2 CH_2), 29.21 (2 CH_2), 28.87 (2 CH_2), 26.09 (2 CH_2), 22.63 (2 CH_2), 14.05 (2 CH_3). FTIR: (v/cm^{-1}): 3148, 2926, 2856 (C-H stretch), 1564 (aromatic C-N stretch), 1465 (aromatic C-C stretch), 1349, 1135 (S=O stretch), 1184 (C-F stretch), 1055 (N-S stretch), 616 (SO_2 bending), 571, 513 (C-F bending). CHN analysis: (calculated for $C_{25}H_{45}N_3O_4S_2F_6 \cdot H_2O$) (647.78 g mol^{-1}): C 46.45% (46.35%), H 7.87% (7.31%), N 6.58% (6.49%).

1,3-Bis(2-ethylhexyl)imidazolium bis(trifluoromethylsulfonyl)imide [EhEhIM][Tf_2N]

Orange oil (2.47 g, 4.31 mmol, 86%). ^{1}H NMR: (300 MHz, $CDCl_3$, δ/ppm): 8.77 (s, 1H, CH), 7.33 (s, 2H, 2 CH), 4.10 (d, 7.5 Hz, 4H, 2 CH_2-N), 1.83 (m, 2H, 2 CH), 1.23 (m, 16H, 8 CH_2), 0.90 (m, 12H, 4 CH_3). ^{13}C NMR: (75 MHz, $CDCl_3$, δ/ppm): 136.13 (N-CH-N), 122.81 (2 CH-N), 119.84 (q, 320 Hz, 2 CF_3), 53.60 (2 CH_2-N), 40.01 (2 CH), 29.82 (2 CH_2), 28.14 (2 CH_2), 23.18 (2

CH_2), 22.73 (2 CH_2), 13.76 (2 CH_3), 10.08 (2 CH_3). FTIR: (v/cm^{-1}): 2963, 2933, 2864 (C-H stretch), 1563 (aromatic C-N stretch), 1462 (aromatic C-C stretch), 1349, 1135 (S=O stretch), 1184 (C-F stretch), 1055 (N-S stretch), 615 (SO_2 bending), 570, 513 (C-F bending). CHN analysis: (calculated for $C_{21}H_{37}N_3O_4S_2F_6 \cdot H_2O$) (591.67 g mol^{-1}): C 43.11% (42.63%), H 7.35% (6.64%), N 7.25% (7.10%).

General reaction procedure for synthesis of tosylate ILs

p-Toluenesulfonic acid is a strong acid with a pK_a of -2.8, therefore the acid was suitable in the metathesis reaction. Acetic acid could be safely removed by evaporation if necessary, due to the high boiling point of the *p*-toluenesulfonic acid. 1,3-Dialkylimidazolium acetate (5 mmol) was dissolved in water and *p*-toluenesulfonic acid (monohydrate, 5 mmol, 0.952 g) was added and the reaction mixture was stirred overnight at room temperature. Depending on the hydrophobicity of the *p*-toluenesulfonate ionic liquids, different purification steps were required. In case of the water-soluble ionic liquids: 1,3-diethylimidazolium tosylate, 1,3-dibutylimidazolium tosylate and 1,3-diisobutylimidazolium tosylate, water and excess of acetic acid were removed by evaporation and further drying on a Schlenk line at 70 °C. For 1,3-di(2-ethylhexyl)imidazolium tosylate and 1,3-dihexylimidazolium tosylate, water-insoluble products were formed, the water layer was separated and ^{1}H NMR indicated that a little excess 1,3-dialkylimidazolium acetate was present in the product. After redissolving the product in water, an excess of *p*-toluenesulfonic acid was added. The remaining *p*-toluenesulfonic acid and acetic acid were washed out with water and the product was dried on a Schlenk line. In the case of 1,3-dioctylimidazolium tosylate and 1,3-didecylimidazolium tosylate, a suspension was formed after reaction. The solid product was separated using a glass filter, washed with water and dried in the vacuum oven.

1,3-Diethylimidazolium tosylate [EEIM][TsO]

Dark brown liquid (1.36 g, 4.59 mmol, 92%). ^{1}H NMR: (300 MHz, $CDCl_3$, δ/ppm): 9.75 (s, 1H, CH), 7.75 (s, 2H, 2 CH), 7.29 (s, 2H, 2 CH), 7.14 (s, 2H, 2 CH), 4.28 (m, 4H, 2 CH_2), 2.34 (s, 3H, CH_3), 1.50 (m, 6H, 2 CH_3). ^{13}C NMR: (75 MHz, $CDCl_3$, δ/ppm): 142.05 (C-S), 140.19 (C-CH_3), 136.52 (CH), 128.81 (2 CH), 125.97 (2 CHN), 121.68 (2 CH), 45.07 (2 CH_2), 21.33 (1 CH_3), 15.34 (2 CH_3). FTIR: (v/cm^{-1}): 3097-2876 (C-H stretch), 1563 (N-C-N

stretch), 1470 (C-C stretch), 1166, 1120 (SO_2 stretch), 1032, 1010, 816 (C-H bending), 679 (S=O stretch), 565 (C-S bending). CHN analysis: (calculated for $C_{14}H_{20}N_2O_3S \cdot H_2O$) (314.4 g mol^{-1}): C 53.50% (53.48%), H 7.88% (7.08%), N 8.07% (8.91%).

1,3-Dibutylimidazolium tosylate [BBIM][TsO]

Light brown liquid (1.76 g, 4.99 mmol, 99%). ^{1}H NMR: (300 MHz, $CDCl_3$, δ/ppm): 9.78 (s, 1H, CH), 7.77 (s, 2H, 2 CH), 7.25 (s, 2H, 2 CH), 7.14 (s, 2H, 2 CH), 4.23 (m, 4H, 2 CH_2), 2.34 (s, 3H, CH_3), 1.81 (m, 4H, 2 CH_2), 1.30 (m, 4H, 2 CH_2), 0.91 (m, 6H, 2 CH_3). ^{13}C NMR: (75 MHz, $CDCl_3$, δ/ppm): 142.20 (C-S), 140.04 (C-CH_3), 137.53 (CH), 128.73 (2 CH), 126.05 (2 CHN), 121.76 (2 CH), 49.76 (2 CH_2), 32.05 (2 CH_2), 21.33 (CH_3), 19.43 (2 CH_2), 13.41 (2 CH_3). FTIR: (v/cm^{-1}): 3097-2874 (C-H stretch), 1564 (N-C-N stretch), 1460 (C-C stretch), 1166, 1120 (SO_2 stretch), 1033, 1010, 816 (C-H bending), 680 (S=O stretch), 566 (C-S bending). CHN analysis: (calculated for $C_{18}H_{28}N_2O_3S \cdot 0.5H_2O$) (361.50 g mol^{-1}): C 59.73% (59.80%), H 8.70% (8.09%), N 7.47% (7.75%).

1,3-Diisobutylimidazolium tosylate [iBiBIM][TsO]

Light brown powder (1.64 g, 4.65 mmol, 93%). ^{1}H NMR: (300 MHz, $CDCl_3$, δ/ppm): 9.78 (s, 1H, CH), 7.76 (s, 2H, 2 CH), 7.23 (s, 2H, 2 CH), 7.15 (s, 2H, 2 CH), 4.10 (m, 4H, 2 CH_2), 2.35 (s, 3H, CH_3), 2.13 (m, 2H, 2 CH), 0.91 (m, 12H, 4 CH_3). ^{13}C NMR: (75 MHz, $CDCl_3$, δ/ppm): 141.85 (C-S), 140.22 (C-CH_3), 137.97 (CH), 128.77 (2 CH), 126.11 (2 CHN), 122.17 (2 CH), 56.79 (2 CH_2), 29.40 (2 CH), 21.34 (CH_3), 19.33 (4 CH_3). FTIR: (v/cm^{-1}): 3141-2982 (C-H stretch), 1565 (N-C-N stretch), 1450 (C-C stretch), 1165, 1119 (SO_2 stretch), 1032, 1009, 817 (C-H bending), 680 (S=O stretch), 565 (C-S bending). CHN analysis: (calculated for $C_{18}H_{28}N_2O_3S \cdot H_2O$) (370.51 g mol^{-1}): C 58.64% (58.35%), H 8.87% (8.16%), N 7.27% (7.56%).

1,3-Dihexylimidazolium tosylate [HHIM][TsO]

Light brown powder (1.36 g, 3.32 mmol, 66%). ^{1}H NMR: (300 MHz, $CDCl_3$, δ/ppm): 10.22 (s, 1H, CH), 7.81 (s, 2H, 2 CH), 7.17 (s, 2H, 2 CH), 7.12 (s, 2H, 2 CH), 4.29 (m, 4H, 2 CH_2), 2.36 (s, 3H, CH_3), 1.86 (m, 4H, 2 CH_2), 1.29 (m, 12H, 6 CH_2), 0.87 (m, 6H, 2 CH_3). ^{13}C NMR: (75 MHz, $CDCl_3$, δ/ppm): 143.79 (C-S), 139.13 (C-CH_3), 138.44 (CH), 128.55 (2 CH), 125.96 (2 CHN), 121.35 (2 CH), 50.10 (CH_3), 31.08 (2 CH_2), 30.18 (2 CH_2), 25.88 (2 CH_2), 22.39 (2 CH_2), 21.30 (2 CH_2), 13.91 (2 CH_3). FTIR: (v/cm^{-1}): 3086-2870 (C-H

stretch), 1565 (N-C-N stretch), 1466 (C-C stretch), 1194, 1121 (SO_2 stretch), 1035, 1012, 814 (C-H bending), 679 (S=O stretch), 561 (C-S bending). CHN analysis: (calculated for $C_{22}H_{36}N_2O_3S \cdot 0.5H_2O$) (417.60 g mol^{-1}): C 63.87% (63.27%), H 8.56% (8.93%), N 7.73% (6.71%).

1,3-Dioctylimidazolium tosylate [OOIM][TsO]

White powder (1.98 g, 4.26 mmol, 85%). ^{1}H NMR: (300 MHz, $CDCl_3$, δ/ppm): 10.24 (s, 1H, CH), 7.82 (s, 2H, 2 CH), 7.15 (s, 2H, 2 CH), 7.13 (s, 2H, 2 CH), 4.29 (m, 4H, 2 CH_2), 2.34 (s, 3H, CH_3), 1.87 (m, 4H, 2 CH_2), 1.27 (m, 20H, 10 CH_2), 0.87 (m, 6H, 2 CH_3). ^{13}C NMR: (75 MHz, $CDCl_3$, δ/ppm): 143.83 (C-S), 139.10 (C-CH_3), 138.40 (CH), 128.55 (2 CH), 125.96 (2 CHN), 121.38 (2 CH), 50.10 (2 CH_2), 31.69 (2 CH_2), 30.24 (2 CH_2), 29.05 (2 CH_2), 28.95 (2 CH_2), 26.23 (2 CH_2), 22.59 (2 CH_2), 21.37 (CH_3), 13.91 (2 CH_3). FTIR: (v/cm^{-1}): 3060-2854 (C-H stretch), 1561 (N-C-N stretch), 1467 (C-C stretch), 1195, 1120 (SO_2 stretch), 1033, 1011, 814 (C-H bending), 678 (S=O stretch), 564 (C-S bending). CHN analysis: (calculated for $C_{26}H_{44}N_2O_3S$) (464.71 g mol^{-1}): C 66.81% (67.20%), H 9.42% (9.42%), N 7.42% (6.03%).

1,3-Didecylimidazolium tosylate [DDIM][TsO]

Light brown powder (2.20 g, 4.22 mmol, 84%). ^{1}H NMR: (300 MHz, $CDCl_3$, δ/ppm): 10.13 (s, 1H, CH), 7.81 (s, 2H, 2 CH), 7.20 (s, 2H, 2 CH), 7.15 (s, 2H, 2 CH), 4.27 (m, 4H, 2 CH_2), 2.34 (s, 3H, CH_3),1.85 (m, 4H, 2 CH_2), 1.24 (m, 28H, 14 CH_2), 0.88 (m, 6H, 2 CH_3). ^{13}C NMR: (75 MHz, $CDCl_3$, δ/ppm): 143.73 (C-S), 139.16 (C-CH_3), 138.25 (CH), 128.58 (2 CH), 125.95 (2 CHN), 121.43 121.38 (2 CH), 50.09 (CH_3), 31.86 (2 CH_2), 30.24 (2 CH_2), 29.47 (2 CH_2), 29.40 (2 CH_2), 29.27 (2 CH_2), 29.00 (2 CH_2), 26.24 (2 CH_2), 22.67 (2 CH_2), 21.30 (2 CH_2), 14.11 (2 CH_3). FTIR: (v/cm^{-1}): 3096-2852 (C-H stretch), 1564 (N-C-N stretch), 1467 (C-C stretch), 1194, 1121 (SO_2 stretch), 1034, 1012, 814 (C-H bending), 679 (S=O stretch), 563 (C-S bending). CHN analysis: (calculated for $C_{30}H_{52}N_2O_3S$) (520.81 g mol^{-1}): C 68.57% (69.18%), H 9.78% (10.06%), N 6.93% (5.38%).

1,3-bis(2-ethylhexyl)imidazolium tosylate [EhEhIM][TsO]

Yellow solid (1.80 g, 3.86 mmol, 77%). ^{1}H NMR: (300 MHz, $CDCl_3$, δ/ppm): 10.05 (s, 1H, CH), 7.80 (s, 2H, 2 CH), 7.16 (s, 2H, 2 CH), 7.12 (s, 2H, 2 CH), 4.19 (m, 4H, 2 CH_2), 2.34 (s, 3H, CH_3), 1.78 (m, 2H, 2 CH), 1.24 (m, 16H, 8 CH_2), 0.88 (m, 12H, 4 CH_3). ^{13}C NMR: (75 MHz, $CDCl_3$, δ/ppm): 143.91 (C-S), 139.21 (C-CH_3), 139.02 (CH), 128.49 (2 CH), 126.01 (2 CHN), 121.77

(2 CH), 53.40 (CH_3), 40.07 (2 CH), 29.95 (2 CH_2), 28.30 (2 CH_2), 23.29 (2 CH_2), 22.83 (2 CH_2), 21.29 (2 CH_2), 13.93 (2 CH_3), 10.34 (2 CH_3). FTIR: (v/cm^{-1}): 3087-2861 (C-H stretch), 1564 (N-C-N stretch), 1460 (C-C stretch), 1192, 1120 (SO_2 stretch), 1033, 1011, 815 (C-H bending), 679 (S=O stretch), 563 (C-S bending). CHN analysis: (calculated for $C_{26}H_{44}N_2O_3S$) (464.72 g mol^{-1}): C 66.32% (67.20%), H 9.32% (9.54%), N 7.73% (6.03%).

General reaction procedure for synthesis of bis(2-ethylhexyl)phosphate ILs

The pK_a of bis(2-ethylhexyl)phosphoric acid (pK_a= 1.47) is not sufficiently low to guarantee a full protonation of the acetate anion to acetic acid (pK_a < 0.7). The sodium salt, sodium bis(2-ethylhexyl)phosphate (NaDEHP) was therefore used. This salt was prepared from the neutralization reaction of bis(2-ethylhexyl)phosphoric acid with sodium hydroxide. Next, the formed water was evaporated, the product was dried on a Schlenk line and in a vacuum oven and stored for further use.

When the metathesis reactions are performed with sodium salts, the crucial step is the removal of the formed sodium acetate. To decrease its solubility, the synthesis was carried out in dry ethyl acetate and under argon atmosphere. The 1,3-dialkylimidazolium acetate (5 mmol) and sodium bis(2-ethylhexyl) phosphate (5 mmol, 1.812 g) were dissolved in ethyl acetate under argon atmosphere (**Scheme 3.3**). A minimum amount of solvent was used (approximately 10 mL), therefore heating was required to dissolve the products. The solution was stirred overnight and cooled down to 0 °C in order to decrease the solubility of sodium acetate, which was separated by filtration with a glass filter. The ethyl acetate was removed with a rotary evaporator. ^{1}H NMR indicated that there was still acetate present in all of the imidazolium DEHP products, which were dissolved in dichloromethane and washed twice with ice water. In case of the more hydrophilic imidazolium cations, centrifugation was needed to separate the two phases completely. This technique resulted in pure 1,3-dialkylimidazolium DEHP for the following cations: $[OOIM]^+$, $[DDIM]^+$ and $[EhEhIM]^+$. The other products contained an excess of NaDEHP, since some imidazolium acetate also migrated to the water phase, leaving NaDEHP behind. To tackle this problem, the product was redissolved in dichloromethane and an excess (2 mmol) of the corresponding imidazolium acetate was added, the phase was carefully

washed with small amounts of ice water. In this way, the remainder of sodium acetate was removed. With this procedure all hydrophobic DEHP ionic liquids could be purified. The most hydrophilic ILs: [EEIM][DEHP], [BBIM][DEHP] and [iBiBIM][DEHP] again contained an excess of NaDEHP in spite of careful washing and could not be purified.

1,3-Dihexylimidazolium bis(2-ethylhexyl)phosphate [HHIM][DEHP]

Highly viscous oil (2.20 g, 3.94 mmol, 79%). ^{1}H NMR: (300 MHz, $CDCl_3$, δ/ppm): 11.04 (s, 1H, CH), 7.09 (s, 2H, 2 CH), 4.35 (m, 4H, 2 CH_2), 3.76 (m, 4H, 2 CH_2), 1.88 (m, 4H, 2 CH_2), 1.31 (m, 30H, 2 CH + 14 CH_2), 0.87 (m, 18H, 6 CH_3). ^{13}C NMR: (75 MHz, $CDCl_3$, δ/ppm): 140.48 (N-CH-N), 120.73 (2 CH-N), 67.70 (2 CH_2-O), 50.01 (2 CH_2-N), 40.47 (2 CH), 31.21 (2 CH_2), 30.22 (2 CH_2), 30.15 (2 CH_2), 29.11 (2 CH_2), 25.99 (2 CH_2), 23.39 (2 CH_2), 23.18 (2 CH_2), 22.42 (2 CH_2), 14.15 (2 CH_3), 13.93 (2 CH_3), 11.01 (2 CH_3). FTIR: (v/cm^{-1}): 2957-2873 (C-H stretch), 1564 (N-C-N stretch), 1461 (C-C stretch), 1239 (P=O stretch), 1038 (P-O-C stretch), 852 815 (C-H bending), 555 (C-S bending). CH analysis: (calculated for $C_{31}H_{63}N_2O_4P{\cdot}H_2O$) (576.83 g mol^{-1}): C 64.68% (64.55%), H 9.81% (11.36%).

1,3-Dioctylimidazolium bis(2-ethylhexyl)phosphate [OOIM][DEHP]

Highly viscous oil (2.97 g, 4.86 mmol, 97%). ^{1}H NMR: (300 MHz, $CDCl_3$, δ/ppm): 11.01 (s, 1H, CH), 7.10 (s, 2H, 2 CH), 4.35 (m, 4H, 2 CH_2), 3.76 (m, 4H, 2 CH_2), 1.89 (m, 4H, 2 CH_2), 1.26 (m, 38H, 2 CH + 18 CH_2), 0.87 (m, 18H, 6 CH_3). ^{13}C NMR: (75 MHz, $CDCl_3$, δ/ppm): 140.50 (N-CH-N), 120.70 (2 CH-N), 67.55 (2 CH_2-O), 50.01 (2 CH_2-N), 40.50 (2 CH), 31.70 (2 CH_2), 30.28 (2 CH_2), 30.17 (2 CH_2), 29.11 (2 CH_2), 29.06 (2 CH_2), 29.05 (2 CH_2), 26.33 (2 CH_2), 23.40 (2 CH_2), 23.18 (2 CH_2), 22.59 (2 CH_2), 14.15 (2 CH_3), 14.04 (2 CH_3), 11.02 (2 CH_3). FTIR: (v/cm^{-1}): 2957-2873 (C-H stretch), 1563 (N-C-N stretch), 1461 (C-C stretch), 1239 (P=O stretch), 1039 (P-O-C stretch), 851 815 (C-H bending), 556 (C-S bending). CH analysis: (calculated for $C_{35}H_{71}N_2O_4P{\cdot}2H_2O$) (650.95 g mol^{-1}): C 64.15% (64.58%), H 10.39% (11.61%).

1,3-Didecylimidazolium bis(2-ethylhexyl)phosphate [DDIM][DEHP]

Highly viscous oil (2.91 g, 4.34 mmol, 87%). ^{1}H NMR: (300 MHz, $CDCl_3$, δ/ppm): 11.06 (s, 1H, CH), 7.09 (s, 2H, 2 CH), 4.35 (m, 4H, 2 CH_2), 3.75 (m, 4H, 2 CH_2), 1.87 (m, 4H, 2 CH_2), 1.26 (m, 46H, 2 CH + 22 CH_2), 0.87 (m, 18H, 6 CH_3). ^{13}C NMR: (75 MHz, $CDCl_3$, δ/ppm): 140.43 (N-CH-N), 120.72

(2 CH-N), 67.61 (2 CH_2-O), 50.02 (2 CH_2-N), 40.48 (2 CH), 31.86 (2 CH_2), 30.30 (2 CH_2), 30.17 (2 CH_2), 29.49 (2 CH_2), 29.42 (2 CH_2), 29.27 (2 CH_2), 29.12 (2 CH_2), 29.11 (2 CH_2), 26.34 (2 CH_2), 23.40 (2 CH_2), 23.19 (2 CH_2), 22.67 (2 CH_2), 14.16 (2 CH_3), 14.10 (2 CH_3), 11.03 (2 CH_3). FTIR: (v/cm^{-1}): 2957-2873 (C-H stretch), 1564 (N-C-N stretch), 1463 (C-C stretch), 1236 (P=O stretch), 1039 (P-O-C stretch), 852 815 (C-H bending), 555 (C-S bending). CH analysis: (calculated for $C_{39}H_{79}N_2O_4P \cdot 2H_2O$) (707.06 g mol^{-1}): C 66.71% (66.25%), H 11.39% (11.83%).

1,3-Bis(2-ethylhexyl)imidazolium bis(2-ethylhexyl)phosphate [EhEhIM][DEHP]

Highly viscous oil (2.65 g, 4.30 mmol, 86%). ^{1}H NMR: (300 MHz, $CDCl_3$, δ/ppm): 10.91 (s, 1H, CH), 7.07 (s, 2H, 2 CH), 4.28 (m, 4H, 2 CH_2), 3.71 (m, 4H, 2 CH_2), 1.82 (m, 2H, 2 CH), 1.26 (m, 34H, 2 CH + 16 CH_2), 0.86 (m, 24H, 8 CH_3). ^{13}C NMR: (75 MHz, $CDCl_3$, δ/ppm): 141.24 (N-CH-N), 121.11 (2 CH-N), 67.76 (2 CH_2-O), 53.29 (2 CH_2-N), 40.45 (2 CH), 40.17 (2 CH), 30.15 (2 CH_2), 30.06 (2 CH_2), 29.11 (2 CH_2), 28.47 (2 CH_2), 23.38 (2 CH_2), 23.35 (2 CH_2), 23.17 (2 CH_2), 22.83 (2 CH_2), 14.02 (4 CH_3), 10.74 (4 CH_3). FTIR: (v/cm^{-1}): 2958-2873 (C-H stretch), 1563 (N-C-N stretch), 1461 (C-C stretch), 1240 (P=O stretch), 1038 (P-O-C stretch), 852 816 (C-H bending), 555 (C-S bending). CH analysis: (calculated for $C_{35}H_{71}N_2O_4P \cdot 2H_2O$) (650.95 g mol^{-1}): C 64.77% (64.58%), H 10.76% (11.61%).

General reaction procedure for synthesis of nitrate ILs

The pK_a of nitric acid is low enough (pK_a = -1.4) to use the acid during the metathesis towards nitrate imidazolium ionic liquids. The removal of the resulting acetic acid is a big concern since nitric acid has a lower boiling point (T_b = 83 °C) than water (T_b = 100 °C) and acetic acid (T_b = 118 °C). Therefore, minor traces of nitric acid left in the solution might evaporate before water and acetic acid. According to the principles of Le Chatelier, these trace amounts will be regenerated and eventually this might result in a significant amount of evaporated nitric acid, leaving acetate anions behind. This would result in contamination by the starting products and impure imidazolium nitrate. Because of this reason, the water-soluble 1,3-diethylimidazolium nitrate, 1,3-dibutylimidazolium nitrate and 1,3-diisobutylimidazolium nitrate were not synthesized in pure form. When the resulting IL is not soluble in water, the acetic acid and excess nitric acid can easily be removed by washing with water. 1,3-Dialkylimidazolium acetate (5 mmol) was dissolved in water and nitric acid (65 wt% in water, 2 eq. 10 mmol, 0.697 mL) was added to the solution. After addition of nitric acid, a water-insoluble product appeared. After two hours, dichloromethane was added to the reaction mixture and the two phases were separated, the organic phase was washed two times with water and the dichloromethane was removed with a rotary evaporator. The last traces of DCM were removed on a Schlenk line at 50 °C.

1,3-Dihexylimidazolium nitrate [HHIM][NO_3]

Dark yellow, viscous liquid (1.05 g, 3.51 mmol, 70%). ^{1}H NMR: (300 MHz, $CDCl_3$, δ/ppm): 10.09 (s, 1H, CH), 7.39 (s, 2H, 2 CH), 4.26 (m, 4H, 2 CH_2), 1.89 (m, 4H, 2 CH_2), 1.30 (m, 12H, 6 CH_2), 0.87 (m, 6H, 2 CH_3). ^{13}C NMR: (75 MHz, $CDCl_3$, δ/ppm): 137.81 (N-CH-N), 122.00 (2 CH-N), 50.14 (2 CH_2-N), 31.03 (2 CH_2), 30.19 (2 CH_2), 25.85 (2 CH_2), 22.38 (2 CH_2), 13.90 (2 CH_3). FTIR: (v/cm^{-1}): 2956-2859 (C-H stretch), 1564 (N-C-N stretch), 1461 (C-C stretch), 1334 (N-O symmetric stretch), 830 (C-H bending). CHN analysis: (calculated for $C_{15}H_{29}N_3O_3$) (299.41 g mol^{-1}): C 59.63% (60.17%), H 9.57% (9.76%), N 14.72% (14.03%).

1,3-Dioctylimidazolium nitrate [OOIM][NO_3]

Brown liquid (1.09 g, 3.07 mmol, 61%). ^{1}H NMR: (300 MHz, $CDCl_3$, δ/ppm): 10.06 (s, 1H, CH), 7.40 (s, 2H, 2 CH), 4.26 (m, 4H, 2 CH_2), 1.89 (m, 4H, 2

CH_2), 1.27 (m, 20H, 10 CH_2), 0.87 (m, 6H, 2 CH_3). ^{13}C NMR: (75 MHz, $CDCl_3$, δ/ppm): 137.71 (N-CH-N), 122.05 (2 CH-N), 50.14 (2 CH_2-N), 31.66 (2 CH_2), 30.24 (2 CH_2), 29.01 (2 CH_2), 28.90 (2 CH_2), 26.23 (2 CH_2), 22.56 (2 CH_2), 14.02 (2 CH_3). FTIR: (v/cm^{-1}): 2956-2856 (C-H stretch), 1564 (N-C-N stretch), 1464 (C-C stretch), 1335 (N-O symmetric stretch), 829 (C-H bending). CHN analysis: (calculated for $C_{19}H_{37}N_3O_3$) (355.52 g mol^{-1}): C 63.26% (64.19%), H 10.04% (10.49%), N 12.63% (11.82%).

1,3-Didecylimidazolium nitrate [DDIM][NO_3]

Brown, viscous liquid (1.71 g, 4.15 mmol, 83%). ^{1}H NMR: (300 MHz, $CDCl_3$, δ/ppm): 10.04 (s, 1H, CH), 7.40 (s, 2H, 2 CH), 4.25 (m, 4H, 2 CH_2), 1.89 (m, 4H, 2 CH_2), 1.27 (m, 28H, 14 CH_2), 0.87 (m, 6H, 2 CH_3). ^{13}C NMR: (75 MHz, $CDCl_3$, δ/ppm): 137.81 (N-CH-N), 121.93 (2 CH-N), 50.15 (2 CH_2-N), 31.84 (2 CH_2), 30.25 (2 CH_2), 29.45 (2 CH_2), 29.38 (2 CH_2), 29.24 (2 CH_2), 28.96 (2 CH_2), 26.24 (2 CH_2), 22.65 (2 CH_2), 14.09 (2 CH_3). FTIR: (v/cm^{-1}): 2956-2854 (C-H stretch), 1564 (N-C-N stretch), 1465 (C-C stretch), 1336 (N-O symmetric stretch), 829 (C-H bending). CH analysis: (calculated for $C_{23}H_{45}N_3O_3 \cdot 0.5H_2O$) (420.63 g mol^{-1}): C 65.56% (65.67%), H 10.59% (11.02%).

1,3-Bis(2-ethylhexyl)imidazolium nitrate [EhEhIM][NO_3]

Dark yellow, viscous liquid (1.43 g, 4.02 mmol, 80%). ^{1}H NMR: (300 MHz, $CDCl_3$, δ/ppm): 10.25 (s, 1H, CH), 7.27 (s, 2H, 2 CH), 4.18 (m, 4H, 2 CH_2), 1.85 (s, 2H, 2 CH), 1.28 (m, 16H, 8 CH_2), 0.88 (m, 12H, 4 CH_3). ^{13}C NMR: (75 MHz, $CDCl_3$, δ/ppm): 139.11 (N-CH-N), 122.13 (2 CH-N), 53.49 (2 CH_2-N), 40.15 (2 CH), 30.00 (2 CH_2), 28.28 (2 CH_2), 23.34 (2 CH_2), 22.84 (2 CH_2), 13.92 (2 CH_3), 10.29 (2 CH_3). FTIR: (cm^{-1}): 2959-2862 (C-H stretch), 1564 (N-C-N stretch), 1461 (C-C stretch), 1335 (N-O symmetric stretch), 829 (C-H bending). CH analysis: (calculated for $C_{19}H_{37}N_3O_3 \cdot 0.5H_2O$) (364.52 g mol^{-1}): C 62.31% (64.19%), H 9.66% (10.51%).

3.3 Results and Discussion

The building blocks for the imidazolium synthesis were an alkyl amine (2 eq.), a 1,2-dicarbonyl compound and an aldehyde. It must be emphasized that the use of enolizable aldehydes and ketones is not compatible with the modified Debus-Radzsizewski reaction. The desired imidazole is formed, yet due to the keto-enol equilibrium, a large variety of aldol-type side-products make purification of the desired product difficult or even impossible. Therefore, the use of enolizable substituents has to be avoided. However, this significantly reduces the number of starting materials that can be used in the synthesis of imidazoles and imidazolium compounds. The most obvious choices of non-enolizable substituents are: hydrogen, trifluoromethyl, trisubstituted carbon atoms and phenyl substituents. Several of these substituents are not compatible in the ionic liquid design. First of all, the ionic liquid should have a low melting point. Therefore, the use of phenyl groups should be limited since the increased intermolecular forces caused by the π-stacking between the aromatic rings will significantly increase the melting point. Next, to get ionic liquids with a green character and a low toxicity, fluorinated carbonyl groups have to be avoided. In case of the trisubstituted carbon as substituent, steric hindrance is the main problem with two of these substituents on neighboring carbonyl groups. Substituting the 1,2-diketone compound with one trisubstituted carbon and one hydrogen atom is theoretically possible, although this would imply the use of the non-readily available 3,3-dimethyl-2-oxobutanal. The only relevant substituent left to use is the hydrogen atom. The corresponding 1,2-diketone compound is glyoxal, the simplest 1,2-dicarbonyl compound. It was used in all further syntheses of both imidazoles and imidazolium compounds. The consequence is that the 4,5-positions remain unsubstituted.

Not only the non-enolizable character of the aldehyde and 1,2-diketone is important, also the reactivity has an influence, as was seen in a test reaction using glyoxal and pivaldehyde (trimethylacetaldehyde) or benzaldehyde. The ^{1}H NMR spectrum taken after these test reactions indicated that considerable amounts of starting reagents were still present as well as the proton peak corresponding to the C2-H of imidazolium. Together with the complete lack of any *tert*-butyl peak for the reaction with pivaldehyde and a deficient signal for aromatic protons for the benzaldehyde reaction, this indicates an unsuccessful synthesis procedure for C2-functionalized ILs since only the

non-substituted acetate ionic liquid was formed. An explanation might be that the glyoxal is incorporated in the ring instead of the mono aldehyde. The imidazole formation then begins with a nucleophilic attack by an unprotonated amine group on glyoxal monohydrate's carbonyl moiety. In a next step, proton transfer and water loss produce an imine which dimerizes and gains a proton to form the five-membered ring, followed by dehydration to form the disubstituted imidazole.[20-23] In a simple test reaction where the equivalent of mono aldehyde was replaced by an extra equivalent of glyoxal, it was proven that imidazolium formation indeed occurs without aldehyde present.

The synthetic procedure for symmetrical 1,3-dialkylimidazolium based ionic liquids was inspired by the procedure described by Zimmermann *et al*.[18] The goal of these authors was to prepare hydrophilic ionic liquids in a continuous way via a microreactor setup. They investigated the influence of the sequence of reactant addition, the effect of reaction time and type of acid. The addition of a mixture of acetic acid and formaldehyde to 2 eq. of amine in a first step and subsequent addition of glyoxal proved to be the best choice. We further optimized the halogen-free synthesis towards 1,3-dialkylimidazolium ionic liquids, using *n*-butylamine. The effect and applicability of different acids on the synthesis were tested with acetic acid, hydrochloric acid, sulfuric acid and *n*-butyric acid. Hydrochloric acid and sulfuric acid were chosen for their availability and low cost, *n*-butyric acid was chosen for its similar acidic properties and more hydrophobic character compared to acetic acid. The physical properties of the acids and the isolated yield of the resulting ionic liquids are given in **Table 3.1**. If any excess of acid would be present in the ionic liquids after reaction, it could be removed by evaporation when the boiling point of the acid is low. Otherwise, more complex purification steps are required, resulting in more synthetic efforts and lower yields. Hydrochloric acid and acetic acid have low boiling points, and under vacuum they can be evaporated at lower temperatures. The boiling point of sulfuric acid is too high (337 °C) and is even under vacuum conditions difficult to remove. Heating the imidazolium compounds to such high temperatures would result in their thermal decomposition.[24]

Table 3.1 pKa and boiling point T_b of the used acids, isolated yields (%) and purity of the resulting 1,3-dibutylimidazolium ionic liquids incorporating the different anions.

Acid	pK_a	T_b (°C)	T_b at 20 mm Hg (°C)	Isolated yield (%)	Pure product after extraction?*
Acetic acid	4.8	118	19.8	77	Yes
HCl	-7.0	<100	<4.6	61	No
H_2SO_4	-3.0	>250	>130.9	83	No
n-Butyric acid	4.8	164	58.5	39	No

* Purity determined via ^{1}H NMR.

n-Butyric acid is an intermediate case having a boiling point of 164 °C. However, experiments showed that removing an excess of *n*-butyric acid from the ionic liquids via evaporation was not possible. The overall yield of the reaction clearly differs from acid to acid. Yet, the yield is not solely determined in the synthetic step, the extraction of the ionic liquid into diethyl ether can also result in losses. More hydrophilic acids result in more hydrophilic anions, and therefore a lower loss of product during extraction. The most important criterion, however, is the purity of the resulting 1,3-dibutylimidazolium salt after the extraction step. The only acid that gave pure imidazolium salts was acetic acid. The use of hydrochloric acid and sulfuric acid resulted in the formation of several side products that could not be removed by extraction. *n*-Butyric acid did not result in any side product formation, but the acid itself was present in excess and could not be removed by evaporation or by a washing step. This indicates that the reaction is dependent on the strength of the acid used: the strong acids (hydrochloric and sulfuric acid) caused several side reactions, while the weak acids (acetic and butyric) did not give such problems. Via ^{1}H NMR spectroscopy, it was found that in case of strong acids, protonation of the amine lead to ammonium based side products which could not be separated from the IL.

Due to the high purity and yield of the acetate ionic liquid obtained, acetic acid was selected for further syntheses. When the formation of 1,3-dibutylimidazolium salts proceeds, the acid is consumed since its conjugate base serves as the anion of the ionic liquid. This might result in a shortage of acid towards the end of the synthesis. To investigate the effect of this phenomenon, the synthesis was carried out with different equivalents of acetic acid. A small increase in yield was observed for higher acid equivalents, an optimum yield of 89% is obtained with 1.5 equivalents of

acetic acid. The research of Zimmermann *et al.* showed similar results, the maximum yield found was 86% for 1.2 equivalents of acid. The effects of larger excesses of acid were not investigated.[18]

The effect of the used amine was tested by performing the reaction with both *n*-butylamine and 2-ethylhexylamine. A much higher yield for *n*-butylamine in comparison with 2-ethylhexylamine was found. The explanation behind this difference in yield might be twofold. First, 2-ethylhexylamine is much more sterically hindered, resulting in a lower reactivity. Nevertheless, this effect seems too weak to result in such a large difference, since both amines are primary which implies no large difference in reactivity is expected. Secondly, the lower yield is again also partly caused by the hydrophilicity of the products and the more hydrophobic cation 1,3-bis(2-ethylhexyl)imidazolium results in more product losses during the washing steps. This is confirmed by the similar yields for different equivalents of acetic acid, indicating that the overall yield is not significantly influenced during the synthetic step but elsewhere, namely in the extraction with diethyl ether. It must be noted that the synthetic method did not work for long-chain amines; *n*-dodecylamine gave virtually no product, while the overall yield of the synthesis with *n*-decylamine was still around 50%.

The optimized reaction conditions were used in the following standard procedure (**Scheme 3.1**). Two equivalents of amine were cooled down to 0 °C in an ice bath, afterwards a mixture of formaldehyde (37 wt% in water, 1 eq.) and acetic acid (1.5 eq.) was added dropwise while keeping the temperature below 10 °C. The mixture was stirred for 30 min at 0 °C, after which the glyoxal (40 wt% in water, 1 eq.) was added and the reaction mixture was stirred overnight at room temperature. The solution was washed with diethyl ether until the organic phase was colorless and the water was removed with a rotary evaporator. The product was dried on a Schlenk line at 50 °C. A total of seven acetate ionic liquids were synthesized via this halogen-free procedure. The full characterization can be found in the experimental section.

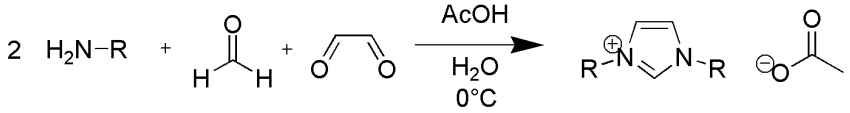

Scheme 3.1 General synthetic procedure for imidazolium acetate ionic liquids.

After the synthesis reactions with the different acids, a correlation between the yield of the imidazolium formation and the hydrophilicity of the anion

(used acid) was observed (**Figure 3.2**). In the Hofmeister series, anions and cations are listed according to their capability to salt-in or salt-out certain compounds from a water phase.[25,26] Since this property is directly linked to their charge density, it is a good indication of their relative hydrophilicity.[25,27] When the anions are listed according to decreasing hydrophilicity in the Hofmeister series, and the butyrate is assumed to be the least hydrophilic (most hydrophobic) of the four anions, the following sequence is obtained: sulfate > acetate > chloride > butyrate.[28] When the acids are ranked according to decreasing yield the same sequence is observed, indicating a correlation between the hydrophilicity of the anion and the reaction yield (**Figure 3.2**). This decrease can be explained by the increased affinity for the apolar diethyl ether phase during the extraction. The less hydrophilic the ionic liquid, the more it is extracted to the organic phase and the lower the reaction yield. The alkyl chains on the imidazolium cation also had an influence on the reaction yield. The same trend as with the anions was observed for the 1,3-dialkylimidazolium cations. When they are listed with increasing number of carbon atoms in the sidechain, the reaction yield decreases (**Figure 3.3**). The branched substituents (isobutyl and 2-ethylhexyl) are indicated with a different symbol since the lower yield might be partially explained by their increased steric hindrance. Since the lowest yield (47%) was observed with the 2-ethylhexyl side chain, this synthesis was repeated to test the effect of another extractant on the yield of the product. Instead of diethyl ether, heptane was used in the extraction, significantly improving the yield to 65%.

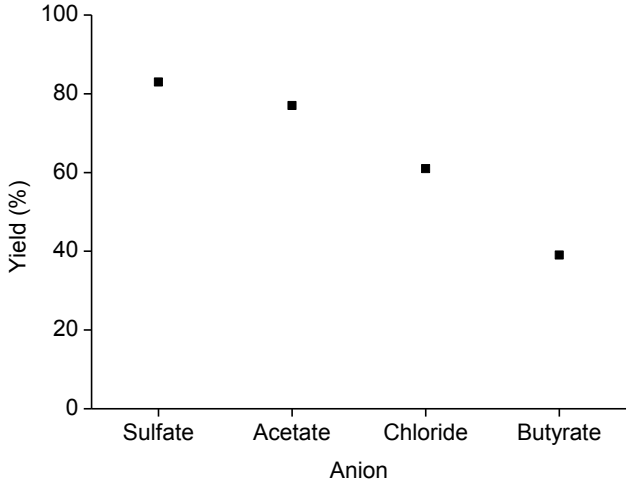

Figure 3.2 Isolated reaction yield (%) as a function of anion hydrophobicity, using different acids in the synthesis of imidazolium ILs.

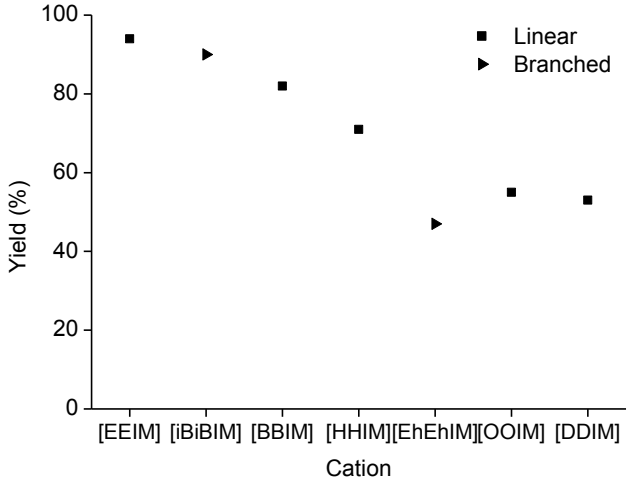

Figure 3.3 Isolated reaction yield (%) as a function of imidazolium cation (diethyl ether as extractant). Listed cations are: 1,3-diethylimidazolium $[EEIM]^+$, 1,3-diisobutylimidazolium $[iBiBIM]^+$, 1,3-dibutylimidazolium $[BBIM]^+$, 1,3-dihexylimidazolium $[HHIM]^+$, 1,3-bis(2-ethylhexyl)imidazolium $[EhEhIM]^+$, 1,3-dioctylimidazolium $[OOIM]^+$, 1,3-didecylimidazolium $[DDIM]^+$.

Several approaches for metathesis reactions starting from acetate ionic liquids were tested. Not all of them were equally efficient with respect to time or yield. Different procedures were required depending on following factors: acidity of the conjugate acid of the anion, the volatility of this acid, and the hydrophilicity of the used reagents and the resulting ionic liquid. If the conjugate acid of the anion is a much stronger acid than acetic acid, its use in the metathesis holds many benefits over the use of the sodium salt of the anion. Most acids are commercially available, and a strong acid will ensure a complete protonation of the acetate with formation of acetic acid, which can be removed by evaporation, an advantage that the procedure with acetate salts does not hold. Therefore, using an acid is beneficial provided that it is strong enough (by convention when $pK_a \leq 0.7$). Looking at the volatility of the acids, the boiling point of the conjugate acid of the new anion is ideally much higher than the boiling point of acetic acid (118 °C). This allows complete removal of acetic acid via evaporation. This technique was successfully applied to the hydrophilic tosylate ionic liquids. Evaporating the acetic acid from ionic liquids synthesized using acids with a boiling point below 118 °C might be troublesome. The extent of this problem was not investigated since the only used acid with a low boiling point was nitric acid, which has the additional problem of being potentially dangerous when heating to high temperatures in the presence of organic materials.[27,29] When the difference in hydrophilicity between the ionic liquid with the new anion and the acetate ionic liquid is large, they can be separated via extraction, as was done for all the water-immiscible ionic liquids (*e.g.* bistriflimide ILs). If the difference in hydrophilicity is too small, for example: [BBIM][TsO], other methods must be applied to purify the ionic liquid, for instance the evaporation of acetic acid. Depending on the properties of the used reagents and the ionic liquid created in the metathesis, different synthetic parameters are required. Most of them easily result in pure ionic liquids, others require intensive purification steps and some could not be synthesized. In general, two main paths were followed, for the bis(trifluoromethylsulfonyl) imide, tosylate and nitrate ionic liquids, acid was added to guarantee full anion exchange (**Scheme 3.2**). In case of the bis(2-ethylhexyl)phosphate ionic liquids, the respective sodium salt was used for the metathesis reaction (**Scheme 3.3**).

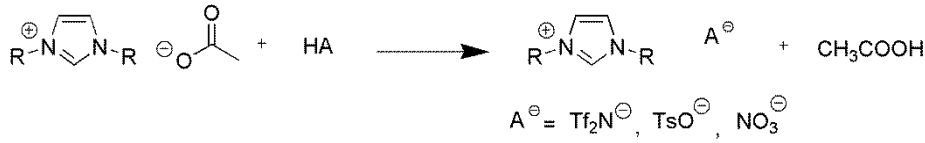

Scheme 3.2 General metathesis reactions by the addition of acid.

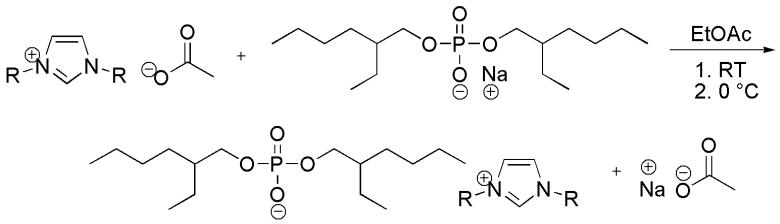

Scheme 3.3 Metathesis reaction by the addition of sodium bis(2-ethylhexyl)phosphate.

Using these synthetic procedures, a library of symmetrical 1,3-dialkylimidazolium ionic liquids was synthesized (**Figure 3.1**). The general characteristics of these ionic liquids were investigated, starting with the thermal properties, since some synthesized ionic liquids were solids at room temperature. Their melting temperatures are listed in **Table 3.3**. These include most of the tosylate ionic liquids and one acetate ionic liquid: 1,3-diisobutylimidazolium acetate. A general rule is that the more symmetrical the compound, the better the crystal packing, the higher its melting point.[30,31] [iBiBIM][AcO] is the only acetate IL that is solid at room temperature with a melting point of 60 °C. It must be noted that this ionic liquid is only solid when completely dry and liquefies when it is exposed to the atmosphere. All tosylate ILs melt above 50 °C, except for the RTILs [EEIM][TsO] and [BBIM][TsO]. The water content of all ionic liquids with a melting point lower than room temperature was measured (**Table 3.3**). This was done after drying them on a Schlenk line at 70 °C. The value of 1,3-diethylimidazolium acetate ([EEIM][AcO]) is not displayed, due to its unusually high water content: 0.73 wt%. The viscosities of all the room temperature ionic liquids were determined using a rotating disk viscometer (**Table 3.3**). Since the viscosities are very sensitive towards contamination of the ionic liquid by water traces, the viscosity of [EEIM][AcO] was not measured due to its high water content: 0.73 wt%. The different anions and imidazolium cations influence the viscosities of the imidazolium ionic liquids. The longer the alkyl substituents on the imidazolium cation, and the higher the degree of branching, the higher the viscosity. This is clearly observed

when looking at the bis(trifluoromethylsulfonyl) imide series: the viscosity increases from 3×10^{1} mPa.s ([EEIM][Tf_2N]) up to 4×10^{2} mPa.s ([EhEhIM][Tf_2N]). These results are in line with the observed trends found in the literature.[31-33] The anions have an even larger effect on the viscosity, the following order is observed: Tf_2N^- < AcO^- < TsO^- / NO_3^- < $DEHP^-$. These results might seem surprising since the two largest anions: Tf_2N^- and $DEHP^-$, give ionic liquids with the lowest and highest viscosities, respectively. However, not only the bulkiness but also the charge delocalization of the anion contributes to the viscosity of the ionic liquid.[31,32] The effect of increasing viscosity with more voluminous substituents is not only clear for the imidazolium cations, but also for the anions. TsO^- and $DEHP^-$ anions have a comparable charged entity (sulfate and phosphate), however the $DEHP^-$ has more, longer and branched substituents. This is translated in a much higher viscosity, even up to 2×10^{4} mPa.s for [EhEhIM][DEHP]. As expected, the bis(trifluoromethylsulfonyl)imide series shows low viscosities due to a good charge distribution over the entire anion structure. The acetate and nitrate anions also show the expected properties: the acetate anion is rather small and has a good charge delocalization therefore having intermediate viscosities. In the nitrate anion two negative charges are delocalized over three oxygen atoms, this increased charge density is translated into higher viscosities.

It is known that intermolecular interactions among anions and cations in ionic liquids greatly determine the properties of ionic liquids.[34] Hydrogen bonding between the ions is evidenced by downfield shifted C-H proton chemical shifts and redshifted C-H frequencies in infrared.[35] Numerous studies on the influence of hydrogen bonding on the properties of imidazolium ionic liquids exist.[34,36,37] A 1,3-dialkylimidazolium ionic liquid has three possible interaction sites at C2, C4 and C5. It has been reported that no shifts are observed for interaction via C(4/5)-H.[38] In the ^{1}H NMR spectra of the different synthesized imidazolium compounds in this study, it can be observed that the peak position of the hydrogen on the 2-position in the imidazolium ring changes with different anion (**Table 3.2**). Bis(trifluoromethylsulfonyl)imide is a weakly coordinating anion, the peak position of the C2-H is the most upfield, as to be expected. The ionic liquids with the bis(2-ethylhexyl)phosphate ($DEHP^-$) show the strongest downfield shift. This indicates that the bond between the bis(2-ethylhexyl)phosphate anion and the C2-H is the strongest hydrogen bond.

Table 3.2 Peak position of C2-H in ^{1}H NMR over the different ionic liquid series.

Ionic liquid series	^{1}H NMR peak position 2-H (ppm)
$[Tf_2N]^-$	8.77-9.18
$[TsO]^-$	9.75-10.24
$[AcO]^-$	9.76-9.98
$[NO_3]^-$	10.03-10.25
$[DEHP]^-$	10.91-11.04

Another aspect to consider is the stability of the synthesized ionic liquids. Thermogravimetric analysis was carried out under nitrogen atmosphere (TGA), the thermal decomposition temperatures ranged from 257 °C to 421 °C with bistriflimide ionic liquids having the highest decomposition temperatures in contrast to the lowest values for the acetate ionic liquids (**Table 3.3**).

Table 3.3. Water content and viscosities of all synthesized room temperature imidazolium ILs (RT IL), melting temperatures of the ionic liquids which are solid at room temperature and thermal decomposition temperature for all synthesized ionic liquids. The viscosity of [EEIM][AcO] was not determined due to the high water content in the IL: 0.73 wt%., with the exception of nitrate ILs (incompatible with Karl Fischer). T_m and T_d are respectively, the melting point and decomposition temperature.

Imidazolium IL	Water content (ppm)	Viscosity (mPa.s) 25°C	T_m (°C)	T_d (°C)
[EEIM][AcO]	0.73 wt%	Water contaminated	RT IL	258
[BBIM][AcO]	7×10^3	5×10^2	RT IL	260
[iBiBIM][AcO]	s	s	60	277
[HHIM][AcO]	4×10^3	7×10^2	RT IL	257
[OOIM][AcO]	4×10^3	9×10^2	RT IL	266
[DDIM][AcO]	2×10^3	5×10^2	RT IL	259
[EhEhIM][AcO]	3×10^3	5×10^3	RT IL	259
[EEIM][Tf_2N]	2×10^3	3×10^1	RT IL	312
[BBIM][Tf_2N]	4×10^2	7×10^1	RT IL	421
[iBiBIM][Tf_2N]	2×10^3	1×10^2	RT IL	353
[HHIM][Tf_2N]	1×10^2	1×10^2	RT IL	406
[OOIM][Tf_2N]	2×10^2	1×10^2	RT IL	416
[DDIM][Tf_2N]	5×10^2	1×10^2	RT IL	414
[EhEhIM][Tf_2N]	1×10^3	4×10^2	RT IL	397
[EEIM][TsO]	5×10^3	1×10^3	RT IL	344
[BBIM][TsO]	4×10^3	2×10^3	RT IL	348
[iBiBIM][TsO]	s	s	95	361
[HHIM][TsO]	s	s	67	342
[OOIM][TsO]	s	s	97	341

Table 3.3 continued.

Imidazolium IL	Water content (ppm)	Viscosity (mPa.s) 25°C	T_m (°C)	T_d (°C)
[DDIM][TsO]	s	s	76	347
[EhEhIM][TsO]	s	s	56	350
[HHIM][DEHP]	8×10^3	8×10^3	RT IL	287
[OOIM][DEHP]	9×10^3	1×10^4	RT IL	288
[DDIM][DEHP]	5×10^3	1×10^4	RT IL	288
[EhEhIM][DEHP]	4×10^3	2×10^4	RT IL	290
[HHIM][NO_3]	i	1×10^3	RT IL	306
[OOIM][NO_3]	i	2×10^3	RT IL	301
[DDIM][NO_3]	i	3×10^3	RT IL	304
[EhEhIM][NO_3]	i	1×10^4	RT IL	321

s: solid, i: incompatible to measure with KF coulometric titration. RT IL no melting point determined.

As a final remark, the environmental concerns and toxicity of these synthesized ionic liquids should be further assessed. The low vapor pressure of ionic liquids causes a minimum risk of air pollution, yet ILs can have a significant water miscibility which inquires a study of aqueous toxicology for ILs. There are five factors that greatly influence the toxicity of an ionic liquid: i) alkyl chain length in the cation, ii) presence of functional groups in the alkyl chain on the cation, iii) anion nature, iv) cation nature, and v) combined influence of anion and cation.[39] Most literature descriptions concerning toxicity of imidazolium ionic liquids only assess the 1-alkyl-3-methylimidazolium ILs. For these types of ionic liquids, a general conclusion was postulated: a clear alkyl chain length-toxicity correlation can be observed in the toxicities of the ILs. Comparisons of different cations demonstrated that phosphonium-based ionic liquids have the highest toxicity whilst morpholinium-based ones are the least toxic.[40,41] An intermediate toxicity was found for the imidazolium ionic liquid when compared to similar alkyl chains. Interpreting these factors to the newly synthesized ILs, we suggest that also here, the longer the alkyl chain length, the higher the toxicity would be, with EEIM having the lowest toxicity and DDIM the highest. It could be assumed that the branched chain ionic liquids will have a lower toxicity due to their reduced lipophilicity when compared to their non-branched counterparts. The effect of the anion nature should be studied further, yet most probably the bistriflimide ionic liquids will have the highest toxicity.

3.4 Conclusions

Imidazolium ionic liquids were synthesized from readily available molecules: formaldehyde, glyoxal, alkyl amines and acids in a halogen-free procedure. The synthesis procedure was investigated for 1,3-dibutylimidazolium ILs testing different acids and acid equivalents. The optimized synthesis involved the synthesis of 1,3-dialkylimidazolium acetate from glyoxal, formaldehyde, a primary amine (2 eq.) and an excess of acetic acid (1.5 eq.). These acetate ILs could be purified by a simple extraction with diethyl ether with excellent yields, depending on the hydrophilicity of the ILs. The yield for the more hydrophobic ILs can be increased by changing the extractant to heptane. Starting from this 1,3-dialkylimidazolium acetate platform, several other 1,3-dialkylimidazolium ILs were prepared via metathesis reactions. If anions were incorporated with an acid which was sufficiently strong (by convention $pK_a<0.7$), the acid was used. The resulting acetic acid could be removed via evaporation. If the acids were not sufficiently strong, sodium salts of the new anion were employed. The completeness of the metathesis reactions in water was influenced by the position of both anions in the Hofmeister series. A general rule for these metatheses is that exchange towards more hydrophobic anions exceeds more efficiently. When the metatheses resulted in hydrophobic ILs, the acetate (salt or acid) was removed by washing with water. The acetic acid could also be completely removed via evaporation, but this step is more time consuming compared to washing the ionic liquid. The evaporation of acetic acid was used to purify water-soluble ILs, since they cannot be purified by washing. Sodium salts were eliminated by precipitation in an apolar solvent. The ILs were fully characterized and their properties listed. The water content in the ionic liquid drops with increasing alkyl chain length on the imidazolium cation as a result of the decreasing hydrophilicity of the cations. Longer alkyl substituents, a higher degree of branching on the imidazolium cation, and a higher coordination between cation and anion increases the viscosity of the ionic liquid.

This research was financially supported by IWT-Flanders (PhD fellowship to DD), the FWO Flanders (research project G.0900.13) and the KU Leuven (projects GOA/13/008 and IOF-KP RARE3). The authors also wish to thank Karel Duerinckx for the help with NMR measurements. Dirk Henot and Danny Vandeput are thanked for performing CHN analysis. Dorien Baeten is thanked for the help with TGA measurements.

3.5 References

1 T. Welton, *Chem. Rev.*, 1999**, 99**, 2071.
2 P. Wasserscheid, W. Keim, *Angew. Chem. Int. Ed.*, 2000**, 39**, 3772.
3 N. V. Plechkova, K. R. Seddon, *Chem. Soc. Rev.*, 2008**, 37**, 123.
4 R. D. Rogers, K. R. Seddon, *Science*, 2003**, 302**, 792.
5 J. D. Holbrey, W. M. Reichert, R. P. Swatloski, G. A. Broker, W. R. Pitner, K. R. Seddon, R. D. Rogers, *Green Chem.*, 2002**, 4**, 407.
6 D. Holbrey, R. Seddon, *J. Chem. Soc. , Dalton Trans.*, 1999**,** 2133.
7 T. L. Merrigan, E. D. Bates, S. C. Dorman, J. Davis, *Chem. Commun.*, 2000**,** 2051.
8 A. E. Visser, R. P. Swatloski, W. M. Reichert, R. Mayton, S. Sheff, A. Wierzbicki, J. Davis, R. D. Rogers, *Chem. Commun.*, 2001**,** 135.
9 L. C. Branco, J. N. Rosa, J. J. Moura Ramos, C. A. M. Afonso, *Chem. Eur. J.*, 2002**, 8**, 3671.
10 S. V. Dzyuba, R. A. Bartsch, *ChemPhysChem*, 2002**, 3**, 161.
11 J. Pernak, A. Czepukowicz, R. Pozniak, *Ind. Eng. Chem. Res.*, 2001**, 40**, 2379.
12 C. Maton, N. De Vos, B. I. Roman, E. Vanecht, N. R. Brooks, K. Binnemans, S. Schaltin, J. Fransaer, C. V. Stevens, *ChemPhysChem*, 2012**,** **13**, 3146.
13 C. Maton, N. R. Brooks, L. Van Meervelt, K. Binnemans, S. Schaltin, J. Fransaer, C. V. Stevens, *ChemPhysChem*, 2013**,** 3503.
14 Debus, H.; *Ueber Die Einwirkung Des Ammoniaks Auf Glyoxal;* WILEY-VCH: Weinheim, 1858, pp 199-208.
15 R. D. Crouch, J. L. Howard, J. L. Zile, K. H. Barker, *J. Chem. Educ.*, 2006**,** **83**, 1658.
16 A. J. Arduengo, F. P. J. Gentry, P. K. Taverkere, H. E. Simmons, Process for Manufacture of Imidazoles, US 6,177,575 B1, **2001**.
17 E. Gelens, F. J. J. De Kanter, R. F. Schmitz, Sliedregt L.A.J.M., B. J. Van Steen, Kruse C.G., R. Leurs, Groen M.B., R. V. A. Orru, *Mol. Divers.*, 2006**,** **10**, 17.
18 J. Zimmermann, B. Ondruschka, A. Stark, *Org. Process Res. Dev.*, 2010**, 14**, 1102.
19 S. N. Suarez, J. R. P. Jayakody, S. G. Greenbaum, T. Zawodzinski, J. J. Fontanella, *J. Phys. Chem. B*, 2010**, 114**, 8941.
20 A. T. Nielsen, R. A. Nissan, D. J. Vanderah, C. L. Coon, R. D. Gilardi, C. F. George, J. Flippen-Anderson, *J. Org. Chem.*, 1990**, 55**, 1459.
21 D. O. D. Haan, A. L. Corrigan, K. W. Smith, D. R. Stroik, J. J. Turley, F. E. Lee, M. A. Tolbert, J. L. Jimenez, K. E. Cordova, G. R. Ferrell, *Environ. Sci. Technol.*, 2009**, 43**, 2818.
22 J. Velisek, T. Davidek, J. Daviek, P. Trska, F. Kvasnicka, K. Velcova, *J Food Sci*, 1989**, 54**, 1544.
23 J. Kua, H. E. Krizner, D. O. De Haan, *J. Phys. Chem. A*, 2011**, 115**, 1667.
24 J. G. Huddleston, A. E. Visser, W. M. Reichert, H. D. Willauer, G. A. Broker, R. D. Rogers, *Green Chem.*, 2001**, 3**, 156.
25 D. Dupont, D. Depuydt, K. Binnemans, *J. Phys. Chem. B*, 2015**, 119**, 6747.

26 L. Cammarata, S. G. Kazarian, P. A. Salter, T. Welton, *Phys. Chem. Chem. Phys.*, 2001**, 3**, 5192.
27 M. G. Cacace, E. M. Landau, J. J. Ramsden, *Q. Rev. Biophys.*, 1997**, 30**, 241.
28 Y. Zhang, S. Furyk, D. E. Bergbreiter, P. S. Cremer, *J. Am. Chem. Soc.*, 2005**, 127**, 14505.
29 S. Wellens, B. Thijs, K. Binnemans, *Green Chem.*, 2013**, 15**, 3484.
30 H. L. Ngo, K. LeCompte, L. Hargens, A. B. McEwen, *Thermochim. Acta*, 2000**, 357–358**, 97.
31 G. Yu, D. Zhao, L. Wen, S. Yang, X. Chen, *AIChE J.*, 2012**, 58**, 2885.
32 A. Ahosseini, A. M. Scurto, *Int J Thermophys*, 2008**, 29**, 1222.
33 H. Tokuda, K. Hayamizu, K. Ishii, Md. A. B. H. Susan, M. Watanabe, *J. Phys. Chem. B*, 2005**, 109**, 6103.
34 K. Fumino, T. Peppel, M. Geppert-Rybczynska, D. H. Zaitsau, J. K. Lehmann, S. P. Verevkin, M. Kockerling, R. Ludwig, *Phys. Chem. Chem. Phys.*, 2011**, 13**, 14064.
35 P. Bonhote, A. P. Dias, N. Papageorgiou, K. Kalyanasundaram, M. Gratzel, *Inorg. Chem.*, 1996**, 35**, 1168.
36 K. Dong, S. Zhang, D. Wang, X. Yao, *J. Phys. Chem. A*, 2006**, 110**, 9775.
37 T. Peppel, C. Roth, K. Fumino, D. Paschek, M. Köckerling, R. Ludwig, *Angew. Chem. Int. Ed.*, 2011**, 50**, 6661.
38 T. Köddermann, C. Wertz, A. Heintz, R. Ludwig, *ChemPhysChem*, 2006**, 7**, 1944.
39 K. S. Egorova, V. P. Ananikov, *ChemSusChem*, 2014**, 7**, 336.
40 S. Stolte, J. Arning, U. Bottin-Weber, A. Müller, W.-R. Pitner, U. Welz-Biermann, B. Jastorff, J. Ranke, *Green Chem.*, 2007**, 9**, 767.
41 J. Ranke, A. Müller, U. Bottin-Weber, F. Stock, S. Stolte, J. Arning, R. Störmann, B. Jastorff, *Ecotoxicol. Environ. Saf.*, 2007**, 67**, 430.

CHAPTER 4

METAL EXTRACTION WITH A SHORT-CHAIN IMIDAZOLIUM NITRATE IONIC LIQUID

This chapter has been published and is reproduced here with permission from The Royal Society of Chemistry.

Depuydt D., Van den Bossche A., Dehaen W., Binnemans K. (2017). Metal extraction with a short-chain imidazolium nitrate ionic liquid. *Chemical Communications, 53* (38), 5271-5274.

The experimental work and writing were executed by the author of this thesis.

The text may deviate from the original publication as the supplementary information is included in the chapter.

Graphical Abstract

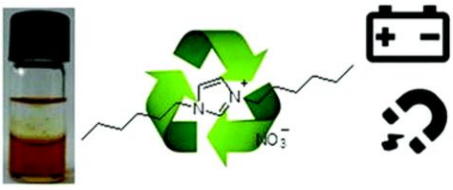

The ionic liquid 1,3-dihexylimidazolium nitrate shows temperature-dependent phase behavior of the UCST-type. The biphasic system efficiently separates rare earths from 3d transition metals, relevant for recycling of batteries (La/Ni) and permanent magnets (Sm/Co).

Inside Cover

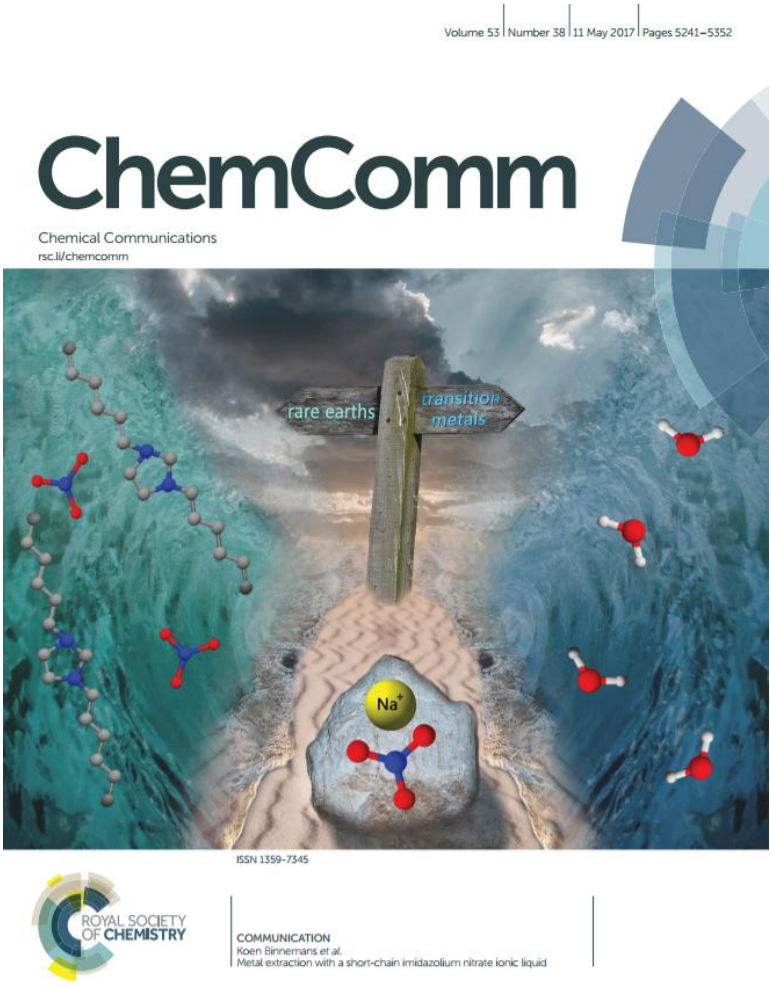

Abstract

A short-chain symmetrical dihexyl imidazolium nitrate ionic liquid for conventional solvent extraction of metals was developed. Rare earths were found to be preferentially extracted over 3d transition metals leading to the application of the ionic liquid system for separation of the Sm(III)/Co(II) and La(III)/Ni(II) pairs, which are relevant for the recycling of SmCo magnets and NiMH batteries.

4.1 Introduction

Solvent extraction systems require solvents of limited miscibility with water, such as toluene, kerosene or dodecane.[1] Most of the solvents used in traditional solvent extraction processes are listed as Volatile Organic Compounds (VOCs). Not only their volatility and flammability are an issue, but these VOCs also have a negative impact on human health if their vapors are emitted into the air. Ionic liquids (ILs) are solvents that consist entirely of ions.[2-4] Their negligible volatility and low flammability, together with the ability to design an IL towards a specific application make them suitable and safer candidates for replacing VOCs.

In many ILs, water immiscibility is reached by using a hydrophobic fluorinated anion like hexafluorophosphate ($[PF_6]^-$), which generates toxic HF due to its hydrolysis in water[5,6] or bis(trifluoromethylsulfonyl)imide (bistriflimide, $[Tf_2N]^-$), which renders ionic liquid synthesis expensive. Alternatives are found in the commercially available ionic liquids tricaprylmethyl ammonium chloride (Aliquat® 336) and trihexyltetradecyl phosphonium chloride (Cyphos® IL 101), where the hydrophobicity is reached by large, bulky cations.[7] However, the long alkyl chains significantly increase the ionic liquid's viscosity. This high viscosity can cause difficulties in solvent extraction applications, because intensive mixing and heating are required to increase mass transfer and speed up the kinetics.[8] The high molar volume of these hydrophobic phosphonium and ammonium ionic liquids is another disadvantage, since it results in a low molar concentration of the ionic liquid. In other words, the anion -which in general plays an important role in the extraction mechanism- is strongly diluted.

Changing the cation to the popular imidazolium heterocycles in combination with non-fluorinated anions generally leads to hydrophilic ionic liquids.[9] Imidazolium ILs with non-fluorinated anions are only water-immiscible if the alkyl chain on the 1-position is sufficiently long, but this leads to unwanted surfactant behavior and formation of emulsions during solvent extraction.[10] Phase equilibria and mutual miscibility of imidazolium ionic liquids with water are a well-studied domain in the literature.[11-16] Some ionic liquids homogenize in water upon heating, this type of phase behavior is known as upper critical solution temperature (UCST) behavior.[17-19] In lower critical solution temperature (LCST) phase behavior, a homogeneous IL solution

phase separates upon heating.[20-22] Ionic liquids with both UCST and LCST have been used for the extraction of metal ions via homogeneous liquid-liquid extraction.[8,23-26]

In this communication, the phase behavior of binary mixtures of the symmetrical dialkylimidazolium ionic liquid 1,3-dihexylimidazolium nitrate [HHIM][NO_3] (**Figure 4.1**) with water was investigated. Additionally, solvent extraction experiments were performed on rare earths and 3d transition metals. Finally, the 1,3-dihexylimidazolium nitrate/water system was used for the separation of Sm(III)/Co(II) and La(III)/Ni(II) pairs.

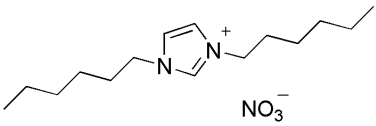

Figure 4.1 Structure of the ionic liquid 1,3-dihexylimidazolium nitrate, [HHIM][NO_3].

4.2 Experimental

4.2.1 Chemicals

Glyoxal (40 wt% in water), sodium nitrate (+99%), nickel nitrate hexahydrate (99%) and cobalt nitrate hexahydrate (99%) were purchased from Acros Organics (Geel, Belgium). Sodium hydroxide (Normapur) and ethanol absolute were obtained from VWR (Heverlee, Belgium). *n*-Hexylamine (99%), nitric acid (65% in water), chloroform-d (99.8 atom% D), deuterium oxide (99.9 atom% D), zinc(II) nitrate hexahydrate (≥98%) and yttrium nitrate hexahydrate (99.9%) and Triton X-100 (laboratory grade) were bought from Sigma-Aldrich (Diegem, Belgium). Dichloromethane (analytical reagent grade), acetic acid (analytical reagent grade) and formaldehyde (37 wt% in water) were obtained from Fisher Scientific Limited (Loughborough, UK). Ammonium nitrate (+99%) was purchased from Chempur (Karlsruhe, Germany). Samarium(III) nitrate hexahydrate (99.9%), lanthanum(III) nitrate hexahydrate (99.9%) and neodymium(III) nitrate hexahydrate (99.9%) were purchased from Alfa Aesar (Karlsruhe, Germany). Copper(II) nitrate trihydrate (≥99.5%) was purchased from Merck (Leuven, Belgium). Scandium(III) nitrate hydrate was synthesized from scandium(III) oxide which was kindly provided by Solvay (La Rochelle, France). All chemicals were used as received without any further purification.

4.2.2 General

The ^{1}H NMR and ^{13}C NMR spectra were recorded on a Bruker Avance 300 spectrometer (operating at 300 MHz for ^{1}H and 75 MHz for ^{13}C). The chemical shifts are noted in parts per million (ppm), referenced to tetramethylsilane (TMS). All solutions were made in $CDCl_3$ or D_2O. The spectra were analyzed with SpinWorks software. Fourier Transform Infrared (FTIR) spectra were recorded on a Bruker Vertex 70 spectrometer, via the attenuated total reflectance (ATR) technique with a Bruker Platinum ATR accessory. The OPUS software package was used for analysis of the FTIR spectra. The water content of the pure, water-saturated and 6 M $NaNO_3$-saturated ionic liquid was determined by respective coulometric and volumetric Karl Fischer (KF) titration using a Mettler-Toledo C30S coulometric KF titrator and a Mettler-Toledo V30S volumetric titrator equipped with a Stromboli Oven. The dynamic viscosity and density of the ionic liquids were measured on an Anton Paar Lovis 2000 M/ME viscometer

equipped with DMA 4500 M density meter. TGA measurements were performed on a TGA-Q500 (TA Instruments). For these TGA measurements, about 10 mg of a water-saturated ionic liquid sample was heated at 10 °C min^{-1} to 120 °C, this temperature was kept for one hour to remove all water, and subsequently the dry ionic liquid was further heated to 500 °C at the same rate of 10 °C min^{-1}. The elemental analysis of carbon, hydrogen and nitrogen (CHN analysis) was performed on a flash 2000 Elemental analyzer of Thermo Scientific Interscience. In order to presaturate the ionic liquid, pure ionic liquid and water or 6 M $NaNO_3$ solution (1:1 w/w) were shaken with an Eppendorf Thermomixer C with a 15 mL SmartBlock (25 °C, 1000 rpm). Extraction mixtures in 2 mL Eppendorf vials were shaken with an Eppendorf Thermomixer C with a 2 mL SmartBlock (25 °C, 2000 rpm). A VWR MiniStar silverline microcentrifuge was used for the centrifugation of the samples. pH measurements were performed with an S220 SevenCompact™ pH/Ion meter (Mettler-Toledo) and a Slimtrode (Hamilton) electrode. A Bruker S2 Picofox total reflection X-ray fluorescence (TXRF) spectrometer was used to determine the metal concentrations in both aqueous and organic (ionic liquid) phase.[27] For the determination of the metal content in experiments involving the Sm/Co and La/Ni pairs, both neodymium and gallium standard solutions were added to the sample as internal references for quantification, in the multi-element screening test only gallium standard solution was used. The sample was further diluted to 1 mL with Triton 100 (5 wt% in water) for aqueous samples, and with ethanol for the ionic liquid phase. The prepared sample solutions were homogenized by vortex mixing and a small droplet (3 µL) was dispensed on a quartz sample carrier. Finally, the carrier containing the sample was dried at 60 °C for 30 min. Prior to dispensing the sample droplet, the quartz carrier was pretreated with a SERVA® silicone solution in isopropanol (30 µL) which was dried at 60 °C for 30 min, in order to make the surface more hydrophobic, to avoid spreading of the sample droplet.

4.2.3 Synthesis

1,3-Dihexylimidazolium nitrate [HHIM][NO_3] was synthesized as described in a previous paper (**Scheme 4.1**).[28] In a first step, 1,3-dihexylimidazolium acetate was prepared from readily available precursors: hexylamine, glyoxal, formaldehyde and acetic acid. 1,3-Dihexylimidazolium acetate (100 mmol) was then dissolved in water and nitric acid (65 wt% in water, 2 eq., 200 mmol, 13.94 mL) was added to the solution. After the addition of nitric

acid, a water-insoluble product was formed. After two hours, dichloromethane was added to the reaction mixture and the two phases were separated, the organic phase was washed two times with water and the dichloromethane was removed with a rotary evaporator. The last traces of solvent were removed on a Schlenk line at 50 °C.

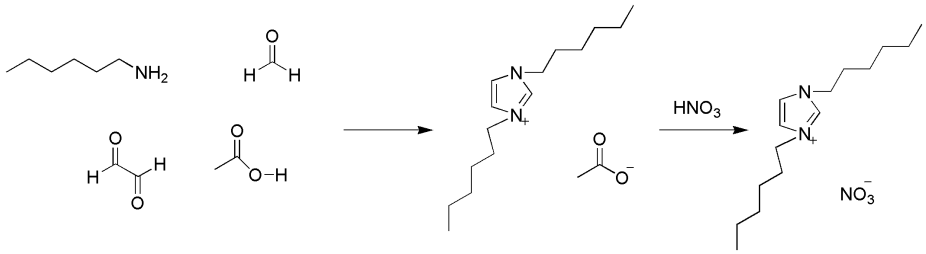

Scheme 4.1 Synthesis of [HHIM][NO_3].

1,3-Dihexylimidazolium nitrate [HHIM][NO_3]

Brown, viscous liquid (26.56 g, 88.72 mmol, 89%). ^{1}H NMR: (300 MHz, $CDCl_3$, δ/ppm): 10.09 (s, 1H, CH), 7.39 (s, 2H, 2 CH), 4.26 (t, 7.5 Hz, 4H, 2 CH_2), 1.89 (m, 4H, 2 CH_2), 1.30 (m, 12H, 6 CH_2), 0.87 (t, 7.0 Hz, 6H, 2 CH_3). ^{13}C NMR: (75 MHz, $CDCl_3$, δ/ppm): 137.81 (N-CH-N), 122.00 (2 CH-N), 50.14 (2 CH_2-N), 31.03 (2 CH_2), 30.19 (2 CH_2), 25.85 (2 CH_2), 22.38 (2 CH_2), 13.90 (2 CH_3). FTIR: (ν/cm^{-1}): 2956-2859 (C-H stretch), 1564 (N-C-N stretch), 1461 (C-C stretch), 1334 (N-O symmetric stretch), 830 (C-H bending). CHN analysis: (calculated for $C_{15}H_{29}N_3O_3$) (299.41 g mol^{-1}): C 59.63% (60.17%), H 9.57% (9.76%), N 14.72% (14.03%).

4.2.4 Extraction experiments

Synthetic solutions of metal nitrates were used in the extraction experiments. All dilutions were made using ultrapure water (18.2 M Ω·cm) which was prepared using a Sartorius Arium Pro ultrapure water system. Presaturation of the ionic liquid [HHIM][NO_3] prior to extraction was necessary to minimize volume changes during the extraction experiments. Equal masses of ionic liquid and water were weighed in a 15 mL vial and shaken for 30 min. After centrifugation, approximately 1 g of the water-saturated IL and 1 g of an aqueous metal solution were added to a 2 mL Eppendorf tube and shaken at 25 °C at 2000 rpm for 30 min (unless stated otherwise). The tubes were centrifuged and a sample of both aqueous and ionic liquid phase was taken to measure the metal content by TXRF. To be noted, experiments involving a metal feed solution containing 6 M $NaNO_3$, were presaturated with a 6 M

solution of $NaNO_3$, in other cases, water was used to presaturate the IL. The distribution ratio *D* and percentage extraction *%E* were calculated according to equation 4.1 and 4.2, respectively:

$$D = \frac{c_{\mathrm{org}}}{c_{\mathrm{aq}}} \tag{4.1}$$

$$\%E = \frac{c_{\mathrm{org}} \cdot m_{\mathrm{org}}}{c_{\mathrm{org}} \cdot m_{\mathrm{org}} + c_{\mathrm{aq}} \cdot m_{\mathrm{aq}}} \times 100\% \tag{4.2}$$

where c_{org} and c_{aq} are the metal concentration in the organic phase (*i.e.* ionic liquid phase) and in the aqueous phase, respectively and m_{org} and m_{aq} are the masses of the organic phase and the aqueous phase, respectively.

4.2.5 Scrubbing experiments

A larger extraction experiment was performed: equal masses of 6 M $NaNO_3$-saturated ionic liquid and 6 M $NaNO_3$ metal feed solution were weighed in a 15 mL vial and shaken for 30 min. After centrifugation, approximately 1 g of the loaded IL and 1 g of an aqueous $NaNO_3$ solution of varying concentration were added to a 2 mL Eppendorf tube and shaken at 25 °C at 2000 rpm for 30 min. Via TXRF, it was found that the IL was loaded with 13.2 g L^{-1} Sm(III) and 5.8 g L^{-1} Co(II) as nitrate salts. After the scrubbing, the percentage scrubbing *%S* was calculated according to equation 4.3:

$$\%S = \frac{\text{amount of scrubbed metal}}{\text{total amount of extracted metal}} \times 100\% \tag{4.3}$$

4.2.6 Quantitative ^{1}H NMR

To determine the amount of IL lost into the water phase, quantitative ^{1}H NMR measurements were performed. After presaturation of the ionic liquid, a 100 mg sample of the water layer was mixed with 10 mg of 1,4-dioxane to obtain approximately equimolar concentrations as the aliquot of water which was saturated with the ionic liquid. 1,4-Dioxane was chosen as internal standard since there is no overlap with the ^{1}H NMR spectrum of the ionic liquid. Via the integration of the peaks in the ^{1}H NMR spectrum of the water samples, the relative concentration versus 1,4-dioxane and the absolute concentration of the different ionic liquids in the water layer were calculated. It is estimated that the measurement uncertainty is less than 1%.[29]

4.3 Results and Discussion

The most popular imidazolium ionic liquids are the 1-alkyl-3-methyl imidazolium salts due to the easy alkylation of commercially available *N*-methylimidazoles.[30-36] In order to obtain hydrophobic cations, a long alkyl chain on the 1-position of the imidazolium has to be incorporated, with unwanted surfactant behavior as a consequence. In order to avoid such surfactant behavior, a symmetrical dialkyl imidazolium ionic liquid was made.[28] The synthesis consisted of two straightforward steps, preparing the acetate form of the 1,3-dihexylimidazolium ionic liquid from readily available starting materials (*n*-hexylamine, formaldehyde, glyoxal and acetic acid) and the addition of nitric acid to obtain the nitrate ionic liquid (**Scheme 4.1**). The benefit of using this method over the conventional quaternization of imidazole with a haloalkane is twofold: 1) this procedure is completely halogen-free, avoiding potentially toxic chloride imidazolium precursors,[37] and 2) higher yields can be reached in shorter reaction times and at lower temperatures.

Properties of the dry ionic liquid, the water-saturated ionic liquid and the ionic liquid saturated with a 6 M $NaNO_3$ solution can be found in **Table 4.1**. The mutual solubility of [HHIM][NO_3] and water was determined to calculate the losses of IL and water to the aqueous phase and the IL phase, respectively. After presaturation, the water content of a sample of the water-saturated ionic liquid was determined by volumetric Karl Fischer titration and was found to be 24 wt% at 25 °C. Quantitative ^{1}H NMR measurements showed that 6 wt% of the ionic liquid dissolved in the aqueous layer. However, most extraction experiments were performed with an aqueous phase containing 6 M $NaNO_3$, wherein the solubility of the ionic liquid is much lower (<0.5 wt%). The high salt concentration also lowers the water solubility in the ionic liquid (11 wt% instead of 24 wt%).

Table 4.1 Properties of ionic liquid [HHIM][NO_3]: water content of IL, solubility in aqueous phase, density ρ, dynamic viscosity η and phase behavior with water.

	H_2O-content IL (wt%)[a]	**Solubility IL in H_2O (1:1 w/w) (wt%)[a]**	**ρ (g·cm^{-3})**	**η (mPa·s)**	**Phase behavior with water**
Dry	n.d.	6	10.233	2×10^3	UCST
H_2O-saturated	24	6	10.153	2×10^1	UCST
6 M $NaNO_3$-saturated	11	<0.5	10.304	5×10^1	2 phases

[a] measured at 25 °C. n.d.: not determined.

As observed in **Table 4.1**, there is a large difference in viscosity between the dry and presaturated ionic liquids at room temperature. In **Figure 4.2**, full temperature scans (from 25 to 75 °C) of the viscosities of the dry, the water-saturated and the 6 M $NaNO_3$-saturated [HHIM][NO_3] ionic liquid are shown. Dry [HHIM][NO_3] is highly viscous (2×10^3 mPa·s at 25 °C) although there is a significant drop in viscosity to approximately 200 mPa·s when the ionic liquid is heated to 60 °C. Water-saturated [HHIM][NO_3] has a viscosity as low as 20 mPa·s at 25 °C, showing the strong effect of the water content on the viscosity. The ionic liquid which was presaturated with a 6 M $NaNO_3$ solution has a slightly higher viscosity than the water-saturated sample, but the viscosity is still lower than 50 mPa·s at room temperature. In comparison, the viscosity of water-saturated trihexyltetradecylphosphonium nitrate is 3×10^2 mPa·s.[38]

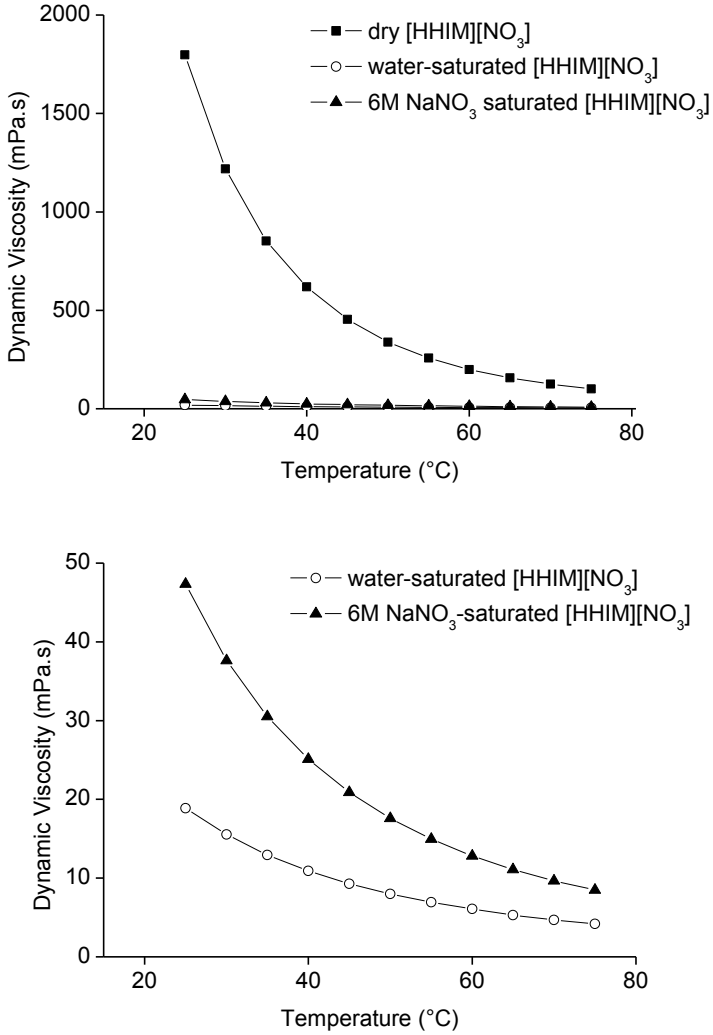

Figure 4.2 Dynamic viscosity of [HHIM][NO_3], top: comparison dry, water-saturated (24 ±0.4 wt% H_2O) [HHIM][NO_3] and 6 M $NaNO_3$-saturated (11 ±0.1 wt% H_2O) [HHIM][NO_3], bottom: detail water-saturated [HHIM][NO_3] and 6 M $NaNO_3$-saturated.

[HHIM][NO_3] shows a UCST phase behavior with water (**Table 4.1**). This thermomorphic behavior occurs upon heating the biphasic mixture to nearly 90 °C, where a clear and transparent solution is observed (**Figure 4.3**). To the best of our knowledge, no nitrate ionic liquid has ever been reported to exhibit temperature-dependent miscibility with water. The exact temperature at which the [HHIM][NO_3]/water 1:1 (w/w) mixture showed a transition between a cloudy, biphasic system and a clear, homogeneous solution was determined to be 84.1 °C. This cloud point temperature was also measured for several different combinations between [HHIM][NO_3] and water, ranging from 6 up to 76 wt% of IL. The liquid-liquid equilibrium phase diagram of the [HHIM][NO_3]/water mixture is shown in **Figure 4.3**. At 90 °C, a homogeneous solution is found for all compositions.

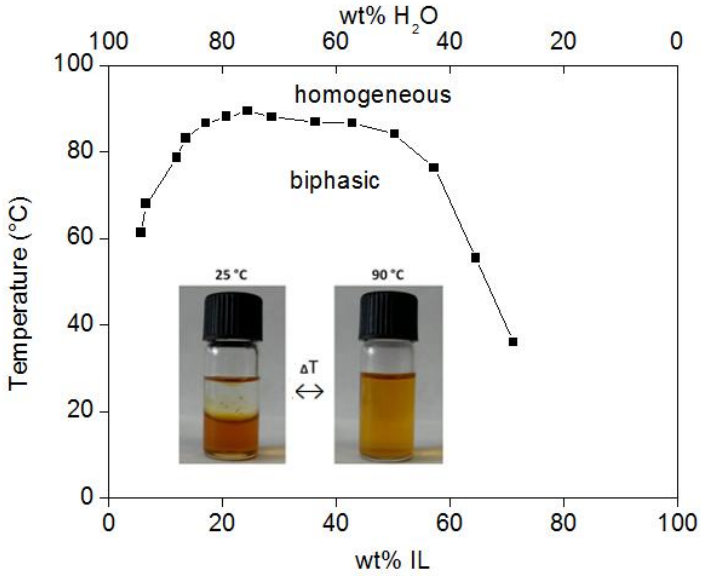

Figure 4.3 Liquid-liquid equilibrium phase diagram of the [HHIM][NO_3]/H_2O binary mixtures. Inset: visual representation of temperature-dependent miscibility of the ionic liquid [HHIM][NO_3] with water.

As discussed before, the total amount of water dissolved in the [HHIM][NO_3] phase at 25 °C was 24 wt% and the amount of IL dissolved in the water phase was calculated to be 6 wt% of the total water fraction. Both these values are also encountered in the phase diagram of [HHIM][NO_3] and water (**Figure 4.3**). Complete miscibility was observed for ionic liquid/water mixtures containing less than 6 wt% or more than 76 wt% [HHIM][NO_3] in water at any given temperature. A thermogravimetric analysis (TGA) of the

water-saturated ionic liquid confirmed the Karl Fischer results as a mass loss of 24% was found when the sample was heated to 120 °C to remove all water. The ionic liquid started decomposing around 280 °C (**Figure 4.4**), although it must be remarked the decomposition temperature is probably lower since a heating rate of 10 °C min^{-1} was used in this experiment.

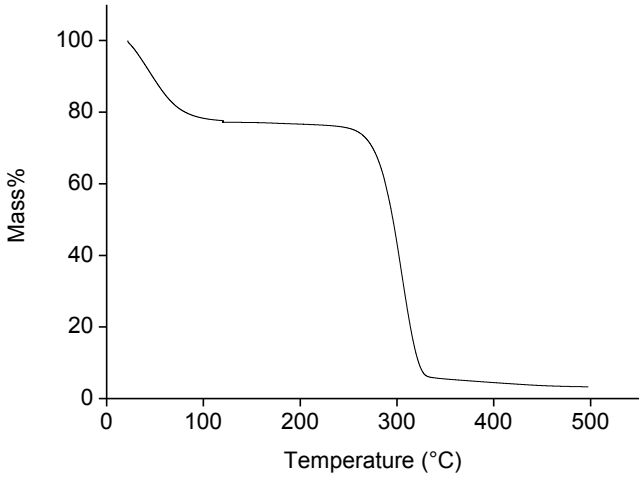

Figure 4.4 Thermogravimetric analysis (TGA) of water-saturated [HHIM][NO_3] (heating rate: 10 °C min^{-1}, N_2 atmosphere).

Addition of salts to the ionic liquid/water system led to the disappearance of any thermomorphic behavior due to the salting-out effect. Therefore, the application of the ionic liquid [HHIM][NO_3] for homogeneous liquid-liquid extraction was not successful. However, for conventional solvent extraction, the use of a non-fluorinated short-chain ionic liquid with a low carbon content is scarce.[39] The commercially available Aliquat® 336 and Cyphos® IL 101 have approximately 30 carbon atoms whilst [HHIM][NO_3] has only half the number of carbon atoms. Still, the [HHIM][NO_3]/water system is a biphasic system, with an ionic liquid solubility of <0.5 wt% in the aqueous phase if the IL was contacted with 6 M $NaNO_3$. The ionic liquid [HHIM][NO_3] was tested for extraction of metal ions. First row transition metals are far less efficiently extracted than the rare earths (**Figure 4.5**). Among the tested transition metals, no clear trend could be observed: all percentage extractions are around 30%. For the rare earths, as the charge density increases (La^{3+} < Nd^{3+} < Sm^{3+} < Sc^{3+}), the *%E* decreases. Larsson *et al.* also found preferential extraction of

light rare earths over the heavy rare earths with Aliquat® nitrate.[40] The similarity of the ionic radius of Y^{3+} to that of the heavier lanthanides is shown here as well, as Y^{3+} is the least extracted of the investigated rare earths.

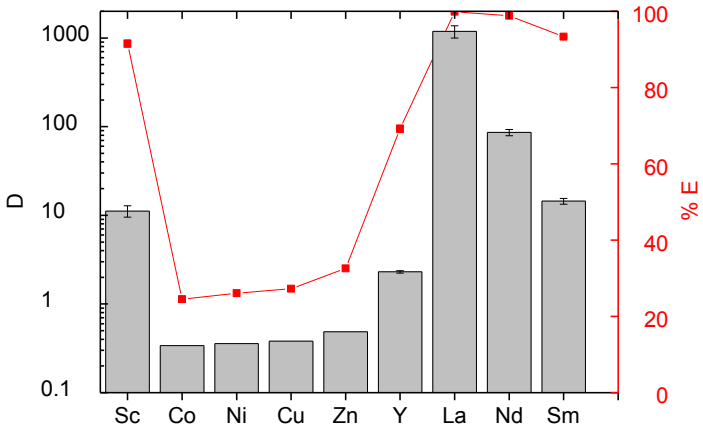

Figure 4.5 *D* (left axis) and *%E* (right axis) values for a selection of REEs nitrate solutions of 5 g L^{-1} and 3d transition metal nitrate solutions of 35 g L^{-1} (mono-element solutions in 6 M $NaNO_3$, 25 °C, 30 min, 2000 rpm). Calculation of error bars based on duplicate experiments.

Separations of the Sm(III)/Co(II) and La(III)/Ni(II) pairs were investigated. For the Sm(III)/Co(II) pair, the ratio of the metals was chosen to mimic that of a $SmCo_5$ magnet. Varying $NaNO_3$ concentrations were added in the aqueous metal feed solution which were then contacted with water-saturated ionic liquid (**Figure 4.6**). The higher the molar concentration of $NaNO_3$, the more Sm(III) was extracted, until at 6 M $NaNO_3$ nearly 100% of the Sm(III) was extracted. However, there was also a significant co-extraction of Co(II), of about 30%.

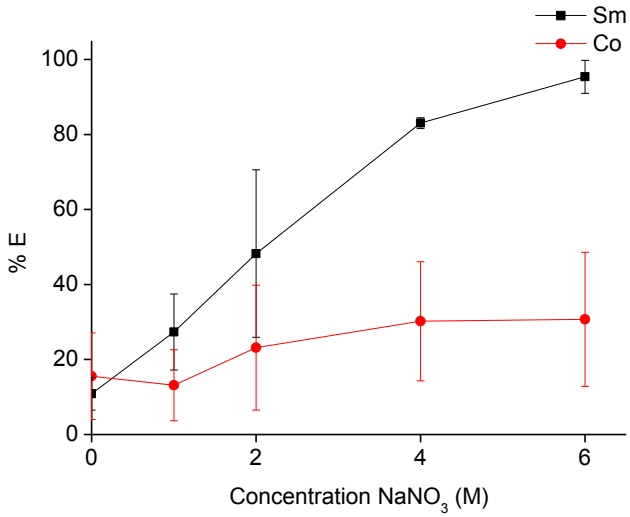

Figure 4.6 Percentage extraction of Sm(III) and Co(II) as a function of varying $NaNO_3$ concentration in aqueous feed solution (1:1 w/w, feed solution: 15.5 g L^{-1} Sm(III) and 36.9 g L^{-1} Co(II) as nitrate salts, 25 °C, 30 min, pH_{eq} =3). Calculation of error bars based on duplicate experiments.

With $NaNO_3$, the maximum nitrate concentration that can be obtained before reaching the solubility limit is about 6 M, also considering the metal nitrate salts present in the aqueous feed. A higher nitrate concentration could be obtained by changing the salting-out agent from $NaNO_3$ to NH_4NO_3 (**Figure 4.7**). The solubility of NH_4NO_3 in water is remarkably higher and a maximum nitrate concentration of 10 M above the nitrate concentration resulting from the metal nitrates could be reached. However, higher nitrate concentrations did not result in a more efficient extraction. In general, higher nitrate concentrations are expected to give higher extraction efficiencies, because in those cases the inner salting-out effect facilitates the extraction. The small, but significant difference in extraction between $NaNO_3$ and NH_4NO_3 can be explained by their respective salting-out effect, or their ability to exclude water from the organic phase. Because Na^+ is a stronger salting-out ion than NH_4^+ according to the Hofmeister series,[41] the lower concentration of 6 M $NaNO_3$ resulted in a better *%E* than 10 M of NH_4NO_3. Therefore, in all following experiments, 6 M $NaNO_3$ was used as optimal condition for the extraction.

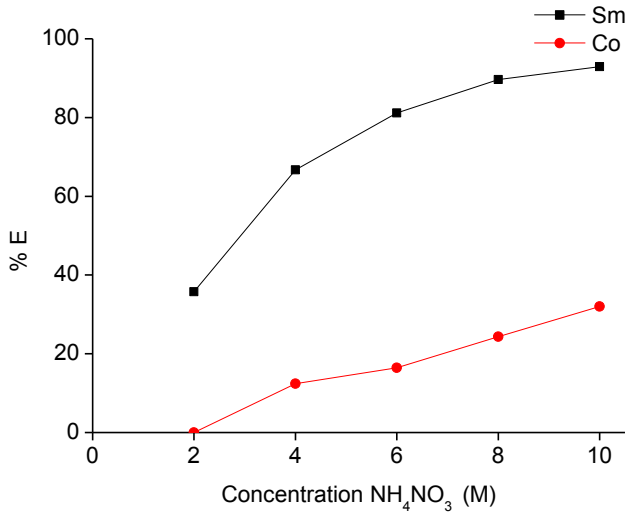

Figure 4.7 Percentage extraction of Sm(III) and Co(II) as a function of varying NH_4NO_3 concentration in the aqueous feed solution (1:1 w/w, feed solution: 15.5 g L^{-1} Sm(III) and 36.9 g L^{-1} Co(II) as nitrate salts, 25 °C, 30 min, pH_{eq} = 3, single experiment).

The low viscosity of water-saturated [HHIM][NO_3] was beneficial for the extraction kinetics. No remarkable changes in percentage extraction of Sm(III) and Co(II) were observed for longer shaking times. Yet, to ensure equilibrium was reached, 30 minutes was selected as the extraction time for further experiments (**Figure 4.8**). Next, the pH of the feed solution was varied. Since no apparent changes were visible, the extraction mechanism does not involve proton exchange (**Figure 4.9**).

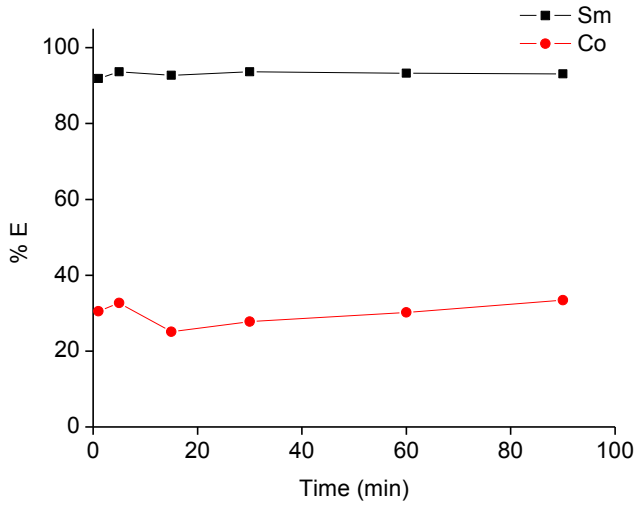

Figure 4.8 Percentage extraction of Sm(III) and Co(II) as a function of time (1:1 w/w, feed solution: 15.5 g L^{-1} Sm(III) and 36.9 g L^{-1} Co(II) as nitrate salts, 25 °C, 6 M $NaNO_3$, single experiment).

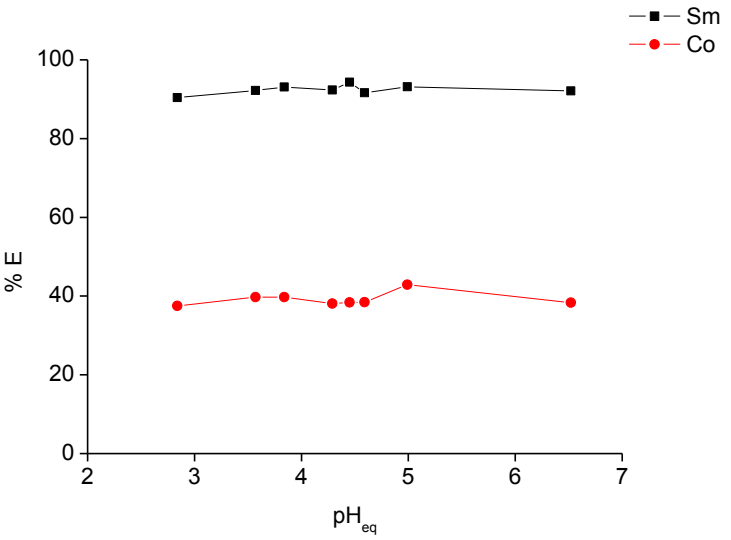

Figure 4.9 Percentage extraction of Sm(III) and Co(II) as a function of the equilibrium pH (pH_{eq}) (1:1 w/w, feed solution: approximately 14.0 g L^{-1} Sm(III) and 33.2 g L^{-1} Co(II) as nitrate salts, 25 °C, 6 M $NaNO_3$, single experiment).

As discussed before, the complete separation of Sm(III) and Co(II) was not feasible in one extraction step as a high amount of Co(II) was co-extracted with Sm(III). Therefore, a scrubbing step was necessary to remove the Co(II) (**Figure 4.10**). Essential in the scrubbing step is to keep the concentration of Sm(III), that is back-extracted to the aqueous phase, as low as possible. The loaded ionic liquid was contacted with different solutions of $NaNO_3$ having various concentrations. Scrubbing the ionic liquid with 6 M $NaNO_3$ removed 65% of Co(II) with a small back-extraction of 5% Sm(III). Repetition of this scrubbing and finalizing by contacting the scrubbed ionic liquid with pure water gave full stripping of Sm(III).

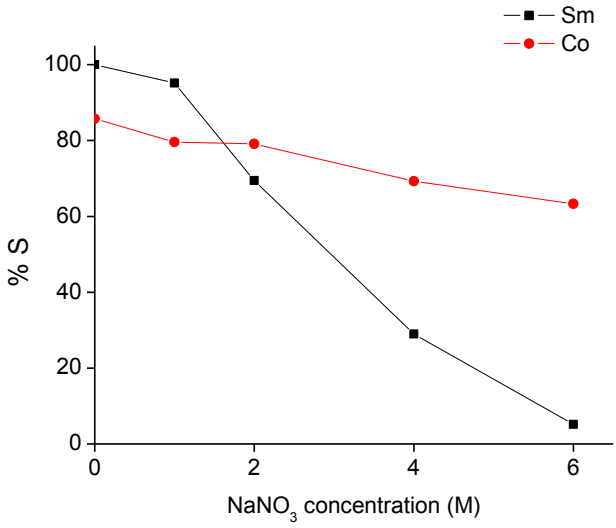

Figure 4.10 *%S* of Sm(III) and Co(II) as a function of varying $NaNO_3$ concentration in aqueous feed solution (1:1 w/w, IL loaded with 13.2 g L^{-1} Sm(III) and 5.8 g L^{-1} Co(II) as nitrate salts, 25 °C, 30 min, single experiment).

Of the REEs, La(III) has the highest distribution ratio, and was thus extracted most efficiently (**Figure 4.5**). Thus, [HHIM][NO_3] was capable to separate the La(III)/Ni(II) pair, which is another relevant separation for recycling end-of-life products, more specifically, nickel metal hydride (NiMH) batteries. A synthetic solution of 9.6 g L^{-1} La(III) and 35.4 g L^{-1} Ni(II) was prepared so that the concentration ratio of the La(III)/Ni(II) pair mimics the concentration ratio of the total rare-earth content to transition metal content in a recycling scheme by Larsson *et al.*[42] In the extraction, La(III) was fully extracted and only 15% of Ni(II) was co-extracted into the ionic liquid phase. In order to remove the Ni(II), the loaded ionic liquid phase was contacted with a fresh solution of 6 M $NaNO_3$, leaving the La(III) in the ionic liquid and removing 76% of the remaining Ni(II). Since the amount of La(III) that was back-extracted to the aqueous phase was low (0.5%), it was no problem to repeatedly contact the scrubbed ionic liquid with 6 M $NaNO_3$ in order to further decrease the amount of Ni(II) in the ionic liquid. Consequently, full separation could be reached with minimal loss of La(III). Final stripping of the La(III) could be achieved by contacting the scrubbed IL with pure water.[38]

4.4 Conclusions

The ionic liquid 1,3-dihexylimidazolium nitrate/water system introduced in this communication contains a relatively small cation whilst maintaining a biphasic system with a non-fluorinated imidazolium ionic liquid. 1,3-Dihexyl imidazolium nitrate is immiscible with water at room temperature, yet becomes fully miscible in all compositions with heating to 90 °C, a feature called upper critical solution temperature (UCST) phase behavior. As the addition of salts to the ionic liquid/water system led to the disappearance of any temperature-dependent miscibility behavior, a fully hydrophobic system was formed at all temperatures. Therefore, the short-chain ionic liquid was tested in conventional metal extraction. The preferential extraction of rare earths over 3d transition metals was observed. This was exploited in the separation of Sm(III)/Co(II) and La(III)/Ni(II) pairs.

This research was financially supported by IWT-Flanders (PhD fellowship to DD), the FWO Flanders (research project G.0900.13) and the KU Leuven (projects GOA/13/008 and IOF-KP RARE3). The authors also wish to thank Dirk Henot for performing CHN analysis. Joris Roosen is thanked for the help with the design of the cover art.

4.5 References

1 Rydberg, J.; Cox, M.; Musikas, C.; Choppin, G. R.; *Solvent Extraction: Principles and Practice;* Marcel Dekker, Inc.: New York, 2004.

2 T. Welton, *Chem. Rev.*, 1999**, 99**, 2071.

3 P. Wasserscheid, W. Keim, *Angew. Chem. Int. Ed.*, 2000**, 39**, 3772.

4 R. D. Rogers, K. R. Seddon, *Science*, 2003**, 302**, 792.

5 R. P. Swatloski, J. D. Holbrey, R. D. Rogers, *Green Chem.*, 2003**, 5**, 361.

6 M. G. Freire, C. M. S. S. Neves, I. M. Marrucho, J. A. P. Coutinho, A. M. Fernandes, *J. Phys. Chem. A*, 2010**, 114**, 3744.

7 T. Vander Hoogerstraete, S. Wellens, K. Verachtert, K. Binnemans, *Green Chem.*, 2013**, 15**, 919.

8 T. Vander Hoogerstraete, B. Onghena, K. Binnemans, *Int. J. Mol. Sci.*, 2013**, 14**, 21353.

9 M. G. Freire, L. M. N. B. Santos, A. M. Fernandes, J. A. P. Coutinho, I. M. Marrucho, *Fluid Phase Equilibr.*, 2007**, 261**, 449.

10 J. Luczak, J. Hupka, J. Thöming, C. Jungnickel, *Colloids Surf A: Physicochem. Eng. Asp.*, 2008**, 329**, 125.

11 J. L. Anthony, E. J. Maginn, J. F. Brennecke, *J. Phys. Chem. B*, 2001**, 105**, 10942.

12 D. S. H. Wong, J. P. Chen, J. M. Chang, C. H. Chou, *Fluid Phase Equilibr.*, 2002**, 194–197**, 1089.

13 H. S. Schrekker, M. P. Stracke, C. M. L. Schrekker, J. Dupont, *Ind. Eng. Chem. Res.*, 2007**, 46**, 7389.

14 M. A. R. Martins, C. M. S. S. Neves, K. A. Kurnia, A. Luis, L. M. N. B. Santos, M. G. Freire, S. P. Pinho, J. A. P. Coutinho, *Fluid Phase Equilibr.*, 2014**, 375**, 161.

15 M. G. Freire, P. J. Carvalho, R. L. Gardas, I. M. Marrucho, L. M. N. B. Santos, J. A. P. Coutinho, *J. Phys. Chem. B*, 2008**, 112**, 1604.

16 U. Domanska, A. Rekawek, A. Marciniak, *J. Chem. Eng. Data*, 2008**, 53**, 1126.

17 P. Nockemann, K. Binnemans, B. Thijs, T. N. Parac-Vogt, K. Merz, A. V. Mudring, P. C. Menon, R. N. Rajesh, G. Cordoyiannis, J. Thoen, J. Leys, C. Glorieux, *J. Phys. Chem. B*, 2009**, 113**, 1429.

18 P. Nockemann, B. Thijs, S. Pittois, J. Thoen, C. Glorieux, K. Van Hecke, L. Van Meervelt, B. Kirchner, K. Binnemans, *J. Phys. Chem. B*, 2006**, 110**, 20978.

19 M. Blesic, H. Q. N. Gunaratne, J. Jacquemin, P. Nockemann, S. Olejarz, K. R. Seddon, C. R. Strauss, *Green Chem.*, 2014**, 16**, 4115.

20 K. Fukumoto, H. Ohno, *Angew. Chem. Int. Ed.*, 2007**, 46**, 1852.

21 Y. Fukaya, H. Ohno, *Phys. Chem. Chem. Phys.*, 2013**, 15**, 4066.

22 Y. Kohno, H. Ohno, *Chem. Commun.*, 2012**, 48**, 7119.

23 T. Vander Hoogerstraete, B. Onghena, K. Binnemans, *J. Phys. Chem. Lett.*, 2013**, 4**, 1659.

24 B. Onghena, J. Jacobs, L. Van Meervelt, K. Binnemans, *Dalton Trans.*, 2014**, 43**, 11566.

25 D. Depuydt, L. Liu, C. Glorieux, W. Dehaen, K. Binnemans, *Chem. Commun.*, 2015**, 51**, 14183.
26 D. Depuydt, W. Dehaen, K. Binnemans, *ChemPlusChem*, 2017**, 82**, 458.
27 S. Riano, M. Regadio, K. Binnemans, T. Vander Hoogerstraete, *Spectrochimica Acta B*, 2016**, 124**, 109.
28 D. Depuydt, A. Van den Bossche, W. Dehaen, K. Binnemans, *RSC Adv.*, 2016**, 6**, 8848.
29 F. Malz, H. Jancke, *J. Pharm. Biomed. Anal.*, 2005**, 38**, 813.
30 J. D. Holbrey, W. M. Reichert, R. P. Swatloski, G. A. Broker, W. R. Pitner, K. R. Seddon, R. D. Rogers, *Green Chem.*, 2002**, 4**, 407.
31 D. Holbrey, R. Seddon, *J. Chem. Soc. , Dalton Trans.*, 1999**,** 2133.
32 T. L. Merrigan, E. D. Bates, S. C. Dorman, J. Davis, *Chem. Commun.*, 2000**,** 2051.
33 A. E. Visser, R. P. Swatloski, W. M. Reichert, R. Mayton, S. Sheff, A. Wierzbicki, J. Davis, R. D. Rogers, *Chem. Commun.*, 2001**,** 135.
34 L. C. Branco, J. N. Rosa, J. J. Moura Ramos, C. A. M. Afonso, *Chem. Eur. J.*, 2002**, 8**, 3671.
35 S. V. Dzyuba, R. A. Bartsch, *ChemPhysChem*, 2002**, 3**, 161.
36 J. Pernak, A. Czepukowicz, R. Pozniak, *Ind. Eng. Chem. Res.*, 2001**, 40**, 2379.
37 M. M. Bailey, M. B. Townsend, P. L. Jernigan, J. Sturdivant, W. L. Hough-Troutman, J. F. Rasco, R. P. Swatloski, R. D. Rogers, R. D. Hood, *Green Chem.*, 2008**, 10**, 1213.
38 T. Vander Hoogerstraete, K. Binnemans, *Green Chem.*, 2014**, 16**, 1594.
39 Y. Zhou, S. p. Boudesocque, A. Mohamadou, L. Dupont, *Separ. Sci. Technol.*, 2015**, 50**, 38.
40 K. Larsson, K. Binnemans, *J. Sustain. Metall.*, 2017**, 3**, 73.
41 D. Dupont, D. Depuydt, K. Binnemans, *J. Phys. Chem. B*, 2015**, 119**, 6747.
42 K. Larsson, K. Binnemans, *Green Chem.*, 2014**, 16**, 4595.

CHAPTER 5

HOMOGENEOUS LIQUID-LIQUID EXTRACTION WITH LCST-IONIC LIQUIDS

This chapter has been published and is reproduced here with permission from The Royal Society of Chemistry.

Depuydt, D., Liu, L., Glorieux, C., Dehaen, W., Binnemans, K. (2015). Homogeneous liquid–liquid extraction of metal ions with non-fluorinated bis(2-ethylhexyl)phosphate ionic liquids having a lower critical solution temperature in combination with water. *Chemical Communications, 51* (75), 14183-14186.

The experimental work and writing were executed by the author of this thesis. The text may deviate from the original publication as the supplementary information is included in the chapter.

Graphical Abstract

Bis(2-ethylhexyl)phosphate ionic liquids show temperature-dependent phase behavior of the LCST-type and can extract transition metal ions very efficiently via homogeneous liquid-liquid extraction.

Abstract

Ionic liquids with an ether-functionalized cation and the bis(2-ethylhexyl)phosphate anion show thermomorphic behavior in water, with a lower critical solution temperature. These ionic liquids are useful for homogeneous liquid-liquid extraction of first period (3d) transition metals.

5.1 Introduction

Ionic liquids (ILs) are solvents that consist entirely of ions.[1-3] They are distinguished from molten salts by their low melting temperature, arbitrarily set at 100 °C. ILs are often considered as environmentally friendly alternatives for molecular solvents in solvent extraction since they have a negligible vapor pressure.[4] The physical properties of ILs depend on their structure. Depending on its composition, an ionic liquid is miscible or immiscible with water, leading to a classification into hydrophilic and hydrophobic ionic liquids. Yet, this classification is ambiguous, since the miscibility of some ILs with water is strongly temperature-dependent. In upper critical solution temperature (UCST) systems, the solubility of the IL in water increases with increasing temperature and a homogeneous system is found above a certain point in the cloud point curve, namely above the upper critical solution temperature, the components are miscible in all concentrations. The opposite happens for the lower critical solution temperature (LCST) systems, in which the homogeneous phase is formed with a decrease of temperature. It has been reported that ILs have temperature-dependent miscibility with different molecular solvents.[5,6,7,8] Ohno and co-workers made seminal contributions to LCST phase changes in ILs.[9-16] They have prepared ionic liquids derived from amino acids that show LCST-type phase changes with water.[17] IL/water biphasic mixtures are of interest for the separation of molecules by solvent extraction. In 2006, we reported on the IL betainium bis(trifluoromethylsulfonyl)imide ([Hbet][Tf_2N]) which, mixed with water, shows an UCST at 55 °C.[18] It has been used in the homogeneous liquid-liquid extraction (HLLE) of metal ions.[19-21] The binary mixture of choline bis(trifluoromethylsulfonyl)imide ([Chol][Tf_2N]) and water shows temperature-dependent phase behavior with an upper critical solution temperature of 72 °C and has been used for the HLLE of Nd(III).[22] A series of ILs based on Girard's reagents have tunable thermomorphism of the UCST type and were used for HLLE of transition metals.[23] In the literature, the LCST behavior of both glycol ether/water mixtures,[24] and functionalized polymers with glycol chains[25] were described. The ionic liquid interpretation of the LCST phase behavior can be comprehended based on the knowledge from polymer studies. Although Ohno and co-workers reported the HLLE of LCST ionic liquids for the extraction of proteins,[26,27] the use of such a LCST system was, until now, never executed for the extraction of metal ions.

In this chapter, ionic liquids having the bis(2-ethylhexyl)phosphate as anion are presented that show lower critical solution temperature phase behavior. A proof-of-principle extraction of first row transition metals by the ionic liquid $[P_{444}E_3][DEHP]$ is the first example of homogeneous liquid-liquid extraction of metal ions with an LCST thermomorphic system. The designed ILs are depicted in **Figure 5.1**.

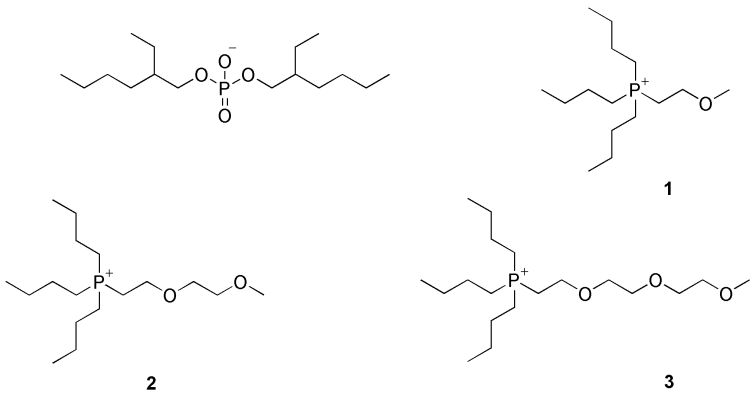

Figure 5.1 Structures of investigated ILs. Anion: bis(2-ethylhexyl)phosphate ($[DEHP]^-$). Cations: 1: tri-*n*-butyl-2-methoxyethylphosphonium ($[P_{444}E_1]^+$), 2: tri-*n*-butyl [2-(2-methoxyethoxy)ethyl]phosphonium ($[P_{444}E_2]^+$), 3: tri-*n*-butyl-{2-[2-(2-methoxyethoxy)ethoxy]ethyl}phosphonium $[P_{444}E_3]^+$).

5.2 Experimental

5.2.1 Chemicals

Tri-*n*-butylphosphine (97%), 2-chloroethyl methyl ether (98%), bis(2-ethylhexyl)phosphate (97%), chloroform (ACS grade), triethylene glycol monomethyl ether (97%), zinc chloride (reagent grade 98%), cobalt chloride (97%), nickel chloride (98%) and magnesium sulfate hydrate were bought from Sigma-Aldrich (Diegem, Belgium). Heptane (99%) and hydrogen peroxide (35wt%) were purchased from Chem-Lab (Zedelgem, Belgium). Acetonitrile (HPLC grade), ethanol absolute, dichloromethane (analytical reagent grade) and sodium hydroxide were obtained from Fisher Scientific Limited (Loughborough, UK). Pyridine was acquired from BDH Laboratory Supplies. 2-(2-methoxyethoxy)ethanol (99%), copper chloride (99%) and thionyl chloride (99.7 %) were bought from Acros Organics (Geel, Belgium). All chemicals were used without purification.

5.2.2 General

^{1}H NMR and ^{13}C NMR spectra were recorded on a Bruker Avance 300 spectrometer (operating at 300 MHz for ^{1}H, 75 MHz for ^{13}C). ^{31}P NMR spectra were recorded on a Bruker AMX 400 spectrometer operating at 162 MHz. The chemical shifts are noted in parts per million (ppm), referenced to tetramethylsilane for ^{1}H and ^{13}C and to 85% H_3PO_4 for ^{31}P NMR. The coupling constants are given in Hertz. Solutions were made in $CDCl_3$. The spectra were analyzed with SpinWorks software. Fourier transform infrared spectra of the ILs were recorded by a Bruker Vertex 70 spectrometer. The attenuated total reflectance (ATR) technique was used for direct examination of the ionic liquids (Bruker ATR platinum sample holder). OPUS software was used for the analysis. The elemental analysis of carbon, hydrogen and nitrogen was performed on a CE-instruments EA-1110 elemental analyzer. The water content was determined by coulometric Karl Fischer titration using a Mettler-Toledo DL39 titrator. The viscosity of the ionic liquids was measured using an automatic Brookfield plate cone viscometer, Model LVDV-II CP (Brookfield Engineering Laboratories, USA). ESI-MS was performed on a Thermo Electron LCQ Advantage ion trap mass spectrometer connected to Agilent 1100 HPLC system coupled to Xcalibur data system. Extraction experiments were performed in a TMS-200 thermoshaker (Nemux Life). A Bruker S2 Picofox total reflection X-ray fluorescence (TXRF)

spectrometer was used to determine the metal concentrations in both aqueous and organic (ionic liquid) phase as well as for the determination of the chloride content of the ionic liquids. For the sample preparation, plastic microtubes were filled with a small amount of aqueous solution (100 mg) or IL sample (10−50 mg), gallium as internal standard (100 or 50 mg) and water or ethanol (800 µL). The microtubes were then vigorously shaken on a vibrating plate (IKA MS 3 basic). Finally, a 5 µL drop of this solution was put on a quartz plate, previously treated with a silicone/isopropanol solution (Serva®) to avoid spreading of the sample droplet on the quartz plate. The quartz plates were then dried for 30 min at 60 °C prior to analysis. Each sample was measured for 200 s. Extraction mixtures were centrifuged using a Heraeus Labofuge 200.

5.2.3 Synthesis

Precursor synthesis

Triethylene glycol monomethylether or 2-(2-methoxyethoxy)ethanol were used in the synthesis of the chloride precursors, a literature procedure was followed (**Scheme 5.1**).[28,29] A solution of thionyl chloride (1.5 mol eq., 75 mmol) in 10 mL of chloroform was added slowly to a stirred solution of triethylene glycol monomethylether or 2-(2-methoxyethoxy)ethanol (1 mol eq., 50 mmol) and pyridine (1 mol eq., 50 mmol) in 20 mL of chloroform under argon atmosphere. The mixture was refluxed at 60 °C for 4 h and then washed four times with water. The organic layer was dried with $MgSO_4$, filtered and the solvent was evaporated. The product was fully dried on a Schlenk line.

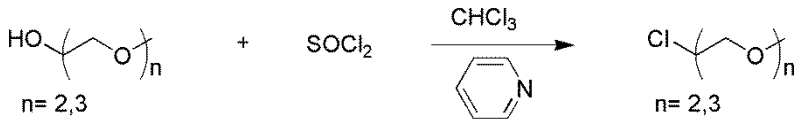

Scheme 5.1 Synthesis of chloride precursors.

1-(2-methoxyethoxy)-2-chloroethane (E_2Cl)

Light brown liquid (2.611 g, 18.84 mmol, 38%). ^{1}H NMR (300 MHz, δ, $CDCl_3$): 3.79-3.74 (2H, m, CH_2), 3.69-3.63 (4H, m, 2 CH_2), 3.58-3.55 (2H, m, CH_2), 3.40 (3H, s, CH_3). ^{13}C NMR (75 MHz, δ, $CDCl_3$): 71.94 (CH_2), 71.37 (CH_2), 70.67 (CH_2), 70.62 (CH_2), 70.61 (CH_2), 59.06 (CH_3), 42.71 (CH_2-Cl). FTIR-ATR: (ν/cm^{-1}): 2877, 1455, 1353, 1200, 1103, 850, 745, 665. CHN

analysis: (calculated for $C_5H_{11}ClO_2$): C 43.82% (43.33%), H 8.30% (8.00%), N 0% (0%).

2-[2-(2-methoxyethoxy)ethoxy]ethylchloride (E_3Cl)

Yellow liquid (6.303 g, 34.5 mmol, 69%). ^{1}H NMR (300 MHz, δ, $CDCl_3$): 3.78 (2H, t, 6.0 Hz, CH_2), 3.68 (8H, m, 4 CH_2), 3.57 (2H, m, CH_2), 3.39 (3H, s, CH_3). ^{13}C NMR (75 MHz, δ, $CDCl_3$): 71.94 (CH_2), 71.37 (CH_2), 70.67 (CH_2), 70.62 (CH_2), 70.61 (CH_2), 59.06 (CH_3), 42.71 (CH_2-Cl). FTIR-ATR: (ν/cm^{-1}): 2874, 1455, 1353, 1200, 1103, 850, 745, 665. CHN analysis: (calculated for $C_7H_{15}ClO_3$): C 45.67% (46.03%), H 9.93% (8.28%), N 0% (0%).

Ether functionalized IL synthesis

Ether functionalization was incorporated in the phosphonium ionic liquids according to literature procedures.[28,30] Tri-*n*-butyl phosphine was reacted with the organic halide containing the desired ether functional group (**Scheme 5.2**). A mixture of tri-*n*-butyl phosphine (1 mol eq., 10 mmol) and oligoethylene oxide chloride precursor (1 mol eq., 10 mmol) in 15 mL of acetonitrile was refluxed for 48 h. On completion, the acetonitrile was evaporated under reduced pressure at 60 °C. The product was washed with 10 mL of heptane under reflux for 1 h. The upper heptane phase was decanted and the process was repeated four times. The product was fully dried on a Schlenk line.

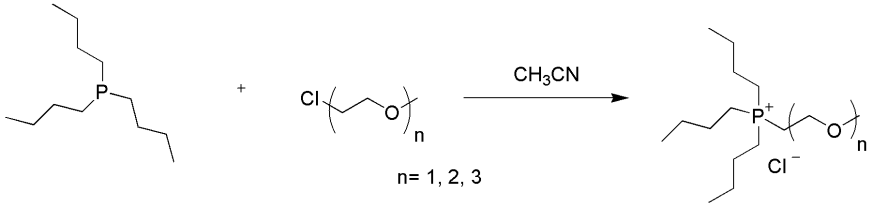

Scheme 5.2 Synthesis of ether-functionalized ionic liquids.

Tri-n-butyl-2-methoxyethylphosphonium chloride
[$P_{444}E_1$][Cl]

Colorless viscous liquid (65%). ^{1}H NMR (300 MHz, δ, $CDCl_3$): 3.85 (2H, m, CH_2), 3.35 (3H, s, CH_3), 3.00 (2H, m, CH_2), 2.43 (6H, m, 3 CH_2), 1.54 (12H, m, 6 CH_2), 0.98 (3H, t, 7.0 Hz, CH_3). ^{13}C NMR (75 MHz, δ, $CDCl_3$): 65.96 (CH_2), 65.86 (CH_2), 58.97 (CH_3), 24.11 (CH_2), 21.51 (CH_2), 20.84 (CH_2), 20.04 (CH_2), 19.42 (CH_2), 13.49 (CH_3). ^{31}P NMR (162 MHz, δ, $CDCl_3$): 34.27. FTIR-ATR: (ν/cm^{-1}): 2958, 2931, 2872, 1722, 1463, 1381, 1235, 1189,

1097, 958, 917, 812, 723. CHN analysis: (calculated for $C_{15}H_{34}ClOP \cdot H_2O$): C 57.22% (57.00%), H 11.93% (11.52%), N 0% (0%).

Tri-n-butyl[2-(2-methoxyethoxy)ethyl]phosphonium chloride
$[P_{444}E_2][Cl]$

Light brown viscous liquid (69%). ^{1}H NMR (300 MHz, δ, $CDCl_3$): 3.90 (2H, m, CH_2), 3.62 (2H, m, CH_2), 3.49 (2H, m, CH_2), 3.34 (3H, s, CH_3), 3.06 (2H, m, CH_2), 2.44 (6H, m, 3 CH_2), 1.53 (12H, m, 6 CH_2), 0.98 (3H, t, 7.0 Hz, CH_3). ^{13}C NMR (75 MHz, δ, $CDCl_3$): 71.40 (CH_2), 70.20 (CH_2), 58.95 (CH_3), 24.00 (CH_2), 19.49 (CH_2), 13.67 (CH_3). ^{31}P NMR (162 MHz, δ, $CDCl_3$): 34.22. FTIR-ATR: (ν/cm^{-1}): 2958, 2931, 2872, 1722, 1464, 1381, 1238, 1198, 1098, 970, 906, 809, 741. CHN analysis: (calculated for $C_{17}H_{38}ClO_2P$): C 59.15% (59.89%), H 11.42% (11.24%), N 0% (0%).

Tri-n-butylphosphonium chloride
$[P_{444}E_3][Cl]$

Light yellow viscous liquid (57%). ^{1}H NMR (300 MHz, δ, $CDCl_3$): 3.55 (2H, m, CH_2), 3.50 (6H, m, 3 CH_2), 3.41 (2H, m, CH_2), 3.24 (3H, s, CH_3), 2.58 (2H, m, CH_2), 2.20 (6H, m, 3 CH_2), 1.53-1.35 (12H, m, 6 CH_2), 0.88 (3H, t, 7.0 Hz, CH_3). ^{13}C NMR (75 MHz, δ, DMSO-d_6): 71.20 (CH_2), 69.42 (CH_2), 58.00 (CH_3), 23.39 (CH_2), 22.63 (CH_2), 18.39 (CH_2), 17.73 (CH_2), 13.17 (CH_3). ^{31}P NMR (162 MHz, δ, $CDCl_3$): 34.22. FTIR-ATR: (ν/cm^{-1}): 2958, 2931, 2872, 1464, 1381, 1350, 1236, 1198, 1101, 1012, 969, 920, 810, 723. CHN analysis: (calculated for $C_{18}H_{40}ClO_3P \cdot H_2O$): C 55.41% (55.58%), H 11.23% (10.88%), N 0% (0%).

Bis(2-ethylhexyl)phosphate anion exchange reaction

The synthesis of the ILs was performed by a metathesis reaction in which the chloride anion of the ether-functionalized ILs was exchanged to the bis(2-ethylhexl)phosphate (**Scheme 5.3**). First, the acid form of the phosphate is neutralized by a base, as found in the literature.[31] To bis(2-ethylhexyl)phosphate in ethanol absolute was added a solution of 20 wt% NaOH until neutral pH was reached. The solvent was evaporated and the product dried in a vacuum oven at 60 °C for 2 h. The phosphate salt (1 mol eq.) and the chloride ionic liquid (1.5 mol eq.) were dissolved in water and stirred overnight. Dichloromethane was added and the product was extracted to the organic phase and washed with water to remove NaCl and the excess of ionic liquid. The organic phase was isolated and evaporated.

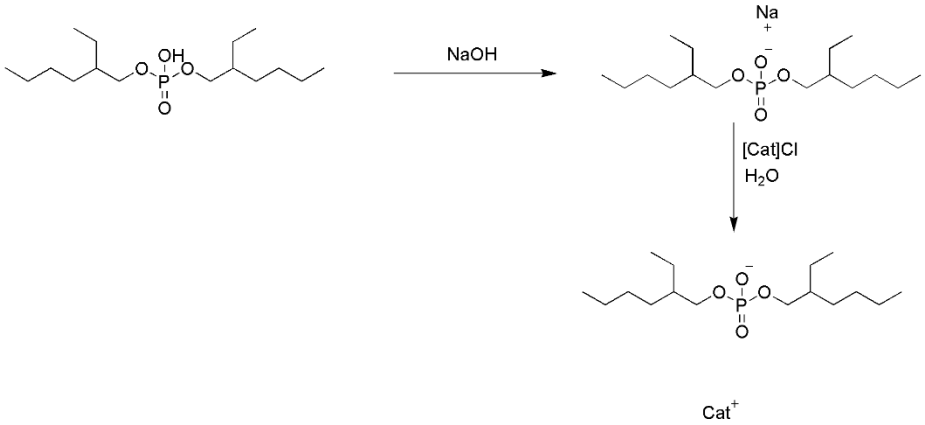

Scheme 5.3 Synthesis of dialkylphosphate ILs.

Tri-n-butyl-2-methoxyethylphosphonium bis(2-ethylhexyl) phosphate [$P_{444}E_1$][DEHP]

Colorless liquid (89 %). ^{1}H NMR (300 MHz, δ, $CDCl_3$): 3.87 (2H, m, CH_2), 3.69 (4H, m, 2 CH_2), 3.33 (3H, s, CH_3), 2.98 (2H, m, 2 CH), 2.35 (6H, m, 3 CH_2), 1.52 (18H, m, 6 CH_2 + 2 CH), 1.27 (12H, m, 6 CH_2), 0.97 (9H, t, 3 CH_3), 0.87 (12H, m, 4 CH_3). ^{13}C NMR (75 MHz, δ, $CDCl_3$): 67.27 (CH_2), 66.07 (CH_2), 58.75 (CH_3), 40.56 (CH_2), 30.20 (CH_2), 29.13 (CH_2), 24.12 (CH_2), 23.91 (CH_2), 23.85 (CH_2), 23.78 (CH_2), 23.42 (CH_2), 23.18 (CH_2), 19.75 (CH_2), 19.12 (CH_2), 14.14 (CH_3), 13.47 (CH_3), 11.03 (CH_3). ^{31}P NMR (162 MHz, δ, $CDCl_3$): 33.64, 0.65. FTIR-ATR: (ν/cm^{-1}): 2958, 2928, 2873, 1462, 1380, 1244, 1054, 810, 532. Cl content: 195 ppm. CHN analysis: (calculated for $C_{31}H_{68}O_5P_2 \cdot H_2O$): C 61.91% (61.97%), H 13.27% (11.74%), N 0% (0%). ESI-MS (MeOH): *m/z* 322.5 (DEHP), 263.4 ($P_{444}E_1$).

Tri-n-butyl[2-(2-methoxyethoxy)ethyl]phosphonium bis(2-ethylhexyl) phosphate [$P_{444}E_2$][DEHP]

Light yellow liquid (97%). ^{1}H NMR (300 MHz, δ, $CDCl_3$): 3.87 (2H, m, CH_2), 3.69 (4H, m, 2 CH_2), 3.59 (2H, m, CH_2), 3.48 (2H, m, CH_2), 3.34 (3H, s, CH_3), 2.99 (2H, m, 2 CH), 2.35 (6H, m, 3 CH_2), 1.52 (18H, m, 6 CH_2 + 2 CH), 1.29 (12H, m, 6 CH_2), 0.97 (9H, t, 3 CH_3) , 0.87 (12H, m, 4 CH_3). ^{13}C NMR (75 MHz, δ, $CDCl_3$): 71.46 (CH_2), 70.09 (CH_2), 67.46 (CH_2), 64.55 (CH_2), 58.72 (CH_3), 40.55 (CH_2), 30.19 (CH_2), 29.12 (CH_2), 24.14 (CH_2), 23.94 (CH_2), 23.85 (CH_2), 23.79 (CH_2), 23.18 (CH_2), 21.20 (CH_2), 19.72 (CH_2), 19.09 (CH_2), 14.15 (CH_3), 13.48 (CH_3), 11.03 (CH_3). ^{31}P NMR (162

MHz, δ $CDCl_3$): 33.56, 0.72. FTIR-ATR: (ν/cm^{-1}): 2958, 2928, 2873, 1462, 1380, 1246, 1053, 809, 554. Cl content: 165 ppm. CHN analysis: (calculated for $C_{33}H_{72}O_6P_2 \cdot 2H_2O$): C 59.78% (59.79%), H 11.44% (11.56%), N 0% (0%). ESI-MS (MeOH): *m/z* 322.5 (DEHP), 307.9 ($P_{444}E_2$).

Tri-n-butyl{2-[2-(2-methoxyethoxy)ethoxy]ethyl}phosphonium bis(2-ethylhexyl)phosphate [$P_{444}E_3$][DEHP]

Light yellow liquid (89 %). ^{1}H NMR (300 MHz, δ, $CDCl_3$): 3.91 (2H, m, CH_2), 3.69 (4H, m, 2 CH_2), 3.58 (6H, m, 3 CH_2), 3.51 (2H, m, CH_2), 3.36 (3H, s, CH_3), 2.98 (2H, m, CH_2), 2.35 (6H, m, 3 CH_2), 1.49 (18H, m, 6 CH_2 + 2 CH), 1.30 (12H, m, 6 CH_2), 0.97 (9H, t, 3 CH_3), 0.87 (12H, m, 4 CH_3). ^{13}C NMR (75 MHz, δ, $CDCl_3$): 71.95 (CH_2), 70.36 (CH_2), 70.16 (CH_2), 67.50 (CH_2), 58.97 (CH_3), 40.59 (CH_2), 30.23 (CH_2), 29.16 (CH_2), 24.17 (CH_2), 23.96 (CH_2), 23.90 (CH_2), 23.83 (CH_2), 23.46 (CH_2), 23.20 (CH_2), 19.76 (CH_2), 19.13 (CH_2), 14.16 (CH_3), 13.52 (CH_3), 11.05 (CH_3). ^{31}P NMR (162 MHz, δ, $CDCl_3$): 33.55, 0.62. FTIR-ATR: (ν/cm^{-1}): 2957, 2928, 2873, 1462, 1245, 1094, 1053, 810, 530. Cl content: 341 ppm. CHN analysis: (calculated for $C_{35}H_{76}O_7P_2 \cdot H_2O$): C 59.41% (59.46%), H 11.15% (11.41%), N 0% (0%). ESI-MS (MeOH): *m/z* 322.5 (DEHP), 352.5 ($P_{444}E_3$).

5.2.4 Transmission measurements

A CW 532-nm laser (Samba 100, Cobolt®) was used as probe laser. The transmitted light was collected by a lens and sent to a photodetector (read by an HP34401A multimeter). The sample cell was situated inside an optical cryostat (Optistat-DN-V, Oxford Instruments®), where the temperature could be regulated by an accompanying temperature controller (ITC 503, Oxford Instruments®). In order to account for possible temperature differences between the cold finger and the sample, a resistive PT1000 thermometer, read by another HP34401A® multimeter, was attached to the sample cuvette, monitoring its temperature nearby the region of probe beam. In the setup, all the instruments are connected to one PC via GPIB interface. For each sample (1:1weight ratio of IL:water), one temperature scan was performed with a step of 0.1 K, and at each temperature 100 pairs of temperature-transmitted light intensity were recorded for averaging.

5.2.5 Quantitative ^{1}H NMR

The amount of IL that is lost into IL phase was determined by quantitative ^{1}H NMR. To 100 mg of the water layer of presaturation of the IL was added 5 mg of pyridine to obtain approximately equimolar concentrations to the aliquot of water presaturated with the IL. Pyridine was chosen as internal standard since there is no overlap with the ^{1}H NMR spectrum of the ionic liquid. The ^{1}H NMR spectrum of the water sample was recorded and the relative concentration versus pyridine and the absolute concentration of the ILs were calculated by integration of the peaks.

5.2.6 Extraction experiments

In a typical extraction experiment, 500 mg of the presaturated IL is contacted with 500 mg of an aqueous metal solution. The mixtures were cooled in an ice bath for several minutes to reach the homogeneous region. Next, the mixtures are left to settle at room temperature for 10 min. A sample was taken from the aqueous layer and analyzed for its metal content by TXRF. The percentage extraction (*%E*) was calculated according to equation 5.1:

$$\%E = \frac{c_{org} \cdot m_{org}}{c_{org} \cdot m_{org} + c_{aq} \cdot m_{aq}} \times 100\% \qquad (5.1)$$

where c_{org} and c_{aq} are the metal concentration in the organic phase (*i.e.* ionic liquid phase) and in the aqueous phase, respectively and m_{org} and m_{aq} are the masses of the organic phase and the aqueous phase, respectively.

5.2.7 Stripping experiments

For a typical stripping experiment, to 500 mg of the loaded IL, equimolar amounts of oxalic acid were added and shaken for 30 min at room temperature. The vials were centrifuged to accumulate all precipitate at the bottom. A sample of the IL phase was taken for analysis of its metal content by TXRF.

5.3 Results and Discussion

The synthesis of the ether-functionalized ionic liquids was based on literature procedures.[29] After tri-*n*-butylphosphine was reacted with a chloride oligo ethylene precursor, a metathesis reaction was performed in which the chloride anion of the ether-functionalized ILs was exchanged to the bis(2-ethylhexyl)phosphate (DEHP) as discussed in the experimental section. The physical properties of the DEHP ILs are listed in **Table 5.1**.

Table 5.1 Viscosity, water content and phase behavior of ether-functionalized ILs.

Entry		Viscosity[a] (mPa s)	Water content (ppm)	Phase behavior with water
1a	$[P_{444}E_1]Cl$	4×10^2	n.d.[b]	miscible[c]
2a	$[P_{444}E_2]Cl$	3×10^2	1×10^3	miscible[c]
3a	$[P_{444}E_3]Cl$	2×10^2	1×10^3	miscible[c]
1b	$[P_{444}E_1][DEHP]$	1×10^2	8×10^2	LCST
2b	$[P_{444}E_2][DEHP]$	5×10^1	9×10^2	LCST
3b	$[P_{444}E_3][DEHP]$	9×10^1	8×10^2	LCST

[a] Viscosity measured at 50 °C. [b] n.d.: not determined. Solid at room temperature, melting point: 31 °C. [c] Fully miscible with water in the temperature range 0-100 °C.

A decrease in viscosity with longer oligo ethylene chain is seen for the chloride ILs (**Table 5.1**). Introduction of the bis(2-ethylhexyl)phosphate anion lowers the viscosity. Regarding the phase behavior of the ionic liquids with water, the structure of the ionic liquid plays a crucial role. Most importantly, the anion drastically changes the miscibility of the ionic liquid with water. All synthesized chloride ionic liquids are fully miscible with water, whilst all the synthesized DEHP ionic liquids show LCST phase behavior. Also, the role of the cation was investigated. The cloud point temperature was determined for the three different ether-functionalized ILs in a 1:1 wt/wt mixture with water. Complete phase diagrams were constructed via visual observation of the cloud

point upon heating the homogeneous mixtures of different compositions (**Figure 5.2**).

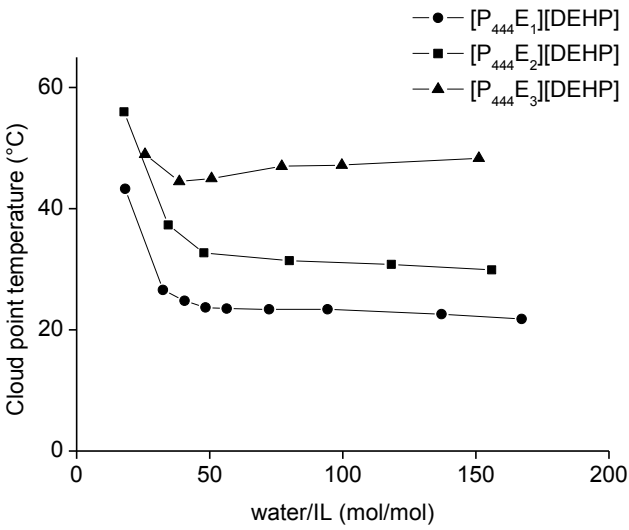

Figure 5.2 Phase diagrams of the binary mixtures of three ether-functionalized ILs with water.

In addition, more accurate but slow transmission measurements were carried out for some of the compounds to verify the visual observations. In this technique, the cloud point temperature was defined as the temperature at which 50% of the initial transmission is reached. Temperatures found are: 34 °C, 38 °C and 44 °C for 1:1 wt/wt binary mixtures with water of $[P_{444}E_1][DEHP]$, $[P_{444}E_2][DEHP]$ and $[P_{444}E_3][DEHP]$, respectively (**Figure 5.3**).

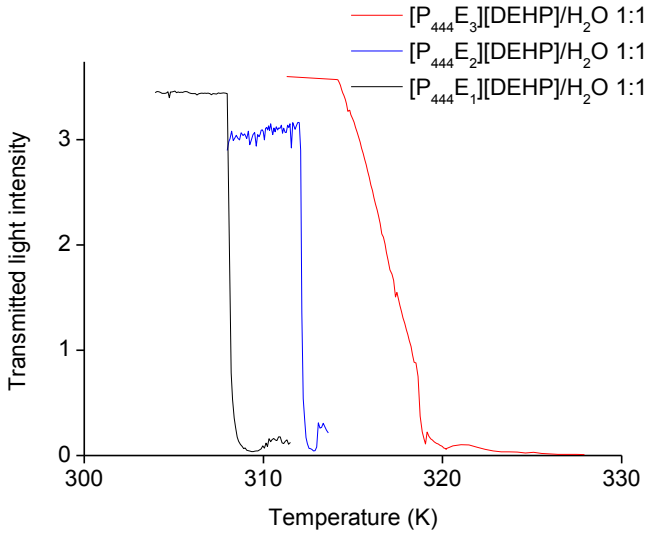

Figure 5.3 Transmitted intensity in function of temperature for the three binary mixtures of IL and water (1:1 wt/wt).

These temperatures are practical for extraction applications, since increasing the temperature by 10 to 20 °C above room temperature is sufficient for complete phase separation. The cloud point temperature increases with increasing oligo ethylene chains. This can be explained as follows. Mixing of the IL and water will occur when the excess Gibbs free energy of mixing $\Delta_{mix}G$ is negative (equation 5.2):

$$\Delta_{mix}G = \Delta_{mix}H - T\Delta_{mix}S \qquad (5.2)$$

In case of LCST phase behavior, $\Delta_{mix}S$ is negative. Below the LCST, the two components are fully miscible due to the formed hydrogen bonds between water and the IL, resulting in a hydration shell around the ions. With increasing temperature, this hydrogen bonding is more and more lost until eventually all water molecules from the hydration shell are expelled into the bulk water. A longer oligo ethylene chain in the ionic liquid has more possibilities for hydrogen bonds with water; hence a higher temperature is needed to break them up. The lower cloud point temperature of $[P_{4444}][DEHP]$/water in comparison with $[P_{444}E_3][DEHP]$/water can be explained in a similar way: $[P_{4444}][DEHP]$ allows for less possible interactions with water, since this IL lacks functional groups (**Figure 5.4**).

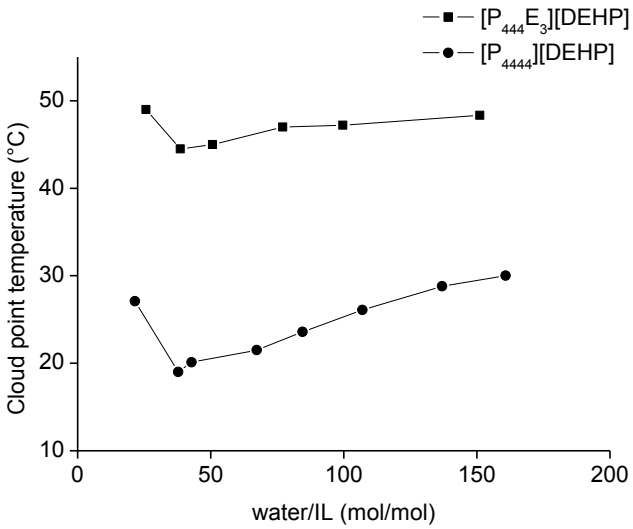

Figure 5.4 Comparison of cloud point temperatures between functionalized ($[P_{444}E_3][DEHP]$) and non-functionalized ($P_{4444}][DEHP]$) ionic liquid.

Bis(2-ethylhexyl)phosphoric acid is a well-known extractant in hydrometallurgical processes for the separation of divalent transition metals.[32-34] Therefore, the bis(2-ethylhexyl)phosphate ILs were tested for homogeneous liquid-liquid extraction of 3d transition metals. The binary mixture of the ionic liquid $[P_{444}E_3][DEHP]$ and water was used for the extraction of cobalt(II), copper(II), nickel(II) and zinc(II). The original cloud point of the 1:1 wt/wt mixture was 44 °C. Yet, the presence of salts in the extraction system influences this cloud point temperature. It is known that the alkaline-earth chloride salts induce a lowering of the lower critical solution temperature.[35] In this case, with the divalent transition metal ions, the cloud point temperature is reduced significantly. The cloud point temperatures are decreased to approximately 20 °C for contacting the IL with an aqueous solution of approximately 5000 ppm of the metal. The reduction in temperature is beneficial for homogeneous liquid-liquid extraction on a laboratory scale, since the homogeneous region is formed by cooling the mixtures down in an ice bath. However, this lowering of the cloud point temperature can also be disadvantageous since it was observed that no metal concentrations higher than 8000 ppm could be used. The high salt concentration induces a lowering of the cloud point temperature outside the window of cooling by ice water (<0 °C).

Prior to the homogeneous liquid-liquid extraction experiments, the IL was presaturated with water to minimize phase changes. A 1:1 wt/wt binary mixture of the IL and water was made. After homogenization and subsequent settling of the two phases, it was found that 18 wt% of water dissolved in the IL phase (Karl Fischer titration) and 6 wt% of IL was lost into the water layer (quantitative ^{1}H NMR). The influence of the extraction time at 0 °C below LCST on the *percentage extraction* (%*E*) was investigated first (**Figure 5.5**). After 5 min, no significant changes in the %*E* were observed, so this cooling time was chosen.

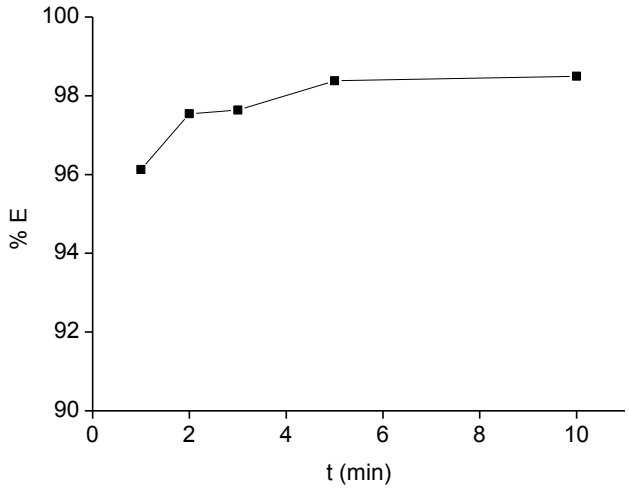

Figure 5.5 Percentage extraction in function of time. (Co(II) concentration: 6866 ppm, pH_{eq}= 3.39, single experiment).

In order to determine the distribution ratios, four different aqueous solutions of approximately 5000 ppm of the metal ($CoCl_2$, $CuCl_2$, $NiCl_2$ and $ZnCl_2$) were mixed with the ionic liquid $[P_{444}E_3][DEHP]$ in the homogeneous phase. After settling at room temperature for 10 min to form the biphasic system again, the mixtures were centrifuged to ensure full phase separation. Then, the aqueous phases were separated and analyzed for their metal content by total reflection X-ray fluorescence (TXRF).

The distribution ratios were calculated as (equation 5.3):

$$D = \frac{c_{\mathrm{org}}}{c_{\mathrm{aq}}} \qquad (5.3)$$

where c_{org} and c_{aq} are the metal concentrations in the initial aqueous phase and the aqueous phase after extraction, respectively.

The distribution ratios listed in **Table 5.2** were measured for chloride solutions of the respective metals with initial pH around 3.5. In **Figure 5.6**, the three stages of the extraction are presented for copper(II).

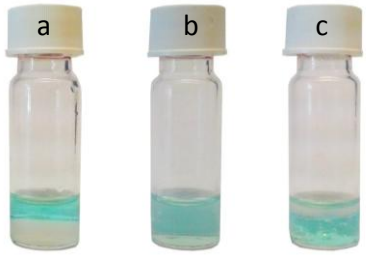

Figure 5.6 Homogeneous liquid-liquid extraction of Cu(II) with $[P_{444}E_3][DEHP]/H_2O$ 1:1 wt/wt mixture (concentration 6866 ppm) a: initial stage, b: homogeneous phase after 5 min in ice bath, c: after settling to room temperature. The upper layer is the aqueous phase; the ionic liquid phase is the bottom layer.

In the Irving-Williams series, the general stability sequence of high spin octahedral metal complexes for the replacement of water by other ligands is given as Co(II) < Ni(II) < Cu(II) > Zn(II).[36] In case of the extraction with the bis(2-ethylhexyl)phosphate anion, the general order is followed, Co(II) is extracted the least, Zn(II) is extracted better and Cu(II) is the metal ion with the highest distribution ratio (**Table 5.2**).

Table 5.2 Extraction of 3d transition metals (Co(II), Ni(II), Cu(II), Zn(II)) with $[P_{444}E_3][DEHP]$, initial metal concentrations in the aqueous phase (c_i) and metal concentration in the aqueous phase after extraction (c_{aq}), the initial pH of the solutions (pH_{in}), their distribution ratios *D* and the percentage stripping *%S* when contacted with solid oxalic acid (for Cu(II), also with H_2SO_4).

Metal ion	$\mathbf{c_i}$	$\mathbf{pH_{in}}$	$\mathbf{c_{aq}}$	***D***	***%S***
Co(II)	6866	3.2	1278	4.4	99
Ni(II)	5578	3.4	286	19	99
Cu(II)	4480	3.9	128	34	58/*99*
Zn(II)	7466	3.0	285	25	91

Stripping was performed by adding a 1:1 molar ratio of solid oxalic acid to the isolated IL phase. After shaking at 40 °C for 30 min at 3000 rpm, a sample of the IL phase was analyzed with TXRF for its metal content (**Table 5.2**). The *percentage stripping* %*S* is defined as follows (equation 5.4):

$$\%S = \frac{c_{org,0} - c_{org,s}}{c_{org,0}} \times 100\% \qquad (5.4)$$

where $c_{org,0}$ is the metal concentration in the IL before stripping and $c_{org,s}$ is the metal concentration in the IL phase after the stripping process. This precipitation stripping technique is advantageous since the metal is removed in one single step. Using oxalic acid as stripping agent, almost all Co(II) and Ni(II) was precipitated as their respective oxalates. The stripping with oxalic acid was still very efficient for Zn(II), more than 90% of the metal was recovered as oxalate. For Cu(II), the IL solution was still very blue colored and only 58% of the metal ion was stripped from the organic phase (**Figure 5.7**). Apparently, the most extracted ion, Cu(II), is also the most difficult to remove from its complex with the addition of oxalic acid. Instead, the stronger acid H_2SO_4 was used to strip Cu(II). 500 mg of the loaded IL phase was contacted with 500 mg of a 1 M H_2SO_4 solution. A light blue precipitate was formed and a percentage stripping of 99% was obtained (**Table 5.2**).

It must be noted that the IL cannot be used for a new extraction step directly after stripping, since the anion is now protonated and the chloride IL reformed. Simply by a washing step with an alkaline solution, the DEHP IL is fully restored and ready for another extraction/stripping cycle.

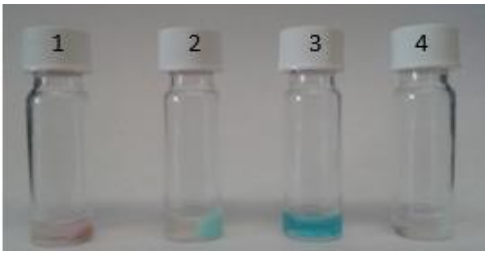

Figure 5.7 Precipitation of the metal oxalates: 1) CoC_2O_4, 2) NiC_2O_4, 3) Cu: small precipitate CoC_2O_4 and highly colored IL phase and 4) ZnC_2O_4.

The coordination of the metal ions by the IL was studied by FTIR spectroscopy. By comparing ATR-FTIR spectra for presaturated IL and the IL loaded with Co(II), an obvious shift to lower wavenumbers was observed for two peaks (**Figure 5.8**). The first one: around 1200 cm^{-1}, a small shift in the peak corresponding to a P=O stretch, and around 1600 cm^{-1}, a larger shift in the peak corresponding to the $P\text{-}O^-$ stretch.[37] As expected, this indicates the interaction between this functional group and the metal cation in the extraction.

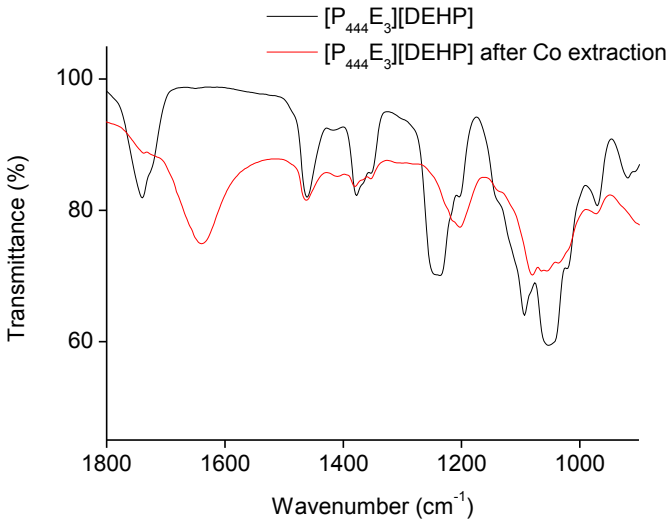

Figure 5.8 ATR-FTIR spectra of IL $[P_{444}E_3][DEHP]$ dry and after extraction of Co(II).

Also, the selectivity towards other metals was investigated. The extraction of CsCl has a distribution ratio of 4.1, even lower than the worst divalent metal ion tested (Co(II)). Taking into account that indium and some rare earths are listed as critical metals in the EU Report because of their high supply risk,[38] and therefore, their recycling demand will increase, these elements were chosen for the study of the selectivity. Unfortunately, these elements form a precipitate when contacted with the ionic liquid. This suggests strong complexation with the bis(2-ethylhexyl)phosphate anion. It is known that the di(2-ethylhexyl)phosphoric acid is an excellent extractant for rare-earth elements and indium.[39,40] Yet, introducing it as an anion in the ionic liquid leads to formation of an insoluble complex, as was confirmed by TXRF measurements.

5.4 Conclusions

We have shown that the introduction of bis(2-ethylhexyl)phosphate as anion in oligo ethylene functionalized phosphonium ionic liquids gives ionic liquids with LCST phase behavior. The cloud point temperature is tunable by making modifications in the structure of the ionic liquid. Longer oligo ethylene chains induce higher cloud points. Addition of a metal chloride salt significantly lowers the cloud point temperature. The ionic liquid $[P_{444}E_3][DEHP]$ was used in this first example of homogeneous liquid-liquid extraction of metal ions with an LCST thermomorphic system. The extraction capacity towards DEHP ionic liquid is excellent for divalent metal ions.

This research was financially supported by IWT-Flanders (PhD fellowship to DD), the FWO Flanders (research project G.0900.13) and the KU Leuven (projects GOA/13/008 and IOF-KP RARE3). The authors also wish to thank Karel Duerinckx for NMR measurements and Dirk Henot for performing CHN analyses.

5.5 References

1 T. Welton, *Chem. Rev.*, 1999**, 99**, 2071.
2 P. Wasserscheid, W. Keim, *Angew. Chem. Int. Ed.*, 2000**, 39**, 3772.
3 N. V. Plechkova, K. R. Seddon, *Chem. Soc. Rev.*, 2008**, 37**, 123.
4 R. D. Rogers, K. R. Seddon, *Science*, 2003**, 302**, 792.
5 J. Lachwa, J. Szydlowski, V. Najdanovic-Visak, L. P. N. Rebelo, K. R. Seddon, M. Nunes da Ponte, J. M. S. Esperança, H. J. R. Guedes, *J. Am. Chem. Soc.*, 2005**, 127**, 6542.
6 J. Lachwa, J. Szydlowski, A. Makowska, K. R. Seddon, J. M. S. S. Esperanca, H. J. R. Guedes, L. P. Rebelo, *Green Chem.*, 2006**, 8**, 262.
7 A. J. L. Costa, M. R. C. Soromenho, K. Shimizu, J. M. S. S. Esperanca, J. N. C. Lopes, L. P. Rebelo, *RSC Adv.*, 2013**, 3**, 10262.
8 S. Dong, B. Zheng, Y. Yao, C. Han, J. Yuan, M. Antonietti, F. Huang, *Adv. Mater.*, 2013**, 25**, 6864.
9 Y. Kohno, H. Ohno, *Aust. J. Chem.*, 2012**, 65**, 91.
10 S. Saita, Y. Kohno, H. Ohno, *Chem. Commun.*, 2013**, 49**, 93.
11 Y. Kohno, H. Ohno, *Chem. Commun.*, 2012**, 48**, 7119.
12 Y. Kohno, H. Ohno, *Phys. Chem. Chem. Phys.*, 2012**, 14**, 5063.
13 Y. Kohno, H. Arai, H. Ohno, *Chem. Commun.*, 2011**, 47**, 4772.
14 Y. Kohno, H. Arai, S. Saita, H. Ohno, *Aust. J. Chem.*, 2011**, 64**, 1560.
15 Y. Fukaya, H. Ohno, *Phys. Chem. Chem. Phys.*, 2013**, 15**, 4066.
16 Y. Fukaya, K. Sekikawa, K. Murata, N. Nakamura, H. Ohno, *Chem. Commun.*, 2007**,** 3089.
17 K. Fukumoto, H. Ohno, *Angew. Chem. Int. Ed.*, 2007**, 46**, 1852.
18 P. Nockemann, B. Thijs, S. Pittois, J. Thoen, C. Glorieux, K. Van Hecke, L. Van Meervelt, B. Kirchner, K. Binnemans, *J. Phys. Chem. B*, 2006**, 110**, 20978.
19 B. Onghena, K. Binnemans, *Ind. Eng. Chem. Res.*, 2015**, 54**, 1887.
20 T. Vander Hoogerstraete, B. Onghena, K. Binnemans, *J. Phys. Chem. Lett.*, 2013**, 4**, 1659.
21 T. Vander Hoogerstraete, B. Onghena, K. Binnemans, *Int. J. Mol. Sci.*, 2013**, 14**, 21353.
22 B. Onghena, J. Jacobs, L. Van Meervelt, K. Binnemans, *Dalton Trans.*, 2014**, 43**, 11566.
23 M. Blesic, H. Q. N. Gunaratne, J. Jacquemin, P. Nockemann, S. Olejarz, K. R. Seddon, C. R. Strauss, *Green Chem.*, 2014**, 16**, 4115.
24 D. Nakayama, Y. Mok, M. Noh, J. Park, S. Kang, Y. Lee, *Phys. Chem. Chem. Phys.*, 2014**, 16**, 5319.
25 S. Sun, P. Wu, *Macromolecules*, 2012**, 46**, 236.
26 Y. Kohno, S. Saita, K. Murata, N. Nakamura, H. Ohno, *Polym. Chem.*, 2011**, 2**, 862.
27 Y. Ito, Y. Kohno, N. Nakamura, Ohno, *Int. J. Mol. Sci.*, 2013**, 14**, 18350.
28 G. Cui, C. Wang, J. Zheng, Y. Guo, X. Luo, H. Li, *Chem. Commun.*, 2012**, 48**, 2633.
29 V. Gudipati, D. P. Curran, C. S. Wilcox, *J. Org. Chem.*, 2006**, 71**, 3599.

30 J. Leicunaite, I. Klimenkovs, J. Kviesis, D. Zacs, J. P. Kreismanis, *C. R. Chimie*, 2010**, 13**, 1335.
31 D. C. Steytler, D. L. Sargeant, G. E. Welsh, B. H. Robinson, R. K. Heenan, *Langmuir*, 1996**, 12**, 5312.
32 Z. J. Yu, T. H. Ibrahim, R. D. Neuman, *Solvent Extr. Ion Exc.*, 1998**, 16**, 1437.
33 T. C. Huang, R. S. Juang, *Ind. Eng. Chem. Fund.*, 1986**, 25**, 752.
34 A. Mellah, D. Benachour, *Chem. Eng. Process.*, 2006**, 45**, 684.
35 D. Dupont, D. Depuydt, K. Binnemans, *J. Phys. Chem. B*, 2015**, 119**, 6747.
36 H. Irving, R. J. P. Williams, *J. Chem. Soc.*, 1953**,** 3192.
37 Stuart, B. H., Organic Molecules, in *Infrared Spectroscopy: Fundamentals and Applications*; John Wiley & Sons: 2004.
38 *Report on Critical Raw Materials for the EU*, European Commission, DG Enterprise & Industry, Brussels, 2014
39 T. Sato, *Hydrometallurgy*, 1989**, 22**, 121.
40 T. Sato, K. Sato, *Hydrometallurgy*, 1992**, 30**, 367.

CHAPTER 6

DOCUSATE IONIC LIQUIDS

This chapter has been published and is reproduced here with permission from Wiley.

Depuydt D., Dehaen W., Binnemans K. (2017). Docusate Ionic Liquids: Effect of Cation on Water Solubility and Solvent Extraction Behavior. *ChemPlusChem, 82* (3), 458-466.

The experimental work and writing were executed by the author of this thesis.

The text may deviate from the original publication as the supplementary information is included in the chapter.

Graphical Abstract

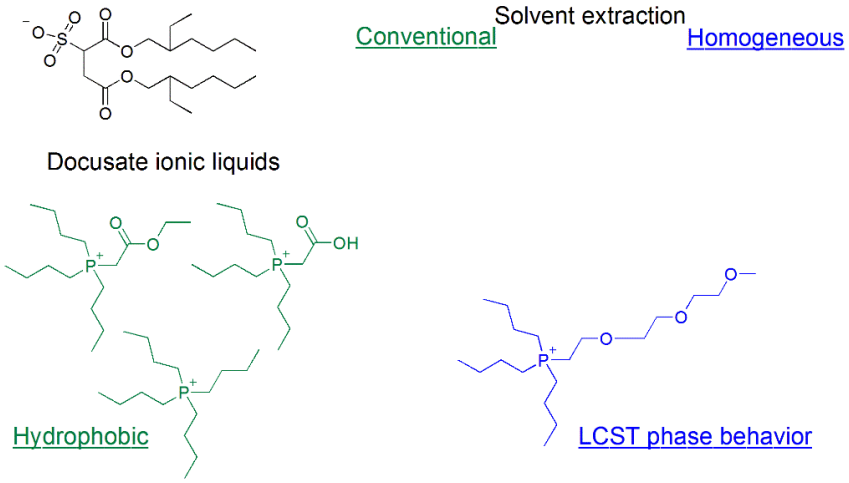

The effect of the cation on the water solubility and solvent extraction capabilities of docusate ionic liquids was investigated.

Abstract

Ionic liquids with the docusate (dioctyl sulfosuccinate or DOSS) anion are described. Docusate was incorporated into several phosphonium ionic liquids, including tetrabutylphosphonium and phosphonium cations functionalized with either an ester, a carboxylic acid or an ethylene glycol group. All synthesized ionic liquids are immiscible with water except the compound with the ethylene glycol moiety in the cation, $[P_{444}E_3][DOSS]$. This ionic liquid exhibits a lower critical solution temperature phase behavior when mixed with water, yielding a homogeneous phase at temperatures lower than 19 °C, resulting in fast kinetics for homogeneous liquid-liquid extraction. The metal extraction capabilities for both divalent and trivalent metal ions were compared for this thermomorphic ionic liquid and the other hydrophobic docusate ionic liquids in an initial screening test. $[P_{444}E_3][DOSS]$ was selected to perform separations on the Sm/Co and La/Ni pairs, because of their relevance to recycling of samarium cobalt magnets and nickel metal hydride batteries. The extraction mechanism was studied and stripping of the metals was investigated.

6.1 Introduction

Ionic liquids (ILs) are solvents that consist entirely of ions.[1-3] There is a particular interest in ionic liquids as alternatives for volatile organic solvents in separation science due to their negligible vapor pressure, low flammability and intrinsic electric conductivity.[4,5] In response to safety and cost issues of fluorinated ionic liquids, non-fluorinated ILs have been introduced for the use in solvent extraction. The commercially available chloride ionic liquids Cyphos IL 101 or Aliquat 336 have large bulky cations, *i.e.* trihexyl(tetradecyl)phosphonium or trioctylmethyl ammonium, and have the hydrophobicity required for solvent extraction processes.[6,7] By selecting ionic liquids with more hydrophobic anions, it is possible to obtain water-immiscible ionic liquids with cations containing shorter alkyl chains than those of Cyphos IL 101 or Aliquat 336. Alkylsulfonate anions are non-toxic and biodegradable, and they are less susceptible towards hydrolysis in comparison to the corresponding alkylsulfates.[8] The docusate (dioctyl sulfosuccinate or DOSS) anion is known to exhibit low mammalian toxicity, and is often applied in food, drugs and cosmetics.[9] Sodium bis(2-ethylhexyl) sulfosuccinate (Aerosol OT or AOT) is a well-known anionic surfactant.[10]

The rich phase behavior of AOT and its ability to form micro-emulsions make this an intensively studied compound.[11] Spontaneous emulsification in oil/water two-phase systems occurs when AOT is added to water[12] or oil.[13,14] Incorporation of docusate as anion into ionic liquids leads to a class of ionic liquids called SAILs (surfactant ionic liquids).[15] A study on the docusate-based room-temperature ionic liquids with quaternary ammonium cations having long alkyl chains showed that spontaneous emulsification did not occur due to the hydrophobicity of the cation used.[16] Docusate-based ionic liquids show potential as antistatic additives for fuel applications and polymer applications because of their partial or full miscibility with hydrocarbons (*e.g.* with hexane).[17] Docusate ionic liquids have also been investigated as plasticizers and antimicrobial agents for medical polymers.[18] Rogers and coworkers have made lidocaine docusate, a room-temperature ionic liquid derived from the local anaesthetic lidocaine.[19] Sulfosuccinate ionic liquids can form ionic liquid crystals with a smectic A phase if an ionic liquid cation with long side chains is used.[20] When considering the phase behavior with water, incorporating the docusate anion often results in highly hydrophobic ionic liquids. Yet, some ionic liquids may become more hydrated when mixed with a certain proportion of water, which results in a change of two phases to a single phase. Davis and coworkers speculated that this unique behavior could be beneficial for some applications in which solubility or insolubility with water is important.[17] To create ionic liquids with so-called thermomorphic behavior (i.e. temperature-dependent miscibility), the balance between hydrophilicity and hydrophobicity needs to be optimized.[21] This thermomorphic behavior can be exploited in homogeneous liquid-liquid extraction (HLLE). Ionic liquids showing upper critical solution temperature (UCST)[22-24] or lower critical solution temperature (LCST)[25] phase behavior have been described as efficient extraction systems for metal ions.

In this chapter, we describe several functionalized docusate ionic liquids (for an overview, see **Figure 6.1**) and the phase behavior of their binary mixtures with water. It is shown that their miscibility with water strongly depends on the type of functional group. Most docusate ILs are hydrophobic and thus immiscible with water; they have been tested in conventional solvent extraction systems. The incorporation of an ethylene glycol moiety induces lower critical solution temperature behavior with water. This novel docusate ionic liquid with an ethylene glycol moiety has been applied in homogeneous liquid-liquid extraction of metals.

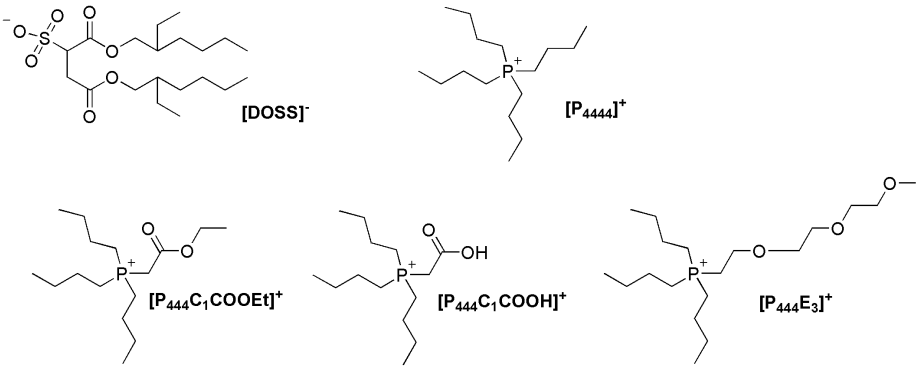

Figure 6.1 Structures of the investigated ILs. Anion: $[DOSS]^-$: dioctylsulfosuccinate (docusate). Cations: $[P_{4444}]^+$: tetra-*n*-butylphosphonium, $[P_{444}C_1COOEt]^+$: tri-*n*-butyl (carboxy-methyl)ethylphosphonium, $[P_{444}C_1COOH]^+$: tri-*n*-butyl(carboxy-methyl) phosphonium, $[P_{444}E_3]^+$: tri-*n*-butyl-{2-[2-(2-methoxyethoxy)ethoxy]ethyl}phosphonium.

6.2 Experimental

6.2.1 Chemicals

Tri-*n*-butylphosphine (97%), sodium docusate (>97%), anhydrous zinc(II) chloride (reagent grade 98%), cobalt(II) chloride hexahydrate (97%), nickel(II) chloride hexahydrate (98%) were purchased from Sigma-Aldrich (Diegem, Belgium). Acetonitrile (HPLC grade), absolute ethanol, dichloromethane (analytical reagent grade) were obtained from Fisher Scientific Limited (Loughborough, UK). Copper(II) chloride (99%) and pyridine (> 99%) were obtained from Acros Organics (Geel, Belgium). Tetrabutyl phosphonium chloride (Cyphos IL 443T) was purchased from Iolitec (Heilbronn, Germany). Dysprosium(III) chloride hexahydrate (99.9%), neodymium(III) chloride hexahydrate (99.9%), yttrium(III) chloride hexahydrate (99.9%), and samarium(III) chloride hexahydrate (99.9%) were obtained from Alfa Aesar (Karlsruhe, Germany). A 1000 $\mu g \cdot mL^{-1}$ gallium and dysprosium standard were obtained from Merck (Overijse, Belgium). The silicone solution in isopropanol was from SERVA Electrophoresis GmbH (Heidelberg, Germany). Indium(III) chloride was obtained from Merck (Darmstadt, Germany). Scandium(III) chloride hydrate and gallium(III) chloride hydrate were prepared from the respective oxides by dissolution in a HCl solution. Scandium oxide was kindly provided by Solvay (La Rochelle, France) and gallium oxide (>99.99%) was purchased from Acros Organics

(Geel, Belgium). All chemicals were used as received without further purification.

6.2.2 General

The ^{1}H NMR and ^{13}C NMR spectra were recorded on a Bruker Avance 300 spectrometer (operating at 300 MHz for ^{1}H, 75 MHz for ^{13}C). ^{31}P NMR spectra were recorded on a Bruker Ascend 400 spectrometer operating at 162 MHz. The chemical shifts are noted in parts per million (ppm), referenced to tetramethylsilane for ^{1}H and ^{13}C and to 85% H_3PO_4 for ^{31}P NMR. The coupling constants are given in Hertz. All solutions were made in $CDCl_3$. The spectra were analyzed with SpinWorks software. The Fourier Transform Infrared (FTIR) spectrum of the ionic liquids was recorded by a Bruker Vertex 70 spectrometer via the attenuated total reflectance (ATR) technique with a Bruker Platinum ATR accessory. The OPUS software package was used for analysis of the FTIR spectra. The water content was determined by coulometric Karl Fischer titration using a Mettler-Toledo DL39 titrator. Extraction experiments were performed in a TMS-200 thermoshaker (Nemus Life). Extraction mixtures were centrifuged using a Heraeus Labofuge 200. A Bruker S2 Picofox total reflection X-ray fluorescence (TXRF) spectrometer was used to determine the metal concentrations in both aqueous and organic (ionic liquid) phases. A small amount (100 mg) of gallium standard solution was added to the sample as a reference for quantification. The sample was further diluted to 1 mL with ultrapure water for aqueous samples, and with ethanol for the ionic liquid phase. The prepared sample solutions were homogenized by vortex mixing and a small droplet (3 µL) was dispensed on a quartz sample carrier. Finally, the carrier containing the sample was dried at 60 °C for 30 min. Prior to dispensing the sample droplet, the quartz carrier was pretreated with a SERVA® silicone solution in isopropanol (30 µL) in order to make the surface more hydrophobic, to avoid spreading of the sample droplet. pH measurements were performed with an S220 SevenCompact™ pH/Ion meter (Mettler-Toledo) and a Slimtrode (Hamilton) electrode. TGA measurements were performed under nitrogen atmosphere on a TGA-Q500 (TA Instruments). The sample (±10 mg) was loaded into an aluminium pan and heated (2 °C min^{-1}) to 110 °C, kept at this temperature for 30 min to remove all water and heated further to 450 °C at a heating rate of 2 °C min^{-1}. CHN elemental analysis was performed on a Flash 2000 Elemental analyzer from Thermo Scientific Interscience. The viscosity of the ionic liquids was measured using a falling-ball type viscometer (Anton Paar, Lovis 2000 ME),

densities were determined using a density meter with an oscillating U-tube sensor (Anton Paar, DMA 4500 M).

6.2.3 Synthesis

The functionalized chloride ionic liquids were synthesized according to literature procedures.[22,23] Tri-*n*-butyl phosphine was quaternized by reaction with the respective chloroester or chloroethylene glycol. The carboxylic acid functionalized ionic liquid was made by hydrolysis of the ester functionalized ionic liquid.

Synthesis chloride ionic liquids

The ether functional group was incorporated in the phosphonium ionic liquid according to literature procedures.[24,25] Tri-*n*-butyl phosphine was reacted with the organic halide containing the desired ether functional group (**Scheme 6.1**). A mixture of tri-*n*-butyl phosphine (1 mol eq., 10 mmol) and oligoethylene oxide chloride precursor (1 mol eq., 10 mmol) in 15 mL of acetonitrile was refluxed for 48 h. On completion, the acetonitrile was evaporated under reduced pressure at 60 °C. The product was washed with 10 mL of heptane under reflux for 1h. The upper heptane phase was decanted and the process was repeated four times. The product was fully dried at a Schlenk line.

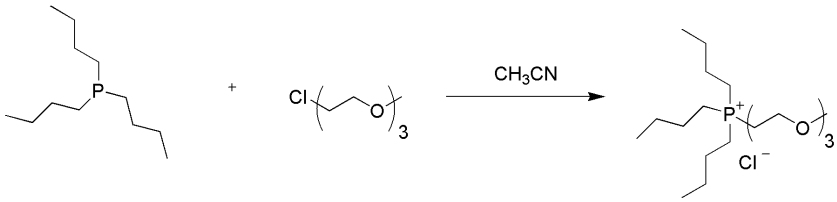

Scheme 6.1 Synthesis of tri-*n*-butyl{2-[2-(2-methoxyethoxy)ethoxy]ethyl}phosphonium chloride.

Tri-n-butyl{2-[2-(2-methoxyethoxy)ethoxy]ethyl}phosphonium chloride $[P_{444}E_3]Cl$

Light yellow viscous liquid (27.76 g, 73.75 mmol, 52%). ^{1}H NMR (300 MHz, δ, $CDCl_3$): 3.55 (2H, m, CH_2), 3.50 (6H, m, 3 CH_2), 3.41 (2H, m, CH_2), 3.24 (3H, s, CH_3), 2.58 (2H, m, CH_2), 2.20 (6H, m, 3 CH_2), 1.53-1.35 (12H, m, 6 CH_2), 0.88 (3H, t, 7.0 Hz, CH_3). ^{13}C NMR (75 MHz, δ, $CDCl_3$): 71.20 (CH_2), 69.42 (CH_2), 58.00 (CH_3), 23.39 (CH_2), 22.63 (CH_2), 18.39 (CH_2), 17.73 (CH_2), 13.17 (CH_3). FTIR-ATR: (ν/cm^{-1}): 2958, 2931, 2872, 1464, 1381,

1350, 1236, 1198, 1101, 1012, 969, 920, 810, 723. CHN analysis: (calculated for $C_{18}H_{40}ClO_3P \cdot H_2O$): C 55.41% (55.58%), H 11.23% (10.88%), N 0% (0%).

The synthesis of the ester and carboxylic acid functionalized ionic liquids $[P_{444}C_1COOEt]Cl$, $[P_{444}C_1COOH]Cl$ was partly based on literature procedures (**Scheme 6.2**).[26,27] A solution of ethyl chloroacetate (100 mmol) in acetonitrile was purged with argon for 10 min. Tri-*n*-butylphosphine (100 mmol) was added dropwise and the mixture was refluxed for 24 h. The solvent was evaporated yielding the $[P_{444}C_1COOEt]Cl$ ionic liquid (31.83 g, 98.01 mmol, 98%). To 40 mmol of the $[P_{444}C_1COOEt]Cl$ a 15 vol% aqueous solution of HCl was added and the solution was refluxed for 5 h. Next, the solvent was evaporated again and the ionic liquid fully dried on a high vacuum line (50 °C). $[P_{444}C_1COOH]Cl$ was formed as a light yellow viscous liquid (11.83 g, 39.86 mmol, 99%).

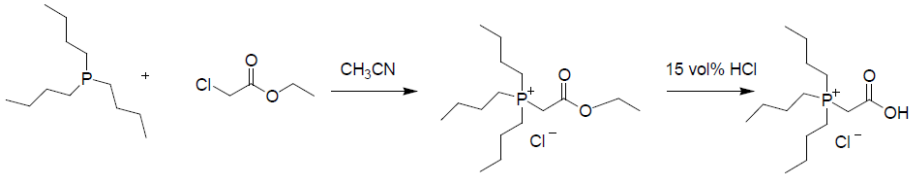

Scheme 6.2 Synthesis of ionic liquids $[P_{444}C_1COOEt]Cl$ and $[P_{444}C_1COOH]Cl$.

Tri-n-butyl(carboxy-methyl)ethylphosphonium chloride
$[P_{444}C_1COOEt]Cl$

White solid (31.83 g, 98.01 mmol, 98%). ^{1}H NMR (300 MHz, δ, $CDCl_3$): 4.22 (4H, m, 2 CH_2), 2.60 (6H, m, 3 CH_2), 1.55 (12H, m, 6 CH_2), 1.30 (3H, t, 7.0 Hz, CH_3), 0.98 (9H, t, 7.0 Hz, 3 CH_3). ^{13}C NMR (75 MHz, δ, $CDCl_3$): 165.99 (C=O), 62.72 (CH_2), 24.04 (CH_2), 23.87 (CH_2), 23.83 (CH_2), 23.81 (CH_2), 19.68 (CH_2), 19.05 (CH_2), 13.98 (CH_3), 13.44 (CH_3). ^{31}P NMR (255 MHz, δ, $CDCl_3$): 32.54. FTIR-ATR: (ν/cm^{-1}): 2961, 2932, 2874, 1724, 1465, 1384, 1366, 1148, 1051, 907, 832, 722. CHN analysis: (calculated for $C_{16}H_{34}PO_2Cl$): C 59.41% (59.15%), H 10.03% (10.55%), N 0% (0%).

Tri-n-butyl(carboxy-methyl)phosphonium chloride
$[P_{444}C_1COOH]Cl$

Light yellow viscous liquid (11.83 g, 39.86 mmol, 99%). ^{1}H NMR (300 MHz, δ, $CDCl_3$): 9.57 (1H, s, COOH), 3.97 (2H, d, 13.0 Hz, CH_2), 2.37 (6H, m, 3 CH_2), 1.51 (12H, m, 6 CH_2), 0.95 (9H, t, 7.0 Hz, 3 CH_3). ^{13}C NMR (75 MHz, δ, $CDCl_3$): 165.89 (C=O), 27.77 (CH_2), 23.98 (CH_2), 23.52 (CH_2), 19.65

(CH_2), 19.01 (CH_2), 13.39 (CH_3). ^{31}P NMR (255 MHz, δ, $CDCl_3$): 32.20. FTIR-ATR: (ν/cm^{-1}): 2960, 2933, 2873, 1713 (C=O), 1464, 1097, 909. CHN analysis: (calculated for $C_{14}H_{30}ClO_2P{\cdot}2H_2O$): C 50.36 % (50.30%), H 10.83% (10.30%), N 0% (0%). ESI-MS (MeOH): m/z 283.5 (100%) $[P_{444}C_1COO]Na^+$.

Metathesis reaction to docusate

The general reaction procedure for the docusate ionic liquids was adapted from a procedure described by Lava *et al.*[17] 1.1 mol eq. of NaDOSS (22 mmol) in water was added to a solution of 1 mol eq. chloride ionic liquid (20 mmol) in water (**Scheme 6.3**). The mixture was refluxed for 3 h, and after cooling to room temperature, ethyl acetate was added. The organic phase separated from the aqueous phase. The organic phase was isolated and the solvent was evaporated. A colorless viscous liquid remained which is further dried on a Schlenk line at 60 °C.

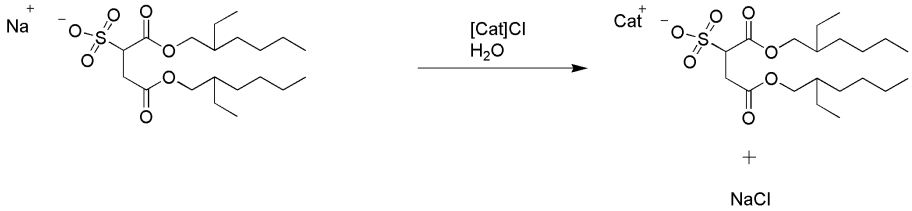

Scheme 6.3 General synthesis procedure of the metathesis reaction to docusate.

Tetra-n-butylphosphonium docusate
$[P_{4444}][DOSS]$

Colorless viscous liquid (13.04 g, 19.16 mmol, 96%). ^{1}H NMR (300 MHz, δ, $CDCl_3$): 4.13-3.93 (5H, m, $2CH_2$ + CH), 3.16 (2H, m, CH_2), 2.31 (8H, m, 4 CH_2), 1.64 (2H, m, 2 CH), 1.55 (16H, m, 8 CH_2), 1.27 (16H, m, $8CH_2$), 0.98 (12H, m, 4 CH_3), 0.88 (12H, m, 4 CH_3). ^{13}C NMR (75 MHz, δ, $CDCl_3$): 171.87 (C=O), 169.17 (C=O), 67.16, 66.87, 65.30, 61.91, 41.99, 38.52, 34.42, 30.09, 28.93, 24.05, 23.90, 23.82, 23.78, 23.68, 23.47, 23.02, 22.97, 18.95, 18.48, 14.06, 13.49, 11.11, 10.96, 10.83. ^{31}P NMR (162 MHz, δ, $CDCl_3$): 32.92. FTIR-ATR: (ν/cm^{-1}): 2958, 2931, 2873, 1731, 1463, 1382, 1322, 1157, 1033, 907, 821, 724. CHN analysis: (calculated for $C_{36}H_{73}PO_7S$): C 63.02% (63.49%), H 10.67% (10.80%), N 0% (0%). Cl content: < 1000 ppm. H_2O content: 84 ppm.

Tri-n-butyl(carboxy-methyl)ethylphosphonium docusate
$[P_{444}C_1COOEt][DOSS]$

Colorless viscous liquid (13.46 g, 19.20 mmol, 96%). ^{1}H NMR (300 MHz, δ, $CDCl_3$): 4.24-3.94 (9H, m, $4CH_2$ + CH), 3.78 (2H, m, CH_2), 3.15 (2H, m, CH_2), 2.41 (6H, m, 3 CH_2), 1.53 (14H, m, 6 CH_2 + 2 CH), 1.31 (19H, m, 8 CH_2 + CH_3), 0.98 (9H, t, 7.0 Hz, 3 CH_3), 0.88 (12H, m, 4 CH_3). ^{13}C NMR (75 MHz, δ, $CDCl_3$): 171.74 (C=O), 169.26 (C=O), 165.88 (C=O), 67.62, 66.97, 62.85, 61.87, 38.52, 34.27, 30.08, 28.89, 26.92, 26.40, 23.99, 23.83, 23.79, 23.74, 23.67, 23.46, 23.01, 22.97, 19.38, 18.90, 14.10, 14.06, 13.99, 13.43, 11.11, 10.96, 10.83. FTIR-ATR: (ν/cm^{-1}): 2959, 2932, 2874, 1730, 1464, 1382, 1312, 1155, 1033, 918, 851, 726. ^{31}P NMR (162 MHz, δ, $CDCl_3$): 32.50. CHN analysis: (calculated for $C_{36}H_{71}PO_9S$): C 60.60% (60.82%), H 10.07% (10.07%), N 0% (0%). Cl content: below detection limit TXRF (LLD 2 mg L^{-1}). H_2O content: 32 ppm.

Tri-n-butyl(carboxy-methyl)phosphonium docusate
$[P_{444}C_1COOH][DOSS]$

White solid (12.86 g, 18.84 mmol, 94%). ^{1}H NMR (300 MHz, δ, $CDCl_3$): 4.20-3.90 (5H, m, $2CH_2$ + CH), 3.74 (2H, m, CH_2), 3.13 (2H, m, CH_2), 2.29 (6H, m, 3 CH_2), 1.50 (14H, m, 6 CH_2 + 2 CH), 1.31 (16H, m, 8 CH_2), 0.98 (9H, t, 7.0 Hz, 3 CH_3), 0.87 (12H, m, 4 CH_3). ^{13}C NMR (75 MHz, δ, $CDCl_3$): 171.30 (C=O), 168.49 (C=O), 165.82 (C=O), 67.86, 67.19, 61.98, 38.54, 33.93, 30.13, 30.08, 29.12, 28.89, 27.34, 26.81, 23.98, 23.82, 23.65, 23.55, 23.50, 22.99, 22.96, 19.29, 18.81, 14.09, 14.06, 13.34, 13.43, 10.96, 10.92, 10.88, 10.81. ^{31}P NMR (162 MHz, δ, $CDCl_3$): 31.69. FTIR-ATR: (ν/cm^{-1}): 2959, 2931, 2874, 1730, 1464, 1382, 1382, 1159, 1097, 910, 853, 726. CHN analysis: (calculated for $C_{34}H_{67}PO_9S$): C 59.54% (59.80%), H 9.89% (9.89%), N 0% (0%). Cl content: below detection limit TXRF (LLD 2 mg L^{-1}). H_2O content: 91 ppm.

Tri-n-butyl{2-[2-(2-methoxyethoxy)ethoxy]ethyl}phosphonium docusate
$[P_{444}E_3][DOSS]$

Colorless viscous liquid (15.11 g, 19.61 mmol, 98%). ^{1}H NMR (300 MHz, δ, $CDCl_3$): 4.14-3.84 (9H, m, 4 CH_2 + CH), 3.60 (6H, m, 3 CH_2), 3.52 (2H, m, CH_2), 3.36 (3H, s, CH_3), 2.77 (2H, m, CH_2), 2.28 (6H, m, 3 CH_2), 1.86 (2H, m, 2 CH), 1.51 (12H, m, 6 CH_2), 1.26 (16H, m, 8 CH_2), 1.00 (9H, t, 7.0 Hz, 3 CH_3), 0.87 (12H, m, 4 CH_3). ^{13}C NMR (75 MHz, δ, $CDCl_3$): 171.83 (C=O),

169.17 (C=O), 71.93, 70.36, 70.27, 70.08, 67.56, 67.48, 64.35, 64.27, 61.89, 58.97, 38.58, 38.52, 34.39, 30.34, 30.08, 28.92, 24.10, 23.95, 23.82, 23.78, 23.68, 23.00, 19.71, 19.24, 14.12, 14.06, 13.49, 10.96, 10.84. ^{31}P NMR (162 MHz, δ, $CDCl_3$): 33.52. FTIR-ATR: (ν/cm^{-1}): 2958, 2930, 2873, 1732, 1463, 1382, 1350, 1143, 1033. CHN analysis: (calculated for $C_{39}H_{79}PO_{10}S$): C 60.11% (60.75%), H 10.30% (10.33%), N 0% (0%). Cl content: below detection limit TXRF (LLD 2 mg L^{-1}). H_2O content: 116 ppm.

6.2.4 Determination of mutual solubilities and phase diagram

The water solubility in the docusate ionic liquids was measured by Karl Fischer titration and the solubility of the docusate ionic liquids in the water phase was determined via quantitative NMR. Both measurements were performed after contacting the ionic liquid with water in a 1:1 (w/w) ratio, shaking the mixture in an ice water bath, and allowing the mixture to settle at room temperature. The complete phase diagram was constructed by visual observations. First, a known mass of ultrapure water was added to a known mass of IL. The mixture was biphasic at room temperature, yet with cooling a homogeneous phase was formed. Upon slow heating, cloudiness appeared, and the temperature at which this occurs is defined as the cloud point temperature for the respective composition of the binary mixture. This procedure was repeated for different compositions of the binary mixture.

6.2.5 Extraction experiments

Prior to extraction, the ionic liquid was contacted with an aqueous solution to presaturate the ionic liquid and to avoid changes in the phase ratio. In a typical extraction experiment, 500 mg of the presaturated IL was contacted with 500 mg of an aqueous metal solution. In case of a hydrophobic ionic liquid, the binary mixtures were heated to 60 °C and shaken for 30 min. The mixture of the thermomorphic ionic liquid $[P_{444}E_3][DOSS]$ and the metal solutions were cooled in an ice bath for several minutes to reach the homogeneous region. Next, the mixtures are left to settle at room temperature for 10 min. Full phase separation is reached by centrifugation at 5000 rpm for 2 min. The aqueous layer was sampled and analyzed for its metal content by TXRF. The distribution ratio *D* and percentage extraction *%E* were calculated according to equations (6.1) and (6.2), respectively:

$$D = \frac{c_{org}}{c_{aq}} \quad (6.1)$$

$$\%E = \frac{c_{org} \cdot m_{org}}{c_{org} \cdot m_{org} + c_{aq} \cdot m_{aq}} \times 100\% \quad (6.2)$$

where c_{org} and c_{aq} are the metal concentration in the organic phase (*i.e.* ionic liquid phase) and in the aqueous phase, respectively and m_{org} and m_{aq} are the masses of the organic phase and the aqueous phase, respectively.

For two metal ions A and B, both distributed between the organic and aqueous phase, a separation factor $\alpha_{A,B}$ can be defined as the ratio of the two corresponding distribution ratios (equation 6.3):

$$\alpha_{A,B} = \frac{D_A}{D_B} \quad (6.3)$$

with $D_A > D_B$. The closer this separation factor approaches unity, the more difficult it will be to separate those two metals ions.

6.2.6 Stripping measurements

Two stripping methods were investigated. To regenerate the IL, it was either stripped with an aqueous solution of HCl or HNO_3 or it was stripped with oxalic acid (precipitation stripping). In the stripping experiments with HCl or HNO_3, 500 mg of the loaded IL was taken and 500 mg of an aqueous HCl or HNO_3 solution with varying concentrations was added. The vials were shaken for 30 min at 70 °C (1700 rpm) and centrifuged to ensure full phase separation. For each precipitation stripping experiment, 500 mg of the loaded IL was taken and known amounts of oxalic acid were added to vary the molar ratios of oxalic acid over metal. The vials were shaken for 30 min at 70 °C (1700 rpm). The vials were centrifuged to accumulate all precipitate at the bottom of the vial. A sample of the IL phase was taken for analysis of its metal content by TXRF. The percentage stripping (%*S*) is defined as equations 6.4 and 6.5:

$$\%S = \frac{\text{amount of stripped metal}}{\text{total amount of extracted metal}} \times 100\% \quad (6.4)$$

Or

$$\%S = \frac{c_{org,0} - c_{org,s}}{c_{org,0}} \times 100\% \quad (6.5)$$

where $c_{org,0}$ is the metal concentration in the IL before stripping and $c_{org,s}$ is the metal concentration in the IL phase after the stripping process.

6.2.7 Quantitative ^{1}H NMR

The amount of IL that is lost into the water phase was determined by quantitative ^{1}H NMR. To 100 mg of the water layer of presaturation of the ionic liquid was added 5 mg of pyridine to obtain approximately equimolar concentrations to the aliquot of water presaturated with the ionic liquid. Pyridine was chosen as internal standard since there is no overlap with the ^{1}H NMR spectrum of the ionic liquid. The ^{1}H NMR spectrum of the water samples was recorded and the relative concentration versus pyridine and the absolute concentration of the different ionic liquids were calculated by integration of the peaks. It is estimated that the measurement uncertainty is less than 2%.[28]

6.3 Results and Discussion

Synthesis

$[P_{444}E_3]Cl$, $[P_{444}C_1COOEt]Cl$ and $[P_{444}C_1COOH]Cl$ were synthesized following literature references.[22,23] All starting materials were readily available, or available in few synthesis steps. In the reaction for the anion exchange from chloride to docusate, the chloride ionic liquid was mixed with a small excess of sodium docusate (1.1 eq.) in water. Boiling water is the preferred solvent since the emulsions which typically form between the ionic liquid and water are easily broken at this high temperature.[14] The mixture was then cooled and ethyl acetate was added. All formed ionic liquids dissolved in the organic phase at room temperature. The organic phase was isolated and the pure products were obtained after removal of ethyl acetate on a rotary evaporator. All synthesis procedures and analytical data for the characterization of the compounds can be found in the experimental section. Detailed FTIR spectra of both the ionic liquid $[P_{444}C_1COOH][DOSS]$ and the zwitterion $P^+_{444}C_1COO^-$ showing the C=O stretch are presented in **Figure 6.2**. Since for the zwitterion the transition attributed to the C=O stretch is found at a lower wavenumber and in the spectrum of the docusate ionic liquid the lower transition is not found, it can be concluded that the ionic liquid is indeed formed and not a mixture of $P^+_{444}C_1COO^-$ and HDOSS.

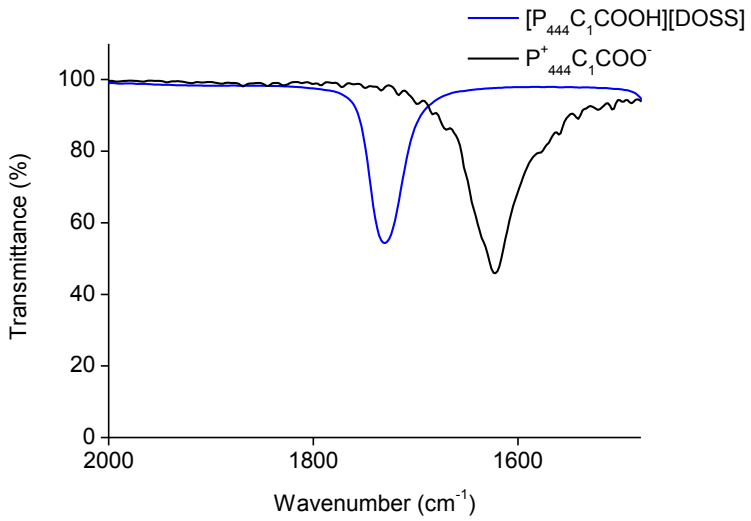

Figure 6.2. Detail of the FTIR-ATR spectra of both the ionic liquid $[P_{444}C_1COOH][DOSS]$ and the zwitterion $P^+_{444}C_1COO^-$ showing the C=O stretch. In the zwitterionic form, the transition is shifted to a lower wavenumber, the spectrum of the docusate ionic liquid does not show this transition, so it can be concluded that the ionic liquid is indeed formed and not a mixture of $P^+_{444}C_1COO^-$ and HDOSS.

Physical and chemical properties

The properties (melting point, glass transition, thermal decomposition temperature, viscosity, density, water content) of the docusate ionic liquids are summarized in **Table 6.1**. The glass transition temperatures all vary around -60 °C, decomposition temperatures are approximately 230 °C. The density values found for all ionic liquids approach unity, which can cause phase reversal if the ionic liquid is contacted with a highly concentrated aqueous phase with higher density. The ionic liquids were dried on a Schlenk line, yielding low water contents (± 100 ppm). The viscosities of the dry ionic liquids are high ($>1\times10^3$ to even 4×10^3 mPa s), which is a disadvantage for application in solvent extraction, because of the slow mass transfer. It must be noted that for this reason generally the water-saturated ionic liquids are used in extraction systems. Functionalized ionic liquids suffer from an even higher viscosity, in particular when these functional groups (*e.g.* carboxylic acid) can form hydrogen bonds. In the case of the $[P_{444}C_1COOH][DOSS]$ ionic liquid, a solid was formed.[29,30] Ionic liquids with an ether-containing side chain have lower viscosities, due to the low rotational barrier in ether functional groups

and therefore higher flexibility of these side chains in comparison to alkyl substituents. This is of course a major advantage of the ethylene glycol functionalized ionic liquids.[29]

Phase behavior with water

Tetrabutylphosphonium docusate [P_{4444}][DOSS] is hydrophobic and not miscible with water at all temperatures.[14] The ester functionalized ionic liquid [$P_{444}C_1$COOEt][DOSS] and the carboxylic acid functionalized ionic liquid [$P_{444}C_1$COOH][DOSS] are both still immiscible with water at all temperatures between 0 and 100 °C. However, the ethylene glycol functionalized ionic liquid [$P_{444}E_3$][DOSS] shows lower critical solution temperature (LCST) phase behavior with water, *i.e* it forms a homogeneous phase upon cooling in ice water. This LCST phase behavior is generally observed for ILs with more strongly hydrated (high charge density) anions.[31] The water content of the docusate ionic liquids was measured by Karl Fischer titration and the solubility of the docusate ionic liquids in the water phase was determined via quantitative NMR, both measurements performed after contacting the ionic liquid with water in a 1:1 w/w (weight/weight) ratio, shaking the mixture in an ice water bath and allowing the mixture to settle at room temperature (**Table 6.1**).

Table 6.1 Glass transition temperature (T_g), decomposition temperature (T_d), viscosity (η), density (ρ), water content, phase behavior and mutual solubility of water and the docusate ionic liquids.

Ionic Liquid	T_g (°C)	T_d (°C)	η (mPa.s)[a]	ρ ($g.cm^{-3}$)[a]	Water content (ppm)	Phase behavior with water[c]	Solubility of H_2O in IL (wt%)[d]	Solubility of IL in H_2O (wt%)[d]
$[P_{4444}][DOSS]$	-58	235	4×10^3	1.004	8×10^1	2 phases	13	9
$[P_{444}C_1COOEt][DOSS]$	-54	225	4×10^3	1.032	3×10^1	2 phases	14	21
$[P_{444}C_1COOH][DOSS]$	-61	239	---[b]	---[b]	9×10^1	2 phases	6	11
$[P_{444}E_3][DOSS]$	-68	240	1×10^3	1.026	1×10^2	LCST: 19 °C	9	8

[a] measured at 25 °C

[b] solid at 25 °C (melting point: 38 °C)

[c] phase behavior measured for 1:1 (w/w) mixtures in a temperature range between 0–100 °C

[d] mutual solubilities determined at room temperature

The binary phase diagram $[P_{444}E_3][DOSS]/H_2O$ is shown in **Figure 6.3**. The binary mixture of water and $[P_{444}E_3][DOSS]$ in a 1:1 ratio (w/w) has a LCST value of 19 °C. Changing the composition to a higher weight percentage of IL or water raises the cloud point temperature. No sharp minimum is observed in the graph, indicating a small change in the cloud point temperature in function of the composition of the binary mixture.

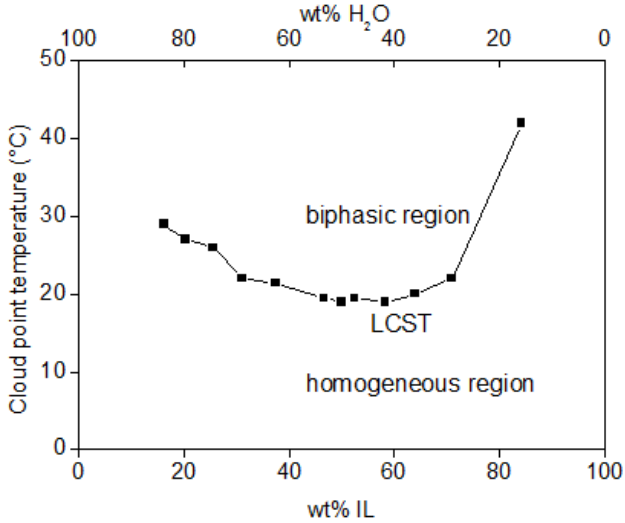

Figure 6.3 Binary phase diagram of $[P_{444}E_3][DOSS]/H_2O$.

Quite remarkably, for some compositions, gel formation was observed after shaking within a certain temperature range. **Figure 6.4** shows the rheopectic gel formation of 10 wt% $[P_{444}E_3][DOSS]$ in water upon shaking at 0 °C. This behavior has previously been described by Ohno and coworkers for tetraoctylphosphonium ethylphosphor amidate.[32] If the aqueous phase contains metal ions, this behavior was not observed for $[P_{444}E_3][DOSS]$, so it has not been investigated further.

Figure 6.4 Rheopectic gel formation of 10 wt% $[P_{444}E_3][DOSS]$ in water upon shaking at 0 °C.

Viscosities and densities of the ionic liquids $[P_{4444}][DOSS]$, $[P_{444}C_1COOEt][DOSS]$ and $[P_{444}E_3][DOSS]$ were measured in function of temperature (**Figure 6.5 and 6.7**). The density and viscosity of dry and water-saturated $[P_{444}E_3][DOSS]$ are compared in **Figures 6.6 and 6.8**. Viscosities below 65 mPa s are reached for the water-saturated IL. The thermal decomposition temperatures of all ionic liquids were determined with TGA (**Table 6.1**). The TGA trace of the ionic liquid $[P_{444}E_3][DOSS]$ is shown in **Figure 6.9**. A mass loss of about 20% was observed at a temperature of 240 °C, indicating loss of oligoethylene glycol. Full decomposition of the ionic liquid was reached at a temperature of 300 °C.

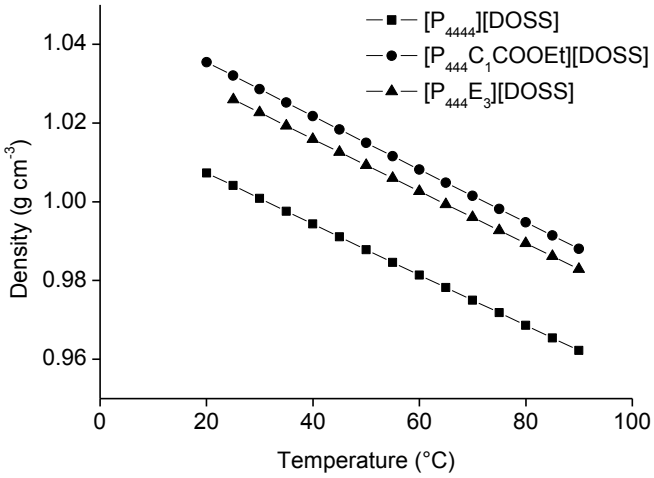

Figure 6.5 Density as a function of temperature for all dry room-temperature ionic liquids.

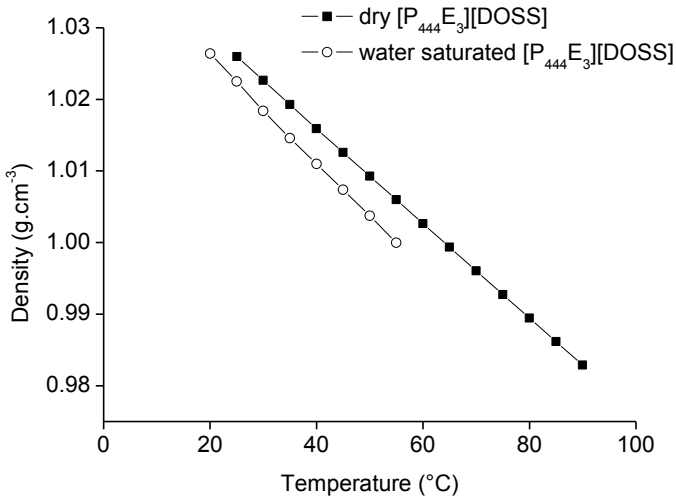

Figure 6.6 Density as a function of temperature for dry and water-saturated $[P_{444}E_3][DOSS]$ (water content 9 wt%).

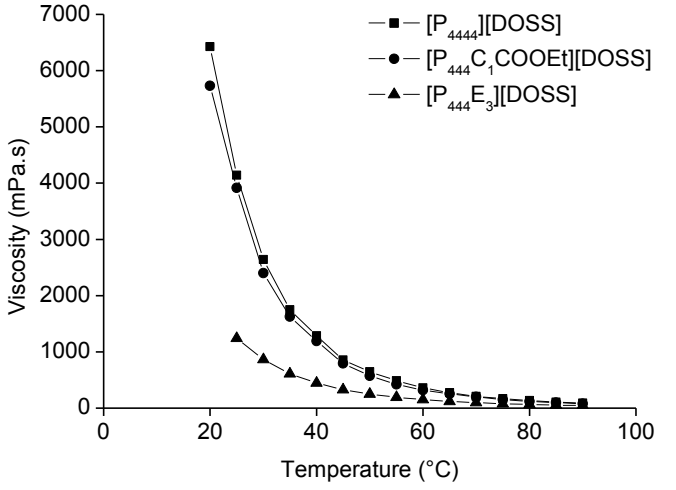

Figure 6.7 Viscosity as a function of temperature for all dry room-temperature ionic liquids.

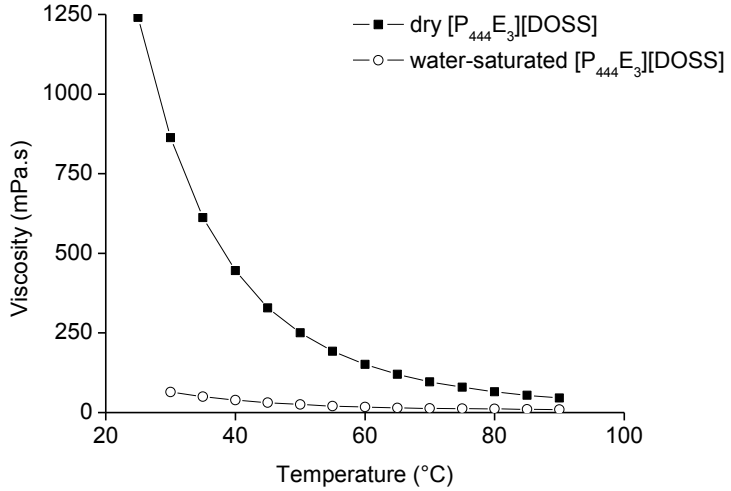

Figure 6.8 Viscosity as a function of temperature for dry and water-saturated $[P_{444}E_3][DOSS]$ (water content 9 wt%).

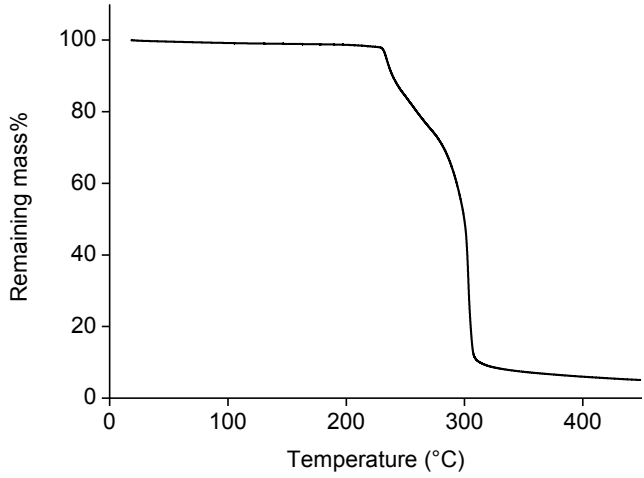

Figure 6.9 TGA trace of $[P_{444}E_3][DOSS]$, measured from 25 °C to 450 °C (2 °C min^{-1}) under a nitrogen atmosphere.

Extraction of metal ions

All synthesized ionic liquids were tested for their extraction capabilities via a multi-element extraction of Sc(III), La(III), Sm(III), Co(II) and Ni(II) (**Figure 6.10**). The high technological interest in Sc(III) and the recycling opportunities of end-of-life nickel metal hydride batteries or SmCo magnets justifies the choice of these metal ions. Since the non-functionalized ionic liquid $[P_{4444}][DOSS]$ has the lowest *%E* for all elements, the cation does play an important role in the extraction mechanism. By functionalization of the cation, the selectivity for a given metal ion was tuned, *e.g.* in $[P_{444}C_1COOH][DOSS]$ Sc(III) was extracted the best. This is in agreement with earlier work where it was shown that an ionic liquid cation with a carboxylic acid group is a good extractant for Sc(III).[23] $[P_{444}E_3][DOSS]$ shows good extraction efficiency for both trivalent and divalent metal ions.

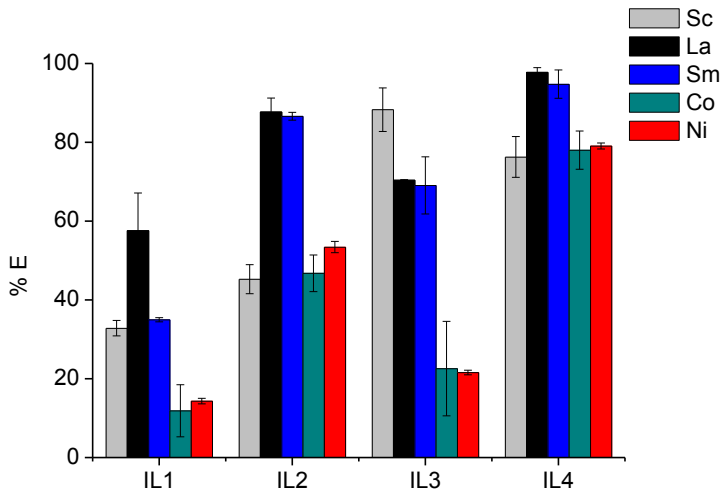

Figure 6.10 Percentage extraction for metals Sc(III), La(III), Sm(III), Co(II) and Ni(II) for all synthesized ionic liquids (multi-element feed solution metal concentration per metal approximately 1000 mg L^{-1}; equilibrium pH, pH_{eq}= 1.7; conditions for extraction: IL1= $[P_{4444}][DOSS]$, IL2= $[P_{444}C_1COOEt][DOSS]$, IL3= $[P_{444}C_1COOH][DOSS]$: 60 °C, 30 min, 1700 rpm; IL4= $[P_{444}E_3][DOSS]$: 0 °C, 2 min). Calculation of error bars based on duplicate experiments.

Special attention was paid to the thermomorphic ionic liquid $[P_{444}E_3][DOSS]$, because of its great potential in homogeneous liquid-liquid extraction (HLLE). In the binary mixture of the ionic liquid $[P_{444}E_3][DOSS]$ and water used for metal extraction, the lower critical solution temperature of the 1:1 w/w mixture was 19 °C. However, the presence of salts in the extraction system influences this cloud point temperature. Metal ions with a high charge density interact more favorably with water and thus have a higher salting-out capacity, leading to a decrease of the LCST. In **Figure 6.11**, the rare-earth metal ions are listed according to increasing charge density from La(III) to Sc(III), and the decrease in cloud point temperature is clearly visible, as cloud point temperatures drop to 3 °C and lower. Systems containing In(III), Sc(III), and Ga(III) do not exhibit any thermomorphic behavior anymore. The discontinuity from Cu(II) to Zn(II) can be explained using the Irving-Williams series which gives the relative stability of transition metal complexes as Co(II) < Ni(II) < Cu(II) > Zn(II), and thus ranks the strength of the interaction of water molecules with these ions or in other words, ranks their salting-out behavior.[33]

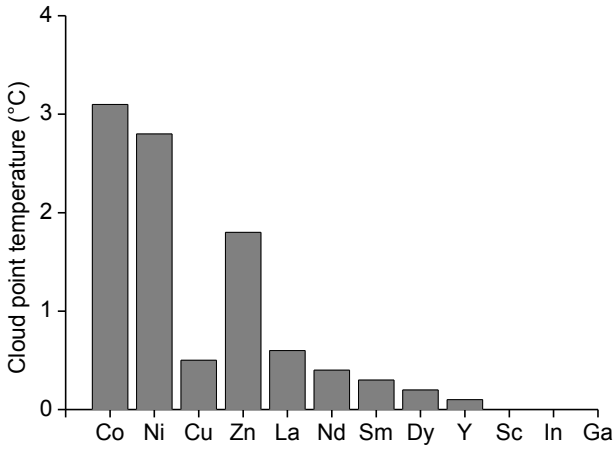

Figure 6.11 Cloud point temperature as a function of the increasing charge density of metal ions (metal concentrations : 5000 mg L^{-1}).

Several mono-element solutions of 5000 mg L^{-1} of metal chloride (Sc(III), Co(II), Ni(II), Cu(II), Zn(II), Ga(III), Y(III), In(III), La(III), Nd(III), Sm(III) and Dy(III)) were made and contacted in a 1:1 ratio (w/w) with the ionic liquid $[P_{444}E_3][DOSS]$. The distribution ratios and extraction efficiencies can be found in **Figure 6.12**. A visual representation of a typical homogeneous liquid-liquid extraction is shown in **Figure 6.13**. Since docusate is a sterically hindered anion, it was assumed that the extraction percentages would decrease with increasing charge density of the metal ion. This statement is only valid for Sc(III), having the lowest percentage extraction and indeed the highest charge density. The 3d transition metals are extracted in the same extent as Sc(III). *%E* for Ga(III) is significantly higher. For the remainder of the extractions of the lanthanide series by the oligoethylene functionalized ionic liquid, a normal extraction sequence is found. So, the higher the charge density, the higher the percentage of extraction, as is usually the case with acidic extractants. Moreover, in previous HLLE work with a similarly sterically hindered anion, namely the bis(2-ethylhexyl)phosphate ionic liquids, rare-earth ions formed a precipitate, while the 3d-transition metals were extracted with high efficiency.[22] In case of the sulfonate anion, no precipitates of rare-earth ions were observed.

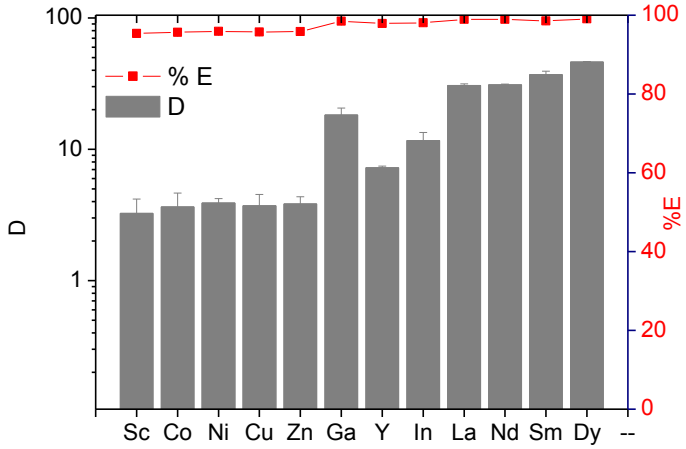

Figure 6.12 $[P_{444}E_3][DOSS]$, *D* (left axis) and *%E* (right axis) for selection of TM and REEs chloride solutions of approximately 5000 mg L^{-1} (mono-element solutions, pH_{eq} ±3, 0 °C, 2 min, manually shaken, settling 10 min, centrifuge). Calculation of error bars based on duplicate experiments.

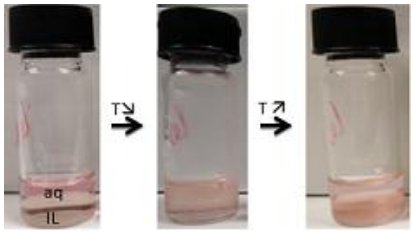

Figure 6.13 Picture showing the phase changes of the mixture of $[P_{444}E_3][DOSS]$ and water when the temperature changes, left: aqueous Co(II) phase of 5000 mg L^{-1}, middle: homogeneous phase and right: Co(II)-loaded IL phase.

Next, the influence of the extraction time at 0 °C (*i.e.* below the LCST) on the percentage extraction was investigated. It was found that once the homogeneous phase was reached, extraction proceeded almost instantaneously, since even after only 30 s no significant changes in the *D* were observed. To ensure that equilibrium was reached, generally the vials were kept in the ice bath for 2 min. The maximum loading of the ionic liquid is defined as the highest concentration of metal ions the ionic liquid can extract. The ionic liquid was put into contact in a 1:1 ratio (w/w) with increasingly higher concentrations of La(III) from 5,000 to 150,000 mg L^{-1}. It is known from the Hofmeister series that salts can have a salting-out effect, disturbing the thermomorphic system.[31] As could be seen in the mono-element extractions (**Figure 6.12**), the binary mixture of $[P_{444}E_3][DOSS]$/water with approximately 5000 mg L^{-1} of Sc(III) in chloride form was already too hydrophobic to reach a homogeneous phase. This can be explained by the small ionic radius and the high charge density of the Sc(III) cation which causes a larger salting-out effect. For La(III), a concentration of 10,000 mg L^{-1} (0.072 mol kg^{-1}) was the highest possible concentration to still have thermomorphic behavior, in that case the cloud point temperature was 0 °C. For higher concentrations, extractions were performed at room temperature in the binary mixtures. An increase in the initial concentration of La(III) causes the percentage extraction to decrease, as expected by the loading effect. In this case, the decrease is significant, to 20% extraction efficiency at initial feed concentrations above 0.40 mol kg^{-1} (**Figure 6.14**). The theoretical maximum loading is not yet reached in these circumstances. Contacting the ionic liquid with an even higher concentration of feed solution is not economically relevant. Thus, in order to fully load the ionic liquid, cumulative loading should be performed. After five consecutive contacts of the ionic liquid with a feed solution of 0.072 mol kg^{-1} La(III), the ionic liquid was finally loaded with 0.29 mol kg^{-1} La(III) and this did not increase further. It was calculated

that this value corresponds to four ionic liquid molecules participating in the extraction of one metal ion.

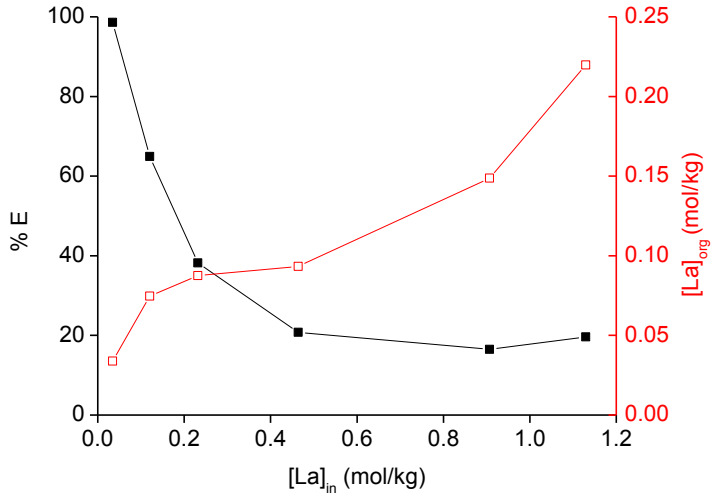

Figure 6.14 Loading of the IL-rich-phase: percentage extraction (■) and La(III) concentration (□) in the IL-rich-phase after extraction as a function of the initial La(III) concentration. ([$P_{444}E_3$][DOSS], room temperature, 2000 rpm, 10 min, single experiment).

To confirm the number of ionic liquid molecules contributing in the extraction, a slope analysis was performed. By changing the concentration of ionic liquid in a toluene phase and measuring the remaining metal concentrations in the water phase, a plausible extraction mechanism could be derived. The extraction mechanism can be generally written as equation 6.6:

$$La^{3+}_{aq} + x\overline{P_{444}E_3DOSS} \rightleftharpoons \overline{La(P_{444}E_3)_{x-3}DOSS_x} + 3P^{+}_{444}E_3 \qquad (6.6)$$

The bar indicates the species in the ionic liquid phase. The extraction constant (K_{extr}) for the extraction is given by equation 6.7:

$$K_{extr} = \frac{[P^{+}_{444}E_3]^3[\overline{La(P_{444}E_3)_{x-3}DOSS_x}]}{[La^{3+}_{aq}][\overline{P_{444}E_3DOSS}]^x} \qquad (6.7)$$

The concentration of $[P_{444}^{+}E_3]$ equals three times the concentration of $[La(P_{444}E_3)_{x-3}DOSS_x]$, which can be abbreviated as $[La_{org}]$. The notation of the extraction constant is now K´ (accent) to denote all constants are included in this value (equation 6.8).

$$K' = \frac{[\overline{La_{org}}]^4}{[La_{aq}^{3+}][\overline{P_{444}E_3DOSS}]^x} \quad (6.8)$$

Rewriting equation 6.8 to equation 6.9 using the abbreviation [IL] for $[P_{444}E_3][DOSS]$ shows that, when plotting $\log([La_{org}]^4/[La_{aq}^{3+}])$ as a function of the log of ionic liquid concentration, the obtained slope will give the number of anions needed in the extraction.

$$\log \frac{[\overline{La_{org}}]^4}{[La_{aq}^{3+}]} = x \log[IL] \quad (6.9)$$

Figure 6.15 shows the plot for the slope analysis of La(III) towards $[P_{444}E_3][DOSS]$ in toluene. The experiment was performed by changing the ionic liquid concentration in toluene with a La(III) solution of 948 ppm. This low concentration ensures that the pH does not vary too much. Measured pH equilibrium values were 3.5 ± 0.3. A value of 3.26 was found for the slope, raising question if 3 or 4 anions are used in the extraction. An objection could be made about the use of toluene as a diluent. However, the use of a diluent is necessary because of the changing concentrations of the ionic liquid phase and the possible phase changes occurring due to the lower critical solution temperature of this ionic liquid. The use of the diluent implies that no direct extrapolation can be performed to the system in which the IL is used in its pure form because diluents can affect the mechanism of extraction. More importantly, in the calculations, concentration was used instead of activity. Since ionic strengths of all solutions will change with varying metal concentrations and small volume changes by ionic liquid dissolution will also affect these values, an error on the calculation is made. From the maximum loading experiment, it was derived that most probably a cation exchange process takes place, in which the metal cation is extracted towards the ionic liquid phase by four anions and a cation and three ionic liquid cations are transferred to the aqueous phase in order to obtain charge neutrality. Yet, further investigation of the extracted species using Extended X-ray Absorption Fine Structure (EXAFS) analysis should confirm these observations.

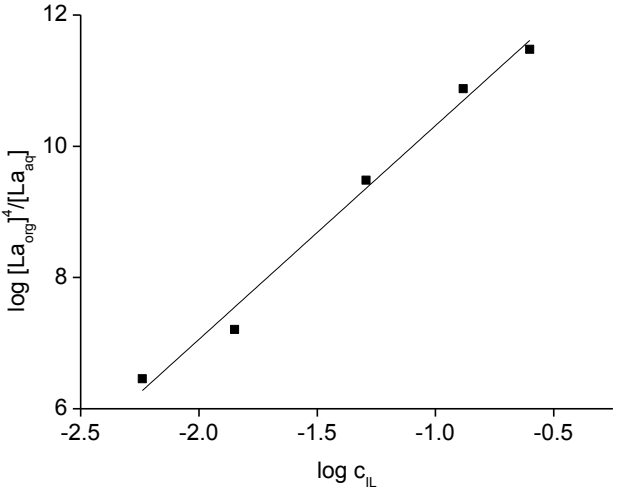

Figure 6.15 Slope analysis of extraction of La(III) towards $[P_{444}E_3][DOSS]$ in toluene. Initial La(III) concentration: 948 mg L^{-1}, slope: 3.26, R^2: 0.99.

Next, the possibility to remove the La(III) from the loaded IL was tested, by examination of two stripping procedures. Both addition of oxalic acid in precipitation stripping (**Figure 6.16**) and addition of acid, HCl or HNO_3 (**Figure 6.17**) resulted in quantitative stripping of La(III). The addition of solid oxalic acid to the ionic liquid phase yields an insoluble lanthanum(III) oxalate complex. 100% stripping efficiency is reached at a molar ratio of 1.5 : 1 of oxalic acid to La(III). The ionic liquid is regenerated and the acid of docusate formed (equation 6.10).

$$3H_2C_2O_4 + 2\overline{La(P_{444}E_3)DOSS_4} \rightleftharpoons La_2(C_2O_4)_3 + 2\overline{(P_{444}E_3)DOSS} + 6HDOSS \quad (6.10)$$

The solid $La_2(C_2O_4)_3$ could be isolated and calcined in an oven at high temperature to form La_2O_3 (equation 6.11):

$$La_2(C_2O_4)_3 + \frac{3}{2}O_2 \rightarrow La_2O_3 + 6CO_2 \quad (6.11)$$

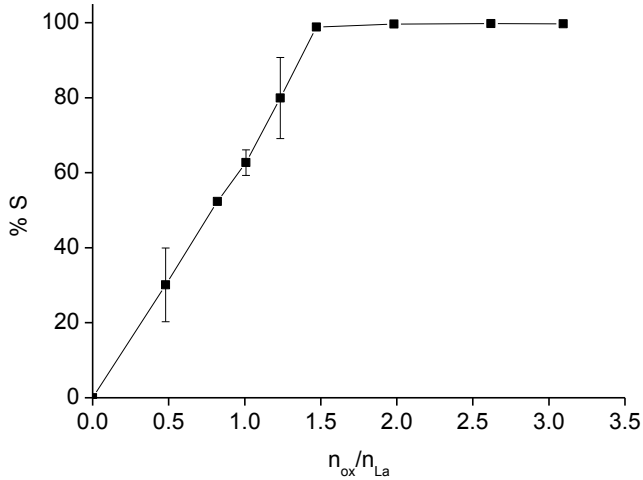

Figure 6.16 Precipitation stripping of La(III) from $[P_{444}E_3][DOSS]$, previously loaded with approximately 10 000 mg L^{-1} of La(III), using pure solid oxalic acid (70 °C, 1700 rpm, 10 min). Calculation of error bars based on duplicate experiments. Error bars that are not visible are smaller than the symbol of the data point.

As was mentioned earlier, ionic liquid cations are lost to the aqueous phase upon extraction of La(III) to the ionic liquid phase (equation 6.6). During stripping, the anion is set free in the form of the conjugated acid HDOSS (equation 6.10). It is thus possible to regenerate the ionic liquid by contacting the aqueous phase and the recycled ionic liquid, simply by the addition of an equivalent amount of NaOH (equation 6.12).

$$P_{444}E_3Cl + HDOSS + NaOH \rightarrow \overline{(P_{444}E_3)DOSS} + NaCl + H_2O \qquad (6.12)$$

Next, the possibility to strip the ionic liquid by contacting the ionic liquid with different concentrations of HCl was investigated (**Figure 6.17**). The ionic liquid could not be fully stripped from its metal content, 20% of La(III) remained in the IL phase at 8 M HCl. Remarkable is the fact that the percentage stripping shows a maximum, with higher concentrations of HCl. This might be due to a change into another extraction mechanism with high chloride concentration, *i.e.* a solvation mechanism. The speciation of La(III) changes from the strongly hydrated La^{3+} to the much weaker hydrated $LaCl_x$ species, which in combination with a protonated docusate can extract and thus stay in the ionic liquid phase. Stripping of La(III) with HNO_3 on the other hand is much more efficient. Again, the strong hydration of chloride, now in

comparison to nitrate lowers its stripping efficiency since the chloride has more water in its coordination sphere and is thus less available for metal ions. By contacting the loaded ionic liquid with a 4 M HNO_3 solution, all La(III) was stripped. A higher concentration of HNO_3 did not yield a drop in stripping percentage.

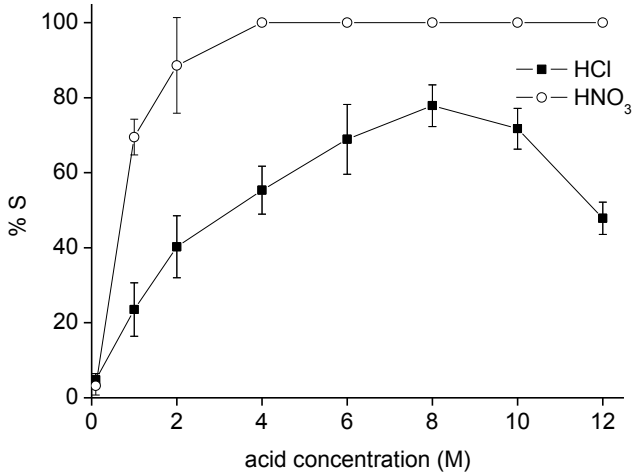

Figure 6.17 Stripping of La(III) from $[P_{444}E_3][DOSS]$, previously loaded with approximately 10,000 mg L^{-1} of La(III) , using different concentrations of acid, both HCl or HNO_3 (70 °C, 1700 rpm, 30 min). Calculation of error bars based on duplicate experiments. Error bars that are not visible are smaller than the symbol of the data point.

The development of routes to recycle rare earths from for instance end-of-life nickel metal hydride batteries, NdFeB or SmCo magnets or other rare-earth containing devices, like fluorescent lamps, is getting a lot of attention.[34-38] Recycling of end-of-life products is increasingly important in the transition to a green economy.[36,39] Here, the ionic liquid $[P_{444}E_3][DOSS]$ was used for the separations of the La/Ni pair, which is relevant for recycling of NiMH batteries and the Sm/Co pair for recycling of SmCo magnets (**Figure 6.18**). Stock solutions containing 2500 mg L^{-1} of both La(III) and Ni(II) or Sm(III) and Co(II) (present as chlorides) were prepared and contacted with the ionic liquid $[P_{444}E_3][DOSS]$. **Figure 6.19** until **Figure 6.22** show the distribution ratio and percentage extractions of the metal ions as a function of pH. It can be concluded that $[P_{444}E_3][DOSS]$ has a high extraction capacity for both the rare-earth elements and transition metals, and that separation by selective extraction is not feasible in one step. Based on the separation factors in **Table 6.2**, the La/Ni separation is easier than the Sm/Co separations since

separations factors of 15 are reached for La/Ni compared to a maximum of 8 for Sm/Co.

Figure 6.18 Picture of Sm/Co pair (pink on the left) and La/Ni pair (green on the right), before (a) and after (b) extraction.

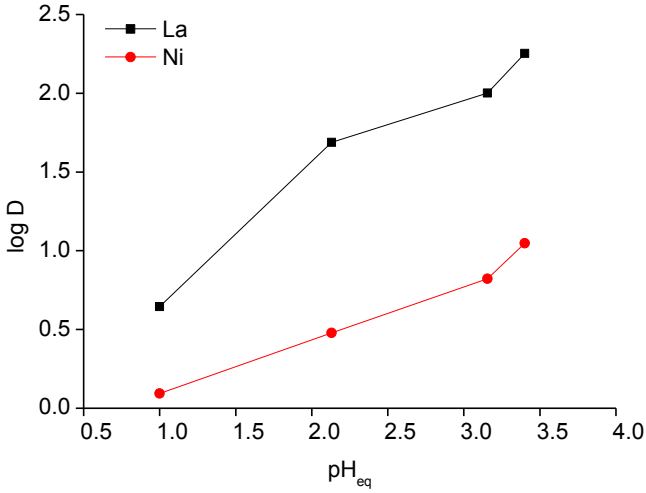

Figure 6.19 Log of distribution ratios of La(III) and Ni(II) in function of the equilibrium pH. (2500 ppm of La(III) and 2500 ppm of Ni(II) at different pH_{eq}, LCST condition: 0 °C in ice water, 5 min)

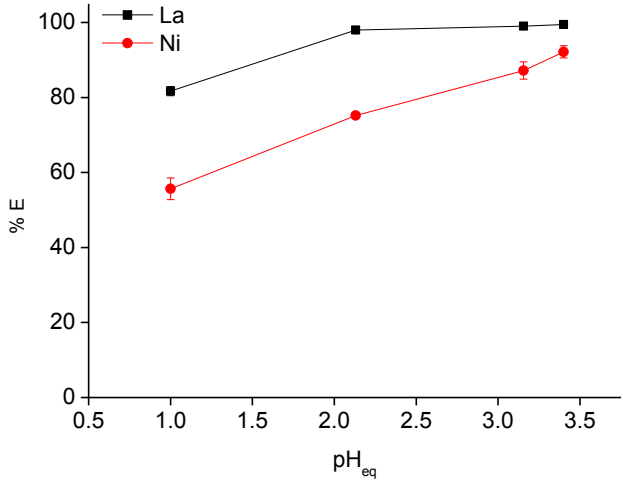

Figure 6.20 Percentage extractions of La(III) and Ni(II) in function of the equilibrium pH. (2500 ppm of La(III) and 2500 ppm of Ni(II) at different pH, LCST condition: 0 °C in ice water, 5 min). Calculation of error bars based on duplicate experiments. Error bars that are not visible are smaller than the symbol of the data point.

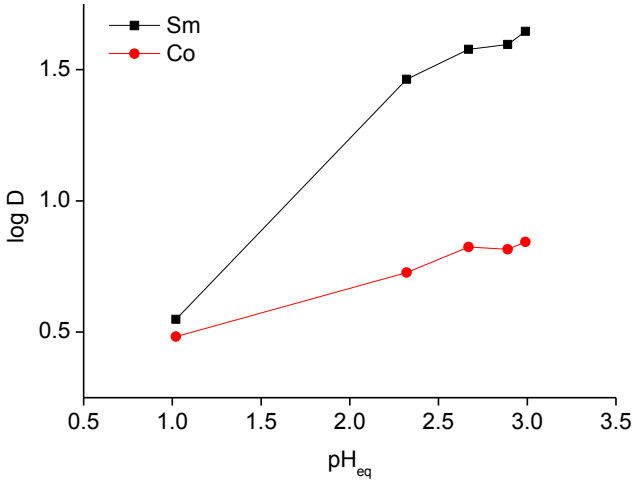

Figure 6.21 Log of distribution ratios of Sm(III) and Co(II) in function of the equilibrium pH. (2500 ppm of Sm(III) and 2500 ppm of Co(II) at different pH, LCST condition: 0 °C in ice water, 5 min)

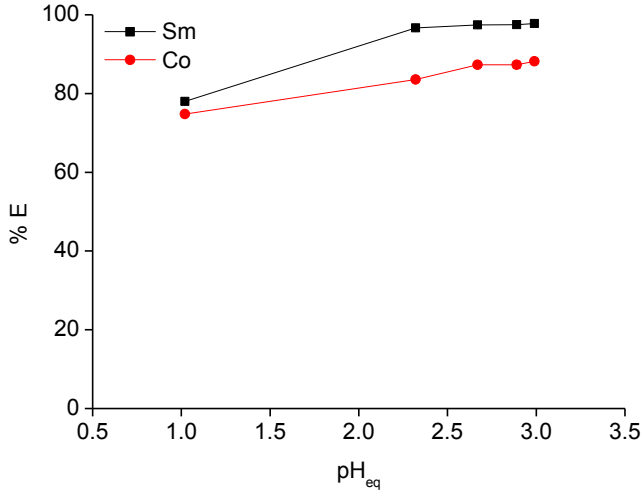

Figure 6.22 Percentage extractions of Sm(III) and Co(II) in function of equilibrium pH. (2500 ppm of Sm(III) and 2500 ppm of Co(II) at different pH, LCST condition: 0 °C in ice water, 5 min). Calculation of error bars (smaller than data point) based on duplicate experiments.

Table 6.2 Separation factors (α) for La/Ni separation and for Sm/Co separation by $[P_{444}E_3][DOSS]$, for different equilibrium pH values, with standard deviation (s), based on duplicate measurements.

pH_{eq}	$\alpha_{La,Ni}$	s	pH_{eq}	$\alpha_{Sm,Co}$	s
1.0	3.51	0.06	1.0	1.31	0.63
2.1	16.08	0.20	2.3	6.24	3.27
3.2	15.83	0.99	2.7	5.89	1.65
3.4	15.11	1.30	2.9	6.06	0.33
			3.0	8.09	1.41

Since separation could not be reached in one single step, it was attempted if a scrubbing step improved the separation. Different methods were tested, including scrubbing with high concentrations of the salts NH_4NO_3 and NaCl, or with the acids HCl, HNO_3 and H_2SO_4 in varying concentrations (**Figure 6.23 until 6.27**). Unfortunately, no selectivity could be achieved by any of these methods. In a next scrubbing experiment, ethylenediaminetetraacetic acid (EDTA) was used as a scrubbing agent (**Table 6.3**). Different concentrations of EDTA at different pH were tested. The difference in stability constants for La(III) and Ni(II), Sm(III) and Co(II) for the formation of complexes with EDTA (*i.e.* logarithms of stability

constants: 15.1 for La(III), 18.2 for Ni(II), 16.8 for Sm(III) and 15.9 for Co(II)[40]) determines the affinity of the ion for the aqueous solution with EDTA. At a concentration of 0.04 M of EDTA with an initial pH of 5.1, all Ni(II) is removed from the ionic liquid. It should be remarked that 10% of La(III) is back-extracted as well. In the ionic liquid phase, now only La(III) remains, which can be stripped using oxalic acid as explained above. In the case of the Sm(III)/Co(II) couple another factor plays a role, causing the Co(II) to be scrubbed more than the Sm(III) although the logarithms of the stability constants state the opposite effect to happen (16.8 for Sm(III) and 15.9 for Co(II)). Most likely, the higher charge density of Sm(III) causes a higher affinity for the docusate ionic liquid than for the EDTA phase. Here, the Co(II) is scrubbed 100% from the ionic liquid by contact with 0.06 M of EDTA, but this is unfortunately associated with a back-extraction of 50% Sm(III). Contacting the ionic liquid with an EDTA solution of pH 12 is unfavorable for selective separations as all metals are removed in that case. Lowering the initial pH of the EDTA solution to 3.8 scrubs 91% of Ni(II) and only 1% of La(III). The separation of Sm(III) from Co(II) is still challenging since a large fraction of Sm(III) is back-extracted in the scrubbing step.

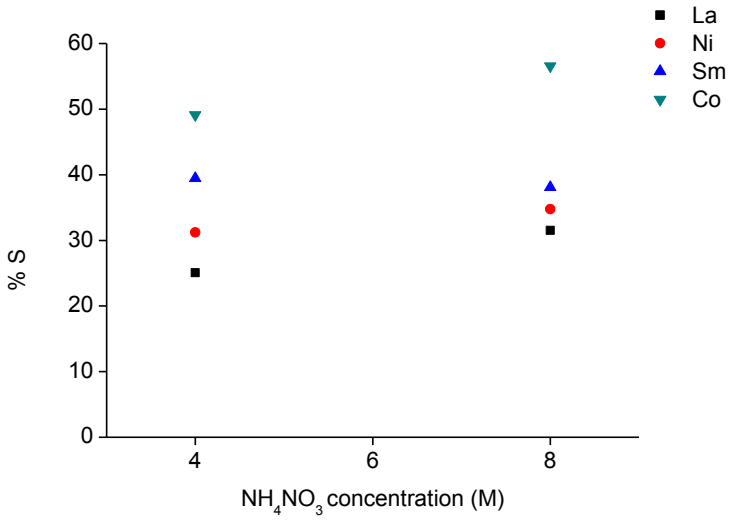

Figure 6.23 Scrubbing of La(III) and Ni(II), Sm(III) and Co(II) with varying NH_4NO_3 concentration (4 and 8 M) (30 min, 50 °C, single experiment).

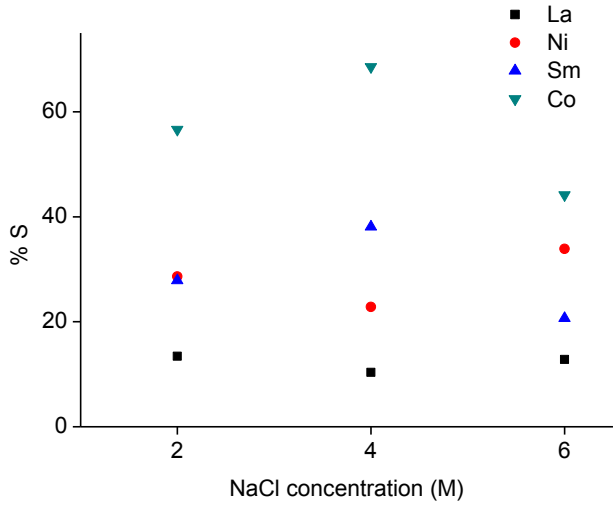

Figure 6.24 Scrubbing of Sm(III) and Co(II) with varying NaCl concentration (30 min, 50 °C, single experiment).

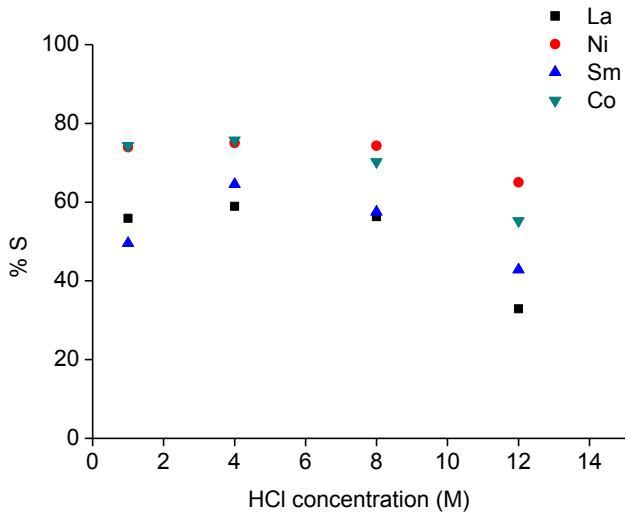

Figure 6.25 Scrubbing of La(III) and Ni(II), Sm(III) and Co(II) with varying HCl concentration (30 min, 50 °C, single experiment).

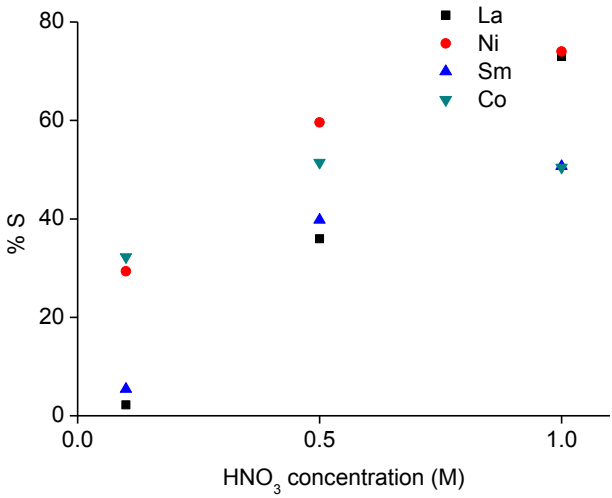

Figure 6.26 Scrubbing of La(III) and Ni(II), Sm(III) and Co(II) with varying HNO_3 concentration (30 min, 50 °C, single experiment).

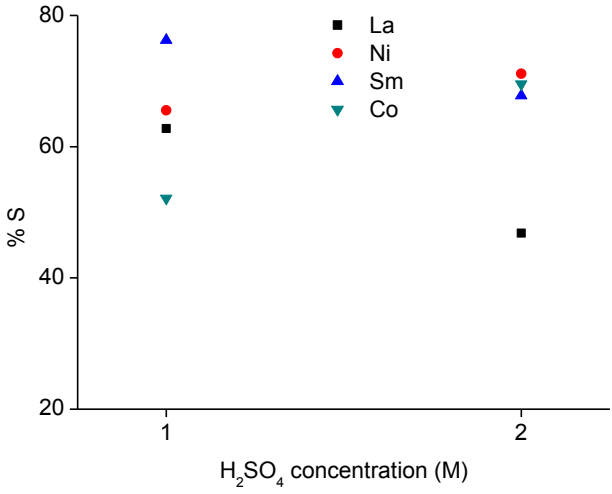

Figure 6.27 Scrubbing of La(III) and Ni(II), Sm(III) and Co(II) with varying H_2SO_4 concentration (30 min, 50 °C, single experiment).

Table 6.3 Scrubbing (*%S*) of La(III) and Ni(II), Sm(III) and Co(II) with varying EDTA concentrations: 0.02 M, 0.04M and 0.06 M, at initial pH, pH_{in} 3.8, 5.1 and 12.1 (0 °C in ice water, 5 min).

EDTA	**pH_{in} 3.8**				**pH_{in} 5.1**				**pH_{in} 12.1**			
	%S La	*%S* Ni	*%S* Sm	*%S* Co	*%S* La	*%S* Ni	*%S* Sm	*%S* Co	*%S* La	*%S* Ni	*%S* Sm	*%S* Co
0.02 M	n.d.	n.d.	n.d.	n.d.	0.36	51	18	67	n.d.	n.d.	n.d.	n.d.
0.04 M	1	91	31	76	10	100	26	87	75	94	100	100
0.06 M	21	95	49	97	17	99	49	100	100	100	100	100

n.d. not determined

6.4 Conclusions

The docusate anion was incorporated into several phosphonium ionic liquids, including tetrabutylphosphonium, and cations functionalized with either an ester, carboxylic acid or ethylene glycol group. The water miscibility of all ionic liquids was tested. Although the docusate anion is a known surfactant, the presence of the ethylene glycol moiety in the cation induced lower critical solution phase behavior when mixed with water. In an initial screening test, both conventional solvent extraction as well as homogeneous liquid-liquid extraction were performed. In general, trivalent metal ions were found to be extracted better than the divalent transition metals. Most attention was paid to the $[P_{444}E_3][DOSS]$/water extraction system since homogeneous liquid-liquid extraction can be performed with this system. The extraction mechanism of La(III) was investigated. The most plausible extraction mechanism extracts the La(III) metal ion with four ionic liquid anions and one ionic liquid cation, transferring three ionic liquid cations to the aqueous phase in order to obtain charge neutrality. These cations can later be recycled by contacting the aqueous phase with the ionic liquid residue after precipitation stripping, fully regaining the functional ionic liquid. The $[P_{444}E_3][DOSS]$/water extraction system was also applied to the La/Ni and Sm/Co pairs in a homogeneous liquid-liquid extraction fashion, as these are relevant separations for the recycling of end-of-life batteries or magnets. The separation could not be achieved by selective extraction, an additional scrubbing step was necessary, in which EDTA performed the best.

This research was financially supported by IWT-Flanders (PhD fellowship to DD), the FWO Flanders (research project G.0900.13) and the KU Leuven (projects GOA/13/008 and IOF-KP RARE^3). The authors also wish to thank Tom Vander Hoogerstraete for scientific discussions, Karel Duerinckx for NMR measurements and Dirk Henot for performing CHN analyses.

6.5 References

1 A. E. Visser, R. P. Swatloski, W. M. Reichert, R. Mayton, S. Sheff, A. Wierzbicki, J. Davis, R. D. Rogers, *Chem. Commun.*, 2001**,** 135.
2 N. V. Plechkova, K. R. Seddon, *Chem. Soc. Rev.*, 2008**, 37**, 123.
3 P. Wasserscheid, W. Keim, *Angew. Chem. Int. Ed.*, 2000**, 39**, 3772.
4 J. N. Chubb, P. Lagos, J. Lienlaf, *J. Electrostat.*, 2005**, 63**, 119.
5 T. Welton, *Chem. Rev.*, 1999**, 99**, 2071.
6 S. Wellens, B. Thijs, K. Binnemans, *Green Chem.*, 2012**, 14**, 1657.
7 T. Vander Hoogerstraete, S. Wellens, K. Verachtert, K. Binnemans, *Green Chem.*, 2013**, 15**, 919.
8 P. P. Gerbino; *Remington: The Science and Practice of Pharmacy;* PA. Lippincott Williams & Wilkins: Philadelphia, 2005.
9 J. Davis, P. A. Fox, *Chem. Commun.*, 2003**,** 1209.
10 S. Nave, J. Eastoe, J. Penfold, *Langmuir*, 2000**, 16**, 8733.
11 S. Nave, J. Eastoe, R. K. Heenan, D. Steytler, I. Grillo, *Langmuir*, 2000**, 16**, 8741.
12 P. Brown, C. P. Butts, J. Eastoe, D. Fermin, I. Grillo, H. C. Lee, D. Parker, D. Plana, R. M. Richardson, *Langmuir*, 2012**, 28**, 2502.
13 N. Nishi, T. Kawakami, F. Shigematsu, M. Yamamoto, T. Kakiuchi, *Green Chem.*, 2006**, 8**, 349.
14 R. Moulton, and J. H. Davis, J. H., Ionic Liquids containing a Sulfonate Anion, US Patent 7,750,166 B2, **2010**.
15 S. Y. Choi, H. Rodriguez, A. Mirjafari, D. F. Gilpin, S. McGrath, K. R. Malcolm, M. M. Tunney, R. D. Rogers, T. McNally, *Green Chem.*, 2011**, 13**, 1527.
16 W. L. Hough, M. Smiglak, H. Rodriguez, R. P. Swatloski, S. K. Spear, D. T. Daly, J. Pernak, J. E. Grisel, R. D. Carliss, M. D. Soutullo, J. Davis, R. D. Rogers, *New J. Chem.*, 2007**, 31**, 1429.
17 K. Lava, Y. Evrard, K. Van Hecke, L. Van Meervelt, K. Binnemans, *RSC Adv.*, 2012**, 2**, 8061.
18 Y. Kohno, H. Ohno, *Chem. Commun.*, 2012**, 48**, 7119.
19 T. Vander Hoogerstraete, B. Onghena, K. Binnemans, *J. Phys. Chem. Lett.*, 2013**, 4**, 1659.
20 M. Blesic, H. Q. N. Gunaratne, J. Jacquemin, P. Nockemann, S. Olejarz, K. R. Seddon, C. R. Strauss, *Green Chem.*, 2014**, 16**, 4115.
21 T. Vander Hoogerstraete, B. Onghena, K. Binnemans, *Int. J. Mol. Sci.*, 2013**, 14**, 21353.

22 D. Depuydt, L. Liu, C. Glorieux, W. Dehaen, K. Binnemans, *Chem. Commun.*, 2015**, 51**, 14183.
23 D. Depuydt, W. Dehaen, K. Binnemans, *Ind. Eng. Chem. Res.*, 2015**, 54**, 8988.
24 G. Cui, C. Wang, J. Zheng, Y. Guo, X. Luo, H. Li, *Chem. Commun.*, 2012**, 48**, 2633.
25 Y. Zhang, S. Zhang, X. Lu, Q. Zhou, W. Fan, X. Zhang, *Chem. Eur. J.*, 2009**, 15**, 3003.
26 Y. Chevalier, P. Le Perchec, *J. Phys. Chem.*, 1990**, 94**, 1768.
27 K. Koumoto, H. Ochiai, N. Sugimoto, *Tetrahedron*, 2008**, 64**, 168.
28 F. Malz, H. Jancke, *J. Pharm. Biomed. Anal.*, 2005**, 38**, 813.
29 G. Yu, D. Zhao, L. Wen, S. Yang, X. Chen, *AIChE J.*, 2012**, 58**, 2885.
30 S. Zhang, N. Sun, X. He, X. Lu, X. Zhang, *J. Phys. Chem. Ref. Data*, 2006**, 35**, 1475.
31 D. Dupont, D. Depuydt, K. Binnemans, *J. Phys. Chem. B*, 2015**, 119**, 6747.
32 Y. Fukaya, T. Nakano, H. Ohno, *Aust. J. Chem.*, 2016.
33 H. Irving, R. J. P. Williams, *J. Chem. Soc.*, 1953**,** 3192.
34 D. Dupont, K. Binnemans, *Green Chem.*, 2015**, 17**, 856.
35 T. Vander Hoogerstraete, B. Blanplain, T. Van Gerven, K. Binnemans, *RSC Adv.*, 2014**, 4**, 64099.
36 K. Binnemans, P. T. Jones, B. Blanpain, T. Van Gerven, Y. Yang, A. Walton, M. Buchert, *J. Cleaner Prod.*, 2013**, 51**, 1.
37 T. Vander Hoogerstraete, K. Binnemans, *Green Chem.*, 2014**, 16**, 1594.
38 K. Larsson, K. Binnemans, *Green Chem.*, 2014**, 16**, 4595.
39 K. Binnemans, P. T. Jones, B. Blanpain, T. Van Gerven, Y. Pontikes, *J. Cleaner Prod.*, 2015**, 99**, 17.
40 G. Schwarzenbach, *Analyst*, 1955**, 80**, 713.

CHAPTER 7

IONIC LIQUID BASED AQUEOUS BIPHASIC SYSTEM

This chapter has been published and is reproduced here with permission from the American Chemical Society.

Depuydt, D., Dehaen, W., Binnemans, K. (2015). Solvent Extraction of Scandium(III) by an Aqueous Biphasic System with a Nonfluorinated Functionalized Ionic Liquid. *Industrial & Engineering Chemistry Research, 54* (36), 8988-8996.

The experimental work and writing were executed by the author of this thesis. The text may deviate from the original publication as the supplementary information is included in the chapter.

Graphical Abstract

The non-fluorinated functionalized ionic liquid $[P_{444}C_1COOH]Cl$ was used in an IL-based aqueous biphasic system for the extraction of scandium.

Abstract

The use of ionic liquids (ILs) as solvents for extraction of metals is a promising development in separation science and technology; yet the viscosities of ILs can be so high that long reaction times are required to reach the equilibrium state. An aqueous biphasic system (ABS) consisting of the non-fluorinated carboxyl-functionalized phosphonium IL $[P_{444}C_1COOH]Cl$ and a 16 wt% NaCl solution is described. The IL-rich phase of the aqueous biphasic system has a very low viscosity in comparison to the pure ionic liquid $[P_{444}C_1COOH]Cl$. This system has excellent extraction properties for scandium. Different extraction parameters were investigated, including contact time and metal loading. The influence of the pH on the solubility of the IL cation in the water-rich phase was determined via quantitative ^1H NMR. The stripping of scandium with oxalic acid from the ionic liquid phase was also investigated. A plausible extraction mechanism is proposed where three IL cations are deprotonated to form zwitterionic compounds that can coordinate scandium(III) ions.

7.1 Introduction

Ionic liquids (ILs) are solvents that consist entirely of ions.[1-3] Because of their low flammability, negligible vapor pressure and thus low volatility, they can be environmentally friendlier and safer to use than conventional volatile molecular solvents. The versatility of ILs, in which the chemical structure can be tuned to fit the requirements of any wanted application, is a great advantage of these solvents. Functionalized ILs contain a functional group in their structure and are also known as task-specific ILs.[4] The carboxyl functional group has proven to be a good moiety for the extraction of metal ions.[5] Carboxylic acids are used as extractants for the separation of copper from nickel and cobalt in hydrometallurgical processes.[6] Given the fact that carboxylic acids are extractants for metal ions in solvent extraction processes, functionalization of an ionic liquid with a carboxylic acid was a logical step. Several examples of carboxyl-functionalized ILs have been described in the literature.s[7-11]

In most studies on solvent extraction processes with ILs, only hydrophobic ILs were considered. The number of hydrophobic ILs is limited and the majority of these ILs have fluorinated anions. Fluorinated ILs are expensive and persistent in nature which makes them difficult to dispose of. Besides

that, in the case of hexafluorophosphate anions, the hydrolysis of the anion leading to the formation of hazardous hydrofluoric acid is a major disadvantage.[12] A first step toward a greener process for solvent extraction of metals was already taken by the incorporation of non-fluorinated ILs in solvent extraction systems. ILs such as Cyphos® IL 101 and Aliquat® 336 are used in extraction systems, yet often with molecular solvents as diluents and thus, undermining the green character of the system.[13-32]

Non-fluorinated ILs with long alkyl chains in their pure form are very viscous. A high viscosity hampers the mass transfer and slows down the kinetics. So, longer mixing times are needed for an exchange across the phase boundary. This can be solved by saturating the ionic liquid with water, by performing the extractions at elevated temperatures, and with lowering the concentrations of metal salts in the aqueous feed solution since viscosity problems mainly arise with high metal loadings.[33] Another way to circumvent the issues related to highly viscous ILs in solvent extraction systems is by using ILs with *thermomorphic behavior*. A two-phase IL/solvent mixture is converted to one homogeneous phase by increasing the temperature in case of a system with an *upper critical solution temperature* (UCST). *Homogeneous liquid-liquid extraction* (HLLE) takes advantage of the homogeneous phase above the UCST. Recently, HLLE processes based on the use of thermomorphic ILs have been developed.[34-36] In this way, the ILs that have a temperature-dependent miscibility with water can also be exploited for solvent extraction, since phase separation is controlled by temperature. Completely hydrophilic ILs have been neglected when it comes to extraction experiments, because they dissolve in water and do not form two phases. However, it is possible to use them in *aqueous biphasic systems* (ABS), also known as a*queous two-phase systems* (ATPS). Conventional aqueous biphasic systems are polymer-polymer, polymer-salt, and salt-salt systems.[37] ABS has been extensively used for separation and analytical studies of biomaterials since Albertsson developed the novel liquid-liquid extraction technique in the 1950s.[38] Aqueous biphasic systems are mainly water-based and they show a large biocompatibility, so that they are being used in the recovery and purification of proteins and nucleic acids,[38,39] and for the preconcentration of solutes from small samples of metal chelates and porphyrins.[40,41] Metal ions can also be extracted with the aqueous two-phase systems, although the number of examples is limited.[42-45] Three different categories of ABS for extraction of metal ions can be defined:

(1) extraction using a water-soluble extractant; (2) extraction of metal ions as metal complexes with inorganic anions and (3) extraction by the polymer-rich phase.[46]

The proof-of-principle for an IL-based ABS was reported by Rogers *et al.* in 2003,[47] and in the past decade, the literature on the theme has increased significantly, including polymer-IL based ABS.[48-57] The aqueous solution of an ionic liquid can undergo a liquid-liquid demixing upon addition of a salting-out agent. In this way, phase separation is chemically induced and a binary system consisting of an IL-rich phase and a salt-rich phase is formed. This implies complete control over the miscibility of the ionic liquid, which is essential for separation technologies. The advantages of IL-based ABS are twofold: the viscosity problem is solved because of the large water content of the IL-rich phase and the possibility to use water-miscible non-fluorinated ILs. The non-fluorinated ILs have great potential in this new separation technique. Moreover, they are less expensive and easier to dispose of than their fluorinated counterparts. The IL-based ABS opens the door to a new, greener solvent extraction system for metals. Although ABS is popular for the extraction of biomolecules,[53,58-60] examples of the use of IL-based ABS for the extraction of metal ions are still rather scarce. Akama *et al.* have reported on aqueous two phase systems with tetrabutylammonium bromide, for the extraction of cadmium and chromium(VI).[61,62]

Scandium is a rare element, and of high technological interest. It can be used as an alloying metal for aluminum,[63] as well as in scandium-stabilized zirconia for solid oxide fuel cells,[64] and scandium(III) triflate is a recyclable Lewis acid catalyst used for the production of fine chemicals.[65] There are no scandium rich deposits, but the element is produced as a byproduct during production of other metals (tin, tungsten, nickel, uranium, tantalum) or recovered from previously processed tailings or industrial process residues.[66] Solvent extraction is the most often used method for the recovery and purification of scandium.[67-75]

In this chapter, the solvent extraction of scandium was performed in an aqueous biphasic system with the water-miscible carboxyl-functionalized phosphonium ionic liquid $[P_{444}C_1COOH]Cl$ (**Figure 7.1**), the aqueous miscibility of which was controlled by the addition of sodium chloride as a salting-out agent. The phase behavior of the ternary system was studied. Different extraction parameters, such as contact time, pH and metal loading

were investigated. Furthermore, the extraction mechanism was examined as well as the stripping of the metal from the ionic liquid.

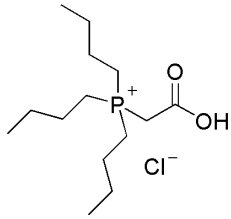

Figure 7.1 Structure of the ionic liquid tri-*n*-butyl(carboxymethyl)phosphonium chloride, $[P_{444}C_1COOH]Cl$.

7.2 Experimental

7.2.1 Chemicals

Tributylphosphine (99%), sodium chloride and scandium(III) chloride hydrate (99.9%) were purchased from Sigma-Aldrich (Diegem, Belgium). Absolute ethanol and hydrogen chloride (37%) were obtained from VWR (Leuven, Belgium). Ethyl chloroacetate (99%) and phenol (99+%) were purchased from ACROS Organics (Geel, Belgium). Sodium hydroxide was acquired from ChemLab (Zedelgem, Belgium). Acetonitrile (HPLC grade) was obtained from Fischer Chemicals (Geel, Belgium). Oxalic acid (> 99.5%) was obtained from JT Baker. A 1000 ppm gallium ICP standard and 1000 ppm lanthanum ICP standard were obtained from Merck (Overijse, Belgium). The silicone solution in isopropanol was purchased from SERVA Electrophoresis GmbH (Heidelberg, Germany). All chemicals were used as received without further purification.

7.2.2 General

The ^{1}H NMR and ^{13}C NMR spectra were recorded on a Bruker Avance 300 spectrometer (operating at 300 MHz for ^{1}H, 75 MHz for ^{13}C). ^{31}P NMR (243 MHz) spectra were recorded on a Bruker AMX 600 MHz spectrometer. ^{45}Sc NMR spectra were recorded on a Bruker AMX 400 MHz spectrometer (operating at 97.2 MHz for ^{45}Sc). The chemical shifts are noted in parts per million (ppm), referenced to tetramethylsilane for ^{1}H and ^{13}C, to 85% H_3PO_4 for ^{31}P NMR and to $ScCl_3$ (1 M) for ^{45}Sc NMR. All solutions were made in $CDCl_3$, except for the ^{45}Sc NMR, where D_2O was used. The spectra were analyzed with SpinWorks software. The Fourier Transform

Infrared (FTIR) spectrum of the IL was recorded by a Bruker Vertex 70 spectrometer via the attenuated total reflectance (ATR) technique with a Bruker Platinum ATR accessory. The OPUS software package was used for analysis of the FTIR spectra. The elemental analysis of carbon, hydrogen and nitrogen (CHN analysis) was performed on a CE-instruments EA-1110 elemental analyzer. The water content was determined by coulometric Karl Fischer titration using a Mettler-Toledo DL39 titrator. The viscosity of the ILs was measured using an automatic Brookfield plate-cone viscometer, Model LVDV-II CP (Brookfield Engineering Laboratories, USA). The error on the viscosity measurements is expected to be < 5%. The density of the ionic liquid was measured using a 5 mL pycnometer. ESI-MS was performed on a Thermo Electron LCQ Advantage ion trap mass spectrometer connected to Agilent 1100 HPLC system coupled to Xcalibur data system. The pK_a of the acidic ionic liquid was measured with a Mettler-Toledo T90 titrator with LabX titration software. Extraction experiments were performed in a TMS-200 thermoshaker (Nemux Life). A Bruker S2 Picofox total reflection X-ray fluorescence (TXRF) spectrometer was used to determine the metal concentrations in both aqueous and organic (ionic liquid) phase. The lower limit of detection for Sc(III) is 2 ppm. Extraction mixtures were centrifuged using a Heraeus Labofuge 200. pH measurements were performed with an S220 SevenCompact™ pH/Ion meter (Mettler-Toledo) and a Slimtrode (Hamilton) electrode.

7.2.3 Synthesis

The synthesis of the ionic liquid $[P_{444}C_1COOH]Cl$ was partly based on literature procedures.[76,77] A solution of ethyl chloroacetate (50 mmol) in acetonitrile was purged with argon for 10 min. Tributylphosphine (50 mmol) was added dropwise and the mixture was refluxed for 24 h. The solvent was evaporated and a 15 vol% aqueous solution of HCl was added and the solution was refluxed for 5 h. Next, the solvent was evaporated again and the ionic liquid fully dried on a high vacuum line (50 °C). A light yellow viscous liquid was formed (14.38 g, 92%).

Tri-n-butyl(carboxymethyl)phosphonium chloride $[P_{444}C_1COOH]Cl$

^{1}H NMR (300 MHz, δ, $CDCl_3$): 9.57 (1H, s, COOH), 3.97 (2H, d, 13.0 Hz, CH_2), 2.37 (6H, m, 3 CH_2), 1.51 (12H, m, 6 CH_2), 0.95 (9H, t, 7.0 Hz, 3 CH_3). ^{13}C NMR (75 MHz, δ, $CDCl_3$): 165.89 (C=O), 27.77 (CH_2), 23.98 (CH_2), 23.52 (CH_2), 19.65 (CH_2), 19.01 (CH_2), 13.39 (CH_3). ^{31}P NMR (255 MHz, δ,

$CDCl_3$): 32.20. FTIR-ATR: (ν/cm^{-1}): 2960, 2933, 2873, 1713 (C=O), 1464, 1097, 909. CHN analysis: (calculated for $C_{14}H_{30}ClO_2P{\cdot}2H_2O$): C 50.36 % (50.30%), H 10.83% (10.30%), N 0% (0%). ESI-MS (MeOH): m/z 283.5 (100%) $[P_{444}C_1COO]Na^+$.

7.2.4 Measurement of phase diagram

The mutual coexistence curve for the $[P_{444}C_1COOH]Cl$/NaCl system was determined via the cloud point method at room temperature.[78] To an aqueous solution of the ionic liquid, the aqueous solution of NaCl was added until turbidity appeared. Then, pure Milli-Q water was added until this cloudiness disappeared again.

Since the ionic liquid $[P_{444}C_1COOH]Cl$ is completely miscible with water and can be salted out with NaCl, the experimental conditions for phase separation were investigated first. Starting from the pure ionic liquid (0.5 g), 0.5 g of aqueous phase was added, so the mass to mass ratio was always 1:1. The IL was contacted with a solution containing a certain weight percentage of NaCl. The total concentration of salt is always half of the initial weight percentage since the mass ratio of IL and aqueous phase is equal. As a first test, a 10 wt% solution of NaCl was added to the pure IL and shaken, after settling, it could be seen that the volumes of the phases were not equal; a lot of water had dissolved in the ionic liquid so that the volume of the ionic liquid phase was larger than that of the aqueous phase. So an overall NaCl concentration of 5 wt% was not enough for good phase separation. The addition of a 20 wt% NaCl solution to the IL resulted in the unwanted precipitation of NaCl; it was concluded that this overall concentration of 10 wt% NaCl in the aqueous biphasic system is too high. It was decided to use an average of 16 wt% solutions of NaCl as aqueous phases in all systems, and thus obtaining an overall concentration of 8 wt% NaCl.

7.2.5 Extraction experiments

Prior to the extraction, the ionic liquid was brought into contact with the 16 wt% NaCl solution in order to presaturate the ionic liquid and avoid changes in the phase volume. In a typical extraction experiment, 500 mg of this presaturated IL was mixed with 500 mg of aqueous feed solution also containing 16 wt% of NaCl. The metal concentration in the aqueous feed was 5 mmol kg^{-1}, unless otherwise stated. The extraction mixture was shaken in a thermoshaker at 2500 rpm at room temperature for 15 min, unless otherwise stated. A sample of 100 mg was taken from the aqueous phase to determine

the metal concentration in this phase with a TXRF spectrometer. A small amount (100 mg) of gallium (measurements of aqueous phases) or lanthanum (measurements of IL phases) ICP standard solution (1000 mg L^{-1}) was added to the sample as a reference for quantification. The sample was further diluted to 1 mL with Milli-Q water for aqueous samples, and with ethanol for the ionic-liquid-rich phase. The prepared sample solutions were homogenized by vortex mixing and a small droplet (5 µL) was dispensed on a quartz sample carrier. Finally, the carrier containing the sample was dried at 60 °C for 30 min. Prior to dispensing the sample droplet, the quartz carrier was pretreated with a SERVA® silicone solution in isopropanol (20 µL) in order to make the surface more hydrophobic and keep the sample droplet in the middle of the carrier. The extraction and stripping were evaluated by calculating the values for the distribution ratio, percentage extraction and percentage stripping respectively. The distribution ratios (*D)* were calculated by the following equation 7.1:

$$D = \frac{c_{org}}{c_{aq}} \qquad (7.1)$$

where c_{org} and c_{aq} are the metal concentration in the organic phase (*i.e.* ionic liquid phase, in mg/kg) and in the aqueous phase, respectively.

The percentage extraction (%*E*) of a metal is defined as:

$$\%E = \frac{\text{amount of extracted metal}}{\text{total amount of metal}} \times 100\% \qquad (7.2)$$

Or

$$\%E = \frac{c_{org} \cdot m_{org}}{c_{org} \cdot m_{org} + c_{aq} \cdot m_{aq}} \times 100\% \qquad (7.3)$$

where m_{org} and m_{aq} are the masses of the organic phase (*i.e*. ionic liquid phase, in mg/kg) and the aqueous phase, respectively.

7.2.6 Stripping experiments

After the extraction of scandium, the IL was regenerated by stripping with oxalic acid. For the stripping of the scandium, a larger extraction experiment was performed. Per stripping experiment, 500 mg of the loaded IL was taken and known amounts of oxalic acid were added to vary the molar ratios of oxalic acid over scandium.

The percentage stripping (%*S*) is defined as:

$$\%S = \frac{\text{amount of stripped metal}}{\text{total amount of extracted metal}} \times 100\% \qquad (7.4)$$

Or

$$\%S = \frac{c_{org,0} - c_{org,s}}{c_{org,0}} \times 100\% \qquad (7.5)$$

where $c_{org,0}$ is the metal concentration in the IL before stripping and $c_{org,s}$ is the metal concentration in the IL phase after the stripping process (both in mg/kg).

7.2.7 Quantitative ^{1}H NMR

The amount of IL that is lost into the salt-rich phase during the extraction was determined by quantitative ^{1}H NMR. A certain amount of phenol (10 mg) was added in approximately equimolar concentrations to an aliquot of water, saturated with the ionic liquid. Phenol was chosen as internal standard since there is no overlap with the ^{1}H NMR spectrum of the ionic liquid. The ^{1}H NMR spectrum of the water sample was recorded and the relative concentration versus phenol and the absolute concentration of $[P_{444}C_1COOH]Cl$ was calculated by integration of the peaks.

7.3 Results and Discussion

Synthesis and characterization of $[P_{444}C_1COOH]Cl$

The ionic liquid $[P_{444}C_1COOH]Cl$ was synthesized by reaction of tributyl phosphine with ethyl chloroacetate, followed by hydrolysis of the formed ester-functionalized ionic liquid by hydrochloric acid. The structure of the product was confirmed by ^{1}H and ^{13}C NMR, ATR-FTIR spectroscopy and CHN analysis. The IL is completely miscible with water and polar solvents such as ethanol in all volume ratios, yet totally immiscible with non-polar solvents such as toluene and heptane. The dried IL still contained 0.12 wt% of water, equivalent to 1159 ppm. This was used as the pure IL. The viscosity of this ionic liquid is very high, > 2×10^4 cP at room temperature. A high viscosity is typical for many functionalized ILs, since the presence of the functional group gives rise to extra intermolecular interactions (*e.g.* hydrogen bonds) in the ionic liquid. The viscosity of the IL-rich phase of the aqueous biphasic system was much lower (4×10^2 cP) at room temperature, which is beneficial for extractions (**Figure 7.2**). The pK_a of the carboxyl functional group is 2.32 in this ionic liquid. The density of the pure ionic liquid is 0.9648 g cm^{-3} at room temperature. After phase separation in water by the salting-out with NaCl, the IL-rich phase will be the upper phase. Even after presaturation, an amount of the IL still dissolves in the salt-rich water phase, this loss was determined by quantitative ^{1}H NMR to be 6 wt%.

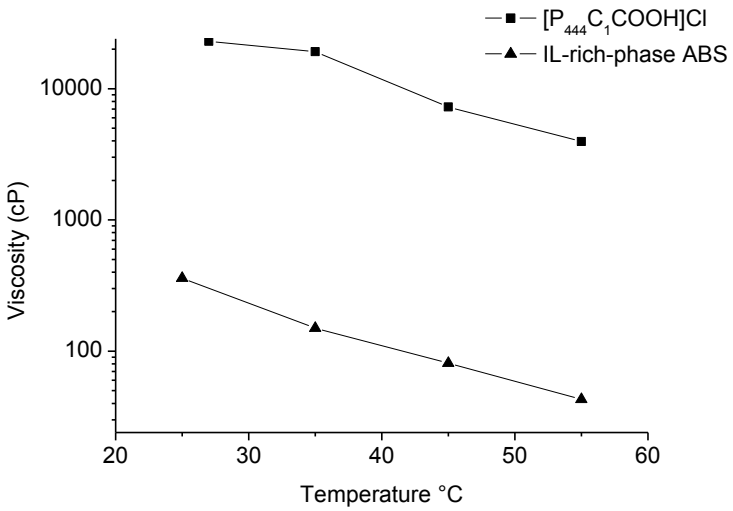

Figure 7.2 Temperature dependence of the viscosities of the pure ionic liquid $[P_{444}C_1COOH]Cl$ and the ionic liquid phase that was contacted with a 16 wt% NaCl solution in Milli-Q water.

Characterization of Aqueous Biphasic System

The mutual coexistence curve for the $[P_{444}C_1COOH]Cl$/NaCl system was determined via the cloud point method at room temperature.[78] Since it is virtually impossible to stir the very viscous pure ionic liquid, the ionic liquid was dissolved in a small amount of water to facilitate the stirring process. To this aqueous solution of 80 wt% ionic liquid, the 16 wt% aqueous solution of NaCl was added until turbidity appeared. Pure Milli-Q water was then added until this cloudiness disappeared again. This procedure was repeated several times until turbidity was no longer observed. The ternary phase diagram of the ABS composed of the IL, NaCl and water is given in **Figure 7.3**. In this orthogonal representation, the water fraction is omitted so that pure water becomes the origin of the axes. Although, in the literature the salts K_3PO_4 or K_2HPO_4 are the most often used,[51] in case of the rare earths, these salts cannot be used since insoluble rare-earth phosphates would be formed. NaCl was preferred as the salting-out agent in the aqueous biphasic system for three reasons: (1) it is an inexpensive and readily available salt with good salting-out behavior, (2) there is no possibility of mixing of anions between the ionic liquid and the salt, and (3) no anionic complexes with rare-earth ions are formed at medium chloride concentrations which avoids complication of the

extraction mechanism. In the extraction itself, not only pure NaCl, but also $ScCl_3$ is present in the system. Therefore, the influence of the addition of 5 mmol kg^{-1} of $ScCl_3$ salt to the ABS was investigated. The $ScCl_3$ solution has a pH of 3, so no hydrolysis of this solution occurs.[79] Taking the amount of scandium(III) chloride salt in the aqueous phase into account, there is definitely a shift to the left in the orthogonal phase diagram (**Figure 7.3**). This is obvious when looking at the salting-out effect: the higher charge density of Sc^{3+} in comparison to that of Na^+ causes a higher hydration energy for Sc^{3+}, since a higher charge density means more strongly hydrated cations. Water molecules form a hydration shell around the cations of the added salt and no longer around the ionic liquid cations, which favors the phase separation of the ionic liquid.

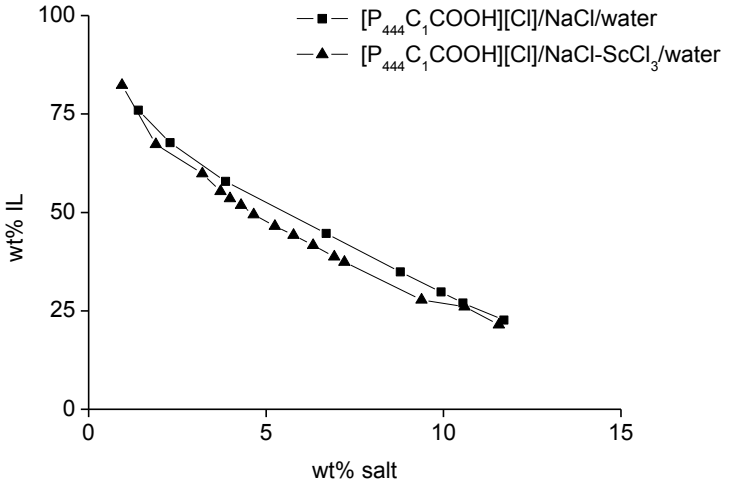

Figure 7.3 Ternary phase diagrams of ABS composed of $[P_{444}C_1COOH]Cl$/NaCl/water (■) and $[P_{444}C_1COOH]Cl$/NaCl-$ScCl_3$/water (▲) at 298 K (values given in units of wt%).

Extraction experiments

The aqueous biphasic system was used for the solvent extraction of scandium(III). Given the fact that carboxylic acids are extractants for metal ions in solvent extraction processes, and are known to be excellent extractants for scandium(III),[34] a carboxyl-functionalized ionic liquid was the ionic liquid of choice. In this way, the extracting group is covalently tethered to the cationic part in the ionic liquid. Prior to the extraction, the ionic liquid was brought into contact with the 16 wt% NaCl solution in order to presaturate the ionic liquid and minimize changes in the phase volume. In every extraction experiment, 500 mg of $[P_{444}C_1COOH]Cl$ (presaturated with 16 wt% NaCl) was mixed with 500 mg of aqueous feed solution (containing 16 wt% NaCl). The metal concentration in the aqueous feed was 5 mmol kg^{-1}, unless otherwise stated. The extraction mixture was shaken in a thermoshaker at 2500 rpm at room temperature for 15 min, unless otherwise stated. The two phases were allowed to settle, a process that was accelerated by centrifugation. A sample of 100 mg was taken from the aqueous phase to determine the metal concentration in this phase with a TXRF spectrometer. To express the efficiency of the extraction system, the distribution ratio (*D*) can be used (equation 7.1). Another possible way is to use the percentage extraction (%*E*), (equation 7.2).

First, the conditions necessary to obtain extraction equilibrium were determined. 0.5 g of $ScCl_3$ solution (5 mmol kg^{-1}) containing 16 wt% NaCl was contacted with 0.5 g of IL (presaturated with 16 wt% of NaCl). Even after 1 min of shaking, 90% of the scandium was already extracted, and 100% extraction was achieved after 10 min (**Figure 7.4**). To ensure full equilibrium was reached, 15 min of shaking at room temperature with a shaking speed of 2500 rpm was maintained for all extraction measurements. The fast kinetics of this extraction system is most likely due to the low viscosity of the water-saturated IL, even when loaded with metals.

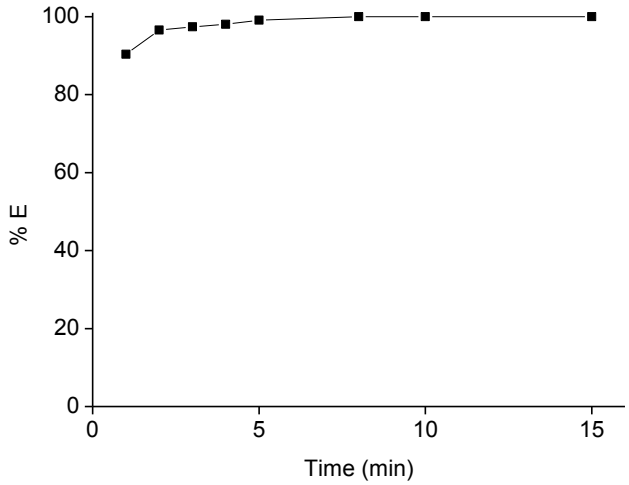

Figure 7.4 Percentage extraction as a function of time ($[P_{444}C_1COOH]Cl$ (presaturated with 16 wt% NaCl), scandium concentration: 5 mmol kg^{-1}, 16 wt% NaCl solution, pH_{eq}= -0.15, room temperature, 2500 rpm, single experiment).

The influence of the pH on the solubility of the IL cation in the water-rich phase was tested. The initial pH was varied from 3.33 to 0 in the aqueous feed solution containing 5 mmol kg^{-1} of Sc and 16 wt% of NaCl similar to that of a regular extraction feed. 500 mg of the presaturated IL was brought in contact with 500 mg of the aqueous layer. The mixtures were shaken for 15 min to ensure equilibrium after which the phases were allowed to settle by centrifuging. Billard and co-workers reported on quantitative NMR studies for the determination of the quantity of both IL cations and anions transferred in the upper phase of biphasic systems.[80] Here, the solubility of the IL cation in the water-rich phase was investigated via quantitative ^1H NMR. So far, little research has been performed on the effect of pH on ABS. Generally, an ABS is more easily formed under alkaline conditions than under acidic or neutral conditions.[51,81] When a citrate salt is used as a salting-out agent, it is observed that a decrease of the pH of the aqueous solution leads to an increase of the homogeneous area of the phase diagram.[82,83] Different surface charges and degree of protonation form the basis of the differences in the ABS formation. This is also visualized in **Figure 7.5**: at lower pH, there is a higher solubility of the ionic liquid cation in the water-rich phase.

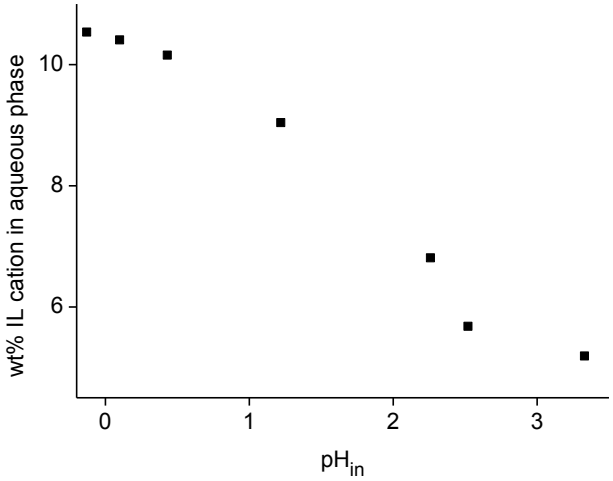

Figure 7.5 Solubility of the ionic liquid cation $[P_{444}C_1COOH]^+$ in the water-rich phase is higher with lower pH_{in}.

It should be remarked the pH of scandium(III) solution should always be kept below pH 4 to avoid hydrolysis of the scandium(III) ions, and prevent precipitation of $Sc(OH)_3$ (K_{sp} ~ 10^{-32}).[79] The solubility of IL cation into the water-rich phase was also determined for the presaturated solution (without $ScCl_3$), this amounted in 6 wt%, with an aqueous solution having a pH of 6.8. This is comparable to the solubility of IL cation contacted with a Sc(III) feed solution of pH 2.5, again showing the favorable salting-out effect of the Sc^{3+}.

In this study, the pH dependence is based on the acid-base equilibrium in the water-rich phase (equation 7.6).

$$[P_{444}C_1COOH]^+ \leftrightarrows P_{444}^+C_1COO^- + H^+ \qquad (7.6)$$

Via titration of the monoprotic acid cation, a complete fractional composition diagram was determined (**Figure 7.6**). It can be seen that for given pH values, there will be a different ratio zwitterion to protonated cation. The formation of the zwitterion is due to the acid donor character of the $[P_{444}C_1COOH]Cl$ with release of HCl, as also seen in betaine hydrochloride $[N_{111}C_1COOH]Cl$.[84]

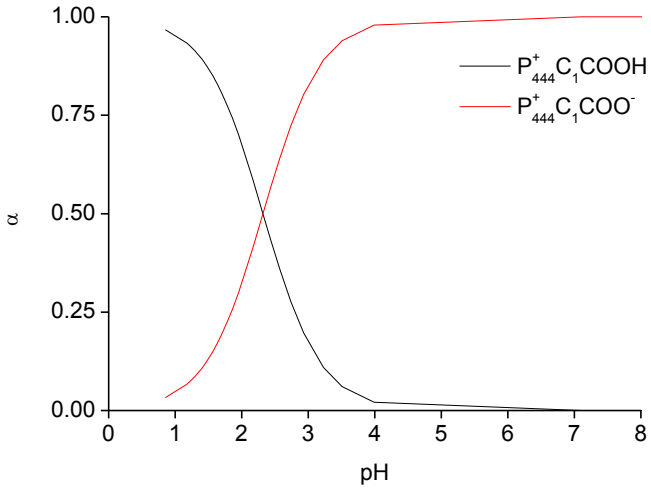

Figure 7.6 Fractional composition (α) diagram of monoprotic acid $P_{444}C_1COOH$ with pK_a= 2.32.

Additionally, quantitative ^{13}C NMR experiments show a steady increase in amount of zwitterions with higher pH (**Figure 7.7**). The zwitterionic form is more hydrophobic and thus a lower solubility is observed at higher pH values.

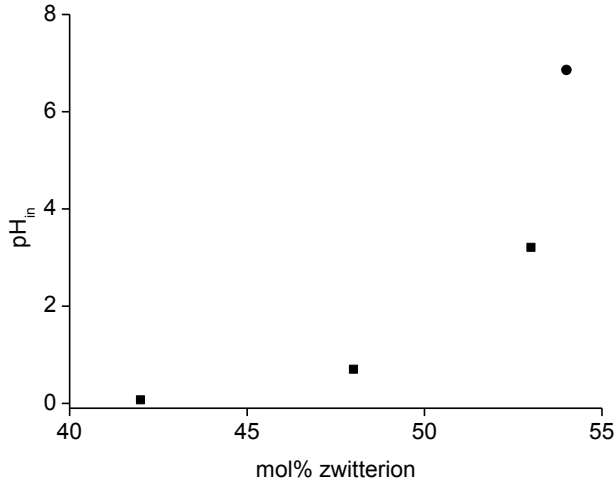

Figure 7.7 Amount of zwitterion (mol%) as a function of initial pH (pH_{in}). (■) IL-rich phase in contact with Sc feed solution of 5 mmol/kg and 16 wt% NaCl, and (●) IL-rich phase in contact with an aqueous solution of 16 wt% NaCl.

The influence of the initial metal feed concentration on the percentage extraction was also investigated. As expected, the percentage extraction lowers with increasing metal concentration, since the distribution of scandium is now influenced by the loading effect. To ensure full equilibrium with the higher metal concentrations, 30 min was taken as shaking time. Until an initial scandium(III) loading of ~ 10 mmol kg^{-1}, 100% extraction efficiency is found. Then, a sharp decrease in extraction efficiency is seen, reaching only 60% extraction for an initial feed of 130 mmol kg^{-1}. For higher initial feed concentrations, the slope of the decrease is lower. At ~ 1.4 mol kg^{-1}, only 30% extraction is reached (**Figure 7.8**). Note that the pH_{eq} is fairly low at -0.3, caused by the protons that are set free during the extraction.

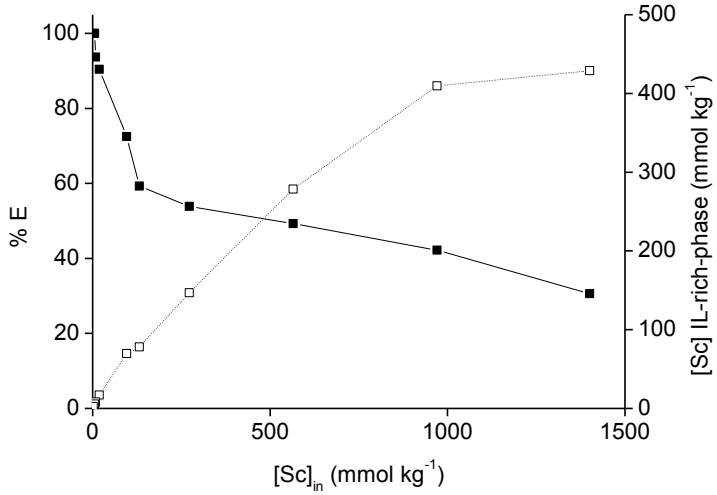

Figure 7.8 Loading of the IL-rich-phase: percentage extraction (■) and scandium concentration (□) in the IL-rich phase after extraction as a function of the initial scandium concentration. ($[P_{444}C_1COOH]Cl$ (presaturated with 16 wt% NaCl), pH_{eq} = - 0.3, 16 wt% NaCl feed solution with varying scandium concentration, room temperature, 2500 rpm, 30 min, single experiment).

The low extraction efficiencies at high initial feed stocks together with the high solubility of the ionic liquid cation in the water layer at these low pH values made further increases in the loading in the IL-rich phase not economical. Yet, another technique to load the IL was performed, the cumulative loading. In this experiment, the ionic liquid is repeatedly brought into contact with a novel Sc(III) feed. The IL-rich phase (500 mg) was contacted with 500 mg of a Sc(III) feed of 0.80 mol kg^{-1} (also containing 16 wt% NaCl). After the first extraction, 0.42 mol kg^{-1} scandium was taken up

in the IL. The IL-rich phase was isolated and after two repeated contacts with the Sc(III) feed, the IL was loaded with 0.95 mol kg^{-1} Sc(III). ATR-FTIR spectra of the IL-rich phase of the extraction, loaded with increasing amounts of scandium (0-0.95 mol kg^{-1}) showed that the scandium ion is coordinated to the ionic liquid via the carboxylic acid function on the cation (**Figure 7.9**). Taking in account the deprotonation of the carboxylic group in $[P_{444}C_1COOH]Cl$ and its affinity to Sc^{3+}, a complex of the form $[(P_{444}C_1COO)_nSc]^{3+}$ must take part in the extraction. The maximum loading was confirmed by ATR-FTIR and is consistent with a ligand-to-metal ratio of 3:1, proposing that the extraction mechanism is occurring via a complex with three IL-zwitterionic molecules.

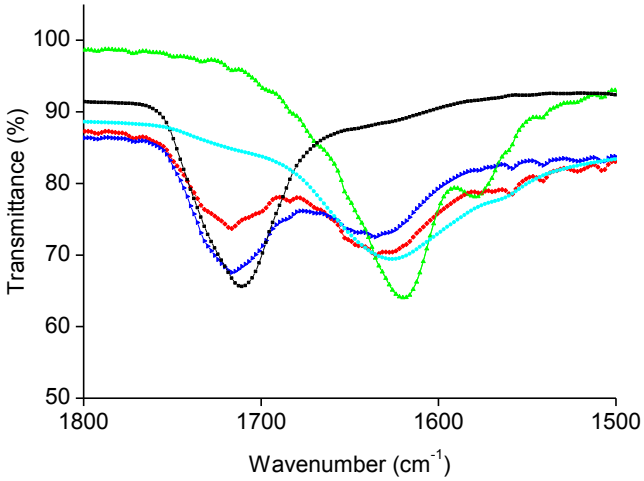

Figure 7.9 ATR-FTIR spectra of the carboxyl peak of $[P_{444}C_1COOH]Cl$. (black symbols: dry IL, blue symbols: IL-rich phase ABS, red symbols: IL-rich phase ABS loaded with Sc (0.2 mol kg^{-1}), light blue symbols: IL-rich phase ABS maximum loading of Sc (0.95 mol kg^{-1}), green symbols: $P^+_{444}C_1COO^-$ zwitterion.

For the carboxyl functionalized ionic liquid $[Hbet][Tf_2N]$, the extraction mechanism has been thoroughly investigated.[85] It has been shown that scandium(III) was extracted as a complex with the zwitterionic betaine in a 1:3 stoichiometry, with three bistriflimide counterions. Proton exchange occurs upon extraction of scandium(III), and three protons are transferred to the aqueous phase. Since (1) the $[P_{444}C_1COOH]Cl$ ionic liquid has a structure similar to that of the ionic liquid $[Hbet][Tf_2N]$ and (2) from the maximum loading, the ligand-to-metal ratio of 3:1 was also confirmed, the suggested

expression for the extraction mechanism of this system is given as equation 7.7:

$$3\,\overline{[P_{444}C_1COOH]Cl} + Sc^{3+} \leftrightarrows \overline{(P_{444}C_1COO)_3ScCl_3} + 3\,H^+ \qquad (7.7)$$

In **Figure 7.10**, ^{45}Sc NMR spectra show a clear difference in peak position for an aqueous $ScCl_3$ complex and the complex formed in the IL-rich phase.

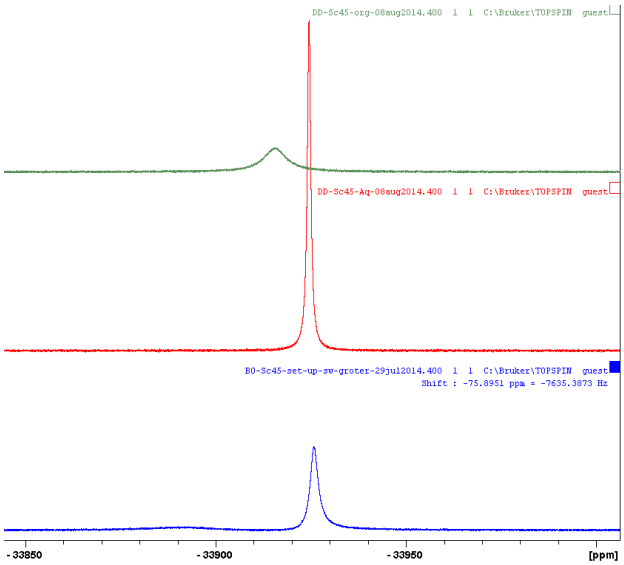

Figure 7.10 ^{45}Sc NMR spectra, green line: Sc complex in the IL-rich phase, red line: $ScCl_3$ in the aqueous phase of the extraction, blue line: reference $ScCl_3$ hydrate in the aqueous phase.

Stripping experiments

After the extraction, it is important to remove the metal ions from the IL-rich phase. This is done during the stripping process, which is usually achieved by the addition of an acid to the IL-rich phase. However, the system is already working at very low pH values and the addition of HCl to the system is troublesome since it induces phase changes. Therefore, a more appropriate technique for removing the metals from the IL is precipitation stripping. This can be easily done via the addition of solid oxalic acid to the IL-rich phase. For the stripping of scandium, a larger extraction experiment was performed. First, the IL-rich phase was loaded with 65 mmol kg^{-1} of scandium. The effect of the molar ratios of oxalic acid over scandium of the same loaded ionic

liquid was then investigated. The stripping efficiency is expressed by the percentage stripping (%*S*) (recall equations 7.4 and 7.5). The stripping efficiency in function of the oxalic acid/scandium molar ratio in the IL-rich phase is given in **Figure 7.11**. In first instance, oxalic acid was added to the scandium-loaded IL-rich phase and the mixture was shaken at 70 °C for 30 min for kinetic reasons. The expected 100% stripping at a molar ratio of 1.5 is not observed. Most likely, this is caused by the presence of HCl in the IL-rich phase after the extraction. In this way, oxalate is present in the protonated form so the precipitation equilibrium is pushed to the left (equation 7.8). With the addition of a 16 wt% NaCl solution, HCl gets isolated from the IL-rich phase and full stripping is obtained. The molar ratios of oxalic acid over scandium *n*(oxalic acid)/*n*(Sc) is 1.5 when a stripping efficiency of 100% is reached (**Figure 7.11**), thus three oxalic acid molecules surround two scandium(III) metal centers (equation 7.8). The big advantage of precipitation stripping is that the scandium(III) oxalate precipitate can be converted to scandium(III) oxide by calcination (equation 7.9). After a calcination step at 950 °C for 2 h, Sc_2O_3 with a purity of 99.45% was obtained. Also, the fact that the IL can be recycled is a major benefit for the system. An extraction efficiency >95% was reached with the recycled IL.

$$2\ \overline{(P_{444}C_1COO)_3ScCl_3} + 3\ H_2C_2O_{4\,(s)} \leftrightarrows Sc_2(C_2O_4)_{3\,(s)} + 6\ \overline{[P_{444}C_1COOH]Cl} \quad (7.8)$$

$$Sc_2(C_2O_4)_{3\,(s)} + \frac{3}{2}O_{2\,(g)} \rightarrow Sc_2O_{3\,(s)} + 6\ CO_{2(g)} \quad (7.9)$$

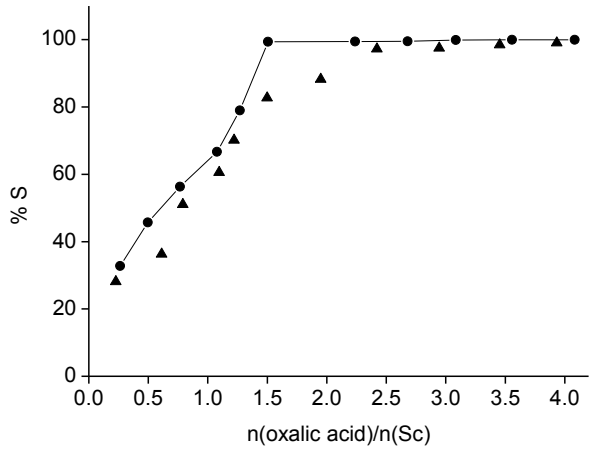

Figure 7.11 Precipitation stripping of the IL-rich phase, percentage stripping as a function of the molar ratio of oxalic acid to Sc(III): (▲) pure IL-rich phase, 70 °C, 30 min, and (●) 16 wt% NaCl solution added to isolate HCl, 30 °C, 1 h. (IL-rich phase loaded with 65 mmol kg^{-1} Sc, 16 wt% NaCl solution, 2500 rpm, single experiment).

7.4 Conclusions

The use of a non-fluorinated, functionalized ionic liquid in an aqueous biphasic system for the extraction of metal ions is shown. With the $[P_{444}C_1COOH]Cl$/16 wt% NaCl/water system, an environmentally friendly solvent extraction process for the extraction of scandium(III) was investigated in detail. The viscosity of the carboxyl-functionalized IL was drastically lowered by contacting it with the 16 wt% NaCl solution. The ternary phase diagram for the system was constructed to determine the suitable working conditions. Fast kinetics, the possibility to extract from fairly low pH and a reasonable metal loading are advantageous in this system. A plausible extraction mechanism is proposed where three ionic liquid cations are involved in the extraction of scandium. The metal ions can be stripped from the IL-rich phase via the addition of oxalic acid and 16 wt% NaCl solution, regenerating the IL that can be used again in an efficient extraction cycle.

This research was financially supported by the FWO-Flanders (Research Project G.0900.13), IWT-Flanders (PhD fellowship to DD), and KU Leuven (Research Projects GOA 13/008 and IOF-KP RARE3). The authors also wish to thank Karel Duerinckx for NMR measurements, Dirk Henot for performing CHN analyses. Bieke Onghena and Tom Vander Hoogerstraete are thanked for useful scientific discussions.

7.5 References

1 P. Wasserscheid.; T. Welton; *ILs in Synthesis;* Wiley-VCH: Weinheim, 2008.

2 N. V. Plechkova, K. R. Seddon, *Chem. Soc. Rev.,* 2008**, 37**, 123.

3 T. Welton, *Chem. Rev.,* 1999**, 99**, 2071.

4 H. Davis, *Chem. Lettt.,* 2004**, 33**, 1072.

5 J. S. Preston, *Hydrometallurgy,* 1985**, 14**, 171.

6 D. S. Flett, D. R. Spink, *Hydrometallurgy,* 1976**, 1**, 207.

7 P. Nockemann, B. Thijs, T. N. Parac-Vogt, K. Van Hecke, L. Van Meervelt, B. Tinant, I. Hartenbach, T. Schleid, V. T. Ngan, M. T. Nguyen, K. Binnemans, *Inorg. Chem.,* 2008**, 47**, 9987.

8 I. A. Shkrob, T. W. Marin, M. P. Jensen, *Ind. Eng. Chem. Res.,* 2014**, 53**, 3641.

9 C. Chiappe, C. S. Pomelli, *Eur. J. Org. Chem.,* 2014**, 2014**, 6120.

10 P. Nockemann, B. Thijs, S. Pittois, J. Thoen, C. Glorieux, K. Van Hecke, L. Van Meervelt, B. Kirchner, K. Binnemans, *J. Phys. Chem. B,* 2006**, 110**, 20978.

11 K. Sasaki, K. Takao, T. Suzuki, T. Mori, T. Arai, Y. Ikeda, *Dalton Trans.,* 2014**, 43**, 5648.

12 R. P. Swatloski, J. D. Holbrey, R. D. Rogers, *Green Chem.,* 2003**, 5**, 361.

13 H. F. Aly, M. El-Garhy, S. El-Reefy, *Microchem. J.,* 1972**, 17**, 431.

14 B. Wassink, D. Dreisinger, J. Howard, *Hydrometallurgy,* 2000**, 57**, 235.

15 T. Sato, T. Shimomura, S. Murakami, T. Maeda, T. Nakamura, *Hydrometallurgy,* 1984**, 12**, 245.

16 F. d. M. Fabrega, M. B. Mansur, *Hydrometallurgy,* 2007**, 87**, 83.

17 K. Campos, T. Vincent, P. Bunio, A. Trochimczuk, E. Guibal, *Solvent Extr. Ion Exc.,* 2008**, 26**, 570.

18 K. Campos, R. Domingo, T. Vincent, M. Ruiz, A. M. Sastre, E. Guibal, *Water Research,* 2008**, 42**, 4019.

19 V. Gallardo, R. Navarro, I. Saucedo, M. Avila, E. Guibal, *Separ. Sci. Technol.,* 2008**, 43**, 2434.

20 M. Regel-Rosocka, *Sep. Purif. Technol.,* 2009**, 66**, 19.

21 A. Cieszynska, M. Wisniewski, *Sep. Purif. Technol.,* 2010**, 73**, 202.

22 D. Kogelnig, A. Stojanovic, F. Jirsa, W. Körner, R. Krachler, B. K. Keppler, *Sep. Purif. Technol.,* 2010**, 72**, 56.

23 R. K. Mishra, P. C. Rout, K. Sarangi, K. C. Nathsarma, *Hydrometallurgy,* 2011**, 108**, 93.

24 A. Comesana, J. Rodriguez-Monsalve, A. Cerpa, F. J. Alguacil, *Chem. Eng. J.,* 2011**, 175**, 228.

25 M. Regel-Rosocka, M. Wisniewski, *Hydrometallurgy,* 2011**, 110**, 85.

26 A. Cieszynska, M. Wisniewski, *Sep. Purif. Technol.,* 2011**, 80**, 385.

27 M. Regel-Rosocka, L. Nowak, M. Wisniewski, *Sep. Purif. Technol.,* 2012**, 97**, 158.

28 T. Vander Hoogerstraete, S. Wellens, K. Verachtert, K. Binnemans, *Green Chem.,* 2013**, 15**, 919.

29 S. Wellens, R. Goovaerts, C. Moller, J. Luyten, B. Thijs, K. Binnemans, *Green Chem.,* 2013**, 15**, 3160.

30 T. Sato, M. Yamamoto, K. Sato, *Solvent Extr. Res. Dev. Jpn.*, 2005**, 12**, 101.
31 T. Sato, M. Yamamoto, K. Adachi, *J. Min. Mat. Process. Inst. Jpn.*, 2005**, 121**, 603.
32 T. Sato, M. Yamamoto, *Bull. Chem. Soc. Jpn.*, 1982**, 55**, 90.
33 S. Wellens, B. Thijs, K. Binnemans, *Green Chem.*, 2012**, 14**, 1657.
34 T. Vander Hoogerstraete, B. Onghena, K. Binnemans, *J. Phys. Chem. Lett.*, 2013**, 4**, 1659.
35 T. Vander Hoogerstraete, B. Onghena, K. Binnemans, *Int. J. Mol. Sci.*, 2013**, 14**, 21353.
36 B. Onghena, J. Jacobs, L. Van Meervelt, K. Binnemans, *Dalton Trans.*, 2014**, 43**, 11566.
37 Hoogenboom, R., Temperature-Responsive Polymers: Properties, Synthesis and Applications, in *Smart Polymers and Their Applications*; Aguilar, M. a. R., Romaín, J. S., Eds.; Woodhead Publishing, Cambridge, U.K., 2014.
38 Albertsson, P. A.; *Partitioning of Cell Particles and Macromolecules;* Wiley: New York, 1986.
39 Zaslavsky, B. Y.; *Aqueous Two-Phase Partitioning;* Marcel Dekkers, Inc.: New York, 1994.
40 H. Watanabe, H. Tanaka, *Talanta*, 1978**, 25**, 585.
41 S. Igarashi, T. Yotsuyanagi, *Mikrochim. Acta*, 1992**, 106**, 37.
42 R. D. Rogers and M. A. Eiteman; *Aqueous Biphasic Separations: Biomolecules to Metal Ions;* Plenum Press: New York, 1995.
43 R. D. Rogers, A. H. Bond, C. B. Bauer, J. Zhang, S. T. Griffin, *J. Chromatogr., Biomed. Appl.*, 1996**, 680**, 221.
44 S. Lahiri, K. Roy, *J Radioanal Nucl Chem*, 2009**, 281**, 531.
45 M. d. C. H. Silva, L. H. M. Silva, F. J. Paggioli, J. S. R. Coimbra, L. A. Minim, *Quimica Nova*, 2006**, 29**, 1332.
46 R. D. Rogers, A. H. Bond, C. B. Bauer, *Sep. Sci. Technol.*, 1993**, 28**, 1091.
47 K. E. Gutowski, G. A. Broker, H. D. Willauer, J. G. Huddleston, R. P. Swatloski, J. D. Holbrey, R. D. Rogers, *J. Am. Chem. Soc.*, 2003**, 125**, 6632.
48 M. H. Abraham, A. M. Zissimos, J. G. Huddleston, H. D. Willauer, R. D. Rogers, W. E. Acree, *Ind. Eng. Chem. Res.*, 2003**, 42**, 413.
49 K. A. Kurnia, M. G. Freire, J. A. P. Coutinho, *J. Phys. Chem. B*, 2013**, 118**, 297.
50 N. J. Bridges, K. E. Gutowski, R. D. Rogers, *Green Chem.*, 2007**, 9**, 177.
51 M. G. Freire, A. F. Claudio, J. M. M. Araujo, J. A. P. Coutinho, I. M. Marrucho, J. N. C. Lopes, L. P. Rebelo, *Chem. Soc. Rev.*, 2012**, 41**, 4966.
52 Y. Pei, J. Wang, L. Liu, K. Wu, Y. Zhao, *J. Chem. Eng. Data*, 2007**, 52**, 2026.
53 Z. Li, Y. Pei, H. Wang, J. Fan, J. Wang, *TrAC Trends in Anal. Chem.*, 2010**, 29**, 1336.
54 J. F. B. Pereira, L. P. Rebelo, R. D. Rogers, J. A. P. Coutinho, M. G. Freire, *Phys. Chem. Chem. Phys.*, 2013**, 15**, 19580.
55 J. F. B. Pereira, K. A. Kurnia, O. A. Cojocaru, G. Gurau, L. P. Rebelo, R. D. Rogers, M. G. Freire, J. A. P. Coutinho, *Phys. Chem. Chem. Phys.*, 2014**, 16**, 5723.

56 L. I. N. Tome, J. F. B. Pereira, R. D. Rogers, M. G. Freire, J. R. B. Gomes, J. A. P. Coutinho, *Phys. Chem. Chem. Phys.*, 2014**, 16**, 2271.
57 H. Rodriguez, M. Francisco, M. Rahman, N. Sun, R. D. Rogers, *Phys. Chem. Chem. Phys.*, 2009**, 11**, 10916.
58 C. Louros, A. Cláudio, C. Neves, M. Freire, I. Marrucho, J. Pauly, J. Coutinho, *Int. J. Mol. Sci.*, 2010**, 11**, 1777.
59 F. J. Deive, A. Rodriguez, A. B. Pereiro, J. M. M. Araujo, M. A. Longo, M. A. Z. Coelho, J. N. C. Lopes, J. M. S. S. Esperanca, L. P. N. Rebelo, I. M. Marrucho, *Green Chem.*, 2011**, 13**, 390.
60 S. Dreyer, U. Kragl, *Biotechnol. Bioeng.*, 2008**, 99**, 1416.
61 Y. Akama, M. Ito, S. Tanaka, *Talanta*, 2000**, 53**, 645.
62 Y. Akama, A. Sali, *Talanta*, 2002**, 57**, 681.
63 J. Royset, N. Ryum, *Int. Mater. Rev.*, 20005**, 50**, 19.
64 S.P.S. Badwal, F. T. Ciacchi, D. Milosevic, *Solid State Ionics*, 2000**, 136**, 91.
65 S. Kobayashi, *Eur. J. Org. Chem.*, 1999**,** 15.
66 W. Wang, Y. Pranolo, C. Y. Cheng, *Hydrometallurgy*, 2011**, 108**, 100.
67 W. Wang, C. Y. Cheng, *J. Chem. Technol. Biotechnol.*, 2011**, 86**, 1237.
68 Z. Zhao, Y. Baba, F. Kubota, N. Kamiya, M. Goto, *J. Chem. Eng. Jpn.*, 2014**, 47**, 656.
69 Q. Bo, J. Lu, D. Li, X. Zhang, W. Ye, *Chinese J. Anal. Chem.*, 2001**, 28**, 45.
70 B. Gorski, N. Gorski, M. Beer, *Solvent Extr. Ion Exc.*, 1991**, 9**, 623.
71 M. Karve, B. Vaidya, *Separ. Sci. Technol.*, 2008**, 43**, 1111.
72 D. Li, C. Wang, *Hydrometallurgy*, 1998**, 48**, 301.
73 D. F. Peppard, G. W. Mason, J. L. Maier, *J. Inorg. Nucl. Chem.*, 1956**, 3**, 215.
74 X. Sun, D. Wu, J. Chen, D. Li, *J. Chem. Technol. Biotechnol.*, 2007**, 82**, 267.
75 X. Sun, Y. Ji, L. Guo, J. Chen, D. Li, *Sep. Purif. Technol.*, 2011**, 81**, 25.
76 Y. Chevalier, P. Le Perchec, *J. Phys. Chem.*, 1990**, 94**, 1768.
77 K. Koumoto, H. Ochiai, N. Sugimoto, *Tetrahedron*, 2008**, 64**, 168.
78 H. D. Willauer, J. G. Huddleston, R. D. Rogers, *Ind. Eng. Chem. Res.*, 2002**, 41**, 2591.
79 D. R. Lide; *CRC Handbook of Chemistry and Physics. 85th Ed.;* CRC Press: Boca Raton, FL, 2005.
80 M. Atanassova, V. Mazan, I. Billard, *ChemPhysChem*, 2015**, 16**, 1703.
81 T. Mourao, A. F. Claudio, I. Boal-Palheiros, M. G. Freire, J. A. P. Coutinho, *J. Chem. Thermodyn.*, 2012**, 54**, 398.
82 M. T. Zafarani-Moattar, S. Hamzehzadeh, *Fluid Phase Equilib.*, 2011**, 304**, 110.
83 T. E. Sintra, R. Cruz, S. n. P. M. Ventura, J. A. P. Coutinho, *J. Chem. Thermodyn.*, 2014**, 77**, 206.
84 R.Vivilecchia, B. Ross, Stabilized pharmaceutical compositions comprising acid donors, US Patent 6,790,861, **2004**.
85 B. Onghena, K. Binnemans, *Ind. Eng. Chem. Res.*, 2015**, 54**, 1887.

CHAPTER 8

CONCLUSIONS AND OUTLOOK

Ionic liquids are solvents that consist entirely of ions. They have special properties such as a negligible vapor pressure and a low flammability. Ionic liquids can be divided into hydrophilic ionic liquids, which are totally miscible with water, and hydrophobic ionic liquids, which are immiscible with water. However, this classification is ambiguous since ionic liquids can also show a temperature-dependent miscibility with water. Some IL/solvent mixtures have an upper critical solution temperature (UCST). They form one homogeneous phase above the UCST and phase separate below this temperature. Other IL/solvent mixtures have a lower critical solution temperature (LCST). They form one homogeneous phase below the LCST and phase separate above this temperature. In this PhD thesis, solvent extraction systems for the separation of metal ions, based on non-fluorinated ionic liquids with this so-called thermomorphic behavior were developed. Intense stirring can be avoided during extraction by the formation of a homogeneous phase. In the homogeneous phase, a fast reaction between the metal ion and the extraction agent can take place. Upon cooling, phase separation occurs with transfer of the metal complex to the IL phase. This separation process is termed as a homogeneous liquid-liquid extraction (HLLE).

In the first part of this PhD thesis, it was shown that the direct synthesis of highly substituted imidazolium ionic liquids (*i.e.* with more than two substituents) was not feasible using enolizable starting materials. A versatile, halogen-free synthesis procedure for 1,3-dialkylimidazolium ionic liquids was developed to obtain a series of acetate ionic liquids which can be transformed into other ionic liquids by anion-exchange reactions. The full characterization of the ILs allowed us to detect some trends in their properties. The water content in the ionic liquid drops with increasing alkyl chain length on the imidazolium cation as a result of the decreasing hydrophilicity of the cations. Longer alkyl substituents, a higher degree of branching on the imidazolium cation, and a higher coordination between cation and anion increases the viscosity of the ionic liquid. One of the synthesized ILs, 1,3-

dihexylimidazolium nitrate ([HHIM][NO_3]) shows UCST phase behavior with water as it is immiscible with water at room temperature, yet becomes fully miscible in all compositions with heating to 90 °C. The addition of salts to the ionic liquid/water system led to the disappearance of the temperature-dependent miscibility, a fully hydrophobic system was formed at all temperatures. Therefore, the short-chain ionic liquid was tested in conventional metal extraction. [HHIM][NO_3] contains a relatively small cation, and the IL/water system remains biphasic even with a non-fluorinated imidazolium ionic liquid. The preferential extraction of rare earths over 3d-transition metals was observed. This was exploited in the separation of Sm(III)/Co(II) and La(III)/Ni(II) pairs.

Next, ionic liquids having LCST phase behavior were discussed. The introduction of bis(2-ethylhexyl)phosphate or docusate as anion in oligo(ethylene) functionalized phosphonium ionic liquids both give ILs that preferentially mix with water at low temperatures and phase separate with heating. The cloud point temperature is tunable by making modifications in the structure of the ionic liquid. For the [DEHP]-ionic liquids, longer oligo(ethylene) chains induce higher cloud points. Also the addition of metal chloride salts has an effect, as it significantly lowers the cloud point temperature. The [$P_{444}E_3$][DEHP]/water system is the first example in the literature for the homogeneous liquid-liquid extraction of metal ions with an LCST thermomorphic system. Divalent metal ions were extracted efficiently towards these types of ionic liquids. The docusate ionic liquids, non-functionalized tetrabutylphosphonium or phosphonium cations functionalized with either an ester, carboxylic acid or oligo(ethylene) group were tested first in conventional solvent extraction. In general, trivalent rare-earth ions were found to be extracted better than the divalent transition metals. The homogeneous liquid-liquid extraction with the [$P_{444}E_3$][DOSS]/water system was studied in detail. The most plausible extraction mechanism describes the extraction of the La(III) metal ion with four ionic liquid anions and one ionic liquid cation, transferring three ionic liquid cations to the aqueous phase in order to obtain charge neutrality. The ionic liquid can be regained and recycled after precipitation stripping of the metal ion. HLLE on La/Ni and Sm/Co pairs with the [$P_{444}E_3$][DOSS]/water extraction system was executed, as these are relevant separations for the recycling of end-of-life batteries or permanent magnets. The separation could

not be achieved by selective extraction, an additional scrubbing step was necessary, in which EDTA performed the best.

The last topic of the PhD thesis is about ionic-liquid based aqueous biphasic systems. Here, the miscibility of the ionic liquid was controlled by the salting-out agent. For instance, $[P_{444}C_1COOH]Cl$ is completely miscible with water, but a biphasic system is formed after the addition of 16 wt% NaCl. This way, the system can be applied as an environmentally friendly solvent extraction process for the extraction of scandium(III). A drastic decrease of the viscosity of the carboxyl-functionalized IL by the creation of the IL-ABS, fast kinetics, the possibility to extract from fairly low pH and a reasonable metal loading are all advantages of this system. Three ionic liquid cations are involved in the extraction process of scandium. Afterwards, the metal ions can be stripped from the IL-rich phase by addition of oxalic acid and 16 wt% NaCl solution, regenerating the IL so that can be used again in an efficient extraction cycle.

Outlook

The key factor to prepare ionic liquids with temperature-dependent miscibility is a perfect balance between hydrophilicity and hydrophobicity. However, it has not been clearly specified how to achieve this balance. Recently, several thermomophic binary mixtures have been listed in literature reviews. Additionally, in the IUPAC Ionic Liquids Database, ILThermo, users can access a data collection containing experimental investigations of thermodynamic, and transport properties of ionic liquids as well as binary and ternary mixtures containing ionic liquids.[i] In Chapter 1, a predictive model for the phase behavior of ILs based on the charge density (hydration) of the IL anion was introduced. UCST phase behavior is found most often with IL/water biphasic systems where the IL has a poorly hydrated anion, whilst the incorporation of a more strongly hydrated anion will give the system LCST phase behavior. However, to date, finding a thermomorphic ionic liquid is still trial-and-error work. The data given in reviews and databases together with the current movement towards open access data will help to gain instructive insights on a better prediction of ionic liquid systems. Additionally, computational software scanning the growing set of known ionic liquids, or calculations based on thermodynamic models (*e.g.* UNIQUAC or COSMO-RS) should be used to find suitable candidates for the specific property of thermomorphic behavior.

All the aforementioned tools can also provide assistance for developing future implementations of ionic liquids in industrial applications. Specifically for hydrometallurgical processes, the use of ionic liquids would ensure a greener, environmentally friendlier and safer alternative for the VOCs currently used. Companies select their extraction process in order to reach targeted objectives of purity, yield, environment, safety and economy. The current high cost of ionic liquids is the major drawback of the technology. However, with growing demands in tons quantities, their prices will drop significantly. In addition, the price-performance ratio is of higher importance than the initial cost. If the ionic liquid outperforms the solvent it wants to replace, less ionic liquid will be required to fulfill a specific task so that the cost is overcome. Also, minimal losses and recycling of ionic liquid after extraction ensure the sustainability and green character of the extraction process. It is possible to minimize the solubility of the ionic liquid by the addition of salts, however, minor losses of especially thermomorphic ionic liquids into the aqueous phase are still an issue. Techniques that can be employed for regeneration and recovery of ILs like vacuum distillation, crystallization, liquid–liquid extraction, *etc.* are not affordable for removing ILs at low concentrations from large waste water streams.[ii] Therefore, the research of nondestructive treatments for removing ILs from wastewater is ongoing. Recent studies focus on the recovery of ionic liquids from the aqueous phase by adsorption with different adsorbents like activated carbon or silica,[iii] or via membrane filtration where a membrane can be selected to retain the ionic liquid.[iv] Other membrane based processes such as pervaporation, reverse osmosis and electrodialysis are promising technologies for the recovery of ILs, however, the practical feasibility of these methods at large scale still needs to be proved.[v]

The right engineering development of process technologies may enable the application of thermomorphic ILs on pilot and industrial scale. A smart design for a possible set-up for homogeneous liquid-liquid extraction was already introduced in Chapter 1. To the best of our knowledge, thermomorphic ILs have not been applied in industry yet. However, with this process, better mass transfer and a higher stage efficiency at a given throughput can be achieved. The combination of this efficient separation battery together with more environmentally friendly ionic liquids for the separation of critical metals from end-of-life products would completely close the materials cycle.

[i]IUPAC Ionic Liquids Database, ILThermo http://ilthermo.boulder.nist.gov

[ii]J.F. Fernandez, J. Neumann, J. Thoeming, *Curr. Org. Chem.*, 2011, **15**, 1992.

[iii]J. Lemus, J. Palomar, F. Heras, M. Gilarranz, J. Rodriguez, *Sep. Purif. Techn.*, 2012, **97**,11.

[iv] S. Judd, B. Jefferson, *Membranes for Industrial Wastewater Recovery and Re-use*, Elsevier Science Ltd: Oxford (UK), **2003**.

[v] N. Mai, K. Ahn, Y. Koo, *Process Biochem*., 2014, **49**, 872.

HEALTH, SAFETY & ENVIRONMENT

All experiments were performed conform the Code of Practice for Safety in the Lab[i] and the Introduction Safety Guidelines of the Department of Chemistry.[ii] The documentation of all risks involving the experiments in the risk assessments always preceded any activity in the lab. Each experiment was recorded in the lab book and a reference was made to the applicable risk assessment.[iii] For personal protection and precaution, gloves, lab coat and goggles were always worn while performing the experiments. At all times, the chemical waste was collected in the designated waste canister. For unsupervised experiments, all necessary information concerning the activity was clearly displayed on the entrance door of the lab and the correct forms with the necessary information were submitted to the Central Dispatch and HSE department.[iv]

The chemicals used in this PhD research did not pose unusual safety risks. Minimal exposure to toxic metal salts, corrosive chemicals (acids/bases) or hazardous organic compounds was ensured. Diethyl ether needed for the purification of the dialkylimidazolium ionic liquids is listed as E4+, as it is highly flammable and may form explosive peroxides. Experiments with phosphines had to be carried out in a nitrogen flushed, closed system in order to minimize the formation of phosphine oxides. Particular care was taken during the handling of solvents, like toluene, methanol or pyridine as they are harmful and irritating.

Safety training courses followed:

- Introductory safety course (start of PhD, 2013)
- Radiation protection: October 15, 2013
- Safety in the lab: November 6, 2013

[i] http://chem.kuleuven.be/en/hse/procedures/liab1.htm
[ii] http://chem.kuleuven.be/veiligheid/documenten/safety-brochure.pdf
[iii] https://www.groupware.kuleuven.be/sites/depchemrisico/Risk%20Assessments/Forms/Per%20division.aspx
[iv] https://admin.kuleuven.be/sab/vgm/kuleuven/EN/riskactivities/ue/continuous-activities

LIST OF PUBLICATIONS

Raiguel S., **Depuydt D.**, Vander Hoogerstraete T., Thomas J., Dehaen W., Binnemans K. (2017). Selective alkaline stripping of metal ions after solvent extraction by base-stable 1,2,3-triazolium ionic liquids. *Dalton Transactions, 46* (16), 5113–5460.

Depuydt D., Van den Bossche A., Dehaen W., Binnemans K. (2017). Metal extraction with a short-chain imidazolium nitrate ionic liquid. *Chemical Communications, 53* (38), 5271–5274.

Depuydt D., Dehaen W., Binnemans K. (2017). Docusate Ionic Liquids: Effect of Cation on Water Solubility and Solvent Extraction Behavior. *ChemPlusChem, 82* (3), 458–466.

Depuydt, D., Van den Bossche, A., Dehaen, W., Binnemans, K. (2016). Halogen-free synthesis of symmetrical 1,3-dialkylimidazolium ionic liquids using non-enolisable starting materials. *RSC Advances, 6* (11), 8848–8859.

Depuydt, D., Dehaen, W., Binnemans, K. (2015). Solvent Extraction of Scandium(III) by an Aqueous Biphasic System with a Nonfluorinated Functionalized Ionic Liquid. *Industrial & Engineering Chemistry Research, 54* (36), 8988–8996.

Dupont, D., **Depuydt, D.**, Binnemans, K. (2015). Overview of the Effect of Salts on Biphasic Ionic Liquid/Water Solvent Extraction Systems: Anion Exchange, Mutual Solubility, and Thermomorphic Properties. *Journal of Physical Chemistry B, 119* (22), 6747–6757.

Glas, D., Van Doorslaer, C., **Depuydt, D.**, Liebner, F., Rosenau, T., Binnemans, K., De Vos, D. (2015). Lignin solubility in non-imidazolium ionic liquids. *Journal of Chemical Technology and Biotechnology*, *90* (10), 1821–1826.

Depuydt, D., Liu, L., Glorieux, C., Dehaen, W., Binnemans, K. (2015). Homogeneous liquid–liquid extraction of metal ions with non-fluorinated bis(2-ethylhexyl)phosphate ionic liquids having a lower critical solution temperature in combination with water. *Chemical Communications, 51* (75), 14183–14186.

Glas, D., Paesen, R., **Depuydt, D.**, Binnemans, K., Ameloot, M., De Vos, D., Ameloot, R. (2015). Cellulose Amorphization by Swelling in Ionic Liquid/Water Mixtures: A Combined Macroscopic and Second-Harmonic Microscopy Study. *ChemSusChem 8* (1), 82–86.

Depuydt, D., Brooks, N., Schaltin, S., Van Meervelt, L., Fransaer, J., Binnemans, K. (2013). Silver-containing ionic liquids with alkylamine ligands. *ChemPlusChem, 78* (6), 578–588.

Schaltin, S., Brooks, N., Sniekers, J., **Depuydt, D.**, Van Meervelt, L., Binnemans, K., Fransaer, J. (2013). Room-temperature silver-containing liquid metal salts with nitrate anions. *Physical Chemistry Chemical Physics, 15* (43), 18934–18943.

LIST OF CONFERENCES AND SEMINARS

Depuydt D., Dehaen W., Binnemans K. Temperature-dependent miscibility of non-fluorinated ionic liquids in water. Chemistry Conference for Young Scientists-ChemCYS 2014, Blankenberge (Belgium) 27-28 February 2014. Poster presentation

Depuydt D., Dehaen W., Binnemans K. Temperature-dependent miscibility of non-fluorinated ionic liquids in water. Workshop Exchange on ionic liquids (EXIL): Liquid-Liquid Extraction with ionic liquids, Strasbourg (France), 24-26 April 2014. Poster presentation.

Depuydt D., Dehaen W., Binnemans K. Solvent extraction of scandium(III) by an ionic-liquid based aqueous biphasic system. EREAN Summer School on Rare Earth Technology, Leuven (Belgium), 18-21 August 2014. Poster presentation.

Depuydt D., Dehaen W., Binnemans K. Temperature-dependent miscibility of non-fluorinated ionic liquids in water. 3rd International Symposium on Green Chemistry (ISGC 2015), La Rochelle (France), 3−7 May 2015. Oral presentation (flash presentation).